Paul Christen Røhr

A hydrological study concerning the southern slopes of Mt Kilimanjaro, Tanzania

Dr.ing.-thesis 2003:39

Faculty of Engineering Science and Technology
Department of Hydraulic and Environmental Engineering

NTNU

URN:NBN:no-3437

NTNU
Norwegian University of
Science and Technology

Faculty of Engineering
Science and Technology
Department of Hydraulic and
Environmental Engineering

A Hydrological Study Concerning the Southern Slopes of Mt Kilimanjaro, Tanzania

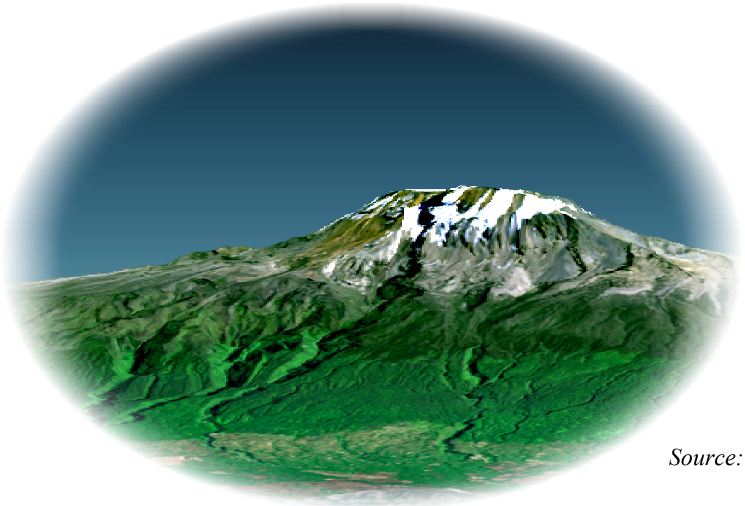

Source: NASA, 2003

By Paul Christen Røhr

A dissertation submitted to
the Faculty of Engineering Science and Technology,
of the Norwegian University of Science and Technology,
in partial fulfilment of the requirements for the degree of
Doctor Engineer.

Trondheim, Norway, 16th June 2003

ISBN 82-471-5589-3

Serial NTNU: 2003:39

URN:NBN:no-3437

URN:NBN:no-3437

ABSTRACT

The hydrological conditions on the southern slopes of Mt Kilimanjaro, Tanzania, are complex and not similar to very many other places. High annual precipitation with complex distribution patterns occurs on these slopes. Extensive water consumption and concentrated groundwater sources of unknown origin are found on the plains. The distribution and utilisation of the scarce water resources can easily be influenced by change in these and in other factors. A hydrological model is developed for the area and used for studying these processes and their influence on potential change in land use and climate.

This study is a part of a cooperative project between the University of Dar es Salaam, Tanzania and the Norwegian University of Science and Technology in Trondheim, Norway, focusing on how changes in land use influence the hydrologic - al responses of a catchment.

Extensive fieldwork has been performed in the course of several stays in the area. Three gauging stations were established on the slopes south of Mt Kilimanjaro for gauging the runoff from areas with and without influence from human activities. Precipitation and temperature measurements from the lower boundary of the forest reserve and up to 4000 metres above sea level (masl) were performed. Extensive field surveys were performed for identifying and understanding the hydrological processes taking place in the catchment. In addition, hydrological data were collected from the regular observation network.

The stream gauging and the precipitation measurements were analysed. The results were used in a water balance assessment of the southern slopes of Mt Kilimanjaro for determination of the extent of infiltration in the higher areas. Based on the results from the three sub-studies, a hydrological model was developed which describes the vertical water balance above and in the soil zone. The model can be used for investigation of the hydrological impact of changes in land use or climate. The model takes meteorological data as an input in addition to parameters describing the land cover and water demand in the catchment. This was applied for analysing the impact of prospective land use and climate changes.

The analysis of the discharge data and field inspections indicated that no surface runoff comes from the area above 2800 masl. The study of the precipitation data

resulted in a function describing the relative distribution of precipitation according to elevation for the southern slopes of Mt Kilimanjaro. The analysis indicates that the maximum precipitation intensity occurs about 400-500 meters higher than previously assumed. The water balance assessment gave indications on the extent of the deep groundwater infiltration on the southern slopes of Mt Kilimanjaro.

These findings were incorporated into the hydrological model, which was calibrated for three catchments on the southern slopes of Mt Kilimanjaro. The calibration for a small 21 km^2 uphill catchment, a mid-hill 52 km^2 catchment and a large 1783 km^2 catchment reaching from the plains to the peak of Mt Kilimanjaro showed good accordance between the simulated and the observed discharge for the three catchments.

The calibrated model was successfully used for simulating the period from 1958 to 2000 for the large catchment and showed good accordance for the simulation period. Simulations with changes in forest cover, water demand and climate were performed. The climate changes simulated were based on the findings from the Intergovernmental Panel on Climate Change and land use and forest cover and were evaluated on the basis of potential management schemes. The simulations indicate that the water demand in the area is not being met, and that changes in water demand are not fully reflected in the river discharge. The results also show that the changes have greater influence in years where the water deficit is already substantial, so called "dry years", than in years with a smaller deficit.

The tools developed and illustrated can be developed further for use in operational water management predicting the hydrological response due to changes in land use and water demand based on various management schemes. It is advised that the infrastructure developed during this work for collecting further measurements concerning the hydrological elements in the area continues to be operated.

PREFACE

My sincere thanks go to professor Ånund Killingtveit at the Department of Hydraulics and Environmental engineering at the Norwegian University of Science and Technology, who has been my guide and supervisor. His encouragement to take up new approaches, and numerous evenings together in the shadow of Mt Kilimanjaro discussing the result of the day's field survey have given me a solid basis for this work.

In addition to personnel at the University of Dar Es Salaam, my great appreciation is also addressed to the Maji Office in Moshi for all their assistance during the collection of data. I am also deeply grateful to the PBWO for their assistance and to the Norwegian Agency for Development Cooperation (NORAD) for funding of the research project.

The multidisciplinary cooperation with the researchers from the university of Dar es Salaam and the Norwegian University of Science and Technology was fruitful and introduced the author to different viewpoints on the topic. I also wish to convey my considerable gratitude to all Tanzanian and Norwegian contacts involved in our discussions over the years.

The spirited environment among my many colleagues at the Department of Hydraulics and Environmental Engineering has resulted in many discussions and to impulses for my study. It has made the daily working environment most pleasurable and my honest thanks are sent to all of them.

Chapter 8 in this thesis is a modified version of an article published in the Hydrological Sciences Journal, 48 (1), February 2003. The introduction has been revised to fit into the context of this thesis and some supplementary comments have been added to the description of the methods for homogeneity testing.

Finally, my heartfelt thanks are due to Sanna for her patience and continuous encouragement during the thesis work. It made the task more manageable than it otherwise would have been.

URN:NBN:no-3437

TABLE OF CONTENT

LIST OF FIGURES

LIST OF TABLES

1. INTRODUCTION

This study is one of the results of a multidisciplinary cooperation project between the University of Dar es Salaam, UDSM, Tanzania, and the Norwegian University of Science and Technology, NTNU, Trondheim, Norway, which started in the autumn of 1997. Joint research, for researchers within geography, botany, economics and hydrology-related issues within water management (preferably within the same physical area in the Pangani River Basin in northeastern Tanzania) was emphasised in this project.

Water is a limiting factor for life and development on the dry plains below the heavily populated southern slopes of Mt Kilimanjaro in Tanzania, East Africa. The major part of the available water falls as rain at altitudes of between 1000 and 3000 masl on the southern slopes of the mountain. The subsequent surface flow is utilized until it vanishes on the lowland plains due to evapotranspiration and major off-takes used for irrigated agriculture, which feed and employ the majority of the population.

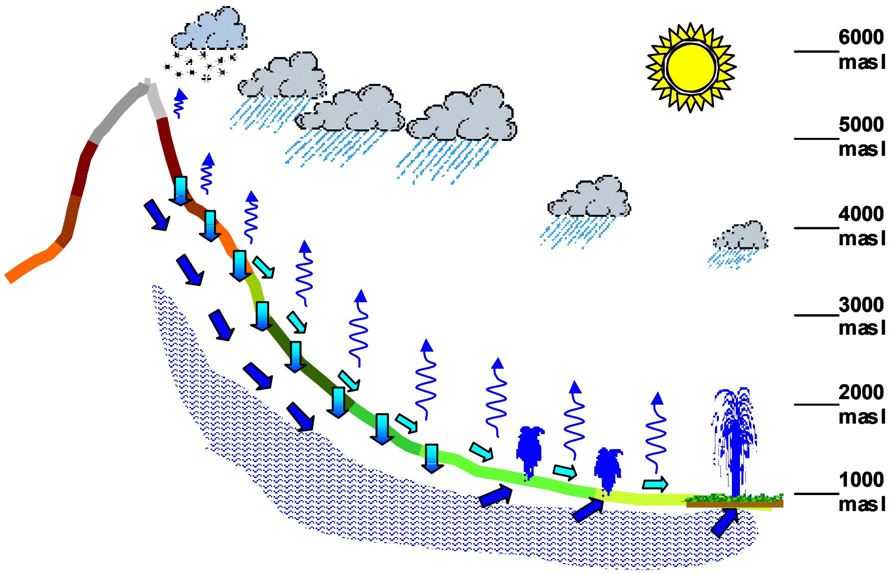

Figure 1.1: Schematic description of the southern slopes of Mt Kilimanjaro. Vertical scale is exaggerated.

The interaction between precipitation, evapotranspiration, surface runoff, infiltration and spring discharge on the mountain slopes and the low-lying plains is a complex mechanism, not easy to understand. Making qualified guesses and assumptions about the interaction is not difficult, but quantitative proofs of the assumptions are scarce and difficult to obtain. A section of the southern slope of Mt Kilimanjaro is shown schematically in Figure 1.1. It illustrates the many hydrological processes that take place on the slopes.

The lowland plains are dry with low precipitation and have a groundwater yield much greater than the annual precipitation on the plains would indicate. The groundwater yield comes mostly from a number of springs, some of them very large, e.g. Chemka Springs with an almost constant flow of nearly 10 m^3/s. Many smaller ones are located on the slopes.   Important questions are how these springs are fed, what are the recharge areas, how stable is the recharge and to what degree will changes in land use influence the recharge and thereby the spring's yield.

The precipitation increases to a maximum of about 2000 mm a year in the middle slopes before decreasing towards the peak, which receives just a few hundred-millimetres, mostly as snow, maintaining the familiar white peak of Mt Kilimanjaro. The groundwater yield on the slopes is limited, compared to the lowland plains. On the other hand, the vegetation is much more extensive on the slopes which are intensively utilized for agricultural production below the forest reserve, starting at about 1600-1800 masl (Martin, 2000). Due to the temperature, the potential evapotranspiration is high throughout the year compared to the strong seasonal variations in temperate areas. However, water supply is a limiting factor for the evapotranspiration, particularly on the lowland plains where extensive irrigation is necessary for securing the crop against poor and erratic rainfall.

The interaction between precipitation, evapotranspiration, infiltration, surface runoff, groundwater yield, irrigation, river discharge and land use is very complex. They are all important and considerable factors in the local hydrological cycle. The extent of irrigation is influenced by the river discharge and vice versa. On the other hand, the land use or cover influences the runoff and maybe the infiltration in addition to the evapotranspiration. The problem is to determine the degree of interaction between all these factors.

The extensive groundwater yield found on the lowland plains is not explicable in terms of the precipitation on the plain itself. The recharge takes place somewhere else, most probably at higher elevations on the slopes of Mt Kilimanjaro. The infiltration that takes place on the slopes is probably influenced by factors such as the soil type and condition in addition to the vegetation. The vegetation will also influence the evapotranspiration, and the extent of irrigation. Or will the irrigation influence the vegetation? The irrigation and the vegetation will both influence the river discharge. All these interactions are complex and depend on each other with unknown mechanisms.

An important parameter influencing many of the processes mentioned above is land use. The land use is the basis for human settlement in the area. Utilisation of the fields is based on a variety of land use, from intensive industrialised agriculture and smallholders to natural and planted forest, bush land, the dry lowland plains and the extreme moonscape-like alpine desert.

Analysis of the relationships between the various processes taking place in the catchment will therefore be a complex matter. Utilisation of computerised simulation models can be used as a method of analysis. It will facilitate the analysis of the interaction between the parameters. It will require detailed knowledge about the processes taking place in the catchment. These must be described properly with subsequent modelling together with their interaction with the other processes in the catchment. With a proper description of the mechanisms involved, changes in land use and climate can be studied, and different scenarios can be presented on the basis of various management schemes. The influence on the hydrological regime in the downstream rivers can be predicted and a beneficial management scheme can be developed.

This is exemplified towards the end of this thesis where the findings are applied to simulate the impact from changes in land use and climate.

URN:NBN:no-3437

URN:NBN:no-3437

2. OBJECTIVE AND DEVELOPMENT OF STUDY

2.1 Objective of the study

The main objective of this study is to study the hydrological processes taking place on the slopes south of Mt Kilimanjaro, in the light of the complex interactions with land use and how land use influences the hydrological response from the catchment. The hydrological processes and the elements within, influenced by land use can be represented in a hydrological model for the investigation of the response from changes in land use on the hydrology. This will assist in developing an improved management of the scarce water resources in the area.

The approach on the mountain slopes south of Mt Kilimanjaro is less straightforward than what would usually be expected. In order to fulfil the main objective of the cooperation between the UDSM and NTNU, a wide view has to be adopted to achieve a solid basis for the study. This is not necessarily part of the main objective of the co-operation.

The main objectives for the study of the southern slopes of Mt Kilimanjaro, can be summarised as follows:

- Collection and analysis of precipitation and runoff data
- Determining the elements of the water balance
- Developing a hydrological model for catchments on the slopes
- Utilisation of the model tool developed

Collection and analysis of precipitation and runoff data are important for a correct presentation in the water balance study. They will form a good foundation for the development of a hydrological model where the response from changes in land use can be evaluated using a reliable presentation of the most important hydrological processes in the catchment.

2.2 Development of study and thesis

In order to determine the changes in hydrological response for a catchment affected by land use changes, it is necessary to utilise a hydrological model for simulating the different alternatives of land use change. However, the required data for a simulation model is often not easily available, if at all. In the Pangani River basin, scarce water resources have put Water Management in focus in recent years (Amland, 1995), Unknown, 1995). Several studies have focused on the lowland plains and their water resources and the distribution between different users (The United Republic of Tanzania (1977c), IVO International Ltd & Norplan AS (1990), Perzyna (1994a) and Rusten (1995)). Less attention has been paid to the uphill areas where most of the water originates.

Four different themes listed in chapter 2.1 were selected for further study. Figure 2.1 illustrates the overall course of the study for determination of the hydrological response due to changes in land use for a catchment on the slopes south of Mt Kilimanjaro taking the complex interactions illustrated in Figure 1.1 into consideration.

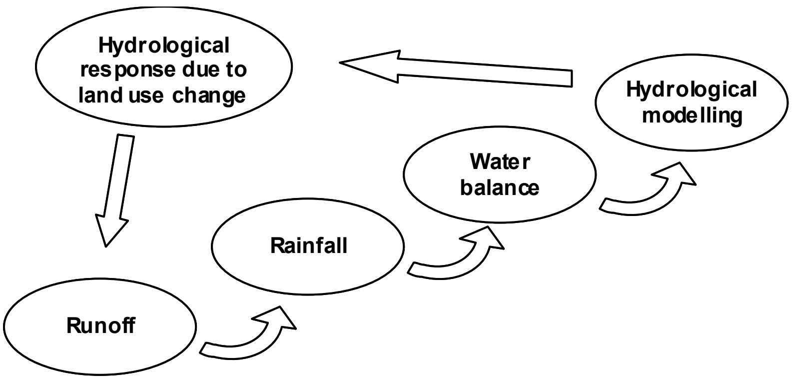

Figure 2.1: The approach applied in this thesis for determination of the hydrological response due to changes of land use on the southern slopes of Mt Kilimanjaro.

On the slopes south of Mt Kilimanjaro, the discharge data are concentrated at a few stations on the lowland plains representing the discharge from the entire catchment with a mixture of different land uses. Little or no information exists about the actual runoff from the upper part of the mountain slopes around Mt Kilimanjaro. Additional discharge observations are therefore required for representative data from different land use types. Discharge data from sub-catchments with a specific land use category can give valuable information about the response from particular types of land use and a better representation of the actual processes taking place in the catchment. In addition to the overall results for the whole catchment, a correct internal representation is important.

Precipitation data represent the input to the simulation model. The amount of precipitation data is bigger than the discharge data. However, very few observations take place above 1500-1600 masl and knowledge about the distribution with elevation is limited, particularly in the uphill area in the forest reserve and above. This is the starting point for many of the rivers in the area. As discussed in chapter 1, the groundwater yield on the lowland plain cannot be explained by the precipitation falling on the plain itself. A water balance taking account of uphill areas can disclose their contribution to groundwater resources and give information about the extent of infiltration in the upper areas.

Knowledge obtained about the hydrological cycle of the catchment, can be assembled and can form a solid basis for hydrological modelling of the catchment with all its different types of land use.

The process of utilizing all the information in the calibration process is summarized in Figure 2.2. In the first instance, small and rather homogeneous catchments are calibrated. The knowledge gleaned from the calibration is then used in considering a medium sized catchment with a more varied pattern of land use including the types of land use, which make up the small catchments. Finally, a catchment stretching from the lowland plains to the mountain peak with its even wider range of land use is modelled utilising all the knowledge obtained from the small and medium sized catchments. Such an approach ensures that processes taking place in the upper part of the catchment are represented in the model describing the whole catchment. Distributed model parameters can be found for the type of land use in the smaller catchment during the first part of the calibration process. These are retained when considering the medium sized and the large catchment. The principle illustrated in Figure 2.1 is repeated for each of the catchments illustrated in Figure 2.2.

The calibration of the large catchment will be more accurate with model parameters representing the actual runoff from its sub-catchment as well as from the catchment as a whole. Adopting the approach above, greater internal consistency in the model is achieved. Changes in land use can more easily be represented in the model parameters since different land uses are "calibrated" separately.

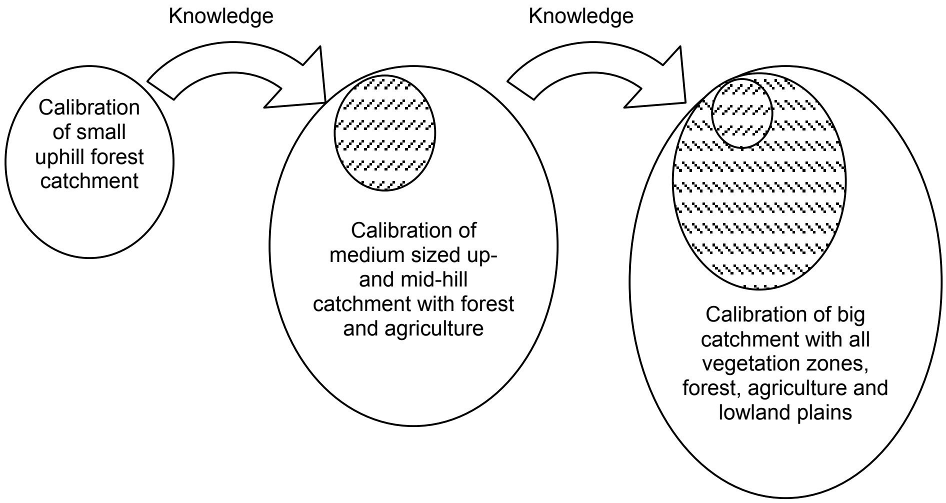

Figure 2.2: Illustration of the calibration process where small catchments are calibrated first. The knowledge obtained, is then used in the calibration process for a bigger catchment and so forth.

Studies of changes in land use and their hydrological impact can adopt various approaches. The selection of research areas must be understood in this context so that co-operation and research take place in the same physical area with a number of researchers. Some parts of the topic in the common research project have been selected for further study using the southern slopes of Mt Kilimanjaro as a research area. In particular, this study focuses on data collection, water balance, development of a hydrological model and examples of utilisation of the developed model focusing on changes in land use and climate. This is a choice made by the author.

The climate changes evaluated towards the end of the thesis are based on the findings of the Intergovernmental Panel on Climate Change. The land use changes are based on potential land use changes, which can take place under different management regimes.

From one point of view, the study of the four separate themes listed in the objective in chapter 2.1 and the overall study of changes in land use illustrated in Figure 2.1

are quite distinct from one another. On the other hand, they are closely linked when considering the water resources within the area. The literature study in chapter three forms the background to the study focusing on water resources and how they are influenced by (and influence) land use. This is done in the light of the overall theme of the cooperation project between UDSM and NTNU of which this study is a part. Literature on the different sub-topics, are treated in the individual chapters.

This approach has resulted in the following structure for the thesis:

Chapter 3: Literature Review
Chapter 4: Study Area and Fieldwork
Chapter 5: Stream Gauging
Chapter 6: Precipitation Distribution
Chapter 7: Water Balance considerations
Chapter 8: Hydrological Modelling
Chapter 9: Use of the Simulation Model
Chapter 10: Conclusions and overall Discussions

The sequence of the thesis is not necessarily similar to the sequence of the actual work as it was carried out. The stream gauge measurements and the study of rainfall distribution required completion of the field measurements that were finished towards the end of the study. On the other hand, the literature review and to some degree the development of the hydrological model did not require completion of the field measurements. This complexity and late receipt of complete measurements gave rise to a "multi-tasked" approach with parallel work on different problems and simultaneous conclusion of the sub-studies.

3. LITERATURE REVIEW

3.1 Introduction to the hydrological impacts of land use change

This literature review will focus on the overall theme of the thesis referred in chapter 1 and 2 forming an appropriate setting for this study. Literature related to particular methods and calculations applied in the following chapters is treated therein.

Modelling of the hydrological responses to changes in land use is somewhat different from modelling the changes in land use itself. Changes in land use can be predicted or estimated in different ways. Either by using regression models which estimate the rate of forestation, deforestation and/or subsequent desertification on the basis of predicted population developments, or by using more complex global models which take meteorological and climatic change into consideration and calculate the resulting change in biomass as a measure of land cover change.

One example of this is Serneels & Lambin (2001) in a study from southwest Kenya. This analyses the driving forces behind land use change without considering the hydrological processes. Spatial and statistical models are applied in order to understand the causes of land use change in the 10 694 km^2 study area. Three processes can largely describe Land use or land cover changes detected over the last 20 years, that is:

- Conversions to large-scale wheat farming
- Smallholder impact through clearing for subsistence agriculture and establishment of permanent settlements
- Rangeland modification through loss of vegetation

Serneels & Lambin (2001) conclude that model tools applied in the study can be used to determine where land cover change is most likely to occur. The difficulty is to determine when the event will actually will take place.

The hydrological response to land use change can be relatively clear. However, it is not necessarily less complex to model. It requires that the parameters influenced by changes in land use should be represented in the model equations forming the basis for the hydrological model applied in a study. In focussing upon the hydrological approach for the southern slope of Mt Kilimanjaro described in chapter 2, a thorough representation of parameters influenced by changes in land use must be represented in a model used for predicting the hydrological response of land use changes in this area.

However, a model must not be so complex and require such a wide range of input data that approximations or estimates must be made for most of the data because of the lack of measurements.

3.2 On land use changes and its general impacts in the tropics

The extent of and reasons for land use change will vary with the character of the change. Tole (1998) reports in a study on the sources of deforestation in tropical countries, a decline in forest area in Tanzania of 1.2 percent a year for the period 1981-1990. This is the 4^{th} highest rate among the tropical countries in Africa. Reasons for this change are analysed through regression and discussed. Tole (1998) points out that deforestation is related to both development and scarcity; development through expanding infrastructure and resource based economic expansion; and scarcity through population pressure, food and land shortages and fuel wood dependency.

In an extensive work Bruijnzeel (1990) draws the following 5 main conclusions concerning the changes in water yield associated with land cover changes in the tropics and sub-tropics after a review of the effects of conversion of tropical forest:

- Selective harvests will have little effect on stream flow
- Removal of natural forest may result in considerable initial increases in water yield
- Thereafter regeneration of vegetation/forest can lead to reductions in stream flow, after the initial increase, but not necessarily always
- Water yield after maturation may remain above the original yield when converted to cropping areas, grassland or tea plantation, and return to the original level with forest cover or in some cases decrease with the introduction of eucalyptus
- Burning of grassland may increase or decrease flow

Bruijnzeel (1990) points out that there are surprisingly few thorough studies involving hydrological modelling of entire basins involving shifting cultivation or removal of tropical forest for annual cropping. This is the case even although these two activities account for the greater part of tropical forest destruction. The reason for much of the increased water yield as mentioned above, is reductions in evapotranspiration when large trees with high evaporation rates are replaced with less extensive and transpiring vegetation.

When considering the base flow, Bruijnzeel (1990) summarizes the processes taking place after forest removal. In general, the base flow decreases, though evapotranspiration may be dramatically reduced when the forest is removed. Removal of the forest may also result in decreased infiltration capacity and increased storm runoff. The removal will also usually result in decreased evapotranspiration, during the dry season when the vegetation absorbs water from the groundwater zone. Theoretically, this will give an increased base flow. However, the process of removing the forest often causes disturbance of the forest floor which results in reduced infiltration capacity. Due to reduced infiltration, a greater part of the water yield leaves the catchment during and immediately after a storm episode and results in lower groundwater recharge and base flow. Bruijnzeel (1990) points out that cases of increased base flow after forest removal have been reported and that the majority of these are from “controlled conditions” and may not be reflected in the real world. Bruijnzeel (1990) argues that the worsened base flow conditions are not necessarily due to the forest removal itself, but due to lack of good land management during and after the clearing, e.g. soil disturbance by unrestricted use of heavy machinery.

Bruijnzeel & Critchley (1994) and Critchley & Bruijnzeel (1996) discuss thoroughly the environmental impacts of logging and conversion of moist tropical forest to agriculture and plantation, and these approximate to the conditions found in parts of the southern slopes of Mt Kilimanjaro. Inevitably, some of this impact will concern the hydrological processes. The lowermost part of the forest reserve around Mt Kilimanjaro, which is under pressure from the densely populated areas below, can risk such conditions. Bruijnzeel & Critchley (1994) describe the processes resulting from the logging of tropical forest. When the intensity of logging is limited and not all the vegetation is cleared, gaps in the forest are created when the large trees are cut down. This can temporarily cause reduced evapotranspiration and additionally more rain reaches the ground due to reduced interception. These factors may lead to increased soil moisture levels. This, in turn, can lead to increased water yield from the catchment. If the soil disturbance due to the logging activities is small, most of the increased water yield may occur as base flow. However, with increasing soil disturbance, the amount of storm flow will increase. In the most dramatic cases, the infiltration capacity will be reduced so much that the base flow will go down. Bruijnzeel & Critchley (1994) also point out that removal of vegetation shortens the response time from the catchment. This means that water reach the streams more quickly during and after a precipitation event instead of filling up the soils storage capacity and depleting it later.

Critchley & Bruijnzeel (1996) focus more on the hydrological impact when converting tropical forest to agriculture or plantations. On agricultural land, the part of the precipitation not infiltrating, but forming direct runoff is often greater than in forest areas. In undisturbed tropical forest, it may be less than 1 percent of the precipitation, while on agricultural land with little or no conservation practices it may be as much as 30 percent. The total catchment yield may increase compared to the undisturbed tropical forest. Typical values are 150-450 mm according to Critchley & Bruijnzeel (1996) depending on annual rainfall. With the increased amount of water available and decreased evapotranspiration, good surface management may lead to increased dry season discharge. In practice however, due to reduced infiltration capabilities, a decline in base flow is often experienced.

Critchley & Bruijnzeel (1996) also discuss the case of so called “fog stripping”, where the amount of water reaching the soil surface is influenced by the presence of trees. Low clouds and fog are blown through the forest canopy and “stripped” of their water by the vegetation. If this is related to land use change on the southern slopes of Mt Kilimanjaro, then we might see that the clearing of forest on the upper slopes which have frequent cloud cover and replacing it with crops, will end this “fog stripping”. Clearing of the forest reserve on the upper slopes of Mt Kilimanjaro is probably not about to happen in the near future. Critchley & Bruijnzeel (1996) raise the question of the influence of land use in the area immediately below the point where such “stripping” takes place. This may have more relevance for the southern slopes of Mt Kilimanjaro. When forest on the lower slopes is cleared, this may lead to a warming up of the overlying atmosphere and to a lifting of the cloud condensation level. If the heating is extensive enough, this might lead to a complete diminution of the cloud cover and bring about changes in the vegetation and water resources on the upper slopes.

A synthesis of French work on the impact of forest conversion from West Africa and Madagascar has been prepared by Adokpo Migan (2000) and this is mainly a review of recent French works. It concludes that forest cover considerably decreases the maximum runoff particularly during extreme floods. It is also clear that forest and eucalyptus have greater evapotranspiration than shrub vegetation. In a study cited, eucalyptus caused a considerable depletion of low flows in four out of seven years, although this effect could not be observed in the natural forest.

In many studies of land use or land cover change, afforestation or deforestation are taken as the most dramatic extremes. Watson et al. (2001) and Calder (1993) highlight two different methods for assessing the changes in river discharge due to various forest treatments:

- Paired catchment approach
- Water balance approach with climatic input

The former is sometimes denoted the paired catchment study and the latter as the single catchment study. The paired catchment approach is based on two catchments with as equal conditions as possible, as regards land use and hydrological conditions. The land use conditions are kept as unchanged as possible in the control catchment, while the other catchment undergoes treatment as regards land use. Regression analysis with the discharge from the undisturbed catchment is used for estimating the undisturbed discharge from the catchment undergoing treatment for the post treatment period. The difference between the measured post-treatment discharge and the estimated undisturbed discharge found through the regression analysis is assumed to represent the effect of the change.

The water balance approach or single catchment study is based on discharge measurements before and after a change in land use or land cover. Based on pre-treatment discharge observations, a water balance or hydrological model is fitted and calibrated to the catchment. The undisturbed post-treatment discharge is then simulated on the basis of meteorological observations. The effect of the treatment is assumed to be the difference between the simulated post-treatment discharge and the observed discharge.

Strictly speaking, the single catchment study does not necessarily require any hydrological modelling. The pre- and post-treatment discharge can be found and computed directly. However, this can give rise to incorrect conclusions concerning the influence of the treatment due to differences in precipitation before and after the treatment.

In the water balance approach, the elements influenced by the treatment of the catchment, are not necessarily reflected directly or indirectly in the model parameters. However, if these elements are reflected in the model parameters, the effect of treatment may be simulated without full-scale field experiments, or the model can be applied on a more extensive basis for other catchments predicting the response from corresponding treatment.

Calder (1993) points out that afforestation and deforestation constitute the most dramatic changes in land use world wide, also as far as hydrological effects are concerned. Areas found unsuitable for agriculture often remain forested. Afforestation processes cause concern for increased interception and depleted downstream water yield. Deforestation may lead to increased erosion, silting up of rivers and streams and more leaching of nutrients. One major factor in the hydrological response to changes in land use is the evapotranspiration. The evapotranspiration will be a result of the balance between available energy, available water and the transport of vapour between the surface and the atmosphere. Changes in land use or land cover can, according to Calder (1993), influence the availability of water through:

- Surface area of free water
- Availability of soil water to plants (different capabilities of absorption from soil)
- Different leaf area or stomata resistance and response

Changes in land use will most probably change one or more of these elements of the evapotranspiration process.

A review of catchment experiments for the determination of the effect of vegetation changes on water yield and evapotranspiration is thoroughly presented by Bosch & Hewlett (1982) with a tabular survey of the 94-catchment experiments reviewed. It is concluded that coniferous forest, deciduous hardwood, bush and grass, in that order, have a decreasing influence on the water yield when these covers are modified. Bosch & Hewlett (1982) find it difficult to draw definite conclusions on water yield changes due to varying forestry practices, for use in planning and prediction of future changes in stream flow. However, for a 10 percent change in cover, the water yield changes for coniferous and eucalyptus; deciduous hardwood and grass and bush land are in the order of 40, 25 and 10 mm respectively, although Bosch & Hewlett (1982) cannot establish any error limits for these numbers.

The influence on water resources due to afforestation and deforestation is analysed by Sahin & Hall (1996) through regression analysis on the basis of data from 145 different experiments. The data from Bosch & Hewlett (1982) is included in this number. The land cover was classified in 7 different cover types. The findings for the cover types relevant for the southern slopes of Mt Kilimanjaro are summarized in Table 3.1. The table indicates that removal of vegetation increased the water yield, while introduction of vegetation decreased the water yield. The individual findings vary somewhat due to a low numbers of data, particularly for the three types of cover shown in Table 3.1. Sahin & Hall (1996) point out that the majority of the results analysed are from small drainage areas not greater than a few hectares. To which degree these results can be transposed to larger areas is subject to discussion. Sahin & Hall (1996) argue that the results from their study can give a "broad-brush" estimate of the magnitude of the yield changes.

Cover type	Yield change for 100 % treatment, mm/year	Yield change per 10% cover change, mm/year
Rainforest	213	10
Scrub (clearing)	92	9
Scrub (planting)	-220	-5

Table 3.1: Results from analysis of land cover vs. water yield change. From Sahin & Hall (1996).

3.3 Water balance studies in tropical areas

Wilk & Hughes (2002a) and Wilk & Hughes (2002b) present a simulation model for the response due to land use change, when not having representative gauging data for different land use regimes within the catchment. A semi-distributed water resource model was calibrated on a monthly basis for a 4100-km^2 catchment with different land use, several reservoirs, hydropower plants and transfer tunnels. The model was divided into 15 sub-catchments. The calibrated model was used to simulate various land use and climate change scenarios relative to the result from the calibrated model for a 21-year modelling period. The greatest increase in runoff was found to be due to conversion from forest and savannah to agricultural land. Land use distribution mapped at the beginning and the end of the modelling period applied in the model, indicated relatively unchanged runoff compared to the control scenario. Wilk & Hughes (2002b) suggest that the mosaic of natural land use changes from the recent past is unlikely to be evident in the runoff records since their impact is negligible.

In their evaluation of the potential for runoff irrigation in the Sahel Zone, Tauer & Humborg (1992) state that some rainfall-runoff models have been developed for quantification of hydrological response to land use change. The definition of the various factors in terms of their impact on the hydrological regime downstream is impossible due to the small scale and their complex interrelationship according to Tauer & Humborg (1992). The influence from scale variation of the model and its parameters is discussed by Refsgaard (1997) in an example of multi-scale validation of a distributed hydrological model for discharge and groundwater head simulation. A 500 m grid is applied to make 1000, 2000 and 4000 m grids. Parameters are interpolated based on the finer grid. The findings indicated that the simulation results declined with a coarser grid.

The changes in runoff due to afforestation or clear felling in 4 small research basins in Zimbabwe and South Africa are considered by Hughes & Smakhtin (1998). Two rainfall-runoff models, one with daily and one with monthly time-steps, were used for the simulations. The change in land use was represented in the models through changes in parameter values for the land use in the model. Examples of parameters are forest area, interception rates, proportion of vegetation cover, leaf area index and canopy capacity. Hughes & Smakhtin (1998) conclude that the models are capable of simulating the general response to afforestation and clear felling, but it was not clear from the study to what extent the models were suitable for simulating the results from thinning and the effect at different stages of growth. This means that the model cannot simulate the response from different planting and management practices when, for example, shifting crops from rice to maize.

Lørup et al. (1998) combine lumped hydrological modelling and statistical tests in six medium-sized (200-1000 km^2) catchments in Zimbabwe for a study of the effect of land use changes on catchment runoff. A hydrological model was calibrated for the six catchments. The six gauging stations used for the calibration were a part of the regular observation network. The hydrological model was calibrated on data from the first half of the reference period. The other half of the reference period was used for verification of the calibrated model. The calibrated model was then run for the entire observation period. The simulated discharges were then compared with the actually observed discharge and a classical hypothesis test was performed on the deviation between the two. The analysis indicated increase in runoff for most of the catchments, but a statistical significance at the 5% level for the increase was only found for one of the six catchments. The largest changes were found to occur where large increases in population and agricultural intensity took place. The considerable increase in population in the area investigated by Lørup et al. (1998) has not resulted in any changes in surface runoff from the catchments.

Post et al. (1996) model a catchment in Australia where 85 percent of the forest has been cut down. Both the periods before and after clear felling were modelled. The model makes it possible to account for possible changes in precipitation from before and after the clear felling as discussed above. The analysis indicated a dramatic increase in runoff from the catchment after deforestation. The increase dropped slowly to the pre-treatment level after about 8 years. Analysis of the model results indicates that the treatment influenced the total runoff volume from the catchment, but had little influence on the quick or slow flow recession.

Calder et al. (1995) studied the effects of land use change from forest to agricultural land in the catchment around Lake Malawi. The lake level was simulated for the period 1896 to 1994. The model was calibrated with respect to forest cover for the period 1954 to 1980 resulting in a 64 percent forest cover for the whole calibration period compared to a 74 percent forest cover for the catchment in 1967 based on a study of aerial photographs. The land use survey from 1967 above and LANDSAT satellite measures from 1990 indicated a 13 percent decline in forest cover in Malawi for the period 1967 to 1990. The 13 percent decline in forest cover, from 64 percent to 51 percent assumed a linear course in the model, and gave a better simulation of the non-calibration period from 1980 to 1994 with an explained variance of 0.91 when incorporated into the model. Without the implementation of the change of forest cover in the model, the lake level towards the end of the simulation period would have been about 1 m lower than actually observed.

Schulze (2000) discuss a southern African perspective on the hydrological response to land use and climatic change. Several issues related to land use change are illustrated with examples from southern Africa.

- Hydrological responses are highly sensitive to and dependent upon, land use and its change
- Abrupt land use changes at local scale are more significant than gradual land cover change on regional or global scale
- Changes in land use are difficult to distinguish from variations in flow regime
- The details of spatial information may be vital in assessing the hydrological responses to critical land uses

These problems can also be found in the area south of Mt Kilimanjaro. The changes in land use from savannah or small-scale agriculture with low population to huge irrigation schemes with extensive irrigation based farming will influence the hydrological regime in the downstream river. Differences in land use obviously also take place on the southern slopes of Mt Kilimanjaro and represent different responses in the hydrological system. The population growth on the mountain slopes has forced the population to find new farming land on the lowland plains (Grove, 1993) where irrigation is a necessity for securing the crop against unreliable rainfall conditions. In the context of the development of irrigated agriculture, it is most probable that a sudden increase in off-take will worsen the already varying flow regimes. However it is also clear the scale of the spatial consideration of the catchment will influence the result. A global vegetation model with let us say, 2^{o} resolution (e.g. Foley et al. (1998)) may simulate well the fluctuations in vegetation over the last 30 years for Africa as a continent, but will probably contribute little to knowledge about the local variations on the southern slopes of Mt Kilimanjaro.

In the wider context of climate change, Schulze (2000) concludes with the question as to whether or not the long-term changes can be detected in a region with high natural variability in both climate and hydrology, but is unable to give an answer. Climate change is represented by small long-term changes, while many tropical areas experience natural dramatic change in hydrological conditions from one year to another.

Sandström (1995) investigated the hydrological implications of deforestation and land degradation in a study of two small catchments in the semi-arid Babati district in north-central Tanzania. The two catchments, one forested and one deforested, were studied for soil properties, runoff and groundwater recharge through both field studies and computer simulations. The findings were partly applied for modelling the bigger Lake Babati catchment downstream. Sandström (1995) found that the groundwater infiltration was almost twice as high in the forested catchment as in the deforested catchment under cultivation. As far as precipitation was concerned, Sandström (1995) was not able to trace any significant trends in the area, but pointed out that there are large inter-annual fluctuations in this area. A simulation model applied for the two small catchments was also fitted for the bigger Lake Babati catchment. Two recorded floods in the past, caused damage to two villages due to high lake level. Sandström (1995) simulates the catchment for forested conditions and finds that it would have resulted in a lower lake level causing less damage compared to the present situation.

An example of modelling the actual land use change including meteorological variables is shown by Stephenne & Lambin (2001). The change is modelled for two time frequencies depending on high frequency climatic or low frequency demographic variability in a study from Burkina Faso. The simulation is based on the variables human population, livestock, rainfall and cereal import for every year. The areas for fuel wood extraction, crops, fallow and pastureland are the output from the model. Changes in cropland simulated by the model, correspond with measurements from case studies based on remotely sensed data. However, this macro scale model does not take any of the hydrological processes in the field into consideration except for the amount of precipitation. It will be difficult to use this model at the local level for operational water management.

Remote sensing utilised in analysis of the hydrological response due to land use changes coupled with hydrological simulations is discussed by Staudenrausch & Flugel (2001). Remote sensing is used for determination of erosion, land use, settlements and vegetation time series for 3 catchments (4400-12000 km^2) in southern Africa for development of a Water Resources System. A web-solution for the operation of the model will make the system available for a wider range of users with actual calculations executed on a central server and this work will be continuously developed.

de Groen & Savenije (1995) studied the relationship between evapotranspiration and rainfall through feedback mechanisms. This was modelled for south-central Africa including Zambia, Zimbabwe and Mozambique. The wet season evapotranspiration was modelled and it was shown that it resulted in precipitation elsewhere in the region at downwind locations. Linking this to land use change, they state that the change in vegetation can influence the hydrological cycle and the precipitation patterns in downwind neighbouring catchments. de Groen & Savenije (1998) point out that it is generally agreed that forest and other bio-diverse areas evapotranspirate considerably more than monocultures in large and intensively utilised irrigation schemes.

3.4 Concluding remarks on the literature

The works by Bruijnzeel (1990), Bruijnzeel & Critchley (1994) and Critchley & Bruijnzeel (1996) described the actual processes taking place. Bosch & Hewlett (1982) and later Sahin & Hall (1996) quantify the yield change based on published catchment experiments. However, it is necessary to agree with Bruijnzeel (1990) that not many studies treat hydrological modelling of entire basins, evaluating the effects of shifting cultivation or changes from forest to annual cropping.

In the last part of this chapter, various investigations of land use changes and hydrological modelling for their determination have been reviewed. Several examples of modelling of pre and post change conditions are referred and put into the context of land use change.

The review has introduced this study of the hydrology of the southern slopes of Mt Kilimanjaro in the light of land use change. Complex processes take place in the area. Some of them are to be revealed and examined in this study and applied in hydrological modelling.

In the hydrological model for the southern slopes of Mt Kilimanjaro knowledge about these processes can be applied including an extensive description of the land use through representation of the vegetation and its immediately influenced surface boundary in the model. It can be used for obtaining new knowledge about the impact of the different factors of land use change in this area and on how the water resources are influenced.

4. STUDY AREA AND FIELDWORK

4.1 The study area

Mount Kilimanjaro with its permanent ice cap reaching 5895 meters above sea level is located only 330 km south of the equator. With its 4600 meters direct rise above the surrounding plains, it is the highest freestanding mountain in the world (NASA, 2002). With Mt Meru it forms the northern most part of the 42200 km^2 Pangani River Basin located on the border between Kenya and Tanzania. This stretches 450 km southeastwards to its outlet in the Indian Ocean near Tanga in Tanzania. See Figure 4.1.

More than 50% of the basin, mainly the lowland plains, are arid or semi-arid with an annual precipitation of 500-600 mm/year (The United Republic of Tanzania, 1977c). High levels of precipitation can be found in the southern slopes of the mountain areas with an annual precipitation of 1000-2000 mm/year (Luhumbika, 1999). The rainfall pattern is bimodal with two distinct rainy seasons, long rains from March to June and short rains from November to December. Population densities of more than 600 persons/km^2 can be found on the mountain slopes of Mt Kilimanjaro (Lein, 2001). The upper part of the basin forming the Kilimanjaro region has a population of 1.1 million (according to the 1988 Census) with an annual growth rate of about 2.2 percent (Nippon Koei CO. Ltd & Pasco International Inc., 1998).

Extensive irrigation, particularly in the upper part of the basin, secures crops against erratic rainfall on the lowland plains and extends the growing of crops like paddy, maize, banana, beans, coffee, vegetables and sugar cane (Daluti, 1999). A total of 95-MW of hydropower capacity is installed in the basin and supplied by water from the Nyumba Ya Mungu, NyM, reservoir in the central part of the catchment. The reservoir has an active storage of 870-mill m^3.

The mountain slopes of Mt Meru and Mt Kilimanjaro have some of the best-developed and best-known traditional furrow irrigation systems in East-Africa (Grove (1993) and Lein (1998)). An extensive network of furrows starts far up in the mountain and transports the water along and across the river valleys to consumers, sometimes far from the source. Uphill, the furrows also act as domestic water supply.

In Tanzania's Structural Adjustment Programme, agriculture, which accounts for half of the GDP and occupies 90% of the labour force, is given high priority (Tanzanian Authorities, 1999). Considerable attention to agricultural development can therefore be expected with continued pressure on already scarce water resources.

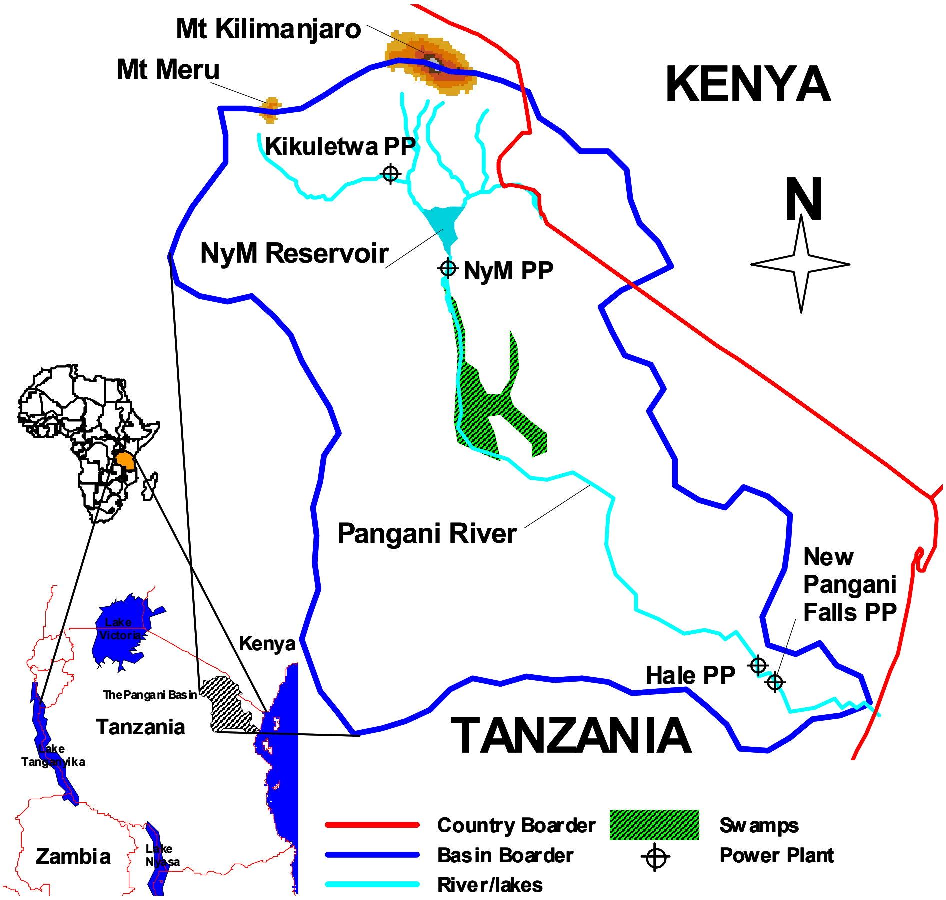

Figure 4.1: Location of the Pangani River Basin.

The mountain slopes of Mt Kilimanjaro can be divided into five ecological zones, the lower slopes, (900-1800masl) the forest (1800-2800masl), the heath and moorland, the highland desert (4000-5000masl) and the summit (above 5000masl) (Martin, 2000). The surrounding area on the plains below can be classified as tropical savannah. The human settlements and agricultural activities are located on the plains and on the lower slopes between 900 and 1800masl. The area above this level forms the Forest Reserve and the Kilimanjaro National Park. In this area, there are, in principle, no settlements, or human activities related to agriculture and land use. Martin (2000) states that fires, illegal timber collecting, land pressure and over usage of natural resources are among Mt Kilimanjaro's biggest problems. The same problems are also described by Yanda & Shishira (1999).

The lowland plains are heavily influenced by extensive human land use through intensive agricultural production based on irrigation undertaken at varying degrees of intensity. The hydrological system is complex with springs, rivers and canals with a large number of off-takes for irrigation as described in the introduction. A few large springs contribute with a yield of 15-20 m^3/s, and these form a major part of the inflow to the NyM reservoir. In addition to irrigation, domestic and industrial water supply and hydropower plants are important, but not major users of water in the area.

4.2 Description of fieldwork and measurements

The introductory description of the complex processes taking place in the catchment demonstrates the need for extensive field data for sorting out some of these processes. Extensive fieldwork has been carried out during this study, mainly in the upper part of the Pangani River Basin. The fieldwork can be summarized as follows:

- Discharge measurements
- Precipitation measurements
- Temperature measurements
- Data harvesting
- Field inspections

An overview of the fieldwork and the equipment used follows with a short description of their use. The fieldwork was carried out during the period from the summer of 1998 to the winter of 2001. The first part of the period was used for installation of equipment. Later, emphasis was shifted to operation and maintenance of the equipment.

As mentioned previously, the multidisciplinary research project concentrated on the same physical area for all disciplines. This was an important principle when choosing the research area, although not a limitation.

4.2.1 Gauging stations

Three new gauging stations were established on the slopes of Mt Kilimanjaro. A previous examination of the files at the local Water Authorities Office by Sivertsgaard & Skau (1996) and later Lefstad & Bjørkenes (1997), revealed that the discharge stations, with one exception at about 1400 masl, are located on the lowland plains between 700 and 900 masl. However, this station has not been operational for several decades. The stations on the lowland plains, give valuable information about the discharge, but unfortunately for the purposes of this study, the majority of the water consumption takes place upstream this stations.

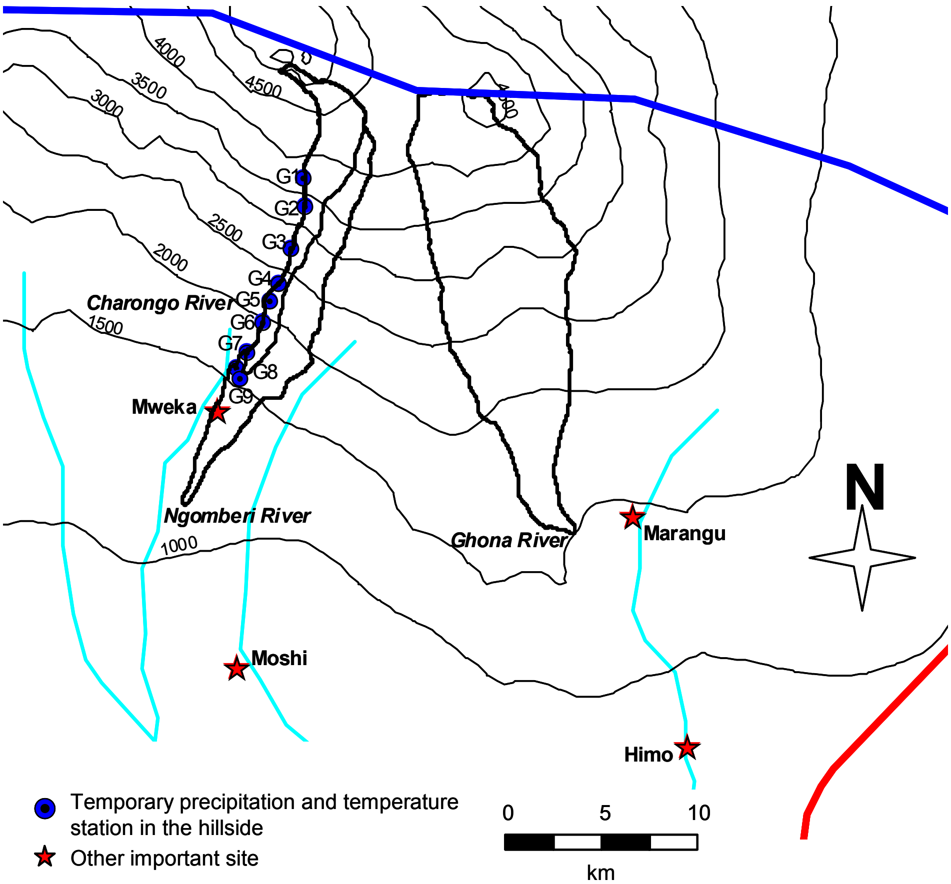

Figure 4.2: The figure shows the location and extent of the three catchments gauged and the 9 temporary precipitation stations. Other important sites are also shown.

After intensive map studies, discussions with other researchers in the multidisciplinary project, with the regional hydrologist at the local Water Authorities Office and the inspection of potential sites, the following three sites were selected:

1. Charongo River at Mweka, just inside the forest boundary
2. Ngomberi River at Kibosho Road Bridge
3. Ghona River at Marangu West

The location of the different gauging stations and their catchment borders can be seen in Figure 4.2. Table 4.1 shows some details of the stations, the catchments and the recordings.

Parameter	**Unit**	**Charongo**	**Ngomberi**	**Ghona**
Lat	dd	3.216	3.277	3.289
Long	dd	37.343	37.316	37.494
Catchment size	km^2	21	52	110
Max elevation	masl	5895	5895	4658
Mean elevation	masl	3940	2602	2879
Min elevation (and loc. of station)	masl	1640	1080	1505
Catchment length	km	16	23	24
Started operating		8th July 1998	14th July 1998	27th October 1998
Recording intervall	hour	1	1	1

Table 4.1: Some information on the three new river gauging station.

A sketch layout for each gauging station is shown in Figure 4.3. A data logger (Aanderaa type 3634), a water level sensor (Aanderaa pressure sensor type 3191 with a compensating unit type 2848) and a power supply form the gauging station. The water level sensor measures the hydrostatic head of water above the sensor. The compensating unit compensates for the effect of barometric pressure on the measurements. The data logger sampled the water level every hour and stored the data until it could be transferred to a portable computer during visits to the gauging station. Further technical details about the equipment can be found in Aanderaa-Instruments (1998) and Aanderaa-Instruments (1997). The equipment is located inside a steel box for protection. In addition to the automatic loggers, there is a staff gauge at each station. A gauge reader, who lives nearby and is familiar with the area, reads the staff gauge frequently. Unfortunately, the gauging station at the Ghona

River was vandalised and the data logger stolen in the spring 2000. In addition to the pressure sensor, several types of precipitation gauges were connected to the data logger for varying periods. Due to operational problems for the precipitation sensors, little and scarce precipitation data was achieved from this activity.

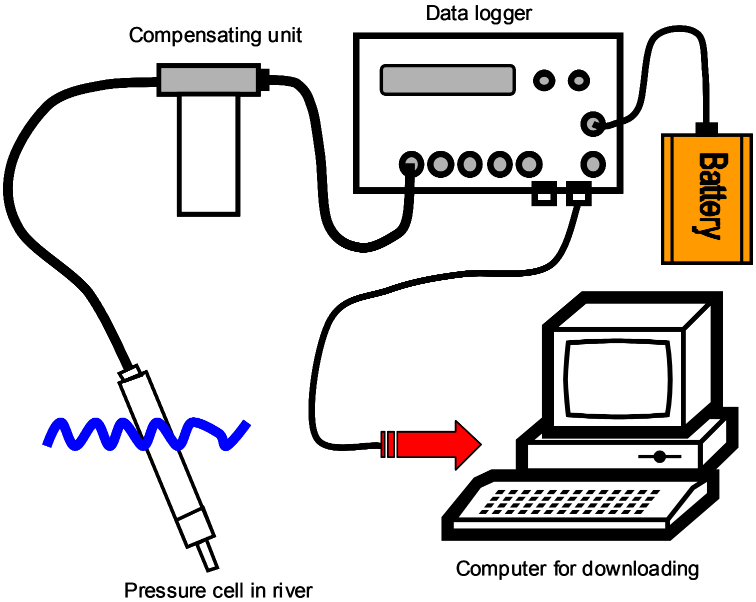

Figure 4.3: The principal set-up for the three new river gauging stations. Data logger, pressure sensor, compensating unit and power supply.

The relationship between the discharge and the recorded water level was determined by discharge measurements. The discharge was measured at various water levels by use of both a current meter and salt dilution measurements. The discharge measurements were performed throughout the recording period. The results from the recording period for the three stations is presented and discussed in chapter 5.

4.2.2 Precipitation measurements

In addition to the occasional precipitation measurements by the sensors connected to the data loggers at the three gauging stations, measurements to determine the precipitation gradient on the southern slope of Mt Kilimanjaro were performed. 9 temporary precipitation gauges, G1 to G9, were installed, located from the gauging station at Charongo and uphill. See Figure 4.2 for details about the location. The precipitation measurements were organised for a period of 2 years from September 1999. The gauges used were made from 5” steel pipes with sufficient volume to store precipitation up to one month between readings. The gauges were manufactured locally and placed between 1500 and 4000 masl in and above the forest reserve around Mt. Kilimanjaro. The vegetation around the gauges was kept down. To prevent evaporation from the gauge, a thin layer of oil was added. The gauges were located on the ground with the rim about 70-80 cm above the ground. An equivalent length of the gauge was buried under the ground for securing a stable installation. Local personnel inspected and read the gauges at every turn of the month. The result from the precipitation gauging is presented and discussed in chapter 6.

4.2.3 Temperature measurements

At each of the 9 temporary precipitation stations, a small automatic temperature logger was installed. The type Tinytalk II data logger or a similar later type was used. The data loggers can store from 1800 readings and more. See Gemini Data Loggers (UK) LTD (1995) for further technical details. The data loggers were located within 100 metres of the precipitation gauge, and programmed to read the temperature every 4 hours. The loggers had a storage capacity for about 10 month reading and more. The data recorded by the loggers were downloaded to regular portable computer and further processed in a spreadsheet. The data were used for the hydrological simulation and for investigation of the temperature gradient from the lowland plains toward the peak of Mt Kilimanjaro.

4.2.4 Other data acquisition

Meteorological data and discharge data were collected from several additional sources. The basis was the work by Sivertsgaard & Skau (1996) and Lefstad & Bjørkenes (1997). Through extensive fieldwork, they collected extensive data material for the Pangani River Basin. This material was updated with recent observations and extended by a few more stations from the area during the project. The information was collected at the local Maji office in Moshi, at University of Dar es Salaam and through field visits to several stations for comparison and by checking several original logbooks. In addition, visits to Kilimanjaro International Airport, Moshi Airport, Tanzania Planting Company and others gave new and valuable information. Kilimanjaro National Park authorities supplied valuable precipitation measurements from the Kilimanjaro National Park used in chapter 6. More detailed description and analysis of the precipitation data is given in chapter 6.

4.2.5 Field inspection

Numerous field inspections and surveys in the area revealed important information about the catchment. Two visits to the area for the gauges G1 to G9 (see Figure 4.2), revealed that the surface runoff from the catchment above about 3000 masl is very limited and if it does exist at all, only occurs during the wet season. Inspection to the northwestern part of the Pangani River basin, that is the area around and south of Arusha town, towards the end of the wet season revealed that this area makes little or no contribution to the river inflow to the Nyumba ya Mungu reservoir.

In addition, a number of stations from which the meteorological observations were taken, were inspected. The extensive field inspections gave valuable information in the work with the hydrology of the area. It gave indications on the processes taking part in the catchment, and helped to form the theories presented here.

4.3 The Water Resources and their use

4.3.1 Water Resources in the upper Pangani River Basin

The water resources in the upper part of Pangani River Basin derive principally from two sources, that is river discharge and groundwater yields. The majority of the rivers have their origin in the forest belt around Mt Kilimanjaro or Mt Meru and drain southwards. As mentioned above, the river discharge from the northwestern most part of the Pangani River Basin, that is the area south of Mt Meru, is scarce or non-existent during a major part of the year. Extensive extractions for domestic and irrigation purposes take place along the river.

The two rivers, the Ruvu River from the northeastern part of Pangani River Basin and the Kikuletwa River from the northwestern part of the basin both drain into NyM. The total river inflow to the NyM reservoir has been estimated in several studies. Nippon Koei CO. Ltd & Pasco International Inc. (1998) estimate the inflow to NyM from Kikuletwa River to 23.5 m^3/s and from Ruvu River as 11.5 m^3/s, a total of 35 m^3/s. Perzyna (1994a) estimate that the total inflow to NyM reservoir was 34.1 m^3/s for the period 1971 to 1996. This was made up of 24.4 m^3/s from Kikuletwa River and 9.7 m^3/s from Ruvu River. The Water Master Plan for the Kilimanjaro region by The United Republic of Tanzania (1977b) estimates the inflow to NyM Reservoir as 19.0 m^3/s from Kikuletwa River and 12.7 m^3/s from the Ruvu River.

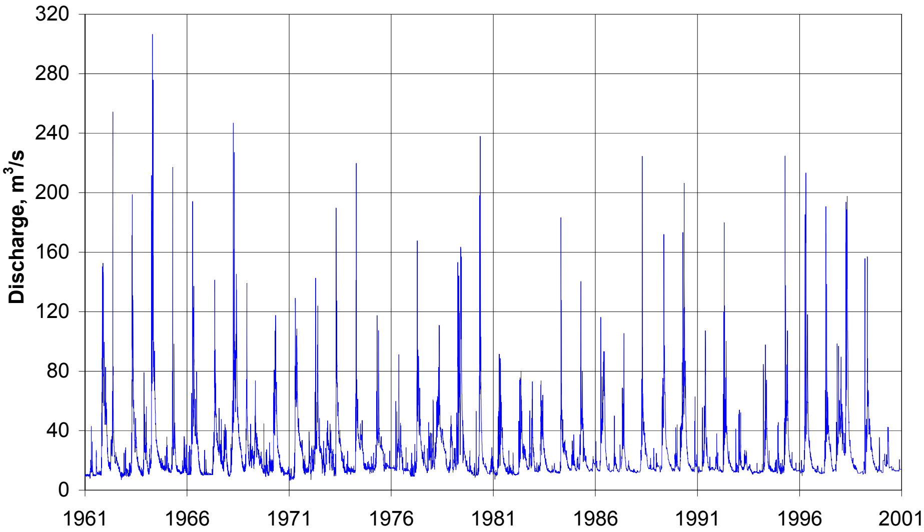

Figure 4.4: Plot of observed discharge at the gauging station 1DD1 for the period 1961-2000

The three estimated inflows to the NyM Reservoir vary from 31.7 m^3/s to 35.1 m^3/s. The average inflow from Kikuletwa River alone varies from 19 m^3/s to 25.1 m^3/s according to these sources. The variation in estimates can be due to the different time periods used. The data acquisition described above involved discharge data from gauging station 1DD1 located upstream from Kikuletwa's inlet to the NyM reservoir. Figure 4.4 shows the daily discharge for the gauging station for the period from 1961 to 2000. If the whole period is taken into consideration, the average discharge at gauging station 1DD1 is 24.6 m^3/s. Some more characteristics of the discharge at gauging station 1DD1 are shown in Figure 4.5. The figure shows the maximum, minimum and 25% percentile of the annual discharge. As seen on the figure, the minimum discharge does not vary much from year to year. Some deviations can be found in the early 1970s and early 1980s, but later the minimum annual discharge has not fallen below 10-12 m^3/s. In addition, monthly values are shown in the appendix in addition to a few years with daily values.

The reason for the relatively stable minimum discharge from one year to another is the groundwater yield, with most of it coming from a few large springs. The groundwater yield is an important source for both domestic and agricultural water supply in the area. Three springs around Moshi town are utilised for water supply. Arusha town utilises a dozen different drilled wells for its water supply. In addition, numerous small wells are utilised on the lower slopes and on the dry lowland plains for domestic water supply. In numbers, these small wells are many, but in terms of the amount of water, they are limited. However, if the water demand for domestic supply is limited, the supply requires a stable and high quality supply throughout the year.

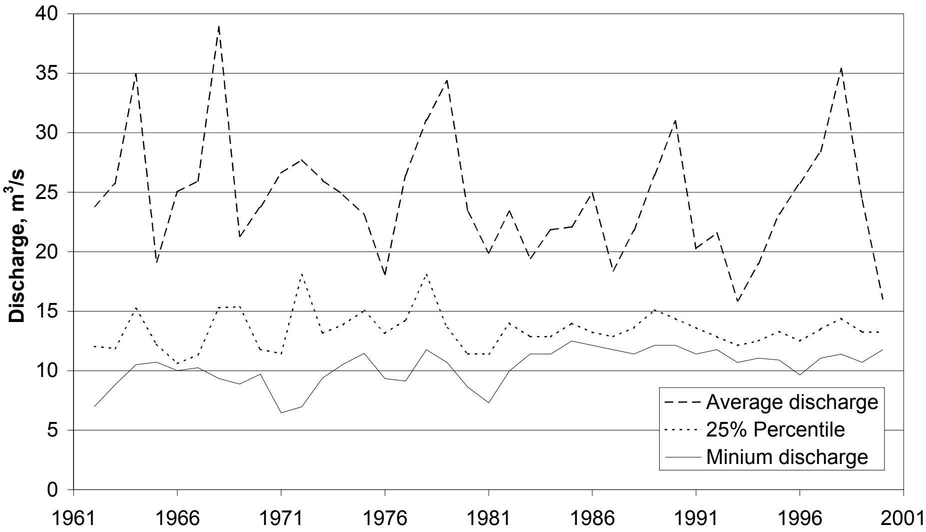

Figure 4.5: Plot of average discharge, minimum discharge and 25% percentile of the discharge at the gauging station 1DD1 for the period 1961 to 2000

For the southern slopes of Mt Kilimanjaro, the majority of the spring yield is found in three limited areas, Kambi ya Chockaa, Chemka and Mwaleni Spring. (The United Republic of Tanzania, 1977b). The two first springs, for which the name Rundugai Springs is also used, drains to Kikuletwa River, while the third drains to the Ruvu River. The United Republic of Tanzania (1977b) estimate that the discharge from the two first springs is about 10 m^3/s. Perzyna (1994b) estimates the runoff from the Rundugai Springs area as about 11 m^3/s.

4.3.2 Water Consumption

The water users in the upper Pangani River Basin are many and have different preferences. The domestic users require a constant, but rather small amount of high quality water. The agricultural industry has a more seasonal demand with high peaks during the growing season. The power producer, Tanzania Electricity Company, can partly transfer water from one season to another by means of reservoirs, but mainly it requires a constant flow for securing power supply. The conflicting interests particularly between agriculture and hydropower generation are also important. Irrigated agriculture consumes the water, while hydropower plants use water. When the former is located upstream, conflicts with the users below over the scarce water resources are inevitable.

Given changes in land use and their impacts on the downstream hydrological regime, water consumption in the agricultural areas is important. All abstractions of water in the area, surface or groundwater, must be based on a so-called Water Right, a legal right for abstracting water. The Pangani Basin Water Office, PBWO, issues the Water Right and keeps registers of all Water Rights and abstractions. A Water Right is given for a particular amount of water to be withdrawn from the river, e.g. 20 l/s or 1.5 m^3/s. The PBWO was formally established in 1991 (Luhumbika , 1999). The introduction and implementation of the Water Right system for a resource, which in the past has been inherited and considered as free, has been a difficult process. Thorough mapping of the river basin by PBWO has exposed a great number of illegal abstractions of water (Luhumbika, 1999), but these probably represent smaller off-takes. It is assumed that the major users have been mapped and been subjected to the Water Right legislation first. In addition to the amount of water, the purpose and the size of farming area is recorded if relevant or available.

The register of Water Rights and abstractions at the PBWO can be used for estimation of the water use in the area. The register gives figures for the maximum allowed off-take of water, but does not say anything about the actual off-takes that take place. Assuming that the stakeholders follow the regulation, the register gives an upper limit for the abstraction, but the Water Rights given for irrigation purposes are probably not utilised fully throughout the year. Additional data are therefore necessary for estimation of the water use for irrigation purposes.

The extent of irrigated areas and irrigation efficiency are estimated in several studies. The Water Master Plan for the Kilimanjaro Region by The United Republic of Tanzania (1977c) estimates that about 18 percent of the agricultural area is irrigated. A later study by IVO International Ltd & Norplan AS (1995) estimates that 25 percent of the agricultural area is under irrigation while an irrigation percentage of 35 is reported for certain parts of the area by The United Republic of Tanzania (1994).

The records at the PBWO have been examined by Lefstad & Bjørkenes (1997) who consider the catchment above discharge station 1DD1. Their findings are summarized in Table 4.2. The irrigated areas were partly given in the records at the PBWO. Missing areas were estimated on the basis of water rights granted or observed off-take. The off-takes in the table above represent the observed off-take at the time of inspection by the PBWO. The actual off-take can vary due to seasonal variations and failure to observe the conditions of the Water Right granted. A search performed by Nippon Koei CO. Ltd & Pasco International Inc. (1998) found that 154 Water Rights had been granted in the catchment above 1DD1 with a total granted off-take of 6.9 m^3/s. However it should be noted that this number represents granted rights, while Lefstad & Bjørkenes (1997) include all off-takes registered by the PBWO, whether legal or not legal.

Crop	**Irrigated area km^2**	**Offtake m^3/s**
Banana	23.5	1.9
Coffee	42.3	3.5
Beans	16.4	1.3
Maize	71.5	5.6
Sugar cane	62.0	5.8
Sum	215.7	18.0

Table 4.2: Irrigated areas and off takes upstream gauging station 1DD1. Modified from Lefstad & Bjørkenes (1997).

A survey by Hunting Technical Services (1996) reveals that about 1010 km^2 of the area upstream station 1DD1 have a land cover suitable for, or capable of being combined with agriculture or related activities. The estimated percentages of irrigated agriculture will then give an irrigated area varying from 182 to 252 km^2. It should be noted that the first estimate is from the 1970s, while the last is from the 1990s. However, the figures support the findings in Table 4.2.

The actual off-take of water over the season must be described on the basis of the water demand for the various crops A method for calculating crop water demand is given in Allen et al. (1998). Based on the areas and crop types found by Lefstad & Bjørkenes (1997) and the cropping pattern for the area described by The United Republic of Tanzania (1994), the actual water demand for the different types of crop can be evaluated based on meteorological data from the area. Meteorological data from station 9337004 and 9337021 were used. The area for cultivation is taken into consideration when calculating the water demand for the different crops. For example coffee is assumed to be cultivated in the higher hill areas and sugarcane is assumed to be cultivated in the lower part of the area. The result from this calculation can be seen in Table 4.3.

The calculated off-take of water is considerably higher than the amount of water granted under the Water Rights for the area, according to Nippon Koei CO. Ltd & Pasco International Inc. (1998). However, it is less than that found by the survey of Lefstad & Bjørkenes (1997). It should be noted that the off-take calculated in Table 4.3 assumes the discharge distributed over the year. The actual off-take will take place only over a part of the year. The off-take may therefore be higher for a period, though the average value for the year should be the same. The calculations in Table 4.3 are also supported by Lugomela et al. (2001) who evaluate the impact of irrigation on water resources in the Pangani River Basin and find an irrigation demand of 11.6 m^3/s for the catchment above gauging station 1DD1.

Crop	Area km^2	Water Demand mm	Offtake m^3/s
Banana	23.5	1281	0.95
Coffee	42.3	991	1.33
Beans	16.4	1214	0.63
Maize	71.5	1926	4.37
Sugar cane	62.0	2062	4.05
Sum			11.3

Table 4.3: Calculated off-take of water for the agricultural area upstream gauging station 1DD1.

In the evaluation of the water demand, domestic water supply has not been considered as a major user. It is an important and favoured user, but the consumption is relatively small compared to the amount consumed by irrigation.

5. STREAM GAUGING

5.1 Three research basins on the slopes

This chapter deals with the results from the stream gauging of the three small catchments on the slopes of Mt Kilimanjaro as described briefly in chapter 4. Table 4.1 give the key data for the three gauging stations. Figure 5.1 shows the location of the three catchments and illustrates the land cover distribution according to Hunting Technical Services (1996). With reference to the description by Martin (2000) cited in chapter 4, there are some deviations. This is particularly the case when considering the extent of the dense bush land at the higher elevations. Inspection in the field indicates that the description by Martin (2000) is more correct as to the extension of the bush land towards the upper limit, while the extension of the forest, particularly towards the lower limit seems to be more in accordance with the description of Hunting Technical Services (1996). However, the description by Martin (2000) is more generally applicable for the whole southern slopes of Mt Kilimanjaro.

For many years a varying number of river gauging stations have been operational in the upper part of the Pangani River Basin. According to Sarmett (1999) 34 stations were operational in the 1950s. The length of the observations varies from a few years in the 1950s and 1960s and up to today but the number of stations in operation now is very limited, though rehabilitation of several stations is under way. Most of the operational stations are located on the lowland plains below the mountain slopes of Mt Kilimanajro and Mt Meru. Very few stations are located on the mountain slopes. A survey performed by Sivertsgaard & Skau (1996) and complemented by Lefstad & Bjørkenes (1997) with the files at the local water authorities, shows that most previous and present stations are located on the lowland area between 700 and 900 masl. Only one station is located up at the forest boundary at 1400 masl but this station has not been operational since the 1970s.

The knowledge on available water resources for the protected and untouched upper slopes area is therefore limited. A gauging station on the border between the heavily exploited and densely populated agricultural area below approximately 1500-1600 masl and the protected and unpopulated forest above, would give new and valuable information about the available water resources. Figure 5.2 shows the hypsographic curves for the three catchments, Charongo, Ngomberi and Ghona. The Charongo catchment forms a sub-catchment within the Ngomberi catchment. Automatic loggers register hourly the water level in addition to manual readings twice a day.

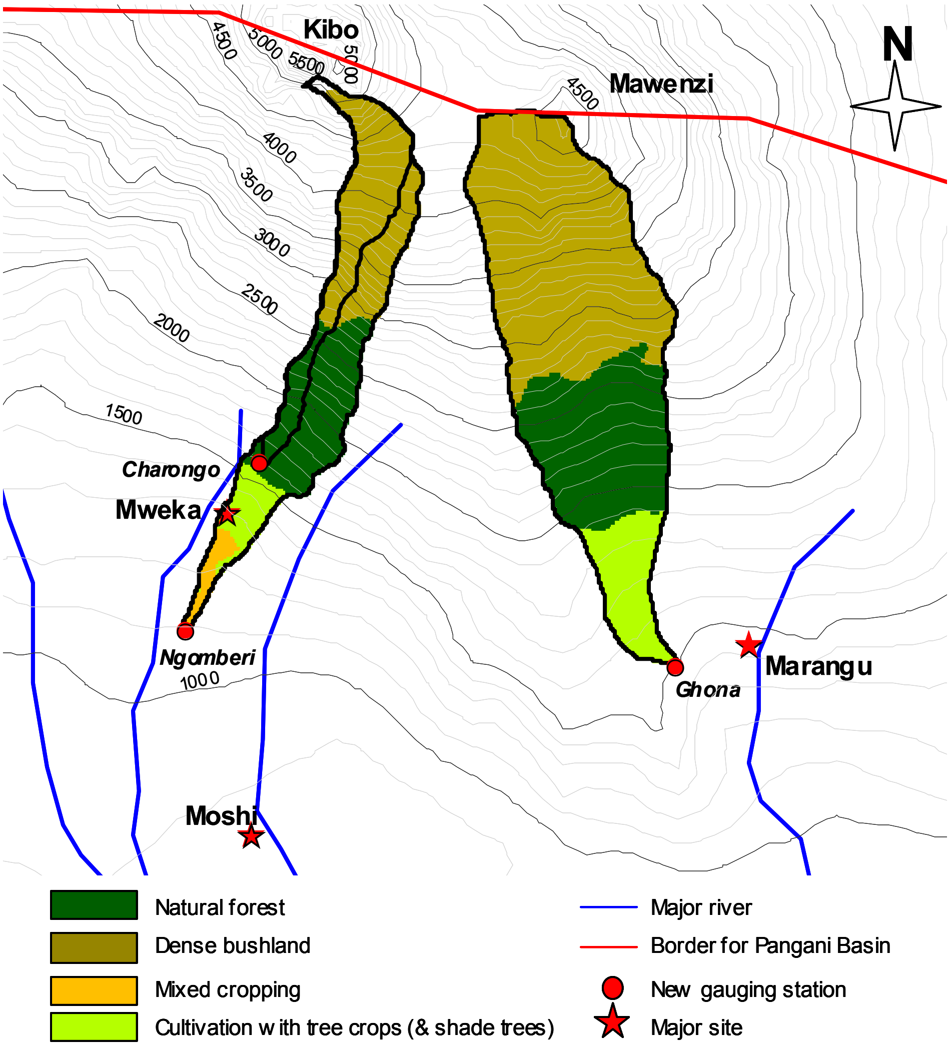

Figure 5.1: Location of the Charongo, Ngomberi and Ghona catchments in the southern hillside of Mt Kilimanjaro and their land cover.

The Charongo drainage basin reaches from the Uhuru peak in the north southwards to Kifura at Mweka. The upper part of the basin is formed by parts of the southern side of the snow-covered summit of Mt Kilimanjaro and a highland desert with poor vegetation. The area above 3000 masl forms the Kilimanjaro National Park. Between approximately the 1550 and 3000 masl a forest reserve limits activities in the area. No agricultural activities, collection of firewood, cattle feed or logging, are allowed in the forest reserve. The lower part of the drainage basin from 1600 masl consists of natural forest up to about 2750 masl where the transition to dense bush land starts and forms the vegetation. The dense bush land changes gradually to no vegetation at all at about 4000 masl from where alpine desert and onwards glaciers prevail. The Ngomberi basin, in which Charongo is located, starts at about 1100 masl. Mixed cropping and cultivation of grain, vegetables and fruit to about 1250 masl dominate the lower part. From about 1250 masl to about 1550 masl the area is dominated by the cultivation of tree crops, i.e. coffee and various fruits are also common here. In this area, shade trees for the coffee crop preventing evaporation are common. From about 1550 masl the natural forest starts and above this upward land cover is similar to the Charongo catchment and is partly formed by this.

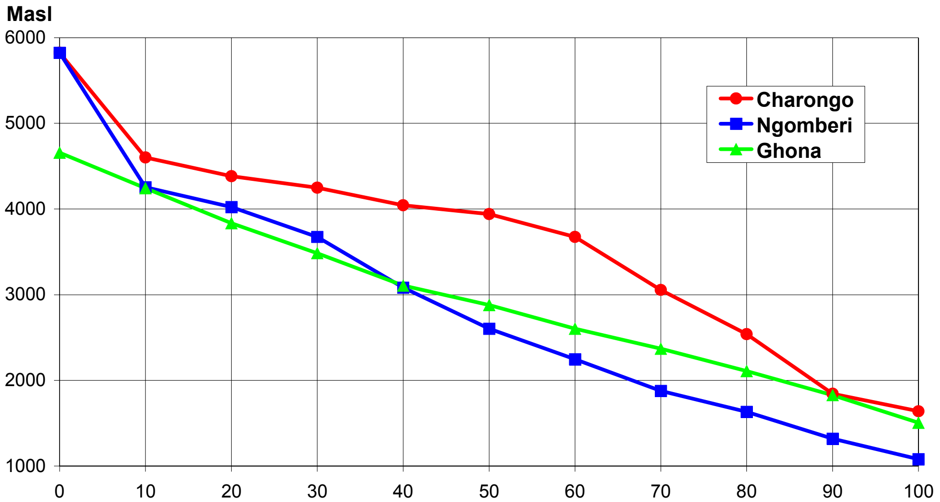

Figure 5.2: Hypsographic curves for the Charongo, Ngomberi and Ghona catchment.

The Ghona drainage basin reaches from the peak of Mwenzi southwards to Marangu West. The upper part consists of the rugged rocks of Mwenzi and its many ridges and ravines. The lower part of the basin from 1500 to about 1850 masl is dominated by cultivation of tree crops, also here with shade trees. Maize is also grown. From 1850 to about 2700 masl the natural forest is dominant. Dense bush land forms the upper parts of the vegetated zone from about 2700 to 4000 masl where a gradual transition to no vegetation takes place. Mawenzi does not have any permanent snow cover, though random seasonal cover can occur.

5.2 Results from the stream gauging

5.2.1 Discharge at the gauging stations

The daily discharge at the three stations is shown in Figure 5.3, Figure 5.4 and Figure 5.5. They show the discharge from installation up to September 2001 for Charongo and Ngomberi and up to May 2001 for Ghona. On the graphs, a minor number of manual readings have been used to fill in missing values from the logger. In addition, some results from the measurements are given in Table 5.1. Tabularised data from daily discharges from each of the three gauging stations can be found in the appendix.

Station	Minimum m^3/s	Maximum m^3/s	Specific runoff $l/s*km^2$
Charongo	0.012	0.485	3.8
Ngomberi	0.000	3.575	4.9
Ghona	0.128	9.959	7.2

Table 5.1: Some results from the gauging period at Charongo, Ngomberi and Ghona.

Charongo River

The station has an increasing discharge from approximately mid March until mid July with frequent fluctuations from day to day. The discharge follows a relatively smooth recession curve from mid July until mid March with some small peaks in November-December. In all three seasons, the minimum discharges occur in February-March. The observed runoff is considerably smaller in the second season than in the first and third. This is due to low rainfall in the region, only about 1/3 of the amount compared to the previous year. The two peaks found in mid January 2001 and early August 2001 are due to sudden precipitation events, that is in August 2001 a 26 mm event is observed at station 9337021 after a period with little precipitation. These peaks can also be found in the observations from the Ngomberi catchment, but not in the Ghona catchment.

Ngomberi River

This station, which is located further down in the same river system as the station at Charongo, is characterised by long periods of no discharge for all three seasons.

During the period of discharge, the station has much of the same characteristics as Charongo, but the increase in discharge starts somewhat later. The recession curve is also steeper. In the second season of measurements, the lack of rain in the area causes very low runoff at the gauging station with only a small fraction of the

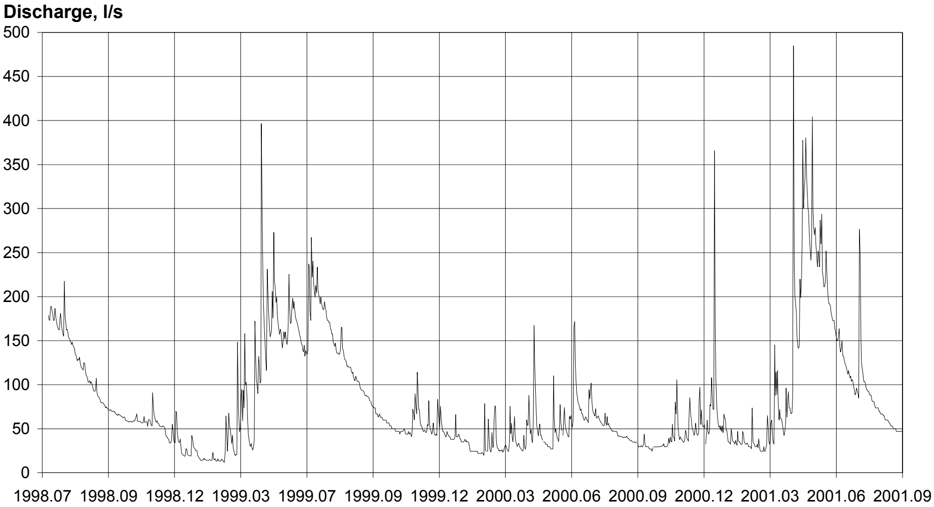

Figure 5.3: Observed daily discharge at Charongo.

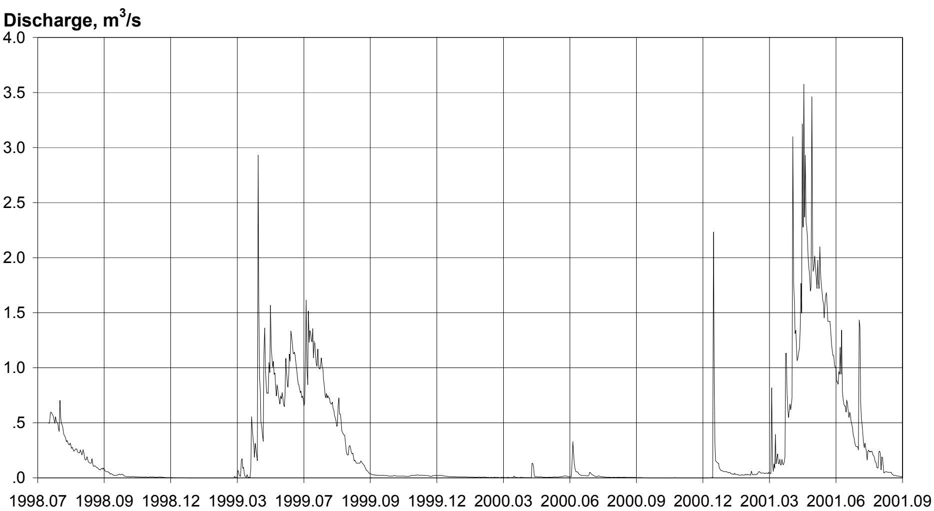

Figure 5.4: Observed daily discharge at Ngomberi.

previous year's runoff volume. Compared to the all-year-discharge at Charongo, the discontinuous discharge at Ngomberi seems to be a limiting factor for extended water consumption further downstream.

Ghona

The recession curve has much of the same characteristics as the two other stations. It continues until end of March 1999, when a sharp rise in the discharge takes place. Frequent fluctuations occur until mid June from when the relatively smooth recession curve continues until end of April. In the 2000 season, there is only a fraction of the previous season's runoff and no clear peak discharge as the previous year. Unfortunately, the third season was interrupted in the end of May 2001.

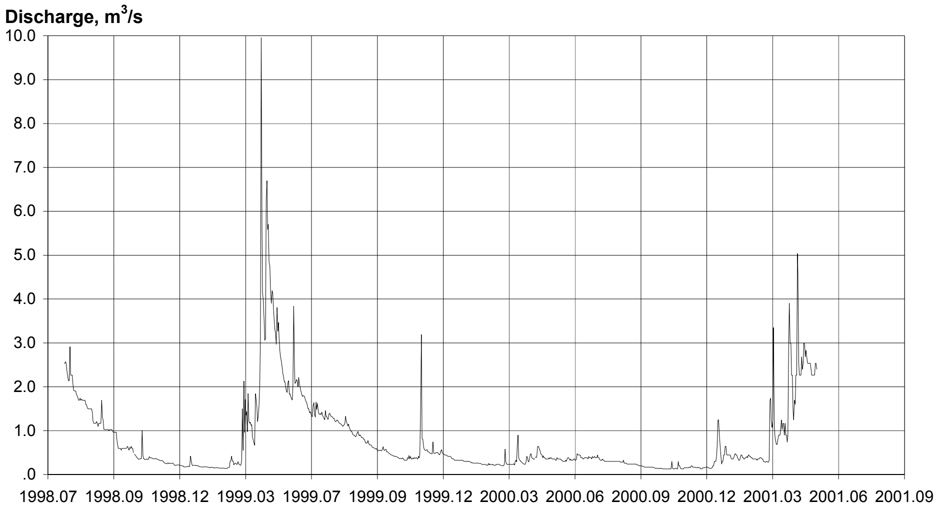

Figure 5.5: Observed daily discharge at Ghona.

5.2.2 Differences in discharge - Charongo vs. Ngomberi

The two catchments have somewhat different behaviour during the first part of the long rains. Figure 5.6 shows the discharge at Charongo and Ngomberi and the precipitation at Charongo during the start of the long rains in the 1999 season. More than 150 mm of precipitation was observed during March before any discharge could be registered at all at Ngomberi the 27th March 1999.

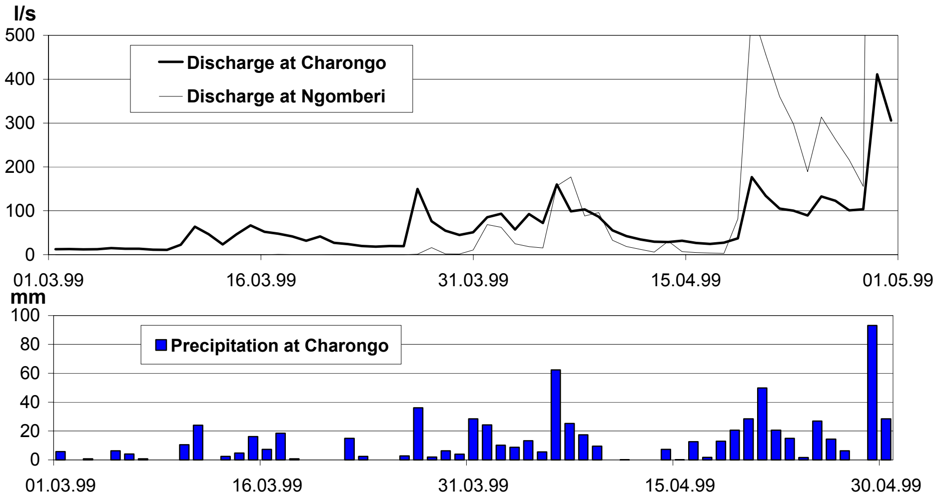

Figure 5.6: Discharge at Charongo and Ngomberi at the start of the long rains in the 1999 season. The precipitation is shown on the lower half of the figure.

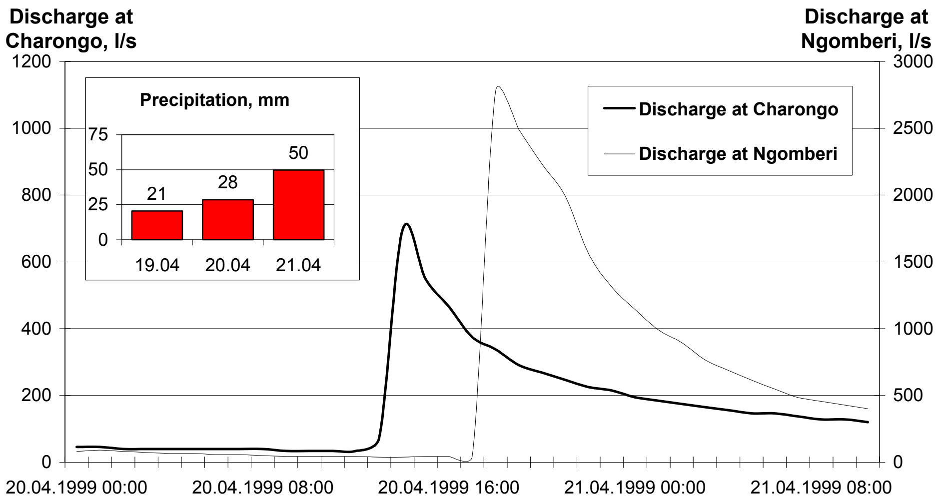

Figure 5.7: Episode with heavy rains and sudden increase in runoff in the Charongo and Ngomberi catchment.

The one-hour resolution of the raw-data makes it possible to observe the flood-peak travelling from the station at Charongo to the station at Ngomberi. Figure 5.7 shows an incident from the 20th - 21st April 1999. The precipitation measurements are done at the gauging station at Charongo. About ¾ of the Ngomberi catchment is located above the rain gauge and ¼ below. The rainfall is indicated in Figure 5.7. During the period 19th -21st April, a total of about 100 mm of precipitation was observed. Previously in March and April, more than 400 mm of precipitation has been observed, so the soil is saturated to some extent. Still the flow at the gauging stations is very low with 34 l/s at Charongo and 44 l/s at Ngomberi. During about one hour, the flood increases by 20 times at Charongo and by 50 times at Ngomberi. The delay between Charongo to Ngomberi is about 4 hours. Other events show the same characteristics of the discharge.

The specific runoff and the differences between the Charongo and Ngomberi catchment can be seen in Figure 5.8. The observed specific runoff seems to be higher for the Charongo catchment during most of the dry season and for the observed short-rain seasons. During and just after the long-rains from about mid April until mid August, the specific runoff is higher at Ngomberi than at Charongo for the first season and the last season.

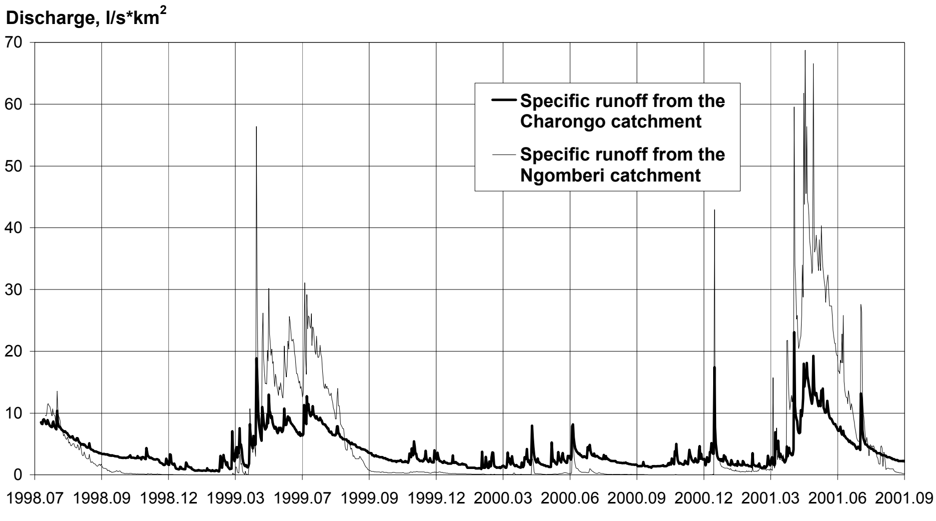

Figure 5.8: Specific runoff for the Ngomberi and Charongo catchment.

Absolute areas	Charongo	Ngomberi	Ghona
"Non-contributing" area above forest, km^2	16.3	22.8	61.9
Forest area, km^2	4.7	21.0	35.9
Agricultural area below forest, km^2	0.0	8.2	11.8
Total, km^2	21.0	52.0	109.6
Contributing area, km^2 (Forest + agricultural)	4.7	29.2	47.7

Relative areas	Charongo	Ngomberi	Ghona
"Non-contributing" area above forest, %	78	44	56
Forest area, %	22	40	33
Agricultural area below forest, %	0	16	11
Total, %	100	100	100

Table 5.2: Simplified land use/cover distribution for the Charongo, Ngomberi and Ghona catchment.

5.3 Discussion of results from the stream gauging

5.3.1 Runoff pattern

During the long rains in the 2000 season, the precipitation at Charongo was about 1/3 compared to the previous year. This can explain the almost total absence of observed runoff at Ngomberi and the reduction at Charongo. This also corresponds with a dry season in the surrounding area with failures in crop cultivation due to lack of rainfall. The major “runoff” season for the drainage basin is from April to August/September. During two different field inspections along the Charongo River, in July 1999 and in June 2000, it was found that the river flow gradually decreased along the Charongo River with increasing elevation. From approximately 2800 masl and above the surface runoff was not significant or non-existent in the Charongo catchment. There were no signs of a “normal” river/stream bed, but a trench, which seemed to have more infrequent discharge patterns, could be observed. Since there was no discharge observed during the inspection just after the long rains, it is most probable that there is no discharge during the other seasons of the year either. This indicates that the contribution to direct river runoff from the upper bush land/alpine desert and melting ice cap is small. Taking account of this area when calculating the relative runoff in Figure 5.8, may lead to drawing the wrong conclusions concerning relative runoff. Table 5.2 shows a simplified overview of the land cover distribution in the three catchments divided into “non-contributing”, forest and agricultural areas. The “non-contributing” area is the area above approximately 2800 masl. An alternative calculation of the specific runoff would be to omit this area in the calculation altogether and only take into account the forest and the agricultural areas.

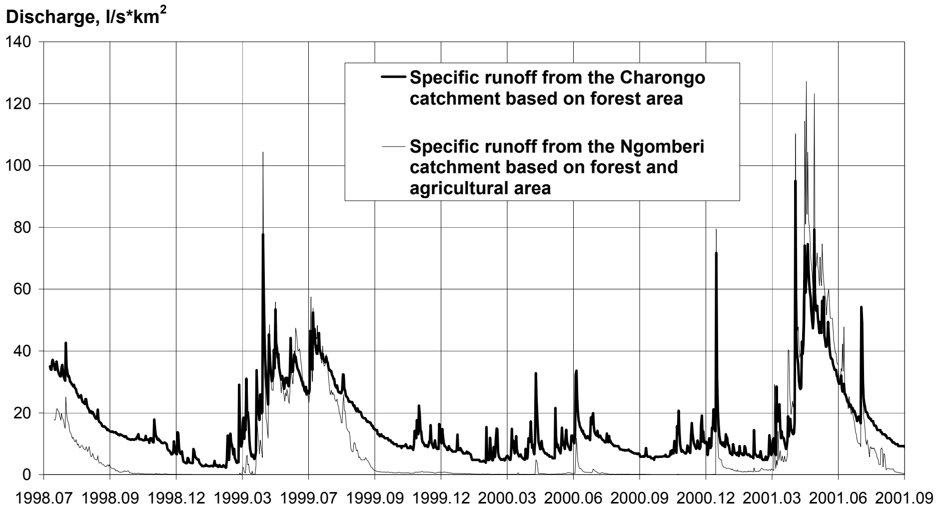

Figure 5.9: Alternative calculation of specific runoff from the Charongo and Ngomberi catchment by use of "contributing" areas only.

The result from such a calculation is shown in Figure 5.9 where only these areas are used in the calculation. Details for the period April to August 1999 are shown in Figure 5.10. The similarities in specific runoff from the two catchments are noticeable compared to the results when applying the whole catchments in the calculations as in Figure 5.8. In absolute size, the “contributing” area in the Ngomberi catchment is about five times the size of the Charongo catchment. The total absence of discharge at the Ngomberi gauge during a number of months every year is probably due to various off-takes between the two gauging stations. The off-take can be due to domestic supply or due to irrigation purposes. It is mainly during the dry season that all the discharge at Ngomberi is utilised.

During the first part of the wet season, most of the rain is absorbed by the soil. Figure 5.6, Figure 5.3 and Figure 5.4 show that a considerable amount of precipitation occurs before the river discharge increases. When the soil is saturated, the need for irrigation is less; the off-take decreases and more water is left in the river. As the wet season ends and the soil dries up, the irrigation requirements increase and with them the off-take of water between the gauging stations. The decreasing discharge and increasing off-take in the recession period will gradually result in a total absence of discharge at the Ngomberi station and a dry river. During the wet season in 2000, there is very little precipitation in the area. This can explain the almost total absence of discharge. The precipitation causes so little discharge that it is all utilised by the off-takes upstream of Ngomberi.

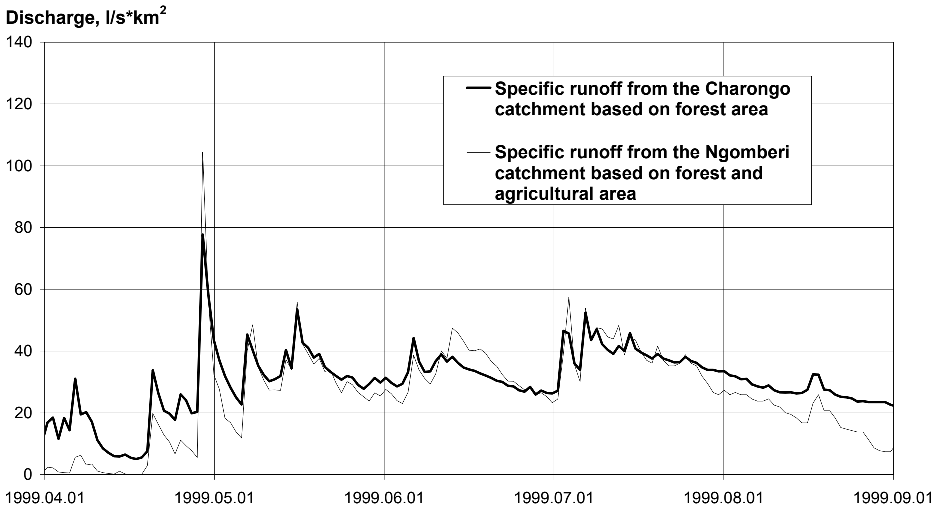

Figure 5.10: Alternative calculation of specific runoff from the Charongo and Ngomberi catchment by use of "contributing" areas only. Details for April-August 1999 are shown.

5.3.2 Water consumption

A simplified calculation of discharge can be set up for the Ngomberi catchment based on the contributing areas in Table 5.2 and the specific runoff from the Charongo drainage basin. It is assumed that the specific runoff from the forest part of the Ngomberi basin is similar to the specific runoff from the forest part of the Charongo basin. The runoff from the agricultural area in the Ngomberi basin is assumed to have the same relative runoff as the forest part of the Charongo basin, but it is corrected for lower precipitation. The calculated river discharge at Ngomberi will then be:

$$Q_{Ng} = q_{Ch} \times \frac{A_{Ng}}{A_{Ch}} + Q_{Offtake} \qquad \textit{(Eq. 5.1)}$$

where Q_{Ng} is the calculated discharge at Ngomberi, q_{Ch} is the observed specific runoff for Charongo catchment on daily basis taking only the forested area into consideration, A_{Ng} and A_{Ch} is the contributing areas found in Table 5.2 for the Ngomberi and Charongo catchment respectively and $Q_{Offtake}$ is the total off-take of water upstream the gauging station. Unfortunately, no continuous measurement of $Q_{offtake}$ exists. A survey performed by the Pangani Basin Water Office, PBWO, in 1995-1996 indicated an off-take of about 375 l/s in the Ngomberi River but this estimate is quite uncertain. However, this value was used for the off-take in the calculation. In addition, it was assumed that the off-take was lower during and immediately after the long rains. The reduction in off-take was assumed 50% for the months of May, June and July. The off-take found by the PBWO and the agricultural areas for the Ngomberi catchment given in Table 5.2, result in an off-take of 35 l/s*km^2 for the agricultural areas. The result from the calculation with the calculated and actually observed discharge at Ngomberi is shown in Figure 5.11 and Figure 5.12.

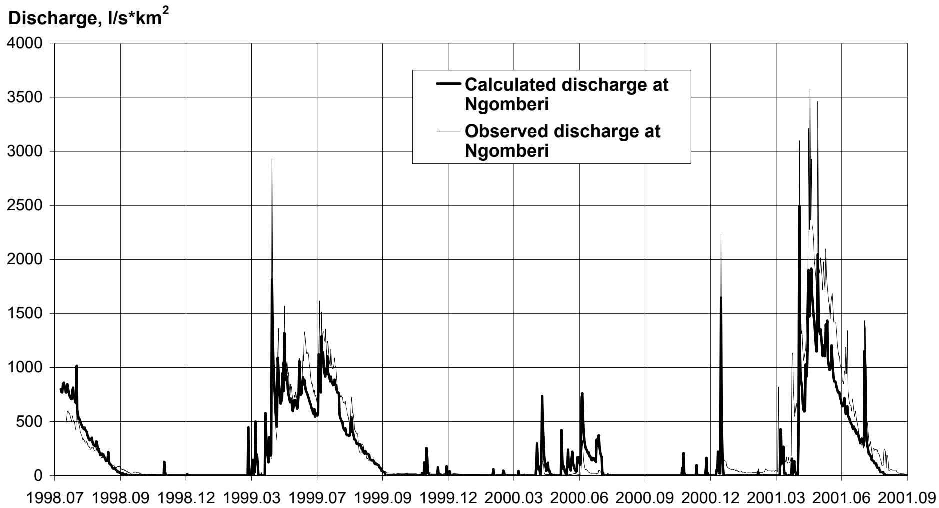

Figure 5.11: Calculated and observed discharge at Ngomberi.

With a theoretical demand of about 35 l/s*km^2 for the agricultural areas according to the observed values from the PBWO, the calculation shows that water demand is greater than the available supply for parts of the year. After some time with drought during the dry season, the demand for water and therefore the off-take of water is at its maximum and often exceeds the actual river discharge. When the rain and the subsequent discharge occur, the off-take from the river will be large. Furthermore, later on in the wet season, the need for water is decreasing, and the off-take is adjusted to a lower level. When the soil starts to dry up, the demand for water increases again, and the off-takes are regulated upwards. The calculated runoff for Ngomberi in Figure 5.11 also has some peaks in the dry period during last half of 1999 and first half of 2000. During the calculations, the runoff from the agricultural area is assumed proportional to the runoff from the forest area. This may not be correct for the dry period, and small adjustments have been made.

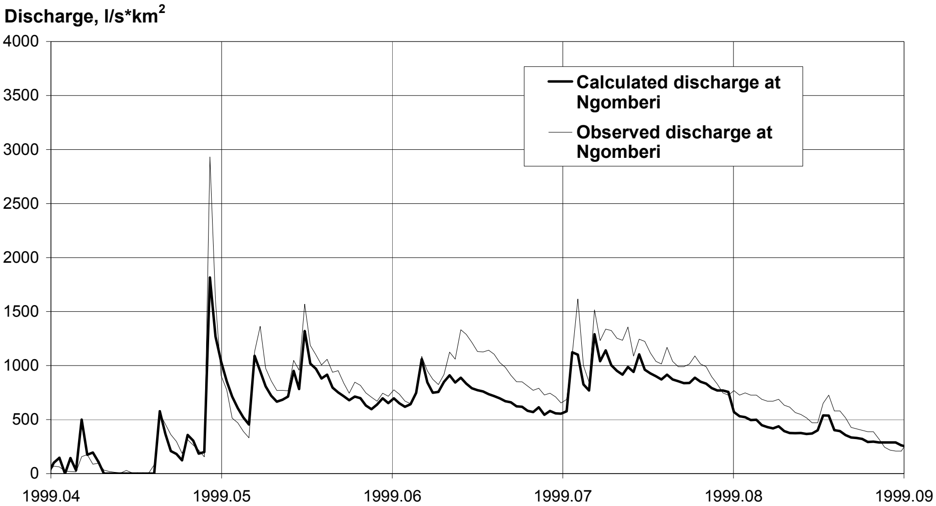

Figure 5.12: Calculated and observed discharge at Ngomberi. Details for April-August 1999 are shown.

5.4 Lessons from the stream gauging

The stream gauging of the three smaller catchments on the southern mountain slopes of Mt Kilimanjaro gave valuable information about the runoff pattern in the area. Field inspections indicated that the there is no contribution to the river discharge from the area above the forest. When applying this information in the calculation of the specific runoff, good correspondence was found between the Charongo and Ngomberi catchment for those parts of the year when the off-take is assumed low.

When applying information about the off-take of water from the PBWO and information about the areas contributing to runoff shown in Table 5.2, the river discharge at Ngomberi can be calculated by use of the observed river discharge at Charongo. For a further understanding of the processes taking place in the catchment, analyses that are more detailed are required. They will be dealt with in chapters 7 and 8.

6. PRECIPITATION DISTRIBUTION

6.1 Introduction to rainfall distribution

This chapter deals with precipitation and its distribution on the slopes south of Mt Kilimanjaro. Precipitation observations from a number of stations, including the results from the 9 new temporary stations on the upper slopes will be evaluated and the distribution of precipitation by elevation will be investigated. A study of the hydrology of the southern slopes of Mt Kilimanjaro requires a detailed knowledge of the distribution of precipitation from the lowland plain at 700 masl to the summit of the mountain at about 6000 masl.

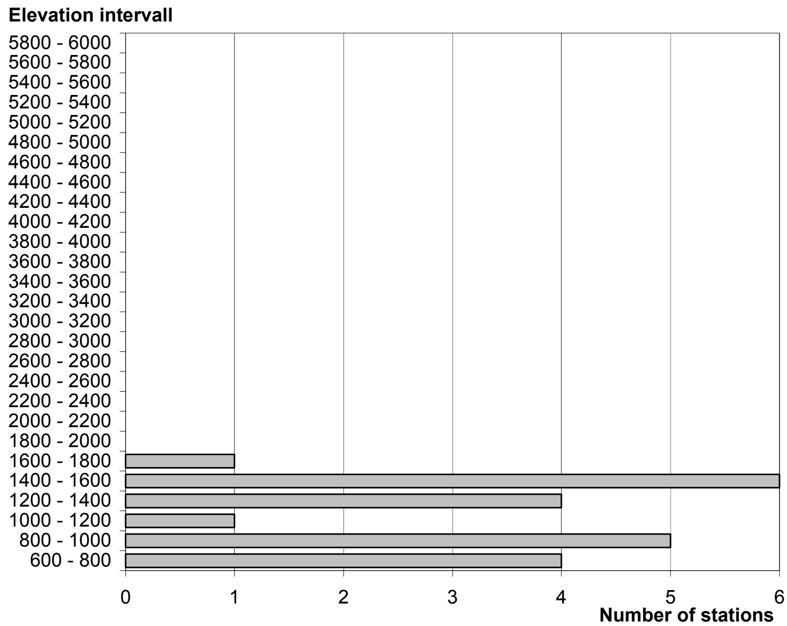

Figure 6.1: Location of present precipitation stations with respect to elevation for the southern slopes of Mt Kilimanjaro.

For the slopes south of Mt Kilimanjaro, precipitation observations can be found back to the early 1920s for a small number of stations. Observation records have been obtained for 21 precipitation stations and many of them are still operational. The series have lengths of 13 to 79 years with varying degrees of missing data. The majority of today's meteorological observations are made below 1500masl. Figure 6.1 illustrates the location of the available stations with respect to elevation. As can be seen, all the stations are located below the forest, and within the populated area. No observations are made on the mid or upper slopes. Extrapolation of results from hydrological analyses of data from the lowland plains to the upper slopes of Mt Kilimanjaro can easily lead to erroneous conclusions.

Griffiths (1972) describe the plains south of Mt Kilimanjaro as being on the border of that area in East-Africa, which has a pronounced bimodal rainfall pattern; the short rains lasting from late October until December and the long rains lasting from March until May. Very little rain occurs in the period between June and September.

Klute (1920) undertook some of the first scientific investigations of the climate around Mt Kilimanjaro. Several precipitation stations were established, but the length of the observations varies considerably, from one season to a few years. Based on these observations, Klute (1920) established the first (?) isohyetal map describing the precipitation distribution around Mt Kilimanjaro.

Teale & Gillman (1935) give a description of the climate and discuss the water problems in the region. They point out that the rapid decrease of precipitation towards the upper reaches of the mountain, which has been investigated by Klute (1920), is supported by indirect observations of morphological and vegetation features observed in the higher parts of Mt Kilimanjaro. Analysis by The United Republic of Tanzania (1977c) indicates that the highest precipitation in the area can be found in the slopes of Mt Kilimanjaro with annual values above 2000mm in smaller parts of the area. Though no stations are present in the upper part of the hillside, detailed precipitation distribution maps are presented in e.g. The United Republic of Tanzania (1977c) and Perzyna (1994a). The United Republic of Tanzania (1977c) develops an isohyetal map for rainfall distribution based on 18 precipitation stations on the lower slopes of Mt Kilimanjaro below 1600masl. No analysis of any trends or documentation of the continuity of each individual station is provided.

6.2 Data availability

Precipitation data for 21 stations was available from various sources for use in the analysis. Digitised readings have been obtained from the University of Dar es Salaam and manual readings have been received from the local Maji Office (Water Authorities office) in Moshi. Nine of the 21 stations have been operational for more than 50 years. Four of the nine stations have between 7 and 28 percent missing values and/or stopped operating 6-10 years ago. They have been discarded from further analysis. The remaining five stations have an observation period of 62 to 79 years and less than 3 percent missing values and were used for further analysis. The other twelve of the 21 stations have been operational for about 20 to 46 years. Six of these stations have more than 12 percent missing values and they were discarded from further analysis. One station lacking 11 percent of the values has partly been used for the analysis. One station had not been operational for 14 years and was discarded from further analysis. The remaining four stations have less than 10 percent missing values. Additionally, two newer stations from the regular observation network have been used for verification purposes.

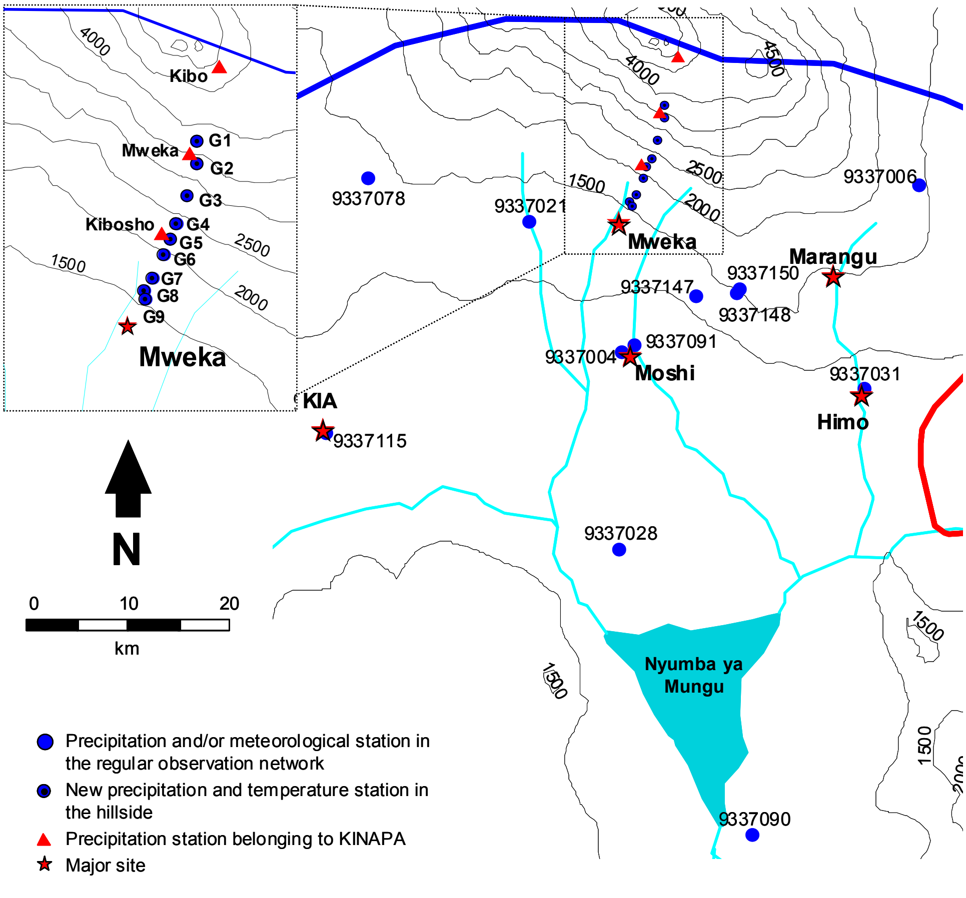

Figure 6.2: Map showing the location of the stations which were used in the analysis of preciptiation distribution. Major sites are also shown.

Station	South, dd	East, dd	Altitude, masl	Start year	End year	Observation period, years	Years of observations, years	Missing data, %
9337004	-3.35	37.33	813	1922	2000	79	79	0.0
9337006	-3.20	37.60	1433	1931	1997	67	65	3.0
9337021	-3.23	37.25	1250	1935	2000	66	66	0.0
9337028	-3.53	37.33	701	1938	2000	63	62	1.6
9337031	-3.38	37.55	960	1938	1999	62	62	0.0
9337078	-3.19	37.10	1249	1954	1999	46	41	10.9
9337090	-3.78	37.45	690	1962	1996	35	35	0.0
9337091	-3.34	37.34	840	1960	2000	40	36	10.0
9337115	-3.42	37.07	891	1972	2000	29	27	6.9
9337147	-3.30	37.40	1050	1980	1999	20	20	0.0
9337148	-3.30	37.44	1470	1975	1999	25	19	24.0
9337150	-3.29	37.44	1590	1987	1999	13	11	15.4

Table 6.1: Details of stations from the regular observation network used for the analysis. In the upper half, 5 stations with relatively long series. In the middle, 5 stations with shorter series, and in the bottom 2 more recently established stations used for verification.

Station	South, dd	East, dd	Elevation, masl	Start month/year	End month/year	
G1	-3.26	37.43	3909	10/1999	09/2001	Stations established during the project
G2	-3.30	37.43	3512	10/1999	09/2001	
G3	-3.39	37.43	2993	10/1999	09/2001	
G4	-3.28	37.38	2626	10/1999	09/2001	
G5	-3.22	37.45	2367	10/1999	09/2001	
G6	-3.22	37.37	2153	10/1999	09/2001	
G7	-3.33	37.45	1863	10/1999	09/2001	
G8	-3.47	37.45	1710	10/1999	09/2001	
G9	-3.28	37.46	1588	10/1999	09/2001	
Kibo	-3.08	37.38	4571	01/1999	01/2000	Stations from KINAPA
Mweka	-3.13	37.37	3505	01/1999	01/2000	
Kibosho	-3.18	37.35	2438	01/1999	01/2000	

Table 6.2: Details of 9 new stations established and 3 stations from Kilimanjaro National Parks authorities, KINAPA.

The 10 stations used in the analysis are located between 690 and 1433masl and are valuable for analysis of the hydrology between these elevations. As far as analysis of the situation in the areas above goes, these are some of the wettest areas in the

Pangani River Basin, so that use of only 10 stations on the lower slopes below 1433masl and on the plain will not be sufficient. A precipitation gradient developed on the lowland plain south of Mt Kilimanjaro will not be relevant for use on the upper slopes towards the summit, above 1500 masl.

Due to the lack of a regular observation network above 1433masl and the importance this area has concerning the availability of water resources, measurements up to the 4000masl were organized for a limited period. In addition, a number of synoptic observations obtained from the Kilimanjaro National Parks, KINAPA, authorities have been used for verification of the findings. All stations used in the analysis are shown in Figure 6.2. Details are given in Table 6.1 and Table 6.2 for the 10 stations used for the statistical analysis, the 9 new stations, the 3 KINAPA stations and the 2 stations used in the verification.

6.3 Homogeneity of precipitation series

6.3.1 Methods for homogeneity testing

Various tests can be applied for checking the quality of precipitation series. The Norwegian Meteorological Institute apply the Alexandersons test on a routine basis together with double mass analysis for checking the homogeneity of precipitation series (Olaussen & Roald, 1996).

Alexandersons test assumes a constant proportionality between the station being checked and the station it is being compared with. The time series to be compared, P_A and P_B, form a new series of ratios between the two. The new series is normalized by use of mean value and standard deviation (Alexandersson, 1986).

$$p_i = \frac{P_{Ai}}{P_{Bi}} \qquad \textbf{(Eq. 6.1)}$$

$$Z_i = \frac{p_i - \bar{p}}{std_p} \qquad \textbf{(Eq. 6.2)}$$

where p_i is the ratio between P_A and P_B, P_{Ai} and P_{Bi} is the observed precipitation at station A or B in year i, Z_i is the normalized value of the ratio for year i, $\bar{p}$ is the average ratio and std_p is the standard deviation for the ratio p_i. Z_i is tested against the two hypotheses:

H_0:	The time series is homogeneous (Null hypothesis)
H_1:	The series is inhomogeneous; break in year m. (Alternative hypothesis)

A test parameter for each of the n years in the observation series is:

$$T(m) = m \times \bar{z}_1^2 + (n - m) \times \bar{z}_2^2 \qquad \textbf{\textit{(Eq. 6.3)}}$$

where $T(m)$ is the test parameter for the year m, $\bar{z}_1^2$ is the mean value from year 1 to year m and $\bar{z}_2^2$ is the mean value from year m+1 to year n. The standard deviation is supposed to be 1 both before and after year m. A high value of T, indicates that the normalised values before and after year m fluctuate significantly from zero and the null hypothesis may be rejected. The highest value for the test parameter is:

$$T_x = \max < T(m), m = \left[1,2,.....,n\right\rangle \qquad \textbf{\textit{(Eq. 6.4)}}$$

The probability for T_x to achieve a certain value provided that the null hypothesis is correct depends only on the length of the time series (Førland et al., 1991). Marginal values for level of significance can be calculated as a function of the length of the observation series. Values for 90 and 95 percent confidence intervals are shown in for example Olaussen & Roald (1996). If a time series is found inhomogeneous, the probability is highest for a break in the year when T equals T_x.

Trends and fluctuations in climatic records can be difficult to trace in standard time series plots. Garbrecht & Fernandez (1994) describe an improved approach for visualization of trends in climatic records based on rescaled adjusted partial sums. A time series of precipitation observations is represented by $Y = \{Y_t; t = 1,...,n\}$ for which the expected value μ_p and variance σ^2 usually is unknown. The value Y is assumed to be normally distributed. The rescaled adjusted partial sum is defined:

$$X_k = \sum_{t=1}^{k} \frac{Y_t - \bar{Y}}{s_y}; k = 1,...,n \qquad \textbf{\textit{(Eq. 6.5)}}$$

where $\bar{Y}$ is the sample mean, s_y^2 is the sample variance, n is the number of values in the series and t is the counter. See Buishand (1982) for details. A test for a change in level based on the adjusted partial sums is:

$$Q = \max_{0 \le k \le n} |X_k| \qquad \textbf{\textit{(Eq. 6.6)}}$$

A high value of Q might be an indication for a change in level. Critical values for the test-statistic as a function of the number of observed values are given in Buishand (1982). Buishand (1982) and Buishand (1984) describe the use of Bayesian procedures for detection of change in the mean. With σ^2 unknown for the distribution, it is replaced with the sample variance in the test static, which give:

$$U = \frac{1}{n(n+1)} \sum_{k=1}^{n-1} X_k^2 \qquad \textbf{\textit{(Eq. 6.7)}}$$

Critical values for the test static can be found in e.g. Buishand (1982). This test gives the same weight for all X_k independent of location in the sample sequence. For emphasizing shifts near the ends of a series of observed values, Worsley's likelihood test based on weighted rescaled adjusted partial sums can be used (Buishand, 1982 and Worsley, 1979). The weighted rescaled adjusted sum is given by:

$$Z_k = \frac{X_k}{\sqrt{k \times (n-k)}}, k = 1, \ldots, n-1 \qquad \textbf{\textit{(Eq. 6.8)}}$$

In the formula, the greatest weight is given for the values at each end of the series and less weight is given for the values in the middle of the series. The test value W is given by:

$$W = \frac{\sqrt{(n-2)} \times V}{\sqrt{(1-V^2)}} \qquad \textbf{\textit{(Eq. 6.9)}}$$

$$V = \max_{1 \le k \le n-1} |Z_k| \qquad \textbf{\textit{(Eq. 6.10)}}$$

Critical test values for W can be found in Worsley (1979).

The double mass analysis (e.g. ASCE, 1996) is based on regional correlation over long time periods, no inconsistency of the stations being compared and that annual precipitation values are utilized in the analysis. The accumulated sums are plotted against each other or against a composite of regional series. A break in the curve can indicate non-homogeneity. If a break occurs around the same time in the compared time series, it can be difficult to trace.

6.3.2 Results from homogeneity testing

The tests with rescaled adjusted partial sums; Bayesian procedures and Worsley's likelihood test are performed on individual series with a significance level of 0,95. The double mass analysis and Alexsandersons test are performed on combination of series. Table 6.3 shows the results from the analysis.

Station number	Calculated test values				Conclusion based on test values			
	$Q/\sqrt{n}$	U	W	T_{max}	$Q/\sqrt{n}$	U	W	T_{max}
9337004	0.650	0.064	0.352	5.335	ok	ok	ok	ok
9337006	1.369	0.419	1.302	16.455	Nonhom	ok	ok	Nonhom
9337021	1.204	0.435	1.792	2.632	ok	ok	ok	ok
9337028	0.876	0.266	1.215	14.066	ok	ok	ok	Nonhom
9337031	1.135	0.327	0.692	5.559	ok	ok	ok	ok
9337078	1.726	0.969	2.003	16.303	Nonhom	Nonhom	ok	Nonhom
9337090	0.706	0.127	0.579	1.211	ok	ok	ok	ok
9337091	0.506	0.036	0.429	3.610	ok	ok	ok	ok
9337115	0.541	0.076	0.501	2.544	ok	ok	ok	ok
9337147	0.644	0.098	0.497	3.674	ok	ok	ok	ok

$Q/\sqrt{n}$ = test value adjusted partial sums. W = test value Worsley's likelihood test
U = test value Bayesian procedures T_{max} = test value Alexandersson's test
ok/Nonhom = Series is homogeneous/Non-homogeneous according to test value

Table 6.3: Results from homogeneity tests of precipitation series. The left half shows the calculated test values. The right half shows the conclusions drawn from the test values.

The results for the five stations with long observation series, shown in the upper half of Table 6.3, indicate that the series from station 9337006 on the southeast side of Mt Kilimanjaro and station 9337028 on the plains below Moshi are non-homogeneous. For the three series found to be homogeneous, double mass analysis was performed for a common, continuous observation period of 62 years from 1938 to 1999. Figure 6.3 shows the double mass curves for each of the three series against a weighted combination of the two others. The series from 9337004 and 9337021 shows moderate changes in gradient, while 9337031 shows some changes, which can be traced to the 1970's. Inspection of the time series shows that the lowest, the fourth and fifth lowest annual precipitation values for the observation period can be found in this decade which may explain the changes. The three series are weighted according to average annual precipitation value and used for forming a reference series. The three individual series and the weighted reference series is shown in the appendix. Double mass curves with the reference series and the other long series, 9337006 and 9337028, show several changes in gradient, and support the conclusion as to non-homogeneity.

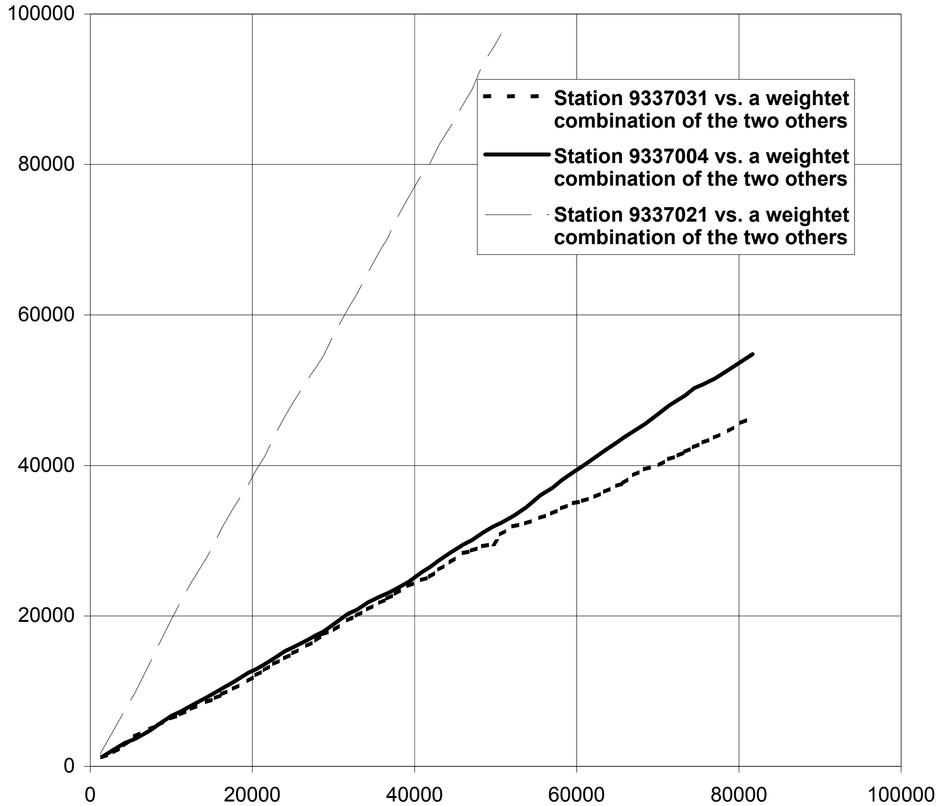

Figure 6.3: Double mass curves for the reference series. The three series are plotted against a combination of the two others.

For station 9337028, the changes can be traced to the mid 1960s. This coincided with the establishment of the Nyumba ya Mungu reservoir. The precipitation station is located about 9 km north of the reservoir (Figure 6.2), which has a surface area of about 160 km^2. The establishment of the reservoir may have caused changes in the local climate. The average annual precipitation for the period 1938 to 1966 is 401 mm while for the period 1967 to 2000 the average annual precipitation is 557 mm, which is a 39 percent increase. On the arid plains, the increased water surface nearby has increased the total evaporation in the area, which may have resulted in increased precipitation.

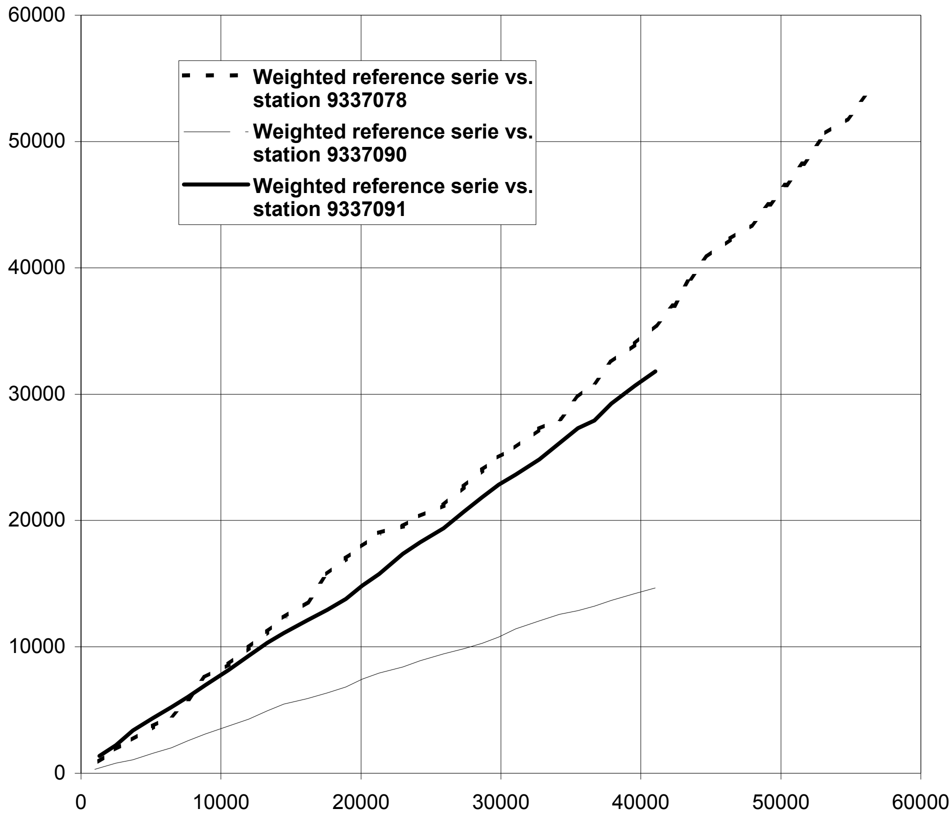

Figure 6.4: Double mass curves for some of the shorter series against the reference serie. Station 9337090 and 9337091 shows little change in gradient. Station 9337078 has several changes in gradient.

The results from the analysis of the shorter series are shown in lower half of Table 6.3. Double mass curves for some of the stations are shown on Figure 6.4. Station 9337078 has several changes of the gradient. The analysis indicates non-homogeneity for station 9337078. This station has observations from 1954 to date, but about 11 percent of the data are missing. The double mass curves indicate a break around 1983. The average annual precipitation from 1954 to 1983 is 1122 mm. For the period 1984 to 1999, the average annual precipitation is 1588 mm. This is an increase of 42 percent, though it should be noted that the missing observations might influence the result.

6.4 Precipitation gradient and elevation

A linear gradient for correcting precipitation data due to change in elevation is commonly used in hydrological analysis and modelling. For most areas, the linear gradient with a constant increase in precipitation with altitude will work satisfactorily, while in certain areas it may give considerable errors. Due to the sparse or completely absent observation network for the upper slopes of Mt Kilimanjaro, a temporary observation network was installed in September 1999 with 9 rain gauges in a transect on the southern slope of Mt Kilimanjaro. These gauges cover the elevation zones from the lowermost border of the forest reserve and into the moorland and alpine desert at 4000 masl. Further details about the stations are shown in Table 6.2 and Figure 6.2.

The gauges were located in clearings in the forest about 1 meter above the ground and the surrounding vegetation was kept down. The gauges perform accumulative measurements of precipitation with a 5” gauge and monthly readings. The results from the 2 years of measurements can be seen in Figure 6.5. The measurements indicate that the maximum precipitation on the southern hillside of Mt Kilimanjaro can be found at about 2200-2300 masl.

From the area below the forest reserve, three stations from the regular observation network were selected to obtain a south north transect for the precipitation distribution as a function of the elevation. Two of the stations, 9337004 and 9337021, were used for establishing the reference series while the station 9337028 was discarded for the same purpose due to non-homogeneity. Before and after the break point in the mid 1960s, the station shows a homogeneous pattern and was used in the study of the gradient. The lack of other alternative stations on the lowland plains was also taken into consideration when applying the data from 9337028.

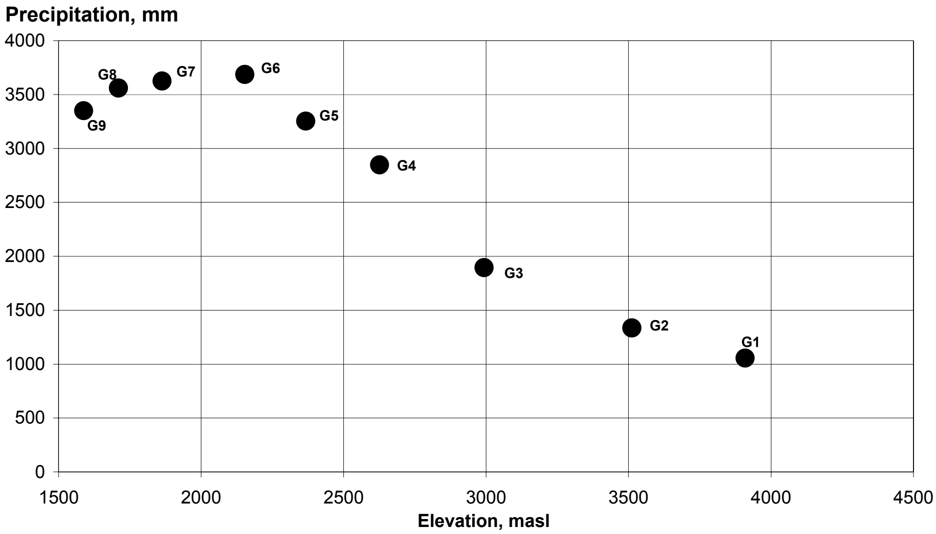

Figure 6.5: The observed precipitation at the 9 new gauges, G1-G9, in the southern hillside of Mt Kilimanjaro for a period of 2 years from September 1999.

The observed precipitation from the nine new stations and from the three stations in the regular observation network was used for fitting a function describing the distribution of precipitation as a function of elevation in the south-north direction. Two types of equations were used. For the distribution below 2700masl a 3rd order polynomial equation was used and for the elevations above 2700masl an exponential equation was used. The least square method was used for fitting the functions. The result can be seen in Figure 6.6. The solid circles show the observed precipitation at different elevations. The three curves are the precipitation from the three stations in the regular observation network corrected for differences in elevation to represent the precipitation at the other 11 observation points. The equation for correcting the precipitation due to change in elevation is based on a ratio between the precipitations at different elevations. A relative precipitation for a random elevation can be expressed as:

$$R = -2.93\times10^{-10}\times X^3 + 7.71\times10^{-7}\times X^2 + 6.15\times10^{-4}\times X - 0.445 \quad \text{for } 680 < X < 2700 \qquad \textbf{\textit{(Eq. 6.11)}}$$

$$R = 5.87\times e^{-6.35\times10^{-4}\times X} \qquad \text{for } 2700 < X < 5895 \qquad \textbf{\textit{(Eq. 6.12)}}$$

where X is the elevation above sea level which is under consideration. If a precipitation station at elevation X_1 has an observed precipitation P_1, the elevation function can be used for finding the precipitation P_2 at elevation X_2 according to the expression:

$$P_2 = P_1 \times \frac{R_2}{R_1} \qquad \textbf{\textit{(Eq. 6.13)}}$$

where R_1 and R_2 is the relative precipitation at elevation X_1 and X_2 respectively. The function was used on precipitation data from each of the three stations from the regular observation network in order to correct for the difference in elevation for each of the other 11 stations forming the three curves at Figure 6.6. The average deviation from the observed precipitation represented by the solid points is about 3 percent.

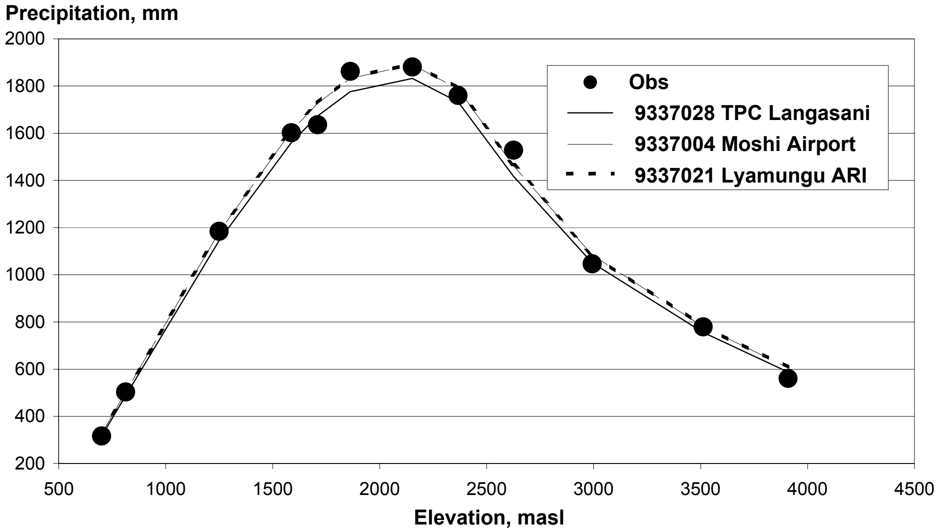

Figure 6.6: Function for correcting precipitation due to change in elevation in a south-north transect on the southern slopes of Mt Kilimanjaro. The three curves are calculated by use of the new function and observations at the stations 9337004/021/028.

For validation of the function for correcting precipitation due to change in elevation, an independent set of data was used. The independent data were obtained from KINAPA and from the regular observation network, both partly from different observation periods. On Figure 6.7, observations from seven different stations are shown. The four observations below 1590 masl are from the regular observation network. The three points located at the 2500, the 3500 and the 4500 masl respectively are from the KINAPA observation network.

An inspection of the KINAPA gauge Kibosho in June 1999, which is located at 2500 masl inside the forest in the southern slopes of Mt Kilimanjaro, revealed that this station was partly covered by vegetation. This will give lower observed precipitation compared to gauges not covered by vegetation, due to interception loss. This station has an observation period from October 1999 to January 2000 coincident with station G5 located at 2480 masl. The nearest area around station G5 has been cleared of vegetation and the station should therefore not be affected by vegetation covering the gauge. A correction factor for the station at Kibosho was calculated based on the coincident observations and applied for the whole observation period. The corrected value is indicated as the non-solid circle on Figure 6.7. The two other stations from the KINAPA observation network, Mweka and Kibo, are located above the forest belt around Mt Kilimanjaro, and will only have minor influence from the surrounding low vegetation.

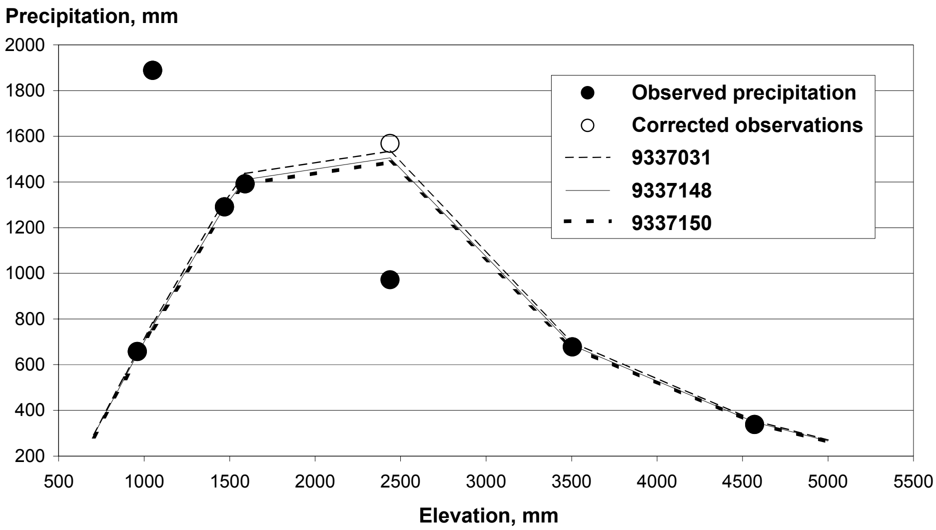

Figure 6.7: Verification of the function for correcting precipitation due to change in elevation with another independent dataset. See text for details.

The new elevation function was applied for correcting three of the precipitation values from the regular observation network and for forming the curves on Figure 6.7. The calculated curves on the figure fit relatively well with the observations in the seven circular points, particularly in the upper slopes of Mt Kilimanjaro. The small discrepancy may be explained by various influences from the vegetation around the gauges in the forest belt.

The deviation from the curves for station 9337147 located at 1050 masl is difficult to explain. No systematic deviation can be found. In the trend analysis, this station was found to be homogeneous. This station had the shortest observation period of the stations used for the analysis. The short observation period may make tests on non-homogeneity less significant. When comparing the observations from station 9337147, located at 1050 masl, and 9337148, located at 1470 masl, for the 10-year period from 1990, it can be observed that station 9337148 located at the highest elevation has the highest annual precipitation for the major part of the period. For some years, however the opposite is the case. This is the case for the period used for the verification of the function for correcting precipitation due to changes in elevation shown on Figure 6.7. Errors in the observations can be one explanation for the deviation from the curve, but it is difficult to say whether one explanation is more trustworthy than another.

6.5 Discussion of the precipitation distribution

The analysis of the precipitation data from the southern slopes of Mt Kilimanjaro has exposed many of the problems connected with precipitation data in third world countries. There are often discontinuities in the observations with a smaller or bigger number of years missing. Changes in observation procedures, lack of procedures or lack of follow up, may have influenced the readings with subsequent non-homogeneity in the observation material. The break in homogeneity can also have been caused by the re-location of the station, growth or removal of vegetation or impacts of new buildings.

The screening and quality check of the data material condensed and focused the most reliable data from the area formed by three precipitation series from the 1930s up to date. These series were used for constructing a reliable reference series, which could be used for verifying and filling in missing data. A larger amount of the data could have been utilized in the analyses with less rigid exclusion of data, and by filling in missing values by various techniques (for example ASCE, 1996). However, such completion of data can make the series more dependent on each other and possibly conceal errors in the observation material.

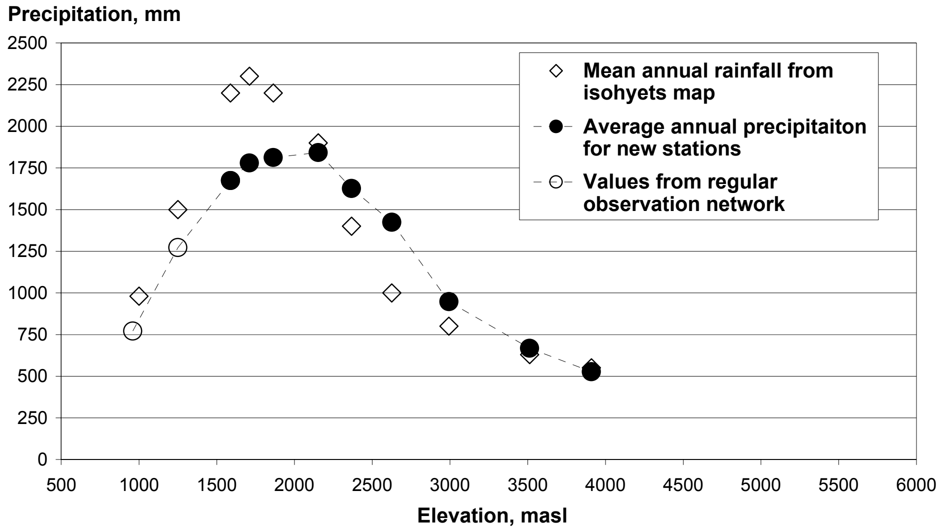

Figure 6.8: Comparison of the new measurements with the existing isohyets map. See text for details.

The 9 temporary stations established in the southern slopes of Mt Kilimanjaro gave interesting new information concerning the precipitation gradient in the southern hillside of Mt Kilimanjaro. A comparison between the isohyetal map presented in The United Republic of Tanzania (1977c) and the observed precipitation from the new stations indicate that the maximum precipitation for a transect on the southern slopes of Mt Kilimanjaro occurs at a higher elevation than previously indicated. The solid circles in Figure 6.8 located above 1500 masl represent the average annual precipitation for the gauges G1 to G9 during the observation period. The two non-solid circles in Figure 6.8 below the 1500 masl are observed values from the regular observation network for the same period. The diamonds represent the values from the isohyetal map presented in The United Republic of Tanzania (1977c). The isohyetal map indicates that the elevation for maximum annual precipitation on the southern hillside is about 1600-1800 masl. The new measurements indicate that the elevation for maximum precipitation in the southern slopes of Mt Kilimanjaro is 2000-2200 masl, which is an increase of 4-500 meters. More of the precipitation therefore takes place in the forest reserve, and not in the heavily utilized, populated and productive agricultural area below approximately 1500-1600 masl as assumed previously.

Though the new observations give some indications at which elevation the maximum precipitation takes place, the magnitude of the annual precipitation cannot be compared. The isohyetal map is constructed on the basis of long-term observations. The new measurements cover only a period of two years and may not be representative for a long-term level of annual precipitation. Yet this study has shown that by use of an elevation function, the existing observation network can be used to determine precipitation in the most intensively used and fertile southern slopes of Mt Kilimanjaro. Extended measurements would be useful in order to confirm the results further and to extend their application east- and westward from the transect under consideration.

URN:NBN:no-3437

7. WATER BALANCE CONSIDERATIONS

7.1 Introduction to the Water Balance considerations

This chapter deals with water balance calculations for three catchments on the southern slopes of Mt Kilimanjaro. The knowledge obtained from the studies of stream gauging and precipitation distribution in the previous chapters will be utilised in the determination of an overall water balance for a typical section of the southern slopes of Mt Kilimanjaro. The overall water balance will be checked against gauged runoff from the three catchments. See Figure 7.1.

The Water Balance for a catchment can be described in a condensed form as:

Water in – Water out = Change in stored water ***(Eq. 7.1)***

A more detailed description of the different elements and use of the equation is discussed by e.g. Black (1991), Maidment (1993), Shaw (1994), Dingman (2002). The different parts of equation 7.1 can be divided into the different components forming the flow of water in and out of the catchment. The basic equation can be expressed as: (Shaw, 1994)

$$E_t = P - R - G \pm \Delta S \qquad \textbf{\textit{(Eq. 7.2)}}$$

where E_t is the evapotranspiration, P is the precipitation, R is the runoff from the catchment, G is the groundwater flow and ΔS is the change in water storage within the time period under consideration. If the factors in equation 7.2 are averaged over a long period, and the conditions elsewhere in the catchment remain unchanged, then the net change in storage can usually be considered as zero (Dingman, 2002). The precipitation and the runoff can usually be measured with the necessary precision. However, it is more difficult to find the groundwater flow and the evapotranspiration. Selecting or assuming a catchment with no subsurface movement of water can eliminate the groundwater flow in equation 7.2. This is not the case for a catchment on the southern slopes of Mt Kilimanjaro where percolation to deep groundwater takes place.

The water balance of a smaller catchment or an elevation interval on the southern slopes of Mt Kilimanjaro will also have additional elements in their local water balance as compared to equation 7.2. The supply of water to the catchment or

URN:NBN:no-3437

elevation interval through irrigation is a frequent occurrence. In addition, water percolates to the deep groundwater reservoir from different elevation intervals on the slope, and then re-emerges on the lowland plains in the form of springs. Some of the elements of equation 7.2 have been described previously. The precipitation distribution with elevation is evaluated in chapter 6 and the runoff on the slopes is discussed in chapter 5. The water consumption is evaluated in the last part of chapter 4. The evapotranspiration in particular, the infiltration and distribution of irrigation will be discussed in this chapter before detailed equations for the water balance at different elevation intervals on the southern slopes of Mt Kilimanjaro are presented.

The United Republic of Tanzania (1977b) simulates the net discharge as a lumped value for four catchments on the southern slopes of Mt Kilimanjaro. The United Republic of Tanzania (1977b) finds that the observation period for discharge is too short for any statistical analysis (3-7 years). The observations are therefore used to make a model for estimation of the specific yield for sub catchments for the present situation. Some of the findings are shown in Table 7.1. The average discharge from the catchments evaluated by The United Republic of Tanzania (1977b) is 376 mm/year.

Catchment	Size km^2	Discharge mm	Effective rainfall mm
Sanya	112.6	227	562
Kikafu	194.9	450	509
Weruweru	150.2	365	617
Karanga	227.1	463	613

Table 7.1: Results from the investigation by The United Republic of Tanzania (1977b)

Perzyna (1994a) estimated the inflow to the Nyumba ya Mungu reservoir located in the central part of the catchment. This work is primarily based on an analysis of observed runoff series in the area upstream of the reservoir, which is formed by two major catchments. Extracting the discharge from catchment 1DD1 in Perzyna (1994a), the estimates vary from 410 to 432 mm/year on average for the whole catchment. The two estimates are based on different lengths of time series considered, that is 1971-1977 and 1971-1993 respectively.

Rusten (1995) calculated a lumped water balance for the catchment above the Nyumba ya Mungu reservoir. The inflow of water to the catchment is based on an estimate of the precipitation in the area. The factors forming the outflow from the catchment are identified on the basis of observed river runoff and on estimates of the evaporation and the groundwater flow. Rusten (1995) estimated the precipitation as 700 mm/year, the runoff as 184 mm/year and the groundwater flow as 158 mm/year. The evapotranspiration is divided into contributions from irrigated land and from other land. The total is found to amount to 815 mm/year. Rusten (1995) commented that the figures for the groundwater flow are associated with uncertainty. The value for runoff is probably the inflow to NyM found by Perzyna (1994a). Rusten (1995) also assumed that the whole area upstream of NyM was contributing to the runoff not excluding the area south of Arusha. This explains the low runoff value.

In a survey, Luhumbika (1999) found 2491 abstractions of water in the Pangani River Basin. However, no exact figures on the actual off-take and the distribution between the different regions in the basin was reported. It was pointed out that the majority of the abstractions were illegal without legal water rights. A survey of groundwater assessment in the Kilimanjaro region reported by Luhumbika (1999) mapped a total of 287 sources, but not all of these were located within the catchment shown in Figure 7.1. No precise value for the groundwater yield was given by Luhumbika (1999) and this would be difficult to determine without extensive fieldwork.

Stiles (1996) reported that a number of the many traditional irrigation systems found in the Kilimanjaro area were also used for domestic water supply, while Sandström (1995) reported that rural life in East-Africa depended on groundwater for at least 6 month every year. According to Ndege (1996), the best-developed irrigated agriculture in Tanzania was to be found in the Pangani River Basin. Further development of agriculture will affect inflow to the downstream reservoir, which may give rise to conflicts with the power producer concerning already scarce water resources.

7.2 The evapotranspiration and its determination

The evapotranspiration formed by evaporation and transpiration is a complex part of the water balance compared to, for example, precipitation and runoff. Direct measurement or calculation based on meteorological parameters may contain errors which are difficult to trace. A brief summary of measuring and calculation methods will be set out before the method applied on the southern slopes of Mt Kilimanjaro will be described in more detail.

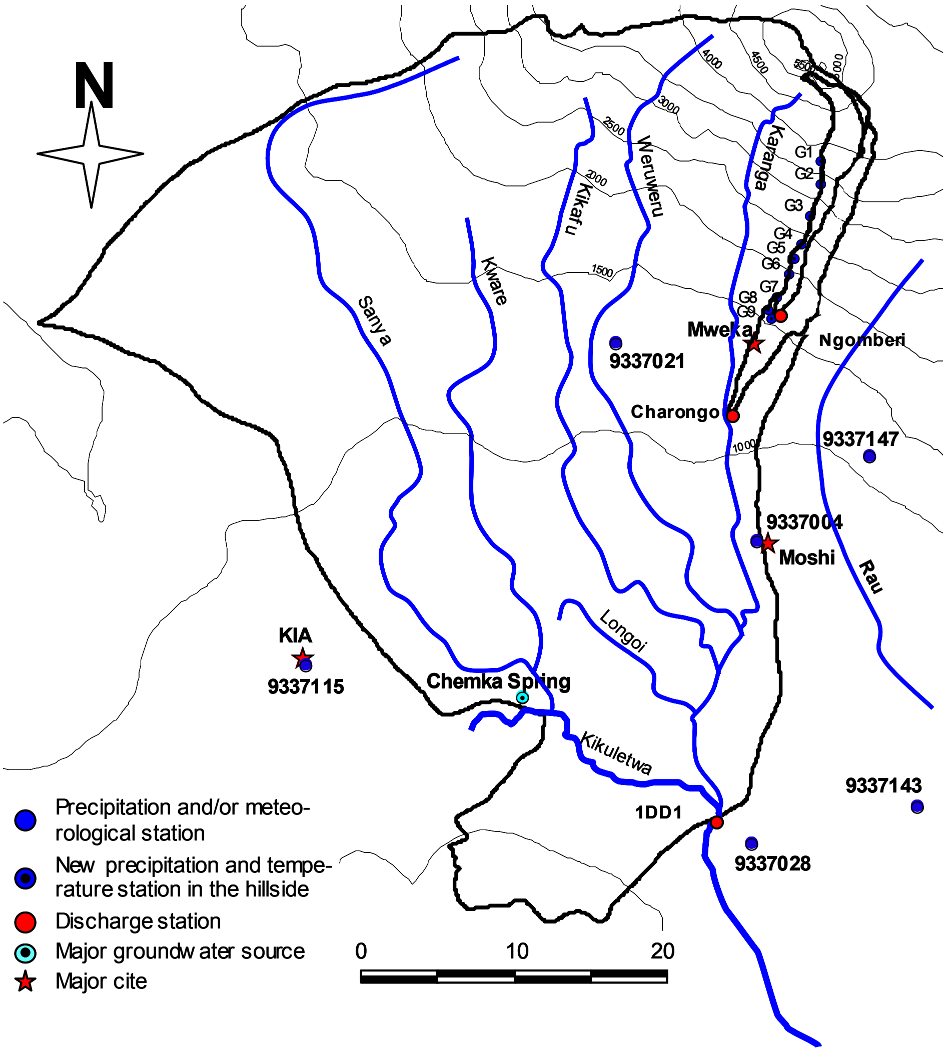

Figure 7.1: Map showing the three catchments for which the water balance calculation has been performed. The 1DD1 gauging station in the south-east. The Charongo and Ngomberi catchments further north-east. Meteorological stations applied are shown.

WMO (1966) define some of the many terms applied in the discussion of evaporation and evapotranspiration. Evaporation is defined as the emission of water vapour by a wet or free surface of water below boiling point. Potential evaporation is the quantity of water vapour, which could be emitted under the present atmospheric conditions by a surface of pure water.

Transpiration is defined as the emission of water vapour to the atmosphere through the pores of the plants. Both transpiration and evaporation will take place in a natural catchment and are termed actual evapotranspiration which is defined as the sum of water emitting from an area under the present meteorological and soil moisture condition. Potential evapotranspiration is defined as the maximum quantity of water that can emit under the present climatic conditions when the soil is kept saturated. It includes both evaporation from the soil and transpiration from plants. The following section deals with the determination of the evapotranspiration.

The evapotranspiration can be determined in several ways by use of an evaporimeter, which measure the evapotranspiration at a given point. Several methods can measure evaporation or evapotranspiration directly or by measurement of parameters affecting the evapotranspiration.

An atmometer has a porous surface, often paper or ceramic, from which the evaporation takes place. In addition, atmometers are supplied with a water reservoir supplying the evaporating surface. The benefits of atmometers are their small size and relatively low cost (WMO, 1966). A major problem connected to the operation of atmometers is to keep the evaporating surface clean (WMO, 1966). Dust and dirt on the evaporating surface will easily influence the result. The fragile atmometer is usually located within a shelter and is not exposed to direct solar radiation.

Pans or tanks filled with water allowing evaporation from a free water surface can be used for determination of the evapotranspiration in an area, with the use of correction factors. An example of this is the Class A pan, a circular 1.21 m diameter and 0.255 m deep steel pan mounted on a frame above the ground. WMO (1966), describe numerous types of pan evaporimeters above, on or set into the ground. Some disadvantages described by WMO (1966), are the problems in tracing leaks, a tendency to gather debris on the ground, difficulties in cleaning, and difficulties in maintaining surrounding vegetation. Pans mounted above ground can, in addition, be exposed to radiation on the sides and in the bottom. Change in colour may also influence the result. The actual evaporation is found through use of pan coefficients that, when multiplied with the measured evaporation, give the correct evaporation for the area.

The above section describes the measurement of evaporation. Direct measurement of evapotranspiration adds the complexity of transpiration from plants and the atmosphere's ability to absorb and transport vapour away. A lysimeter is a buried tank filled with the same soil as the surroundings and with its top at the same level as the surrounding surface (Manning, 1997). The percolation through the soil in the tank and sometimes the weight change of the tank can be measured. The evapotranspiration is found by calculating the water balance between rainfall, percolation and weight change.

In the area south of Mt Kilimanjaro, measurement of actual evaporation from a water surface is carried through pan evaporation at station 9337004 (See Figure 7.1 for location) and station 9337021 with observations of varying frequency and quality. Pan evaporation can be used for estimating the actual evapotranspiration.

With a lack of satisfactory measurements, the actual evapotranspiration can be estimated from climatic data. The basis for the estimates is often a wide range of meteorological parameters, which must be measured in or nearby the catchment. Dingman (2002) describes several approaches for estimating the actual evapotranspiration from a catchment:

- Water balance
- Potential Evapotranspiration
- Advection-Aridity approach
- Penman-Monteith
- Bowen-Ratio
- Eddy Correlation

By measuring the input and output of water from a catchment and compensating for changes in storage, the evapotranspiration can be found through a water balance approach. However, when considering a catchment on the slopes of Mt Kilimanjaro, the definition of the input and particularly the output can be difficult.

The potential evapotranspiration can be estimated in several ways based on observed meteorological parameters. Methods commonly applied in hydrological studies, are as follows, according to Dingman (2002):

- Temperature based
- Radiation based
- Combination
- Pan based

The temperature-based methods apply the air temperature and in some case the day length in the calculation. The monthly average temperature can also serve as the basis for the calculation. The radiation method considers the net radiation and the temperature above and the area for determination of the potential evapotranspiration. The combination method considers the net radiation and the air temperature in addition to the wind speed and relative humidity. The net radiation can be measured or estimated from meteorological data. The pan method is based on the correlation between measured pan evaporation and the potential evapotranspiration, which can be corrected for wind speed, temperature and humidity.

The advection-aridity or complementary approach mainly considers a large, uniform surface evaporating at potential rate. When the soil starts to dry out and the soil moisture decreases and with it the water supply slows the evapotranspiration, the energy not used for the evapotranspiration will increase the air temperature in the surroundings. The potential evapotranspiration will then increase. With the assumptions above, a relationship between the actual evapotranspiration, the potential evapotranspiration for the drying area and the potential evapotranspiration for an assumed wet area can be worked out. (Morton (1983b), WMO (1994)). The relationship is often termed the complementary relationship. The advection-aridity approach has the benefit of applying only routinely measured meteorological variables (Brutsaert & Stricker, 1979).

The Penman-Monteith approach treats the tree canopy as one big leaf. The surface resistance will represent the biological control of transpiration. The model requires sub-models for surface resistance and its use is therefore restricted WMO (1994).

The Bowen ratio approach utilises the mass transfer between two levels near the surface and the Bowen ratio to eliminate the need for wind speed measurements and roughness length estimates. The temperature and the vapour pressure have to be measured at two different levels above the ground to be applied in the calculation.

The eddy correlation is a complex and fragile way of actually measuring the parameters directly influencing the actual evapotranspiration. The vertical flux of the humidity can be found by use of instantaneous values for vertical wind speed and humidity. However, continuous measurements of these variables are not suitable for routine field measurements (WMO, 1994).

The methods applicable for calculating the actual evapotranspiration are restricted in a catchment on the southern slopes of Mt Kilimanjaro with only routine meteorological variables as temperature and vapour pressure being available in the area on regular basis as time series for several decades. The advection-aridity approach (Brutsaert & Stricker, 1979) has the advantage of applying these readily available data and requires no calibration to a specific site.

7.3 Finding actual evapotranspiration using the complementary relationship

Morton (1983a) uses the complementary relationship approach for development of the Complementary Relationship Areal Evapotranspiration, the CRAE-method, for determination of the actual evapotranspiration for an area without any prior calibration. The necessary calculation procedure will be described briefly below. Further details can be found in e.g. Morton (1983a), WMO (1994), and Dingman (2002). A simplified explanation of the complementary relationship will be set out below.

In an extensively wet area with an unlimited supply of water, the actual areal evapotranspiration will equal the potential evapotranspiration. If the actual areal evapotranspiration for some reason is falls below the potential rate for some reason, the released energy can be expressed as follows:

$$\lambda E_{TW} - \lambda E_T = Q \qquad \textbf{\textit{(Eq. 7.3)}}$$

where E_{TW} is the wet environment potential evapotranspiration, E_T is the actual evapotranspiration, Q is the released energy due to decreased evapotranspiration and λ is the latent heat of vaporisation of water. The released energy due to reduced evapotranspiration will influence the meteorological variables in the area, which will result in a new value for the potential evapotranspiration, E_{TP}. The difference between potential evapotranspiration before and after the change can be expressed as:

$$\lambda E_{TW} - \lambda E_{TP} = Q \qquad \textbf{(Eq. 7.4)}$$

where E_{TP} is the potential evapotranspiration after the change. Assuming E_{TW} is the potential evapotranspiration under the present meteorological conditions, with an unlimited supply of water and E_{TP} is the potential evapotranspiration under the present meteorological conditions with the present supply of water, equation 7.3 and equation 7.4 can be used to present an expression for the actual evapotranspiration:

$$E_T = 2E_{TW} - E_{TP} \qquad \textbf{(Eq. 7.5)}$$

where E_T is the actual evapotranspiration for an area found through the CRAE approach. The potential evapotranspiration under present meteorological conditions and water supply, E_{TP}, is found by use of the equilibrium temperature when the energy balance and the vapour transfer equation give the same result for a moist surface. Morton (1983a) uses the following equations for representing the energy balance and vapour transfer:

$$E_{TP} = R_T - \lambda_P f_T (T_P - T) \qquad \textbf{(Eq. 7.6)}$$

$$E_{TP} = f_T (\upsilon_P - \upsilon_D) \qquad \textbf{(Eq. 7.7)}$$

where E_{TP} represents the potential evapotranspiration in the units of latent heat under present meteorological and moisture conditions, where R_T is the net radiation for the area under investigation under present meteorological conditions, where f_T is the vapour transfer coefficient, where T_P is the equilibrium temperature found through the iteration process of solving equation 7.6 and equation 7.7, where T is the air temperature under present meteorological conditions, where ν_P is the saturation vapour pressure at equilibrium temperature, where ν_P is the saturation vapour pressure at dew-point and where λ_P is given by:

$$\lambda_P = \gamma p + 4\varepsilon\sigma (T_P + 273)^3 / f_T \qquad \textbf{(Eq. 7.8)}$$

where γ is the psychrometric constant, p is the atmospheric pressure, ε is the surface emissivity and σ is Stefan-Boltsmann constant.

For each time step, the elements in equation 7.6 and equation 7.7 are found and the equation solved with respect to the equilibrium temperature. The net radiation is calculated on the basis of observed sunshine hours, which are available for some stations on the slopes south of Mt Kilimanjaro. The maximum and minimum air temperatures are utilised with dew temperature where available or alternatively humidity measurements.

When the equilibrium temperature is found, the potential evapotranspiration under present meteorological condition, E_{TP}, using the equilibrium temperature is calculated using either equation 7.6 or equation 7.7. For wet environment potential evapotranspiration, E_{TP}, Morton (1983b) found the following general expression:

$$E_{TW} = 0.49 + 0,042\left(\frac{\gamma p}{\Delta_p + \gamma p}\right)R_{TP} \qquad \textbf{\textit{(Eq. 7.9)}}$$

where γ is the psychrometric constant, p is the atmospheric pressure, Δ_p is the slope of the saturation vapour curve at equilibrium temperature, T_p and R_{TP} is the net radiation for the surface at T_P.

The results from equation 7.6 or 7.7 and equation 7.9 are inserted in equation 7.5 and the actual evapotranspiration is found.

Further details on the elaborate calculations can be found in Morton (1983a). An example showing the calculation of the actual evapotranspiration for one month for a particular elevation level on the southern slopes of Mt Kilimanjaro will be shown later.

Morton (1983a) points out that the CRAE approach cannot be used on a daily basis due to changes in the storage of heat in the subsurface and atmospheric boundary and the vapour in the atmospheric boundary due to changes in meteorological conditions. The calculations are performed in monthly time steps.

The development of the complementary relationship and Morton's use of it are discussed in many works. Granger (1989) discusses the potential evapotranspiration and its definitions. Nash (1989) points out the connection between the CRAE and

Penman's concept of potential evapotranspiration. Penman calculated actual evapotranspiration according to the formula:

$$E_a = \Phi \times E_p \qquad \textbf{\textit{(Eq. 7.10)}}$$

where E_a is the actual evapotranspiration, E_p is the calculated potential evapotranspiration and Φ is a function of availability based on an empirical relationship. The proportionality between the actual and the potential evapotranspiration and Penman based formulas is thoroughly discussed in Morton (1994) and Morton (1991). Brutsaert & Stricker (1979) discuss the concept of symmetry between the potential and actual evapotranspiration. When applied to a rural catchment in the eastern Netherlands, good degree of agreement is found for daily values of evapotranspiration during a period of severe drought for which the concept is tested.

Karongo & Sharma (1997) conclude that the Morton model can be used for estimation of actual evapotranspiration on a monthly basis for tropical African catchments. The Morton model was used for calculating actual evapotranspiration in four small (<100 km^2) humid catchments in Kenya. The land cover in three catchments is a mix of pasture, crop and forest while the fourth is dominated by forest. The result shows an 8 percent overestimation of the actual evapotranspiration. Karongo & Sharma (1997) emphasise the benefit of the Morton model in using only meteorological data that are already available. The calculations were based on 34 years of daily runoff and precipitation measurements from the four catchments. The mean rainfall for the catchments varies from 1500-2180 mm within the elevation levels of 1600-2640 masl. The actual evapotranspiration found by the Morton model varies from 1051-1345 mm for the four catchments.

Chiew & Mcmahon (1991) compare the potential evapotranspiration of Penman with the wet environmental calculation of Morton, as both represent the upper constraint on actual evapotranspiration, and find that under moderate climatic conditions; they yield similar results when applied to 26 climatic stations all over Australia. The two estimates are found to be more even during wetter conditions than drier ones. Chiew & Mcmahon (1991) apply wet and dry bulb temperature, wind speed and sunshine hours for a period of 15 years in their study.

Doyle (1990) model catchment evapotranspiration with the same two approaches for catchments in Ireland. The Morton model is found to give marginally better results in the 27-year water balance considered for the 10 412-km^2 catchment studied. The calculations are performed on a monthly basis for the period under consideration. The annual precipitation and runoff in the studied catchment is 1044 and 543 mm respectively.

Meteorological data and 700 days of lysimeter evapotranspiration are used by Ali & Mawdsley (1987) for testing a CRAE-identical model at three different sites in the UK with barley, turf and rye grass. The study compares daily data but it is pointed out that with a correlation coefficient of 0.7, there is room for improvement. The model tends to overestimate the evapotranspiration under dry conditions and to underestimate for wet conditions. In addition to the lysimetric data the data measured in the study were, temperature, humidity, rainfall and wind speed.

Hobbins et al. (2001) perform long-term water balance calculations for 120 basins all over northern America ranging in area from 5000 km^2 to more than 100 000 km^2 for evaluation of the CRAE model. Their findings indicate that the CRAE model slightly underestimates the actual evapotranspiration in humid climates and slightly overestimates in arid climates. The performance of the CRAE model in the estimation of evapotranspiration in different climatic regions is emphasised. Local dramatic disturbances to the hydrological cycle such as extensive irrigation or groundwater pumping are accounted for in the model without any particular adjustments to local conditions due to the assumption that the result from the CRAE model accounts for all surface hydrology in the catchment under consideration.

7.4 Water balance calculation

As described in chapter 4 and 5, new discharge measurements have been performed for three catchments on the slopes of Mt. Kilimanjaro. In addition, long-term measurements are available from gauging station 1DD1. Principally, three different water balance calculations can be performed for three different catchments. These three catchments are located within each other. The findings from a smaller catchment can therefore be used for sorting out some of the unknown elements in the water balance for the bigger catchment as illustrated in Figure 2.2. Separate Water Balance calculations are therefore performed for the three catchments shown in Figure 7.1, Charongo, Ngomberi and 1DD1. A brief description of the catchment

1DD1 will be given. The description is also valid for the Ngomberi and Charongo catchment for the corresponding elevations.

7.4.1 The calculation method

The land use in the catchment above gauging station 1DD1 is mainly various types of cropping with a total of 1010 km^2 under varying types and intensity. Table 7.2 shows in detail the land cover distribution for the catchment above gauging station 1DD1, which is shown in Figure 7.1. Figure 7.2 show the hypsographic curve for the catchment. The elevation intervals in the table are selected with respect to size, elevation differences and the location of gauging stations and will be used later in the calculation.

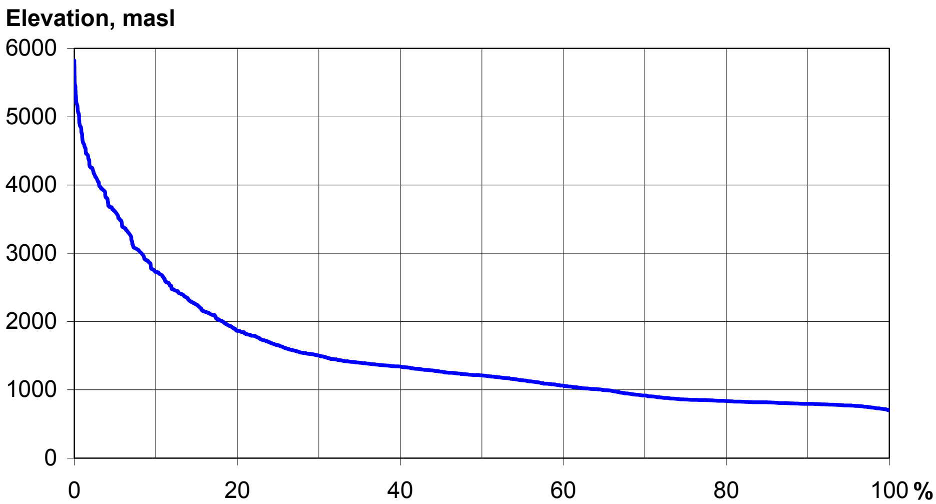

Figure 7.2: Hypsographic curve for the catchment above gauging station 1DD1.

Mainly mixed cropping with maize, rice or beans and cultivation with various types of tree crop like coffee or banana are to be found. On the lowland plains, sugar cane is also cultivated. Coffee cultivation mainly takes place in the middle area of the slope above 1000-1100masl where the temperate conditions, water and shadow trees make conditions favourable. About 25% of the agricultural area is under irrigation (Rusten, 1995), see chapter 4 for further details about water use. Other major land cover types are various combinations of wood-; bush- and grassland constituting 428 km^2 in addition to the forest belt around Mt Kilimanjaro that form about 295 km^2 of the total area. The majority of the forest is located in the forest reserve between approximately 1500-1600 masl and 2750masl. A more detailed illustration of the land cover distribution can be seen in Hunting Technical Services (1996). The different types of land cover have various influences on the water balance. Irrigated land will, for example, be more water consuming than bush land.

Elevation	Agricultural area	Forest	Open bush/ woodland	Dense bushland	Swamp/ Marsh/ Ice	Urban
masl	km^2	km^2	km^2	km^2	km^2	km^2
5825					0.4	
5468				1.7	3.8	
4915				7.1	5.1	
4463				19.9	1.8	
3998				37.2		
3489		0.4		48.2		
2961		3.6		34.8		
2737		11.8		19.0		
2474		25.3		19.2		
2250		42.5		13.4		
2000	0.5	66.0		4.0		
1747	6.9	56.3				
1636	30.1	34.8				
1499	148.5	34.0	3.6		0.1	0.1
1250	205.4	17.7	18.5		0.1	0.5
1100	140.8	2.6	21.4			0.8
1000	192.3		61.5		0.2	3.0
813	208.7		86.4		15.7	3.1
700	76.4		31.4		15.4	0.4
Sum	1009.6	295.0	223.0	204.5	42.7	7.9

Table 7.2: Simplified tabularised distribution of the different land covers with elevations in the catchment above gauging station 1DD1.

Figure 7.3 shows a schematic view of the southern slopes of Mt Kilimanjaro and the various elements in the water balance for the slope. Elements such as precipitation and evaporation will exhibit significant changes with elevation. For a detailed water balance consideration of the whole catchment, the different elements and their contribution should be analysed for various elevation intervals.

In the following section, the expression *global groundwater* is applied for the overall groundwater in the catchment under consideration. The expression *groundwater* means the groundwater within the elevation interval currently under consideration.

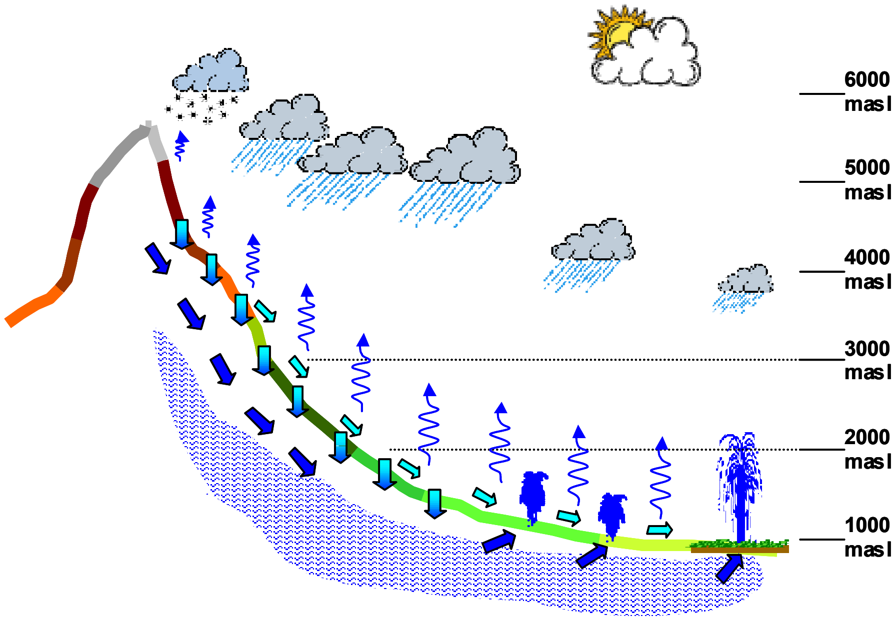

Figure 7.3: Figurative illustration of the southern hill slope of Mt Kilimanjaro and the major processes in its Water Balance.

The left side of Figure 7.4 illustrates the water balance for an elevation interval in a random catchment. The major elements of equation 7.1 are illustrated with the water in and out of the catchment represented by precipitation P, evapotranspiration E, and runoff R. For a catchment not exposed to lateral transport of water and a period of consideration selected so that no changes in storage take place, this will represent the water balance properly.

The river discharge from areas located above the elevation interval under consideration, are excluded from the calculation. It will represent the lateral transport of water and does not influence the water balance for the catchment under consideration, with some exceptions. When comparing the runoff from the water balance against the observed river discharge in the field, the sum of all R from the sub-catchments will represent the total river discharge from the catchment.

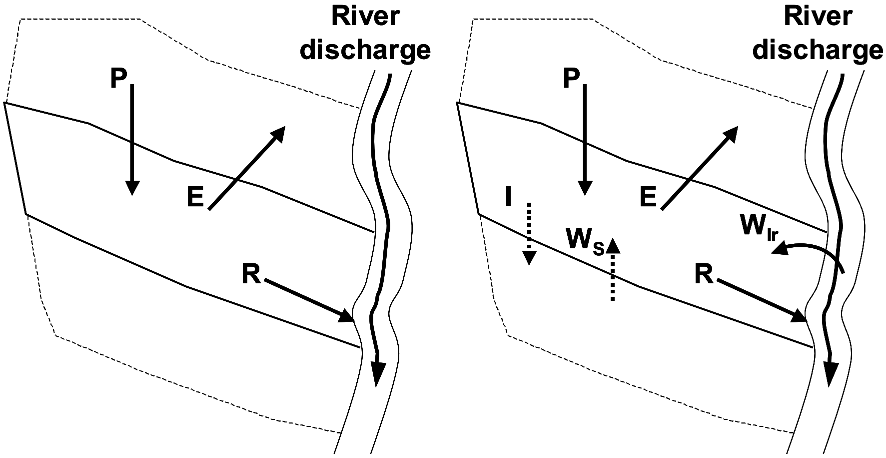

Figure 7.4: Illustration of the water balance for an elevation zone in the hillside south of Mt Kilimanjaro. The simplified water balance on the left and the more extended with all elements on the right. See text for description of variables.

On the hill slopes south of Mt Kilimanjaro, lateral transport of water takes place for a number of elevation intervals. The lateral transport from uphill areas can consist of groundwater infiltration and spring sources in addition to water for irrigation. These elements can be a result or effect of processes taking place at another elevation interval. For example, irrigation at a lower elevation interval obviously pre-supposes runoff from the elevation interval above. This will be discussed below.

The right side of Figure 7.4 and Figure 7.5 shows an isolated elevation interval with the various elements of the surface water balance. Figure 7.4 illustrates the water balance calculation for each elevation interval where the river discharge is excluded from the calculation. In principle a simplified water balance can be expressed as follows::

$$P + W_{Ir} + W_S = E + R + I \qquad \textbf{(Eq. 7.11)}$$

where the left side represents the "water flux" into the elevation interval and the right side represents the "water flux" out of the elevation interval under consideration. P is the precipitation, W_{Ir} is the irrigation water supply, W_S is the spring yield, E is the evaporation, R is the runoff and I is the infiltration or groundwater recharge.

The contribution to change in global groundwater storage from one elevation interval can be expressed:

$$\Delta W_G = I - W_S \qquad \textit{(Eq. 7.12)}$$

ΔW_G is the change in the "global" groundwater storage. A difficulty in considering a smaller part of a bigger catchment is the uncertainty related to transport of water in and out of the control volume under consideration. This is particularly the case on the slopes of Mt Kilimanjaro where intense rainfall is concentrated on the slopes, while extensive groundwater utilisation and consumption are concentrated to the dry lowland plains.

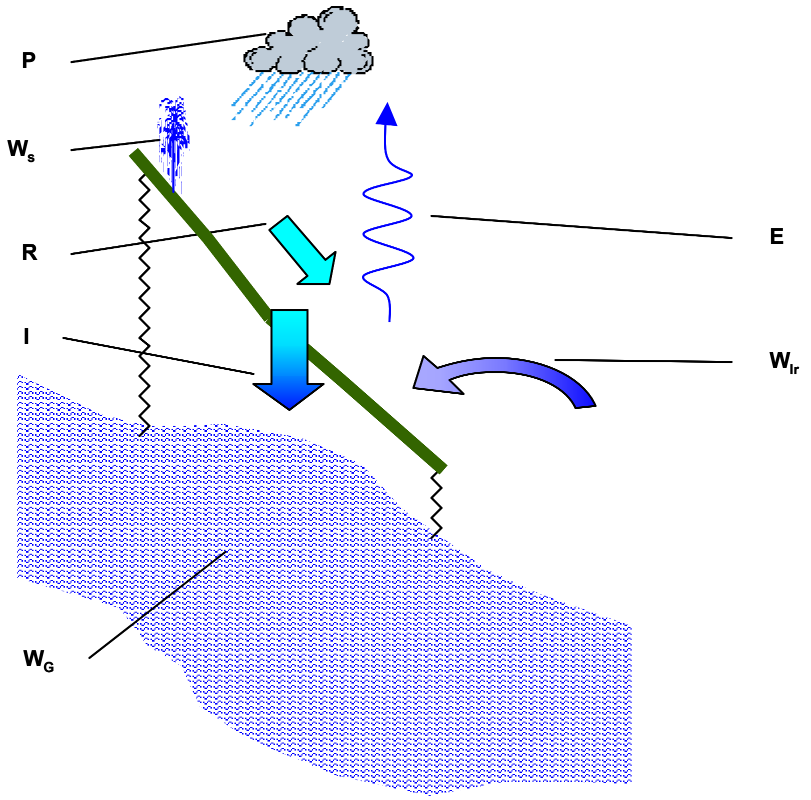

Figure 7.5: Identification of the elements in the Water Balance at a random elevation interval. See text for explanation of variables.

Assuming no change in or out of the global groundwater storage from one year to another and no lateral transport of water, the total global groundwater yield over the season for the whole catchment will be the sum of the infiltration in all the elevation intervals:

$$W_{Gw} = \sum_{i=1}^{n} \Delta W_{Gi} \qquad \textbf{\textit{(Eq. 7.13)}}$$

where ΔW_{Gi} is the contribution from each elevation interval i and n is the number of elevation intervals.

For comparison of the calculated runoff for all the elevation intervals with the observed value for a catchment, the following equation can be put forward with reference to the right side of Figure 7.4:

$$Q = \sum_{i=1}^{n} R_i - \sum_{i=1}^{n} W_{Ir\,i} + W_{Gw} \qquad \textbf{\textit{(Eq. 7.14)}}$$

where Q is the river discharge, n is the number of elevation intervals and W_{Gw} is the spring yield if it exists in the catchment under consideration. This will be discussed later.

7.4.2 Calculating the variables in the Water Balance

The meteorological data used for the water balance calculations and evaluations were taken from several stations in and close to the catchment above station 1DD1. An overview of the different data utilised can be seen in Table 7.3 and their location in Figure 7.1. The calculations were performed for various periods for the different catchments depending on the availability of data. All calculations were based on annual averages except for the actual evapotranspiration, which was calculated on a monthly basis with subsequent determination of annual values. For the Charongo and Ngomberi catchments, the calculations were performed for the two-year period from October 1998 to September 2000. For the 1DD1 catchment, the calculations were performed for the period from 1970 to 1996. For the two smaller Charongo and Ngomberi catchhments, the data from Table 7.3, which were most representative for the catchment concerning geographical location, were utilised. The determination of the different elements in the water balance illustrated in Figure 7.3, Figure 7.4 and Figure 7.5 are described in detail below.

Rainfall

Determination of the rainfall is based on the analysis of the rainfall distribution as a function of elevation found in chapter 6. The analysis was based on the new observations on the slopes of Mt Kilimanjaro and the regular observation network in the area. See chapter 6 for further details. The stations from Table 7.3 were utilised and an annual average was calculated for the period under consideration. The annual average was corrected for the considered elevation interval and the stations were given different weights depending on their location in or relative to the catchment. Stations in the central and upper part of the catchment were given higher weights than stations on the lowland plain and outside the catchment. The number of stations at the different elevations was also taken into consideration.

Station	Elevation masl	P mm	T_{Max} °C	T_{Min} °C	RH %	Sun hrs
9337004	813	x	x	x	x	x
9337021	1250	x	x	x	x	x
9337028	701	x				
9337115	891	x				
9337143	705	x				
9337147	1050	x				

Table 7.3: Overview of meteorological data used in the water balance caclualtion.

Evaporation

Area evapotranspiration is calculated by using the CRAE (Morton, 1983a). For catchment 1DD1, the area evapotranspiration was calculated for four different elevations for the period 1970 to 1996 for which period the necessary data were available or could easily be estimated. At station 9337004 and station 9337021, elevation 813 and 1250masl respectively, measured data from the meteorological stations was used.

The CRAE approach described previously in this chapter involves a range of complex equations for calculating the actual evapotranspiration on a monthly basis. A simplified example is illustrated in appendix 5 for the year 1976. The monthly values for temperature, humidity and sunshine hours are used for the calculations. The elements of equation 7.6 and 7.7 are found and the two equations are solved with respect to T_P which is shown in appendix 5. Equation 7.6 or 7.7 and equation 7.9 are then used to find the elements of equation 7.5 by use of T_P. The calculated actual evapotranspiration is then found for each month as shown in the appendix.

For a period of about two years, the temperature was measured automatically 6 times a day at 9 different elevations between 1500masl and 4000masl on the southern slopes of Mt Kilimanjaro. The locations of the 9 temperature stations can be seen in Figure 7.1 and they are identical in location to the 9 new precipitation gauges described in chapter 4. The new temperature measurements together with simultaneous observations from the regular meteorological stations in the area, were used for finding a temperature gradient. The gradient was used for estimation of temperature series for the 1970 to 1996 period at elevations 2000 masl and 3000 masl based on the observations at station 9337021. The minimum temperature was used for estimation of dew point at the two highest elevations due to lack of humidity measurements. The area evapotranspiration calculated at the 4 different elevations was used for interpolating the evapotranspiration at intermediate elevations. For the Charongo and Ngomberi catchments, some of the observation series from the 9 temperature stations were applied directly for the two-year period of monthly calculations of evapotranspiration. The monthly calculations were averaged over the year and an annual value utilised during the calculations for all the three catchments.

The water evapotranspirating from the different elevations under consideration consists of precipitation and a small amount from the rivers, which in this case is ignored. However, it should be noted that the majority of the water supplied by irrigation also evapotranspirates. In the calculations, the water supplied to each elevation level as irrigation is used for “filling up” the evapotranspiration “demand”. Thus, a smaller amount of precipitation will evaporate and e.g. form runoff or infiltration instead.

Runoff

Surface runoff measurements from station 1DD1 at the outlet of the catchment back to 1960 were used for determination of the total runoff from the catchment. The control volume formed by the catchment upstream station 1DD1 is assumed to have no lateral transport of water in or out of the catchment in addition to the components identified in Figure 7.3. The measurements from station 1DD1 will therefore

URN:NBN:no-3437

represent all the runoff from the catchment, including groundwater yield within the catchment.

The discharge measurements at station 1DD1 cannot give very much information concerning the runoff processes actually taking part within the catchment. No conclusions based on the measurements at gauging station 1DD1 can be made as to which part of the catchment actually contributes to the runoff, or whether there is an equal contribution to the runoff from the whole catchment.

Discharge measurements for the two catchments Charongo and Ngomberi indicated in Figure 7.1 can give more information about the runoff situation in the catchment. Gauging records are available for a period of 2.5 years. Refer to chapter 5 for further details. The records have been used for determination of annual runoff from these catchments. The smaller catchment consists of forest, bush- and high land desert with little or no activities influenced by humankind. The lower of the two catchments is more influenced by agriculture and irrigation activities. Field inspection has shown that the upper part of the catchment above about 2700-2800masl does not have any surface runoff. The runoff from these two smaller catchments was considered representative for the runoff from the same elevation interval in the whole 1DD1 catchment. The figures found for the two smaller catchments, were corrected for differences in annual precipitation between the period of water balance calculation for the whole catchment, 1970-1996 and the 2-year observation period considered for the Charongo and Ngomberi catchments.

The distribution of runoff within each catchment below 2800 masl, is assumed to be proportional to the distribution of precipitation. A simpler approach would have been to apply the runoff constant to the whole catchment. However, the assumption as to proportionality with precipitation seems more likely. The findings for Charongo were utilised in the Ngomberi catchment and the findings from both catchments were then utilised in the 1DD1 catchment making compensation for the differences in annual precipitation for the 1998-2000 period versus the 1970-1996 observation period.

Infiltration and spring yield

The infiltration was found for each elevation interval through a “local” water balance for each elevation level under consideration. For each elevation level, the actual evapotranspiration, the precipitation and the runoff could be found. In addition, the irrigation is determined for some elevation intervals. A local water balance for the elevation interval under consideration, will then give the value of the unknown infiltration according to the following equation. See also Figure 7.4 for illustration.

$$I = P - E - R + W_{Ir} \qquad \textbf{\textit{(Eq. 7.15)}}$$

where all terms are defined above. This equation is very similar to equation 7.11 except that the spring yield is omitted. Equation 7.15 assumes that the spring yield on the hillside is small compared to the lowland plains where major groundwater sources can be found, e.g. Chemka Spring, see Figure 7.1.

The findings from the Charongo catchment were utilised in the Ngomberi catchment, but when considering the 1DD1 catchment, the precipitation and evapotranspiration are different and they give somewhat different infiltration values. The difference is due to period under consideration, which is the period 1998-2000 for the Charongo and Ngomberi catchments and the period 1970-1996 for the 1DD1 catchment.

Irrigation

The extent of irrigated areas and determination of water demand are described in chapter 4. The agricultural areas found by Lefstad & Bjørkenes (1997) were applied in addition to the water demand calculated according to Allen et al. (1998). The irrigated areas were distributed between the different elevation levels according to the following rules and priorities based on observations in the field:

- No irrigation above 1640 masl
- Coffee cropping from 1100 masl and above
- Sugar cane cropping at 813 masl and below
- Irrigated areas distributed according to the hypsographic curve

The calculation resulted in a distribution of irrigated areas and irrigation demand as shown in Table 7.4. The irrigation demand is given in mm for each elevation interval. The large variations are due to both crop and irrigated areas within each elevation interval. The total irrigation demand is found to be equal to a constant off take of 11.3 m^3/s. It should be noted that the off take given in Table 4.2 is based on actually observed off take during inspection from PBWO and does not represent the actual Water Rights which are lower. Since it is a "point observation", it is probable that the off take can vary over the year with higher values in the cropping season.

Elevation masl	Area km^2	Coffee km^2	Sugar km^2	Banana/ beans/maize km^2	Irrigation demand mm
5895	0.4				
5500	5.5				
5000	12.2				
4500	21.8				
4000	37.2				
3500	48.7				
3000	38.5				
2750	30.8				
2500	44.5				
2250	55.8				
2000	70.5				
1750	63.1				
1640	65.0	4.8		5.3	211
1500	186.3	13.7		15.3	211
1250	242.2	17.8		19.9	211
1100	165.5	6.1		13.6	175
1000	257.0			21.1	139
813	313.8		34.6	25.8	366
700	123.9		27.4	10.2	594
Average for catchment					201

Calculating equivalent discharge		
Irrigation demand	201mm x 1783km^2 =	11.3 m^3/s

Table 7.4: Assumed distribution of irrigated areas and determination of the irrigation demand in the 1DD1 catchment.

For the Ngomberi catchment, the calculation of water demand is more difficult. No exact figures for irrigated areas are available for this area. The records from PBWO indicate granted water rights of about 374 l/s for this catchment, but some of the water redrawn from the river might be utilised outside the catchment. The runoff from the Ngomberi catchment is assumed to correspond with the runoff from the Charongo catchment. However, the discharge at the gauging station at Ngomberi is even less than at Charongo for the same period, though it is located further down the same river. This can indicate some major off takes between the two gauging stations. The off take in the Ngomberi catchment is therefore adjusted so that the river discharge fits the observed discharge on annual basis. The distribution of the off take between the elevation intervals is assumed proportional to the evapotranspiration.

Groundwater storage and yield

The total groundwater resources in the catchment will not emerge directly from the water balance calculations. If the assumptions of no lateral transport of water in or out of the total catchment are correct nor that there will be any change in the global groundwater storage, then the total groundwater yield from the catchment will be the sum of the infiltration contribution from all the elevation intervals. This value is applied when calculating the river discharge in Table 7.7. The distribution of groundwater yield between the different elevation intervals will be difficult to calculate using this approach. For the 1DD1 catchment, the larger part of the groundwater yield takes place in the Chemka Spring area (see Figure 7.1), which is located in the lower most elevation interval.

7.5 Results and discussions

7.5.1 Results

The results from the water balance calculations can be seen in Table 7.5, Table 7.6 and Table 7.7 representing the results from Charongo, Ngomberi and 1DD1 catchment respectively. The elevation interval, the area of the elevation interval, A, the precipitation, P, the evapotranspiration, E, the runoff, R, the infiltration, I, and the irrigation, W_{Ir}, are shown for each elevation interval. The calculated values are average values for the considered elevation interval.

An additional summary of the results can be seen in Table 7.8 and Table 7.9. Table 7.8 shows the summary of the water balance for the three catchments indicating the average value for the catchment of the elements that have been calculated. The average values for each catchment are a result of area-weighted average of all the elevation intervals within.

Table 7.9 shows the calculation of the river discharge. For the Charongo and Ngomberi catchment, the river discharge has been used for determination of the runoff values. They therefore obviously correspond well with the observed discharge from these two catchments.

Elevation masl	A km²	P mm	E mm	R mm	I mm
5895	0.0	207	207		0
5500	0.4	266	242		24
5000	1.4	365	301		65
4500	4.3	502	382		120
4000	5.7	689	493		197
3500	3.2	946	645		301
3000	1.5	1300	854		445
2750	0.8	1523	876	373	274
2500	0.4	1988	898	486	603
2250	0.6	2242	924	548	770
2000	1.2	2272	949	556	767
1750	1.0	2118	982	518	617
1640	0.5	2003	997	490	516

Table 7.5: Result from the Water Balance calculation for the Charongo catchment. See text for details.

Elevation masl	A km²	P mm	E mm	R mm	I mm	W_{Ir} mm
5895	0.0	207	207		0	
5500	0.3	266	242		24	
5000	1.7	365	301		65	
4500	4.9	502	382		120	
4000	7.4	689	493		197	
3500	5.7	946	645		301	
3000	3.1	1300	854		445	
2750	2.5	1523	876	373	274	
2500	3.0	1988	898	486	603	
2250	3.5	2242	924	548	770	
2000	4.2	2272	949	556	767	
1750	3.9	2118	982	518	617	
1640	3.0	2003	997	490	1169	653
1500	3.8	1822	1029	442	1025	674
1250	3.3	1424	1093	356	690	716
1100	1.6	1153	1135	305	457	744

Table 7.6: Results from the Water Balance calculation for the Ngomberi catchment. See text for details.

Of interest is the good correspondence between the observed and calculated values for the 1DD1 catchment. The observations at station 1DD1 represent an average discharge of 23.7 m^3/s for the period 1970-1996, while the calculated values in

Table 7.7 give an average discharge of 22.2 m^3/s. The deviation is about 6 percent between the observed and calculated discharge.

Elevation masl	A km²	P mm	E mm	R mm	I mm	W_{Ir} mm
5895	0.4	252	252		0	
5500	5.5	324	311		13	
5000	12.2	446	410		35	
4500	21.8	612	546		66	
4000	37.2	840	733		108	
3500	48.7	985	851		134	
3000	38.5	1154	989		165	
2750	30.8	1858	994	502	362	
2500	44.5	2424	998	655	771	
2250	55.8	2734	1003	739	992	
2000	70.5	2770	1007	749	1014	
1750	63.1	2583	1076	698	809	
1640	65.0	2442	1106	660	887	211
1500	186.3	2222	1145	596	693	211
1250	242.2	1736	1214	480	254	211
1100	165.5	1406	1173	411		175
1000	257.0	1177	1146	169		139
813	313.8	740	1096	10		366
700	123.9	478	1065	6		594

Table 7.7: Results from the Water Balance calculation for the 1DD1 catchment. See text for details.

It should be noted that the elements in the water balance of 1DD1 are calculated independently of the observed discharge. The precipitation is calculated from the elevation function and observations from the regular observation network. In the calculations the following are used: the evapotranspiration from Morton's CRAE-method, the infiltration is estimated as a balance between the other elements, the irrigation is based on the water demand for the crop in the area and the runoff is based on the findings from the Charongo and Ngomberi catchment for the upper part of the 1DD1 catchment. The runoff is compensated for differences in precipitation by multiplying with the ratio for the period 1970-1996 and 1998-2000, but otherwise the values are the same. This means that all the elements in the water balance are found independently of the actually observed discharge at the outlet of the catchment.

Element of Water Balance		Charongo catchment	Ngomberi catchment	1DD1 catchment
Precipitation	**P, mm**	996	1396	1481
Actual Evapotranspiration	**E, mm**	-597	-783	-1088
Runoff	**R, mm**	-108	-259	-319
Infiltration	**I, mm**	-291	-510	-275
Irrigation	**W_{Ir}, mm**		155	201
Sum		0	0	0

Table 7.8: Summary of results from water balance calculation for the three catchments.

Element of Water Balance		Charongo catchment	Ngomberi catchment	1DD1 catchment
Runoff	**R, mm**	108	259	319
Irrigation	**W_{Ir}, mm**		-155	-201
Spring yield (only 1DD1)	**W_G, mm**			275
River discharge	**Q, mm**	108	104	393
	Q	72 l/s	171 l/s	22.2 m^3/s

Table 7.9: Discharge calculation for the outlet of the three catchments under consideration.

The groundwater yield for the 1DD1 catchment estimated at 15.6 m^3/s shows some correspondence to the findings by Perzyna (1994b). Perzyna (1994b) estimates only the groundwater yield for the limited Rundugai area. Additional groundwater yield is not included. The United Republic of Tanzania (1977a) describes the use of 14 boreholes for irrigation purposes. The exact location is not given, but several must be located within the 1DD1 catchment. A rough estimate based on the figures in The United Republic of Tanzania (1977a), gives a groundwater yield of about 1-2 m^3/s, though no figures are given in The United Republic of Tanzania (1977a). In addition, there are numerous smaller groundwater sources and springs on the slopes, but no detailed overview is found for these.

7.5.2 Discussion of the calculations

Rainfall

The rainfall distribution is based on an analysis of rainfall measurements back to the 1920-1930s and up to to-day's date for the lowland plains. The new precipitation gauging on the middle and the upper hill slopes have only been undertaken for a period of two years. There is a question as to how representative the distribution of precipitation with elevation for the two-year observation period is for the whole calculation period. Compared with no or little information about the precipitation distribution due to elevation on the upper slopes it probably represents an improvement. With the use of the regular observation network in the area, the increase and consecutive decrease of precipitation towards the peak of Mt Kilimanjaro is difficult to trace and develop a mathematical description for, though it is quite likely that it exists. It should be noted that the new measurements have only been used for determination of the precipitation distribution with elevation and not for representing the actual amount of precipitation. Questions can also be raised as to whether the distribution of precipitation with elevation varies with wet and dry years, but this has not been evaluated.

Evaporation

The calculation of actual evaporation is difficult, particularly when the meteorological observations are limited. Numerous choices had to be made throughout the process. Using the complementary relationship for calculation of the area evapotranspiration can of course be called into question. The effect of the upwind boundary may not influence the calculations on the lowland plains, which form the larger part of the area, while on the slopes this may have some influence. Brutsaert (1982) defines actual evaporation as the average value from a large uniform surface involving characteristic scale length in the order of 1-10 km. On the slopes of Mt. Kilimanjaro, such scale length may result in 2-3000 meter change in elevation, and in some cases changes in the parameters used for the calculation. Use of the minimum temperature for some cases when calculating the dew point temperature can give rise to errors, but was accepted on the higher hill slopes where the minimum temperature is lower and closer to the actual dew point compared to the dry lowland plains.

On the slopes, the temperature is relatively low and the humidity high. A decrease of some degrees in temperature during the night will bring it relatively close to the dew point. On the lowland plains, the humidity is lower and the temperature higher. A decrease of some degrees in temperature during the night may not bring it much closer to the dew point. This may give rise to errors in the calculation of the evapotranspiration at the lowland plains.

The sunshine hours observed at elevation 1250masl may not be representative for the higher elevations. The number of observed sunshine hours at elevation 813 is about 20 percent higher than at the 1250masl. The cloud cover which partly surrounds Mt Kilimanjaro will reduce the number of sunshine hours on the middle slopes, but it is unclear how far up this effect will extend, or if or how much the number of sunshine hours will increase on the higher slopes.

In general, the evaporation calculations for higher altitudes are more uncertain than for lower slopes and plains due to a lack of actual observations and dependence on extrapolated variables. Some of the extrapolations of the data may be extended some distance taking the high elevation differences within the limited physical distance into consideration. On the other hand, it should be noted that the upper slopes constitute a rather small part of the total catchment. Only 10 percent of the total catchment area is located between the 2000 and 3000masl and only 7-8 percent above that.

Runoff

The assumption about the control volume formed by the catchment upstream 1DD1 is rather difficult to validate. The overview on Figure 4.1 and with more details on Figure 7.1, showing the river Kikuletwa draining from the Arusha region seems to contribute some discharge to station 1DD1. Field observations have indicated that this river is mostly dry, even during the wet season and very seldom contributes any runoff to the Kikuletwa River and to the Nyumba Ya Mungu reservoir. On the lowland plains, it might be difficult to determine the exact border between the catchments due to the small elevation differences. Irrigation canals in the extensively utilised agricultural area may also lead water between the catchments, but the extent is difficult to determine. Particularly on the border between the Karanga and Rau River on the lowland plain, Figure 7.1, short distances and small elevation differences may increase the risk of interchange of water between the catchments.

The runoff conditions in the catchment above 1DD1 might be different to the west as compared to the conditions in the gauged eastern Charongo and Ngomberi catchments. Differences in land cover may also have an influence. When we look at Figure 9.1, we will see that the forest reaches both a lower and a higher elevation interval more to the west in the 1DD1 catchment compared to the two smaller catchments. This can result in other runoff characteristics in the 1DD1 catchment than in the Charongo and Ngomberi catchments.

The lack of discharge measurements in the elevation interval between the two new gauging stations on the slopes and the discharge at station 1DD1 may also conceal important knowledge concerning the discharge in this area. The calculations assume that the measurements from the two new gauging stations are representative for their elevation levels in the rest of the 1DD1 catchment. The lower of the two new gauging stations, Ngomberi, is located at approximately 1080 masl. From the hypsographic curve for the 1DD1 catchment in Figure 7.2, it can be seen that 40% of the catchment is located below the 1080 masl. In this area, agricultural activities are most intense, but the rainfall is erratic and unreliable. Many of the streams in this area are dry during parts of the year due to increased abstractions (Mujwahuzi, 1999). All available water resources within each elevation level are consumed for irrigation or other purposes, though the former is the major consumer. For the lowland plains, there is a water deficit. This has to be compensated for either by an increased off-take from the river or from spring yield, particularly when the rivers have dried up. Unfortunately, there are no measurements being made between the 700 masl and 1080 masl. It is therefore difficult to provide evidence of the actual conditions in this area. This knowledge has to be based on learning from the area above and the total response from the 1DD1 catchment.

Infiltration and spring yield

Infiltration is one of the most difficult elements to check in the water balance calculations. For the upper slopes, the findings can be supported directly by observations and calculations of the other elements of the local water balance for the elevation intervals under consideration. The spring yield will provide a check on the total infiltration where there is no lateral transport of water in or out of the catchment under consideration. Various investigations have been performed, but no extensive survey of the spring yield in the area exists. When considering the gauging station 1DD1, the annual minimum daily discharge during the observation period is 10.2 m^3/s and the 25 percentile is 13.3 m^3/s for the catchment.

Comparing this with the infiltration found through the local water balance for each elevation level in Table 7.7, a spring yield equal to 15.6 m^3/s is given which is somewhat higher than the 10-11 m^3/s refereed in chapter 4. However, this value represents only the spring yield from the Chemka Spring area. Assuming some spring yield is also distributed at other elevation intervals ---- though it will be difficult to determine which ones ---- there is a correspondence between the spring yield and infiltration taking place largely between 1500 and 3000 masl on the southern slopes of Mt Kilimanjaro.

Outside the wet season, observations in the field show that the discharge in the rivers often decreases towards the lowland plains before vanishing completely during some times of the year, mainly towards the end of the dry season. The majority of the discharge at station 1DD1 thus consists primarily of spring yield (Perzyna, 1994b) during the low flow periods and little or no local runoff.

Irrigation

The lack of a detailed description of the extent of irrigation in the catchment can give rise to misinterpretation. The percentage of irrigated land given in Rusten (1995) is for the whole of the Kilimanjaro region, including areas east and west of catchment 1DD1. The use of this value requires that the 1DD1 catchment is representative for the whole Kilimanjaro region. When comparing the value given by Rusten (1995) on the land cover suitable for cropping with the actual estimate for the catchment above 1DD1 in Lefstad & Bjørkenes (1997), 252 km^2 and 216 km^2 respectively, we find a deviation of about 15 percent. The cause of this deviation can be non-representative figures or errors in one of the two estimates of irrigated area.

The return flow was estimated at some 25 percent and was not included in the irrigation water requirements. Walker (1989) suggests that a 40 percent return flow is a safe estimate, but local conditions with poor permeability particularly on the lowland plains and relatively flat fields in parts of the irrigated area, may justify a somewhat lower return flow value. On the other hand, this can be a matter for discussion and is difficult to prove.

The surveying behind the map in Hunting Technical Services (1996), consists of aerial photos and field studies from the period 1994-1996. This is towards the end of the period for the calculation. This description of land cover and land use might not be representative for the whole period 1970-1996 and may thus introduce errors, e.g. in the estimate of the irrigated areas. Obviously, errors in the meteorological data may also give erroneous crop water estimates, rainfall distribution and actual evapotranspiration.

7.5.3 Discussion of the results

In the water balance calculation for the catchment above station 1DD1, certain elements shown in Figure 7.5 are more difficult to determine than others. The reliability of the precipitation, evaporation, runoff and irrigation is probably higher than for the scarce and unevenly distributed figures for the spring yield. The former factors have been estimated at each elevation level based on observations in the field.

The water balance calculation for the catchment above gauging station 1DD1 assumes that the agricultural activities, runoff characteristics, etc. are evenly distributed within each elevation interval. Field inspections indicate that the irrigated agriculture and the spring yield, for example, are more concentrated to the east but no figures emerge to support this view. In this case, the measurements in the two smaller catchments will not necessarily be representative for the areas further west on the slope.

The function for correcting precipitation for change in elevation is based on observations from the recent years, from October 1999 to October 2001. The function developed is then used for the whole calculation period from 1970 to 1996. This assumes that changes in the catchment do not influence the precipitation distribution with elevation. It is also assumed that no change in land cover took place during the period under consideration with respect to agricultural areas. This is somehow not so important for the evapotranspiration calculation since the CRAE model is assumed to represent the total surface hydrology in the catchment.

The calculations are averaged annually for both the period 1970 to 1996 and over the year. The values resulting from the calculations are average values for the whole year and for the whole elevation interval under consideration. None of these values can therefore actually be observed in any of the rivers in the area. Also the calculation of total evapotranspiration for the 1DD1 catchment is averaged, but the CRAE approach ensures that changes in the vegetation are reflected in the calculation result since evapotranspiration is calculated on a monthly basis for the calculation period and thereafter used for finding an average annual value for the calculation period.

In the catchment above station 1DD1, the spring yield is not taken into consideration as an independent variable, except when calculating the river discharge in the bottom of Table 7.7 where the sum of the infiltration in the different elevation intervals is assumed to represent the total groundwater yield. In addition to irrigation, spring yield is also used for domestic water supply. The town of Moshi, located just on the border of the catchment, with approximately 145 000 inhabitants (Mbonile, 1999) and the surrounding rural areas, with approximately 450 000 inhabitants (Mbonile, 1999) are extensive consumers who are not taken into consideration as a separate variable in the water balance assessment. With the targeted water supply as described by Ndege (1996), this represents a demand of less than 4 mm a year, or about 0.2 m^3/s and cannot explain the deviation from closing the water balance calculation. To what extent domestic water supply can be considered as merely on loan from Nature and will returned to the system, or whether it will be removed permanently, is also open to discussion.

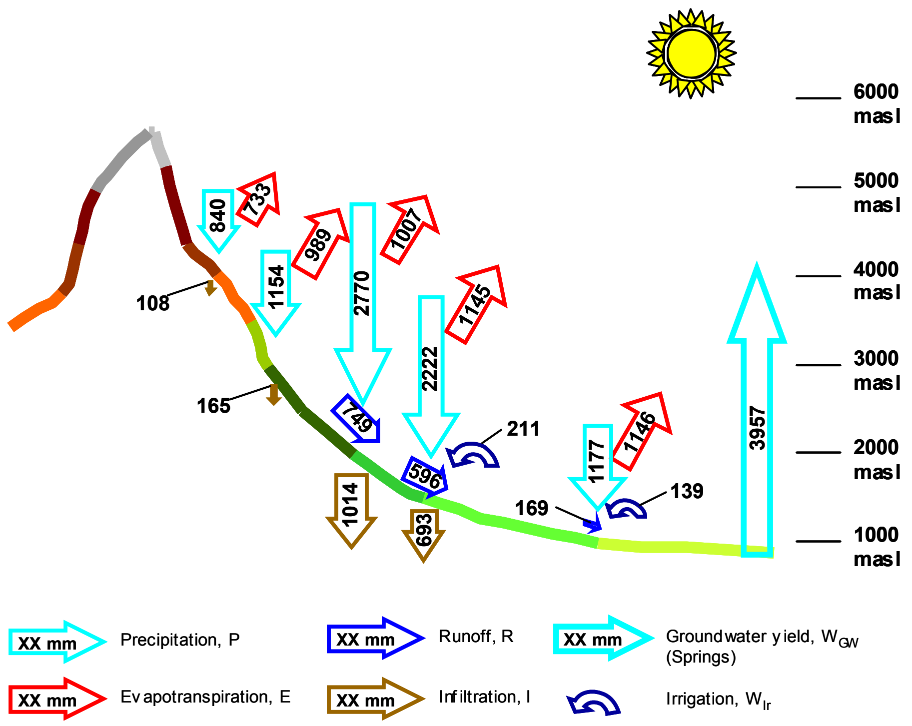

Figure 7.6: Illustration of the water balance for a section on the southern slope of Mt Kilimanjaro. See text for description.

Considering a section on the southern slopes of Mt Kilimanjaro, the instant values of the different elements of the water balance are illustrated on Figure 7.6 for some elevation intervals. The numbers can be recognised in table Table 7.7. The groundwater yield found mainly in the Chemka Spring area in the lowest elevation interval, causes an extraordinary inflow of water to this elevation interval. This value forms the sum of all the infiltration elements from the above elevation intervals. Figure 7.6 illustrated that the infiltration is small on the uppermost slopes towards the peak, reaches a peak on the mid slopes, decreases, and vanishes towards the lowland plains.

To conclude the discussion regarding water balance by pointing to the source for the deviation between the observed and calculated runoff from the 1DD1 catchment is difficult. The only safe conclusion is that all the elements of the water balance are uncertain. There are probably heterogeneities in the precipitation in the area. The calculation of evapotranspiration may also contain errors, or the assumptions for the CRAE approach are not fulfilled. The readings at the gauge at 1DD1 too can be erroneous or the rating curve may have changed. Furthermore, the actual off take of water can vary. The calculations assumes a constant off take from one year to another, while in reality, the off take will be higher in dry years than in wet years, that is in inverse proportion to the supply. Finally, checking the actual infiltration at each elevation interval is difficult and the assumptions really are assumptions.

Most of the deviation from closing the water balance can probably be explained through the evapotranspiration and conditions of no lateral exchange of water, though it is difficult to postulate that these are the actual sources of error. The error can also be found in the other elements of the water balance, but evapotranspiration is a complex process and is calculated from a relatively limited number of observations. The reliability of the method adopted can have introduced errors into the calculation. However, extensive field survey is required for a thorough examination of this theory and for obtaining enough parameters for a different approach to the calculation of the area's evapotranspiration.

All the conditions and elements of the water balance calculation are accounted for and discussed in this chapter. As far as these are found to be valid, the water balance assessment made here will be representative for the actual conditions found in the field.

8. HYDROLOGICAL MODELLING

8.1 Introduction to hydrological modelling

This chapter deals with the development of a hydrological model for use on the southern slopes of Mt Kilimanjaro. As described in chapter 1, the hydrological processes involved are complex and possess characteristics found in few other places. The peak of Mt Kilimanjaro rises 5000 meters above the surrounding plains. Within a few kilometres of horizontal distance, elevation changes thousands of meters on the mountain slope. A distinct transition from dry lowland plains, through a precipitation rich mountain slope towards a snowy peak takes place. Some of the meteorological processes, which occur in this area, have been investigated in the previous chapters. The findings are applied in the model development and incorporated where meaningful. The model developed here is thereafter calibrated for three catchments on the southern slopes of Mt Kilimanjaro; one small uphill catchment, one medium size mid hill catchment and a large catchment reaching from the lowland plains to the peak of Mt Kilimanjaro.

8.2 A distributed approach

Rinde (1998) describes the hydrological modelling tool applied in the development of the hydrological model here. In Rinde (1999), the modelling tool was used for evaluating the quantitative influence of the change in land use on the yield from a catchment in central Norway. A distributed hydrological model using the parameters influencing the land use and combining them with hydro-meteorological parameters for simulation of the yield was developed. A distributed description of high and low vegetation, snow cover, surface and root zones was used for calculating the processes across the catchment. The interception, evapotranspiration, snow distribution, infiltration, soil water and surface runoff were taken into consideration for each area element in addition to the total runoff from the catchment. The vertical water balance above, on and including the root zone was described distributed. The model can therefore determine the influence from land use changes involving changes in these zones. Lateral transport of water is not described distributed.

The model required further development before it could be used on the southern slopes of Mt Kilimanjaro. The processes describing the vegetation on the surface and its interaction with the atmosphere were kept, while a number of processes had to be changed or added for a correct representation of the hydrological processes on the southern slopes of Mt Kilimanjaro. The major improvements are:

- A “global” groundwater routine
- A relative precipitation function of elevation
- A distributed description of water demand

On the hill slopes of Mt Kilimanjaro where the rainfall is most intensive, the surface runoff is small compared to the actual rainfall. On the lowland plains, extensive groundwater yields can be found which do not correspond to the precipitation and size of the surrounding area. This requires a model where precipitation in one part of the catchment can infiltrate to a “global” groundwater reservoir and occur as a groundwater yield elsewhere in the same or in a neighbouring catchment.

On the hill slopes of Mt Kilimanjaro, the elevation gradient is high with up to 4000-meter elevation differences within a 10-12-kilometre distance. Often precipitation is corrected by a simple linear gradient with elevation during the hydrological simulation and this can be satisfactory in many cases. However, the precipitation on the lowland plains below Mt Kilimanjaro increases to a maximum at around 2200 masl before decreasing towards the peak. With a limited number of observation stations, primarily located on the plains and on the lower hill slope, a linear precipitation gradient does not reproduce the parabolic shaped precipitation distribution on the slopes of Mt Kilimanjaro. This requires a change in the routine for correcting precipitation with elevation. This is treated in chapter 6, which describes the development of a function for distribution of precipitation with elevation.

In many temperate areas, e.g. Norway, irrigation does not play an important role in the water balance. In tropical areas where erratic rainfall makes irrigation a necessity for securing the success of the crop, irrigation will form a major component of the water balance in some regions, particularly where water resources are scarce. The modified concept of the model by Rinde (1999) is shown in Figure 8.1 with the distributed vertical water balance illustrated on the right hand side of the figure. The calculation of the vertical water balance is repeated for all area elements in each time step. The runoff response and the global groundwater recharge contribution is summarised for all area elements in the catchment under consideration and forms an input to the response routine and global groundwater reservoir respectively, for determination of the hydrograph for river discharge and spring yield.

8.3 Model description

The description of the features present in the model is based partly on the work by Rinde (1999). In addition, a description of the necessary improvements of the model for application on the southern slopes of Mt Kilimanjaro is added. However, features described in the original work by Rinde (1999) not relevant for the southern slopes of Mt Kilimanjaro are omitted.

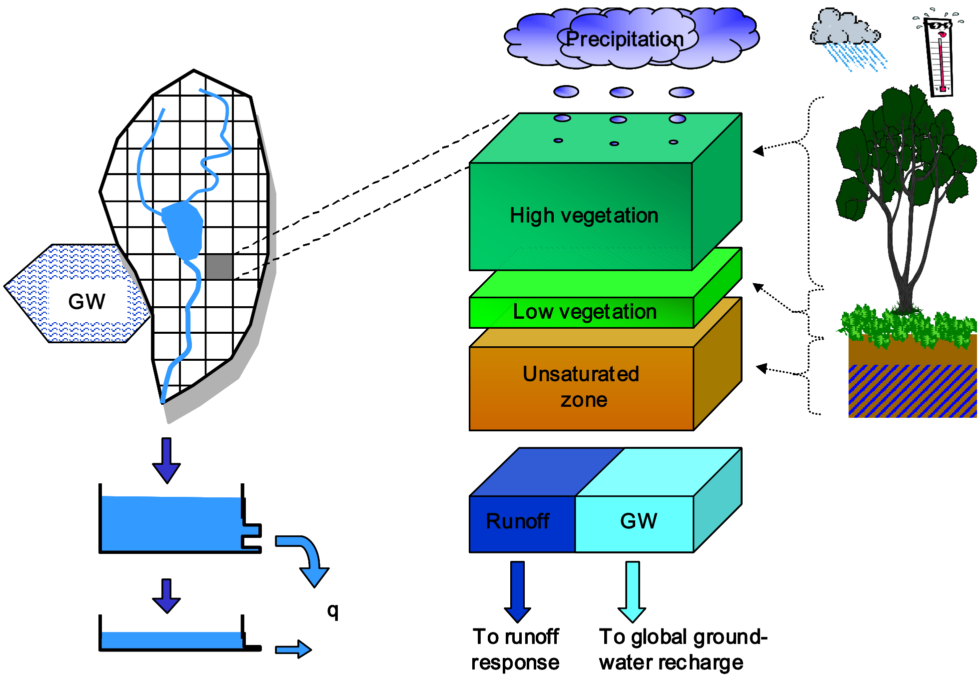

Figure 8.1: Illustration of the model concept with emphasis on the vertical water balance and distribution between contribution to runoff response and global groundwater recharge.

8.3.1 Model equations

In the event of a precipitation event over a vegetated area, the rain will first strike the high vegetation as illustrated on Figure 8.1. A part of the rain will wet this first. The precipitation not wetting the high vegetation will fall through and strike the low vegetation. Furthermore, a part of the rain will wet the low vegetation. The precipitation not wetting the high and the low vegetation, will strike the ground. This is named throughfall. The water wetting the vegetation will evaporate from the vegetation itself and not from the ground or through transpiration. The process of wetting and evaporation is called interception (Maidment, 1993).

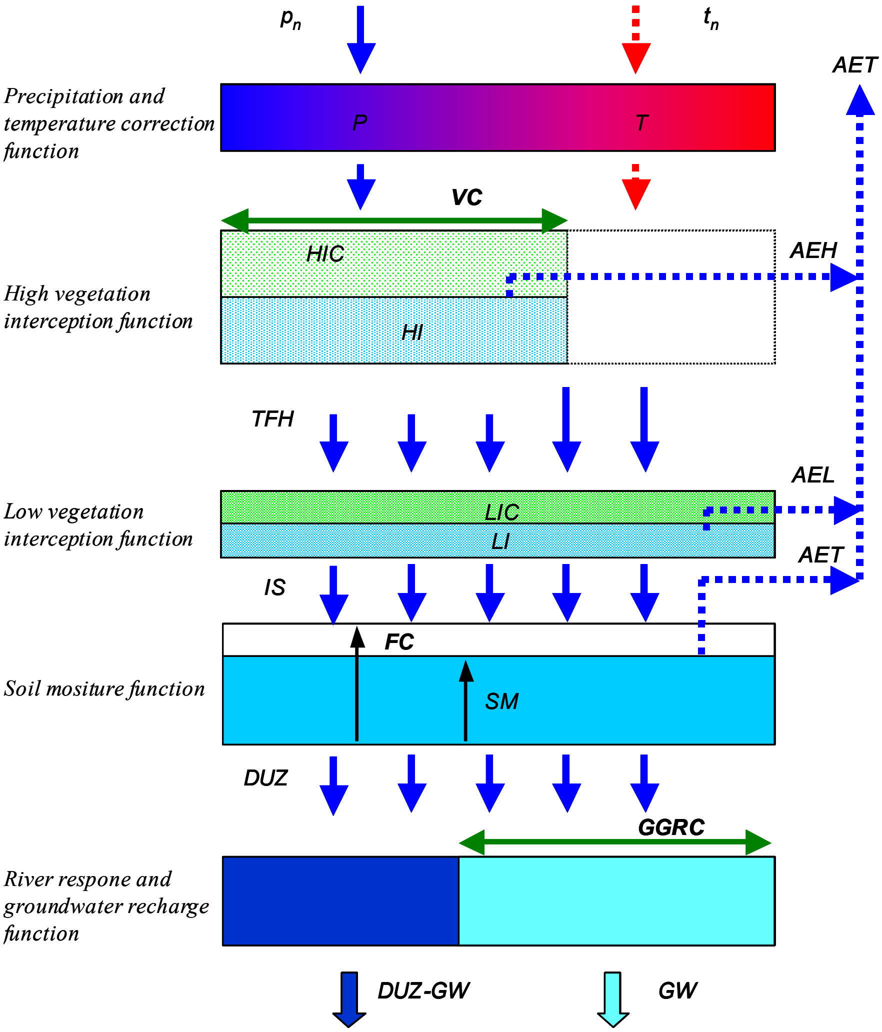

Figure 8.2: Illustration of the vertical water balance above, on and in the soil zone.

A schematic outline of the processes in the distributed water balance above, on and including the root zone for each area element is shown in Figure 8.2. Some of the distributed variables are indicated in upper case and distributed parameters are shown in upper case bold on the figure. A detailed explanation will be given later.

The precipitation enters from the upper part of Figure 8.2 and is routed through the different routines in the model. The point observations of precipitation and temperature in the catchment are used to calculate a representative value for each area element. The interception of precipitation in the high and the low vegetation is modelled with separate routines as illustrated on Figure 8.2. The vegetation cover $\boldsymbol{VC}$, adjusts the area in which high vegetation interception take place. Furthermore, the routine modelling the low vegetation interception and the function for soil moisture can also be found. From all these three routines, evapotranspiration takes place. Intercepted water from the high and low vegetation evaporates and direct soil evapotranspiration take place from the soil moisture routine. The lowermost routine in Figure 8.2 distributes the water between the global groundwater recharge and river runoff response.

A more detailed description of the hydrological processes and the equations within each routine will be given below. The expression "*average values*" means that the value from each area element in the catchment under consideration is summarized and an average value for the whole catchment is calculated. All average values are expressed in lowercase in the text.

In the following, the parameters are indicated in bold and the variables or model states in regular font. Lumped values are written in lower case and distributed values in upper case. Variables are expressed in the figures in the following, while parameters are indicated on the right hand side.

Name	Unit	Description
p_1, p_2, p_3	mm	Timeseries with observed precipititation
t_1, t_2, t_3	^oC	Timeseries with observed temperature
w	m/s	Timeseries with observed windspeed

Table 8.1: The input variables for the simulation model.

Meteorological input

The routine for correction and determination of meteorological data for each area element is illustrated in Figure 8.3 where the parameters are shown on the right side. The meteorological input applied in the calculation is shown in Table 8.1 and it includes temperature, precipitation and wind speed. Data from up to three different precipitation and three different temperature stations are applied in the calculations. The precipitation and temperature stations can be situated in different locations. The coordinates and the elevation of the meteorological stations are given in the parameter file for the simulation model.

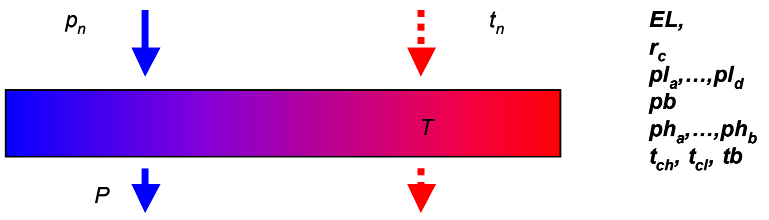

Figure 8.3: Illustration of the routine for correction and determination of meteorological data for each area element.

The observed point values form the basis for calculation of the precipitation and temperature in each area element considered in the distributed water balance. For finding the precipitation and temperature for each area element, the observed point values are corrected for elevation and distance from the observation point depending on how many point observations are used in the calculation. The temperature and the precipitation observations can be made in different locations. The temperature at a particular location, is calculated in accordance with the formula:

$$T = t_n + \boldsymbol{t_{lapse}} \times (\boldsymbol{EL} - \boldsymbol{Ht_n}) \qquad \textit{(Eq. 8.1)}$$

where t_n is observed temperature at station n, $t_{lapse} = \boldsymbol{t_{ch}}$ for $\boldsymbol{EL} \geq \boldsymbol{tb}$ - in the higher areas and $t_{lapse} = \boldsymbol{t_{cl}}$ for $\boldsymbol{EL} < \boldsymbol{tb}$ - in the lower areas, $\boldsymbol{tb}$ is the elevation for change in temperature gradient, $\boldsymbol{EL}$ is elevation of the area element under consideration and $\boldsymbol{Ht_n}$ is elevation of temperature station n. A brief analysis of the temperature data for the meteorological station in the area and from the 9 temporary temperature stations indicated a temperature gradient for the lower slopes $\boldsymbol{t_{cl}} = -1.0$ and for the higher slopes $\boldsymbol{t_{ch}} = -0.55$ per 100 m increase in elevation. Little or no difference was found for days with and without precipitation events. The precipitation is corrected for point errors in the observed values, and adjusted for differences in elevation between the observation point and the area element under consideration according to equation: 8.2. The point error can arise, for example, from distance to obstructions like trees or houses, observer errors, splash, evaporation and wetting loss (Dingman, 2002).

$$P_n = \boldsymbol{r_c} \times p_n \times \frac{R(\boldsymbol{EL})}{R(\boldsymbol{Hp_n})} \qquad \textbf{\textit{(Eq. 8.2)}}$$

where P_n is the elevation corrected precipitation at the considered area element based on the observed precipitation from station n, p_n is the observed precipitation at station n, $R()$ is the relative precipitation function with elevation as argument, $\boldsymbol{EL}$ is the elevation of the area element under consideration and $\boldsymbol{Hp_n}$ is the elevation of precipitation station n. The general function for relative precipitation is expressed by equation 6.11 and equation 6.12 depending on the elevation of the area element under consideration. The relative precipitation is calculated for both the precipitation station and the area element under consideration. A ratio is formed and the precipitation for the area element under consideration can be calculated. For more details, see chapter 6. When temperature and precipitation data from several stations are used, the precipitation for the area element under consideration is interpolated and the inverse distance weighting according to Dingman (2002) is applied. For example, where three precipitation stations are applied in the calculation, the weighted precipitation in the area element under consideration will be:

$$P = \left(\frac{P_1}{d_1} + \frac{P_2}{d_2} + \frac{P_3}{d_3}\right) \times \left(\frac{1}{\frac{1}{d_1} + \frac{1}{d_2} + \frac{1}{d_3}}\right) \qquad \textbf{\textit{(Eq. 8.3)}}$$

where P_n is the elevation corrected precipitation from station n and d_n is the distance from station n to the area element under consideration. The equation above shows an example with three different precipitation stations. If precipitation or temperature data are missing from one or two stations, the remaining data are used for the calculation and weighted according to their distance from the area element under consideration.

Interception capacity

Valente et al. (1997) describe an interception model for areas with sparse vegetation, which divides the area between vegetated and non-vegetated areas. The interception only takes place in the vegetated areas. A simplified version of the model for high vegetation is illustrated on Figure 8.4. A tank with no outlet and a threshold *IC* for overflow describes the interception. The precipitation will first fill the tank. The threshold *IC* represents the amount of precipitation necessary for wetting high vegetation on Figure 8.4. When the tank is full, the excess precipitation will form throughfall to the low vegetation. There is no throughfall before the tank is filled up. The water evaporates from the tank and the tank is emptied. The rate of evaporation depends on the meteorological conditions. If all the water in the tank is not evaporated before the next precipitation event, the interception will be reduced correspondingly.

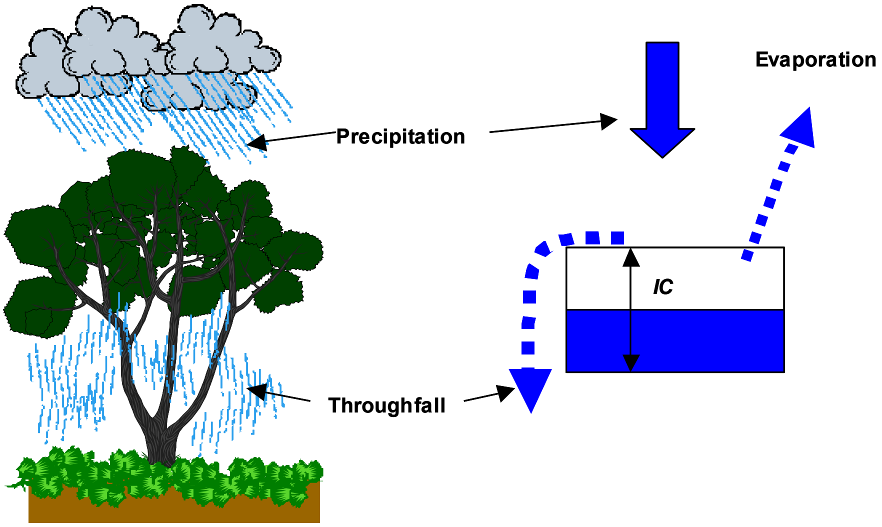

Figure 8.4: Illustration of the modelling of the interception process in high vegetation.

The interception is modelled separately for high and low vegetation using the approach described above. Dingman (2002) give 0.15 mm as a guide for precipitation necessary for wetting per unit LAI, while Valente et al. (1997) refers to values from 0.2 to 1.0 mm as canopy storage.

The interception capacity is calculated separately for high and low vegetation by use of four distributed and two lumped parameters. ***LAI*** and ***LAIU*** represent the leaf area index for the forest and undergrowth respectively. ***VH*** and ***VC*** represent the vegetation height and coverage of high vegetation. $\boldsymbol{laicap}$ is the storage capacity per leaf area index and $\boldsymbol{dvh}$ is the average vegetation height.

The interception capacity in high vegetation is calculated according to the formula:

$$HIC = \boldsymbol{LAI} \times \boldsymbol{laicap} \times \boldsymbol{VC} \times VGC \qquad \textbf{\textit{(Eq. 8.4)}}$$

where HIC is the interception capacity for high vegetation, VGC is correction factor for tree height given with the formula:

$$VGC = \left.\frac{\boldsymbol{VH}}{\boldsymbol{dvh}}\right|_{\min=0}^{\max=1} \qquad \textbf{\textit{(Eq. 8.5)}}$$

The parameter $\boldsymbol{VC}$ adjusts for non-complete forest cover for the area element under consideration. The parameter VGC adjusts for the height of forest deviating from the average height. The interception capacity in low vegetation is calculated according to the formula:

$$LIC = \boldsymbol{LAIU} \times \boldsymbol{laicap} \qquad \textbf{\textit{(Eq. 8.6)}}$$

where LIC is the interception capacity for the vegetation.

For lakes and waters, the interception capacity is put at zero for both high and low vegetation. This is controlled through the land use, $\boldsymbol{LU}$, parameter.

Potential evapotranspiration

The potential evapotranspiration is pre-calculated on a monthly basis for the catchment and is given as input to the model. More details on the calculation of the evapotranspiration can be found in chapter 7. The evapotranspiration can be influenced by meteorological and vegetation factors in the catchment Ward (1990). The wind speed can influence the exchange of vapour between the surface and the air and the LAI will influence the area from which transpiration actually takes place.

The potential evapotranspiration in the area element under consideration is expressed by the formula:

$$PE = \boldsymbol{ep}_{\boldsymbol{month}} \times TC \times \boldsymbol{HC} \times WC \times PC \qquad \textbf{\textit{(Eq. 8.7)}}$$

where $\boldsymbol{ep_{month}}$ is the monthly average potential evapotranspiration calculated for the area for month 1 to 12. This is given as an input to the model. TC is a correction factor for deviation from the average monthly temperature in the catchment and is expressed by the equation:

$$TC = 1.0 + \boldsymbol{et} \times (T - \boldsymbol{tp_{month}}) \qquad \textit{(Eq. 8.8)}$$

where $\boldsymbol{et}$ is the sensitivity of the potential evapotranspiration on deviation from the average temperature, T is the corrected temperature for the area element under consideration and $\boldsymbol{tp_{month}}$ is the average monthly temperature for month 1 to 12 given in the parameter file. $\boldsymbol{HC}$ makes adjustments for deviations from standard vegetations' height in the catchment. The layer where the vapour exchange takes place is thicker in high forest than in low forest. The air movements increase with elevation above the ground, see for example Dingman (2002) and contribute to a higher vapour exchange where the trees are high. Usually high vegetation also has a bigger interception reservoir, which makes more water available for evapotranspiration. The adjustment for differences in vegetation height is expressed:

$$\boldsymbol{HC} = 1.0 + \boldsymbol{ehgt} \times (\boldsymbol{VH} - \boldsymbol{dvh}) \qquad \textit{(Eq. 8.9)}$$

where $\boldsymbol{ehgt}$ is the evapotranspiration dependency of deviation from standard vegetation height, $\boldsymbol{VH}$ is the average vegetation height in the area element under consideration and $\boldsymbol{dvh}$ is the standard vegetation height in the catchment.

Wind speed will also influence the potential evapotranspiration, and is corrected by the following formula:

$$WC = 1.0 + \boldsymbol{ew} \times w \qquad \textit{(Eq. 8.10)}$$

where $\boldsymbol{ew}$ is the dependency of changes in wind speed on potential evapotranspiration. w is the observed wind speed. If daily wind data are not available, average wind speed for the actual month, $wp_{1,\ldots 12}$, is used. In addition, there is a reduction factor for a rainfall event. The potential evapotranspiration decreases during rainfall events due to increased vapour pressure. The correction is expressed by the formula:

$$\begin{aligned} PC &= 1.0 && \text{for } P = 0.0 \\ PC &= \boldsymbol{epr} && \text{for } P > 0.0 \end{aligned} \qquad \textbf{\textit{(Eq. 8.11)}}$$

where $\boldsymbol{epr}$ is a reduction factor for potential evapotranspiration during days with rainfall events.

Interception and evapotranspiration in the vegetation

The rainfall events occurring at the individual area elements are corrected for intercepted precipitation, first in the high and then in the low vegetation according to Rinde (1999). The water in the high vegetation is assumed to evaporate first; thereafter the water from the low vegetation and the water from the soil zone will do so, until the evapotranspiration reaches the potential level for evapotranspiration. The routine for the high and the low vegetation is illustrated on Figure 8.5.

The precipitation is first used for filling up the interception reservoir in the high vegetation. The precipitation not intercepted in the high vegetation, forms throughfall to the low vegetation below. The throughfall from the high vegetation, TFH is calculated according to the following formula:

$$THF = P - (\boldsymbol{HIC} - HI') \,\Big|_{\min=0.0} \qquad \textbf{\textit{(Eq. 8.12)}}$$

where P is the precipitation in the area element under consideration, $\boldsymbol{HIC}$ is the interception capacity in the high vegetation and HI' is the intercepted precipitation in the high vegetation from the previous time step. The throughfall has a minimum value of zero. The actual interception in the high vegetation is calculated according to the formula:

$$HI = HI' + P - AEH \,\Big|_{\min=0.0}^{\max=\boldsymbol{HIC}} \qquad \textbf{\textit{(Eq. 8.13)}}$$

where HI is the intercepted precipitation with a minimum value of zero and maximum value of $\boldsymbol{HIC}$, interception capacity. HI' is the remaining intercepted water from the previous time step which has not evaporated. The precipitation, P, in the time step under consideration is added to the remaining water in the interception reservoir and together they form the total amount of intercepted water. The actual evaporation of the intercepted water in the high vegetation AEH is given by the formula:

$$AEH = PE \times \mathbf{VC} \Big|_{\min=0.0}^{\max=\mathbf{HIC}} \qquad \textit{(Eq. 8.14)}$$

where $\mathbf{VC}$ is the coverage of high vegetation on the area element under consideration. The evapotranspiration from the high vegetation can have a minimum value of zero and a maximum value equal to $\mathbf{HIC}$ depending on the conditions.

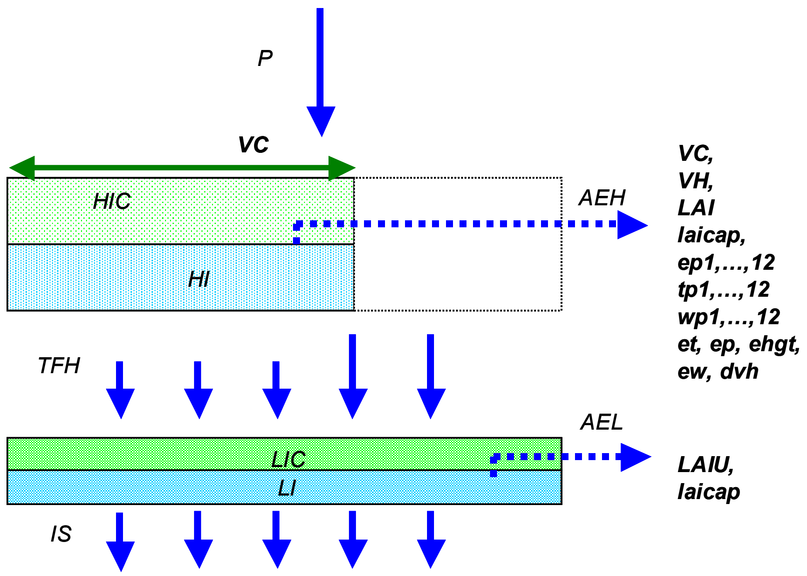

Figure 8.5: Illustration of the routine for high and low vegetation interception for each area element.

The throughfall from the high vegetation will be used for filling up the interception reservoir in the low vegetation that is the grass, crops and other vegetation on the surface. The outflow from the low vegetation is the precipitation not intercepted by the low vegetation and forms the inflow to the soil zone:

$$IS = TFH - (\mathbf{LIC} - LI') \Big|_{\min=0.0} \qquad \textit{(Eq. 8.15)}$$

where TFH is the throughfall from the high vegetation, $\mathbf{LIC}$ is the interception capacity in the low vegetation and LI' is the intercepted precipitation in the low vegetation from the previous time step. The inflow to the soil zone, IS, has a minimum value of zero. The interception in the low vegetation, LI, is:

$$LI = LI' + TFH - AEL \Big|_{\min=0.0}^{\max=\boldsymbol{LIC}} \qquad \textit{(Eq. 8.16)}$$

where LI' is the remaining intercepted water in the low vegetation from the previous time step which has not evaporated, TFH is the throughfall from the high vegetation and AEL is the actual evapotranspiration from the low vegetation. LI has a minimum value of zero and a maximum value equal to $\boldsymbol{LIC}$ depending on the availability of precipitation for filling up the interception reservoir. The actual evapotranspiration from the low vegetation is calculated as follows:

$$AEL = PE - AEH \Big|_{\min=0}^{\max=\boldsymbol{LIC}} \qquad \textit{(Eq. 8.17)}$$

where PE is the potential evapotranspiration for the whole catchment, and AEH is the actual evapotranspiration from the high vegetation and is subtracted from the PE so that total actual evapotranspiration does not exceed PE. AEL has a minimum value of zero and maximum value $\boldsymbol{LIC}$.

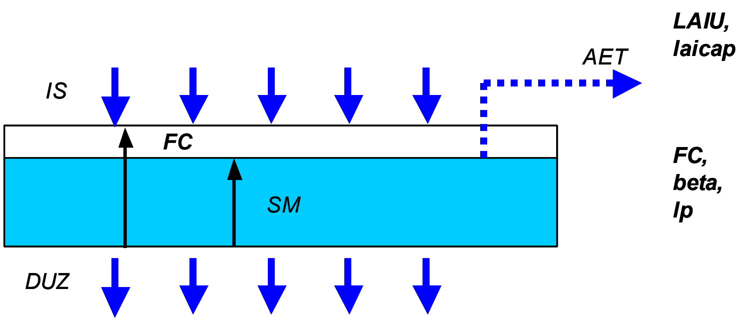

Figure 8.6: Illustration of the soil moisture routine.

Soil moisture

The soil zone routine illustrated on Figure 8.6 has a non-linear response equivalent to the HBV-model (Bergstrøm & Forsman, 1973). The maximum storage capacity in the soil zone is defined by the distributed parameter $\boldsymbol{FC}$, field capacity. The inflow to the soil zone, IS, is used partly for increasing the saturation of the soil zone and partly for runoff and increase of the global groundwater reservoir. The soil zone is drained through evapotranspiration. The evapotranspiration rate depends on the relative saturation of the soil zone. The water balance for the soil zone can be expressed by :

$$SM = SM' + IS - DUZ - AET \Big|_{\min=0}^{\max=\boldsymbol{FC}} \qquad \textbf{\textit{(Eq. 8.18)}}$$

where SM is the soil moisture content of the soil zone, SM' is the soil moisture content from the end of the previous time step, IS is the inflow to the soil zone from the low vegetation, DUZ is the outflow from the soil zone, or more correctly the inflow to the soil zone not used for increasing the soil moisture and AET is the evapotranspiration from the soil zone. The soil moisture has a minimum value of zero and a maximum value equal to the field capacity, which describes the maximum water storage capacity in the soil zone. If the soil moisture increases above $\boldsymbol{FC}$, then the excess water is added to the outflow from the soil zone.

The outflow from the soil zone, DUZ is described as:

$$DUZ = IS \times \left(\frac{SM}{\boldsymbol{FC}} \right)^{\boldsymbol{\beta}} \qquad \textbf{\textit{(Eq. 8.19)}}$$

where IS is the inflow from the low vegetation, SM is the soil moisture, $\boldsymbol{FC}$ is the field capacity and $\boldsymbol{\beta}$ is the parameter describing the non-linearity of the soil moisture zone. The evapotranspiration from the soil zone is described by:

$$AET = (PE - AEH - AEL) \times SMC \qquad \textbf{\textit{(Eq. 8.20)}}$$

where AET is the evapotranspiration from the soil zone, PE is the potential evapotranspiration for the area element under consideration, AEH is the actual evapotranspiration from the high vegetation, AEL is the actual evapotranspiration from the low vegetation and SMC is a correction factor reducing transpiration from the soil zone at low soil moisture content. The correction factor is:

$$SMC = \left(\frac{SM}{\boldsymbol{lp} \times \boldsymbol{FC}} \right) \Big|_{\min=0.0}^{\max=1.0} \qquad \textbf{\textit{(Eq. 8.21)}}$$

where SM is the soil moisture, $\boldsymbol{FC}$ is the field capacity and $\boldsymbol{lp}$ is the threshold for full evapotranspiration from the soil zone. It results in a linear decline in the evapotranspiration from the soil zone when the SM falls below $\boldsymbol{lp} \times \boldsymbol{FC}$.

Global groundwater recharge and water demand

The outflow from the soil zone, DUZ, is distributed between the two components river discharge and recharge of the global groundwater reservoir as illustrated in Figure 8.7. The global groundwater reservoir makes it possible to model a situation where infiltration in one part of the catchment forms a concentrated spring yield in other parts of the catchment or in a neighbouring catchment. The contribution to the global groundwater recharge from the area element under consideration is:

$$GW = DUZ \times \boldsymbol{GGRC} \qquad \textbf{\textit{(Eq. 8.22)}}$$

where GW is the global groundwater recharge from the area element under consideration, DUZ is the outflow from the soil zone and $\boldsymbol{GGRC}$ is the relative distribution between global groundwater recharge and river discharge. $\boldsymbol{GGRC}$ can have a value between 0 and 1. It is a distributed parameter found through the calibration process. For determination of the global groundwater reservoir for the whole catchment, the contributions from all area elements are summarized and added to the global groundwater reservoir:

$$gws = gws' + \left(\frac{1}{n}\sum_{i=1}^{n} GW\right) - q_{gws} \qquad \textbf{\textit{(Eq. 8.23)}}$$

where gws is the storage in the global groundwater reservoir, gws' is the storage in the global groundwater reservoir at the end of the previous time step, GW is the contribution from the area element and time step under consideration and n is the number of area elements in the catchment.

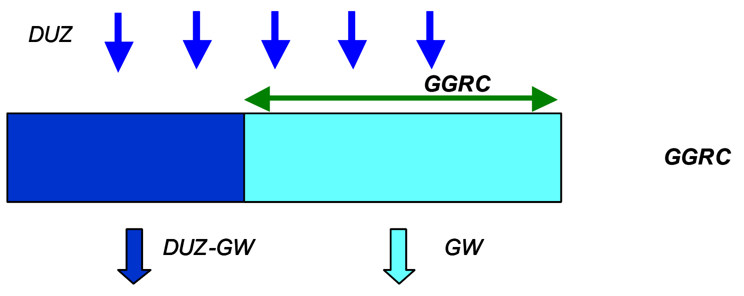

Figure 8.7: Illustration of the routine for global groundwater recharge and runoff response distribution.

The irrigation demand in the catchment is expressed as a distributed parameter defining the water demand in each area element. The irrigation demand varies over the season from its maximum value during the growing season towards zero in the fallow season. The total water demand in the whole catchment due to irrigation demand in a given time step is:

$$awd = \frac{1}{n}\sum_{i=1}^{n} \mathbf{WD} \times wd_m \qquad \textit{(Eq. 8.24)}$$

where awd is the average water demand in the catchment, $\mathbf{WD}$ is the water demand for the area element under consideration, wd_m is a correction factor depending on the month under consideration varying from $m = 1,....,12$ and n is the number of area elements in the catchment. The water demand in a catchment is illustrated in Figure 8.8 where the water demand is described for each area element in the grid and summarized for finding the total demand from the catchment.

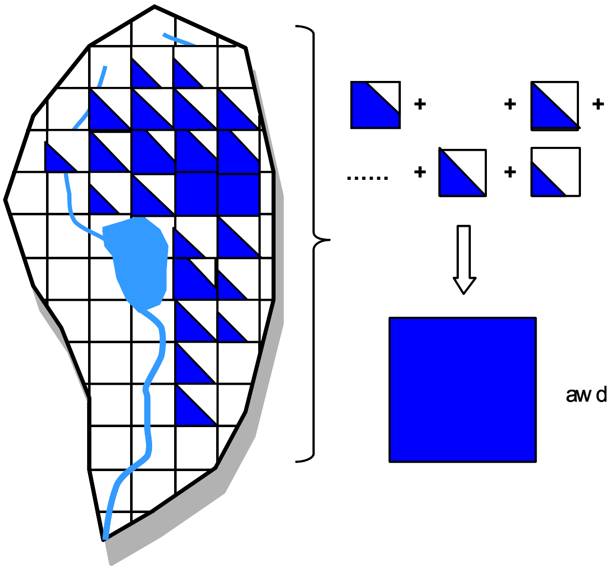

Figure 8.8: Illustration of water demand for the catchment. The distributed value is summed up for finding the total demand for the whole catchment.

From catchment runoff to actual river discharge

The response from the catchment forming the river discharge is not described in a distributed way, meaning that the present model does not calculate lateral water transport between grid cells within the catchment. Instead, a simplified response function using a lumped averaged value over the catchment as a whole is applied. The total response function including both the river discharge and the groundwater yield from the model is illustrated in Figure 8.9. The entire contribution from all the area elements is summarized and forms an input to the response routine for the river discharge or input to the global groundwater reservoir. The water is depleted through both response routines, and compensated for by water demand in the catchment before forming the river discharge at the outlet of the catchment.

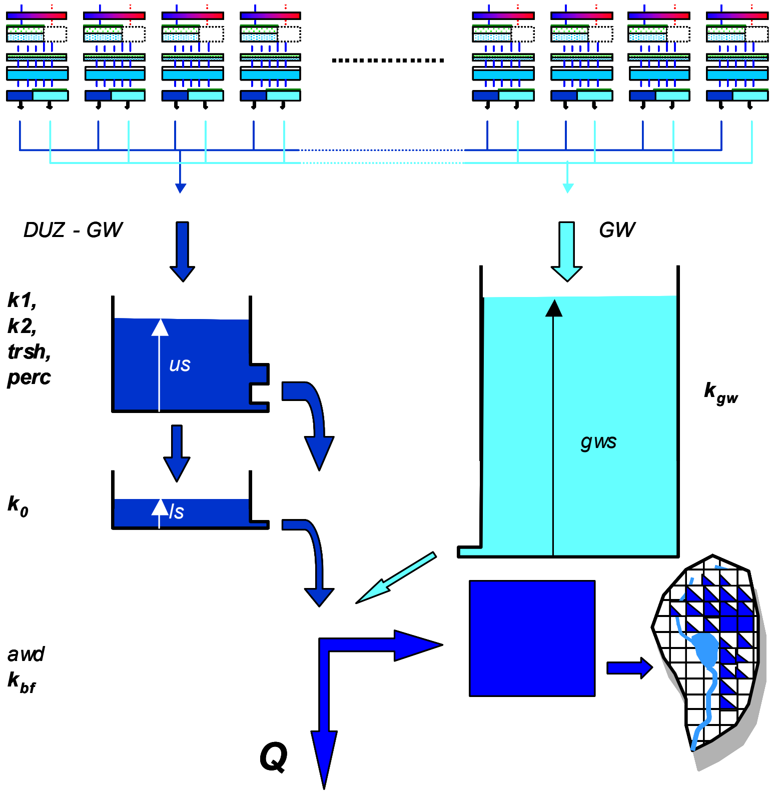

Figure 8.9: Illustration of the response function in the model. The distributed vertical water balance sends water to direct catchment response and global groundwater recharge. Water demand is subtracted before final river discharge is obtained.

The inflow to the response routine for river discharge is:

$$aduz = \frac{1}{n}\sum_{i=1}^{n}\left(DUZ - GW\right) \qquad \textbf{\textit{(Eq. 8.25)}}$$

where $aduz$ is the average inflow to the lumped response routine, DUZ is the outflow from the soil zone from each area element, GW is the global groundwater recharge contribution from each area element and n is the number of area elements in the catchment under consideration.

The upper and the lower zones forming the river discharge component of the runoff from the catchment are equal to the response functions in the HBV model (Bergstrøm & Forsman, 1973). The river discharge is represented through a lumped value for the whole catchment under consideration, but can also be found for sub-basins depending on the distribution of catchment borders within the model. Though lateral water transport is not described in a distributed fashon in the model, lumped values for sub-basins can be found and describe the discharge in sub-catchments. If required, a routing function can be established between the sub-catchments for a better simulation of the resulting runoff hydrograph from the catchments. A routing function would improve the simulation of the runoff hydrograph from the catchment, particularly if shorter time steps were applied. However, with the present 24-hours time step, routing procedures were found unnecessary.

The lower zone represents groundwater reservoirs and lakes along the rivers and the upper zone represent rivers and canals in the catchment. The upper zone will drain away relatively fast, while the lower zone will represent a base flow in the dry season and form the "local" groundwater depletion. The outflow from the response routine is given by the following three equations:

$$q_l = \boldsymbol{k_0} \times lz \qquad \textbf{\textit{(Eq. 8.26)}}$$

$$q_{u1} = \boldsymbol{k_1} \times uz \qquad \textbf{\textit{(Eq. 8.27)}}$$

$$q_{u2} = \boldsymbol{k_2} \times (uz - \boldsymbol{trsh}) \,\Big|_{\min=0.0} \qquad \textbf{\textit{(Eq. 8.28)}}$$

with total outflow from the response routine:

$$q_r = q_l + q_{u1} + q_{u2} \qquad \textbf{\textit{(Eq. 8.29)}}$$

where $\boldsymbol{k_0}$ is the recession coefficient for the lower zone, $\boldsymbol{k_1}$ is the recession coefficient for the slow outlet from the upper zone, $\boldsymbol{k_2}$ is the recession coefficient for the fast outlet from the upper zone. q_l, q_{u1} and q_{u2} are the corresponding outlet, $\boldsymbol{trsh}$ is the threshold for fast outflow from the upper zone, uz is the storage in the upper zone and lz is the storage in the lower zone. The water balance for the upper zone gives the following storage:

$$uz = uz' + aduz - \boldsymbol{perc} - q_{u1} - q_{u2} \Big|_{\min=0.0} \qquad \textit{(Eq. 8.30)}$$

where uz' is the storage at the end of the previous time step, $perc$ is the percolation from the upper zone to the lower zone. The water balance for the lower zone give the following storage:

$$lz = lz' + \boldsymbol{perc} - q_l \qquad \textit{(Eq. 8.31)}$$

where lz' is the storage at the end of the previous time step. The percolation only takes place when there is enough water available in the upper zone. If there is no water stored in the upper zone, there will be no percolation to the lower zone.

The outflow from the global groundwater reservoir or the spring yield in the catchment, q_{gws}, is:

$$q_{gws} = \boldsymbol{k_{gw}} \times gws \qquad \textit{(Eq. 8.32)}$$

where $\boldsymbol{k_{gw}}$ is the recession coefficient for the global groundwater reservoir and gws is the storage in the global groundwater reservoir.

The total discharge at the outlet of the catchment is found by adding up q_r, the outflow from the response routine, awd, the average water demand and q_{gws}, the contribution from the global groundwater reservoir. A routine for utilisation of the groundwater yield is incorporated in the final stage of the model. In this particular case the reason is the exceptional groundwater yield found at Chemka Spring, see Figure 7.1 or Figure 8.11 for location. The off take between the spring and the gauging stations is limited. In the general case, this routine can also secure restrictions on the groundwater utilisation if this is desired.

A limit on the groundwater utilisation is therefore incorporated in the final stage of the model. The simulated runoff from the catchment by the model will therefore be:

$$Q = Q_{CR} + \boldsymbol{k_{bf}} \times q_{gws} \quad \textit{(Eq. 8.33)}$$

where

$$Q_{CR} = (q_r + (1 - \boldsymbol{k_{bf}}) \times q_{gws} + awd)\big|_{\min = 0} \quad \textit{(Eq. 8.34)}$$

and $\boldsymbol{k_{bf}}$ is the coefficient for the distribution of groundwater yield between the conserved base flow and the utilised spring resources within the catchment. The value $(1 - \boldsymbol{k_{bf}})$ therefore represents the part of the spring yield that can be withdrawn from the river and utilised within the catchment above gauging station 1DD1. Naturally, additional utilisation of the spring yield can be made further down in the river below the gauging station. The value Q is the simulated river discharge at the outlet of the catchment under consideration. The introduction of $\boldsymbol{k_{bf}}$ secures a correct representation of the groundwater based base flow during the dry season. $\boldsymbol{k_{bf}}$ is found through calibration. However, it only applies to the biggest of the three catchments where the groundwater yield is more extensive than in the two smaller catchments. In the smaller catchment, Charongo and Ngomberi, the groundwater yield is ignored in the simulation model.

8.3.2 Parameters

Both lumped and distributed parameters are utilized in the model. A range of distributed parameters describes the land use and the physiographic conditions in the catchment. Table 8.2 shows an overview of the distributed parameters utilized in the model. The confined distributed parameters can be determined from map-studies alone or in combination with analysis of the vegetation. An example of these parameters is illustrated in Figure 8.10 for the catchment above gauging station 1DD1. The elevation and the coverage of high vegetation are shown on the figure. Both parameters are found from map studies and used in the calculation. The free distributed parameters cannot be found through any map study and must be determined through a process of calibration.

The free distributed parameters found through calibration are for example the Field Capacity, FC, and the relative distribution of water from soil zone to groundwater recharge or runoff response, $GGRC$. In principle, the free distributed parameters can vary independently from one pixel to another. However, for example the FC is assumed to vary with the border of the vegetation cover. The border for change of the FC will follow the vegetation border.

Name	Unit	Description
EL	m	Elevation
FC	mm	Field capacity
GGRC	-	Relative distribution from soil to groundwater recharge
LAILOW	-	Leaf area index for undershrub
LAI	-	Maximum leaf area index
LU	-	Landuse - land or water
VC	%	Coverage of high vegetation
VH	m	Average tree height
WD	mm	Water demand
ISS	%	Initial soil saturation at start of simulation

Table 8.2: The distributed parameters applied in the simulation model.

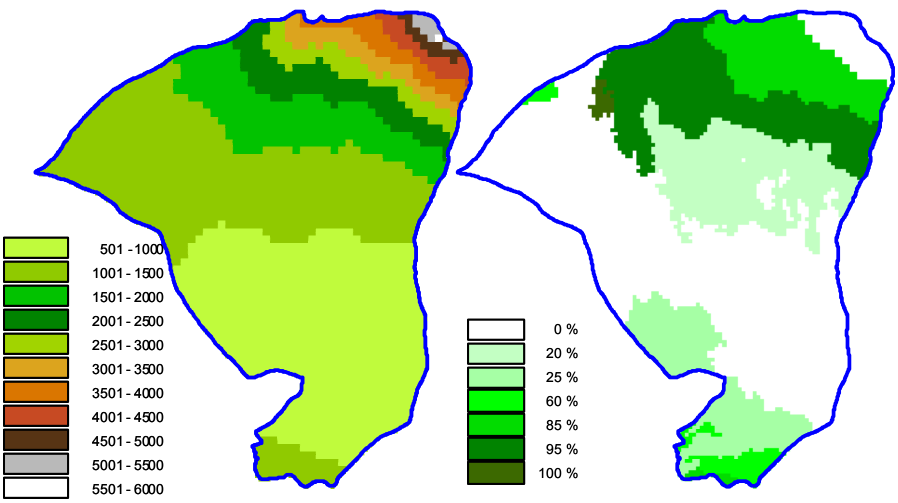

Figure 8.10: Example of distributed parameters applied in the model. The elevation is shown on the left and the coverage of high vegetation is shown on the right.

The lumped parameters and some lumped input or initial values are shown in Table 8.3. Some meteorological input data and initial conditions are given in the upper part

URN:NBN:no-3437

of the table. Also coordinates for the meteorological stations applied in the simulations are given.

Name	Unit	Description
Input and initial data for model		
$ep_{1,...,12}$	mm/d	Normal potential daily evapotranspiration for month 1-12
$tp_{1,...,12}$	^{o}C	Normal daily temperature for month 1-12
$wp_{1,...,12}$	m/s	Normal wind speed for month 1-12
us	*mm*	*Initial storage in upper tank*
ls	*mm*	*Initial storage in lower tank*
gws	*mm*	*Storage in global groundwater reservoir*
Coordinates for precipitation and temperature stations		
Nt_1, Np_1,…	m	North coordinate for temperature and precipitation stations
Et_1, Ep_1,…	m	East coordinate for temperature and precipitation stations
Ht_1, Hp_1,…	masl	Elevation for temperature and precipitation stations
Parameters for precipitation correction		
r_c	-	Point correction for precipitation
$pl_{a,...,d}$	-	Constants for correcting precipitation in lower areas (Eq. 6.11)
pb	masl	Elevation for change of cor. funct. for precip. (From Eq. 6.11 to Eq. 6.12)
$ph_{a,b}$	-	Constants for correcting precipitation in higher areas (Eq. 6.12)
Parameters for temperature correction		
t_{ch}	$^{o}C/100m$	Temperature lapse rate in higher areas
t_{cl}	$^{o}C/100m$	Temperature lapse rate in lower areas
tb	masl	Elevation for change of laps rate for temperature (From t_{cl} to t_{ch})
Parameters for calculating the evapotranspiration		
laicap	mm/m^2	Storage capacity per LAI
et	-	Dependency of potential evapotranspiration on temperature
epr	-	Relative magnitude of pot. evap. during precipitation
dvh	m	Average vegetation height
ehgt	-	Dependency of pot. evap. on average vegetation heigth
ew	-	Dependency of pot. evap. on wind speed
lp	-	*Threshold value for pot. evap. from soil moisture*
Parameters for calculating the runoff-response		
$wd_{1,...,12}$	-	Water demand correction for month 1-12
β	-	*Non-linearity of soil water retention curve*
k_2	-	*Fast outflow coefficient for upper tank*
k_1	-	*Slow outflow coefficient for upper tank*
k_0	-	*Slow outflow coefficient for lower tank*
perc	*mm/stp*	*Percolation from upper to lower tank*
trsh	*mm*	*Threshold heigth for fast outflow from upper tank*
Parameters for calculating the groundwater reservoir response		
kgw	-	*Recession coefficient of the groundwater reservoir*
k_{bf}	-	*Distribution between utilisable and non-utilisable spring yield*

Table 8.3: The lumped parameters and the input data applied in the simulation model.

URN:NBN:no-3437

Furthermore, the parameters are sorted according to which routine they are first applied. The confined parameters are shown in regular font and the free parameters in italic.

The confined parameters are found though an evaluation of observations from the catchment, literature, maps or consideration of the physical processes occurring in the catchment. The lumped parameters found through the calibration process are related to the evapotranspiration and recharge from the soil zone, the response function forming the runoff hydrograph from the catchment and the groundwater processes. This is done in addition to setting the initial conditions at the start of the simulation period.

Station	Precipitation	Temperature	Discharge
9337004	X		
9337021	X		
9337028	X	X	
9337115		X	
Gauge 2 (See Figure 4.2 or Figure 8.11)		X	
Gauging station at Charongo			X
Gauging station at Ngomberi			X
Gauging station 1DD1			X

Table 8.4: Input data used for development and calibration of the model. The discharge is utilised for the respective catchments. The discharge data is only applied for the respective catchments.

8.4 Simulation and calibration procedure

8.4.1 Input data

For securing a wide area of application, the amount of input data for the model is kept low. The majority of the input data are time series of precipitation and temperature from meteorological stations in the area. Wind data can also be utilised if present, but they are not required. The input data used in the model, is shown in Table 8.4. All the input data are lumped. In addition results from the stream gauging of three different catchments is utilised for the evaluation of the model performance during the calibration procedure.

8.4.2 Simulation

The hydrological model was calibrated for the three different catchments Charongo, Ngomberi and 1DD1. The catchments can be seen in figure Figure 8.11 with the biggest catchment above station 1DD1 and the smaller Ngomberi and Charongo

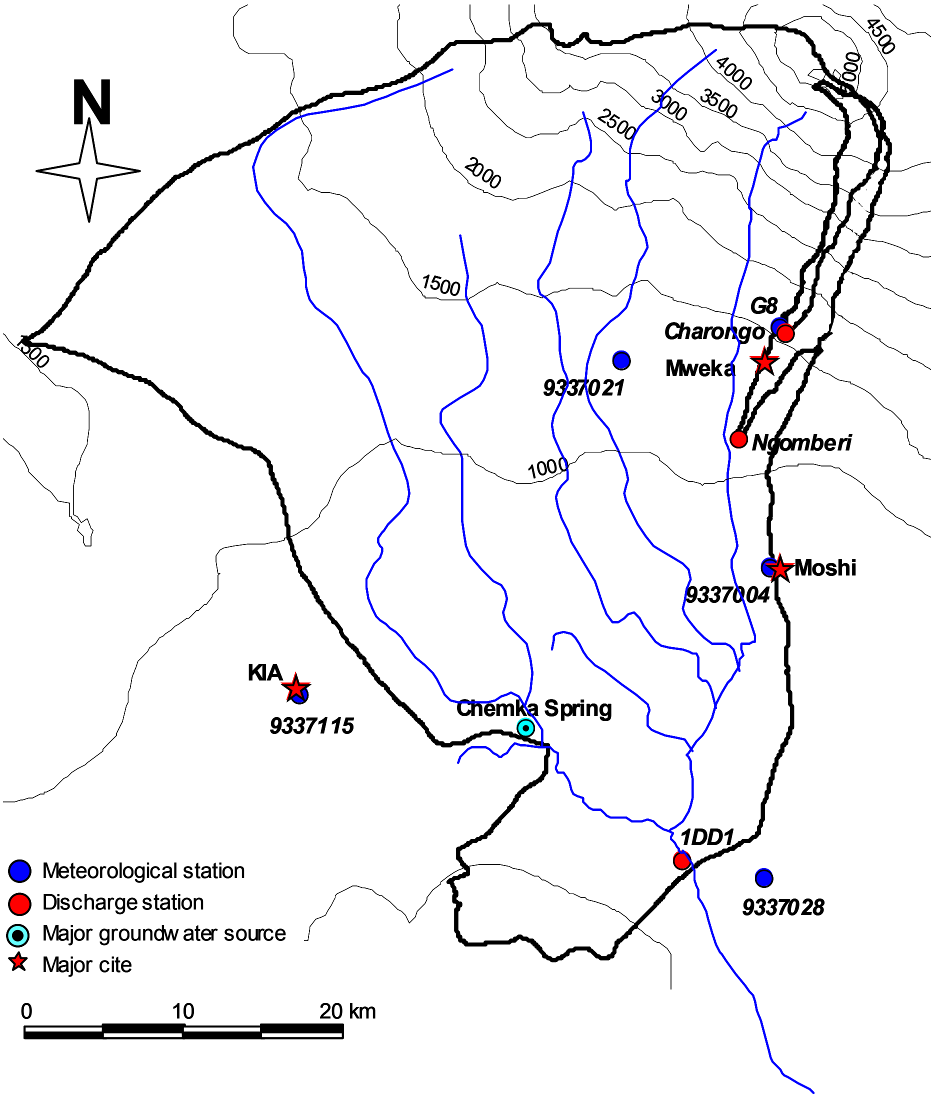

Figure 8.11: Map showing location of the three catchments for which the model was calibrated. The Charongo, the Nbomberi and the 1DD1 catchment. Meteorlogical and discharge stations applied in the simulation are shown on the map.

catchment contained within it on the southern slopes of Mt Kilimanjaro. Details on the catchments are given in Table 8.5. In principle, the calibration procedure was as shown in Figure 2.2. Firstly, a smaller catchment in the upper hillside was calibrated. The parameters found for the smaller catchment, were then used for comparable features in the bigger catchment. For example, the FC found for the forest in Charongo, were also applied for the forest in Ngomberi within the same elevation interval. Furthermore, the parameters found for the agricultural areas in Ngomberi, were also applied for the agricultural areas in the 1DD1 catchment for the same elevation interval. These parameters, which were found in the smaller catchment, and later applied in the larger, were not changed during the calibration process of the larger catchment. In principle, the distributed parameters in the hatched area in Figure 2.2 were not calibrated further. However, some of the lumped parameters in the response routine were changed during the calibration process.

Parameter	Unit	Catchment		
		Charongo	Ngomberi	1DD1
Catchment size	km^2	21	52	1783
Max elevation	masl	5895	5895	5895
Mean elevation	masl	3940	2602	1211
Min elevation	masl	1640	1080	700
Length	km	16	23	52
Timestep	hrs	24	24	24

Table 8.5: Details of the three catchment the simulation model was calibrated for.

8.4.3 Tools applied

The source code of the model was written and compiled within the Microsoft Visual C++ system, version 6.0. The map analysis was performed by use of the ArcView GIS, version 3.1 from Environmental Systems Research Institute, ESRI and partly the Grassland GIS, version 1.1 from Logiciels et Aplications Scientifique Inc. In addition, regular text editors were used to edit the parameter files for the simulation model and various spreadsheet solutions were developed for facilitation of comparison and evaluation of the simulated discharges.

8.4.4 Evaluation of simulations

The observed values of river runoff were compared with the simulated values from the model described above. Various criteria and methods were used for determination of the goodness of fit for developing as well calibrated model as possible. Some are:

- Study of time series plot
- R^2, explained variance
- Control of water balance
- Calibration of sub-catchments

The time series plot is the subjective method to decide the goodness of fit between the observed and the simulated discharge. It gives good indications of how the model simulates the discharge compared to the observed values and is particularly helpful during the first part of the calibration process. The explained variance can be used to determine smaller changes in fit, which are difficult to work out from a time series plot. The explained variance is given by the equation:

$$R^2 = \frac{\sum\left(Q_o - \overline{Q_o}\right)^2 - \sum\left(Q_s - Q_o\right)^2}{\sum\left(Q_o - \overline{Q_o}\right)^2} \qquad \textit{(Eq. 8.35)}$$

where Q_o is observed discharge, $\overline{Q_o}$ is average observed discharge and Q_s is simulated discharge. Explained variance is also named the Nash-Sutcliffe efficiency criterion. R^2 may vary from $-\infty$, to 1.0 for a perfect model. See ASCE (1996) and Maidment (1993) for further details.

The control of the water balance is given by:

$$\Delta Q = \sum\left(Q_o - Q_s\right) \qquad \textit{(Eq. 8.36)}$$

The ΔQ, the accumulated difference between observed and simulated discharge, should be as small as possible. It will ensure that the simulation model produces the same runoff as the natural system with the same input.

Calibration of sub-catchments is by first calibrating the Charongo catchment, thereafter the Ngomberi and lastly the 1DD1 catchment.

The internal states in the model are also considered during the calibration procedure and their values evaluated. This evaluation is based on the subjective experience and opinions of the author. Several combinations of parameters can simulate the runoff pattern of the catchment. However, inspection and plot of the internal states and results of the model can exclude the combinations of parameters, which have little or no interest. This can for example be the case for changes in groundwater storage where a continuous increase in the storage through the calibration period is an unrealistic pattern.

8.5 Results from the calibration

The results from the calibration of the three catchments are shown in Figure 8.12, Figure 8.13 and Figure 8.14. The best fit is evaluated on the basis of objective and subjective criteria as described above.

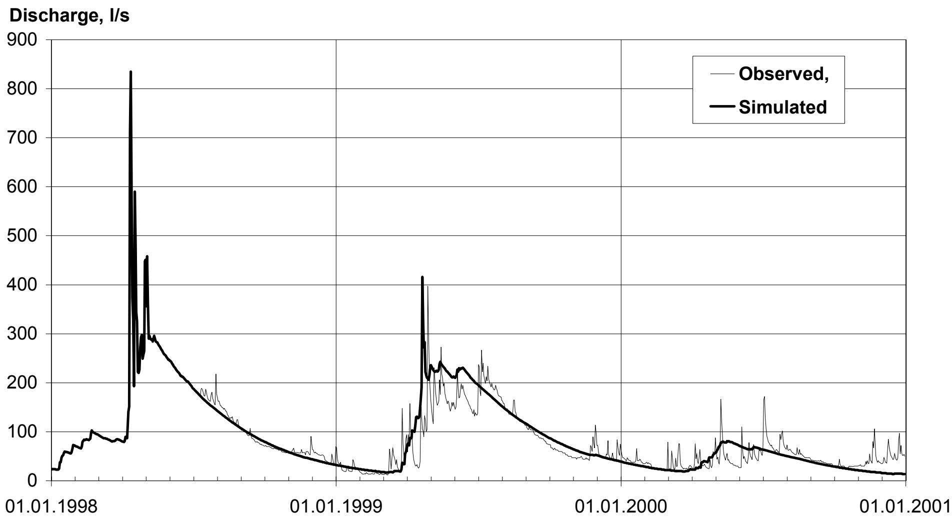

Figure 8.12: The result from the calibration of the Charongo catchment.

8.5.1 A catchment on the upper slopes

The small Charongo catchment on the upper slopes of Mt Kilimanjaro was calibrated first. The result from the calibration period can be seen in Figure 8.12. The simulated discharge shows a relatively good fit with the observed discharge. The model simulates an increase in discharge during the beginning of the wet season, and the recession afterwards for the two first seasons. However, during the third season, the simulated low flow discharge is too low.

8.5.2 On the mid slopes

The bigger Ngomberi catchment was then calibrated using the knowledge obtained from the Charongo catchment. The distributed parameters found through calibration of the Charongo catchment were applied for the Ngomberi catchment for similar land use conditions, e.g. field capacity for the forest and the relative distribution between global groundwater recharge and catchment runoff. The result from the calibration is shown in Figure 8.13. The model simulates the increased discharge at the beginning of the wet season and the recession curve afterwards. However, during the third season, the model tends to overestimate the discharge dramatically compared to the actually observed discharge. This is discussed below.

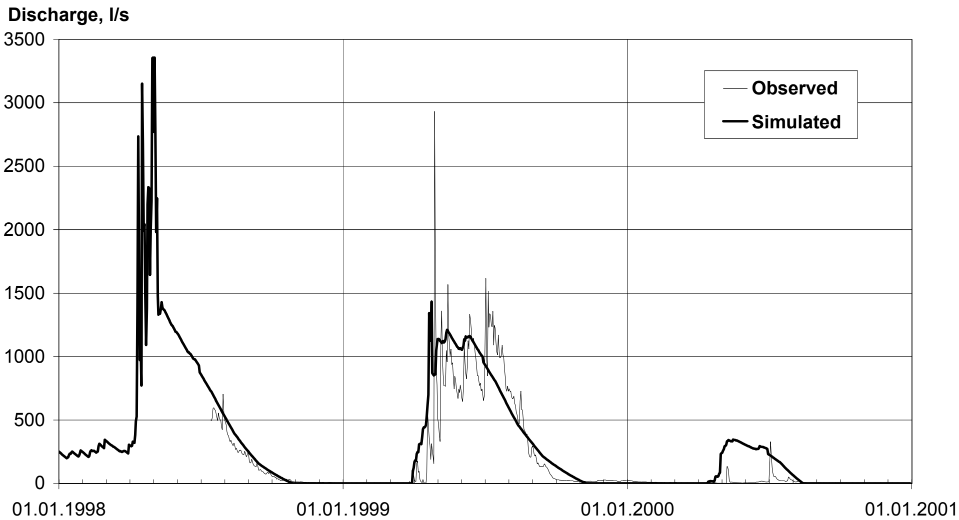

Figure 8.13: The result from the calibration of the Ngomberi catchment.

8.5.3 From the plains to the peak

Finally the whole catchment above gauging station 1DD1 containing the two other catchments, was calibrated. The distributed parameters found for the Ngomberi catchment, were applied for the 1DD1 catchment in the same manner as from the upper to the mid slopes catchment. The result from the calibration procedure is shown in Figure 8.14. The model simulates well the river discharge based on the meteorological input to the model. Both the rise in discharge during the start of the wet season and the recession afterwards is simulated well by the model. Also the simulated discharge in the low flow period shows a good agreement with the observed discharge. The model does not simulate some rainfall events in the recession period properly, for example in November-December 1999.

The sudden increase in observed discharge found in March 1999, cannot be traced to any precipitation events. No precipitation events, which can explain such a sudden increase in discharge, can be found in the preceding days. An error in the observation material is therefore the most probable reason for the sudden change, but verification of this assumption has not been possible. Also, this event cannot be seen at any of the above-located measurements.

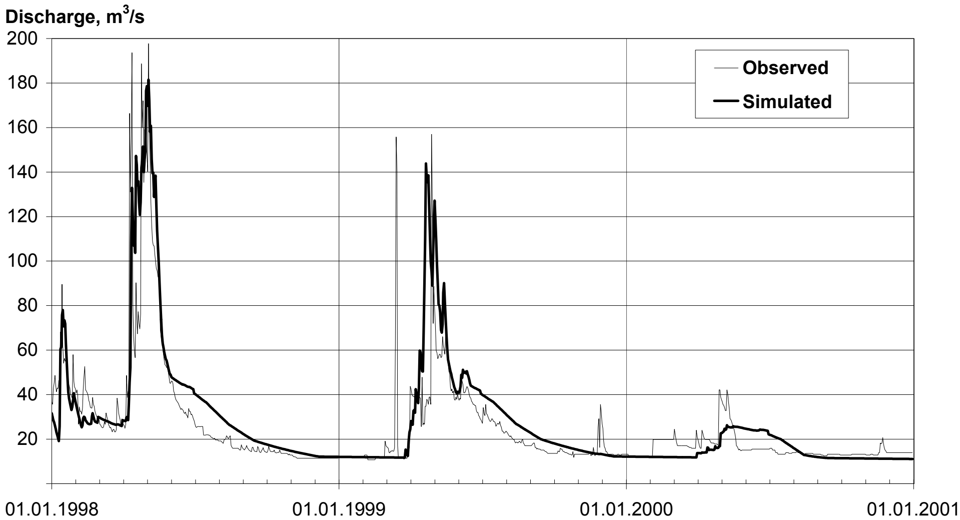

Figure 8.14: The result from the calibration of the 1DD1 catchment.

The results from all the simulations are summarised in Table 8.6, which also give the objective criteria, R^2 for fit between simulated and observed values. The observed and simulated discharges are averaged for each month of the simulation period. The average value shows relatively good accordance except for the Ngomberi catchment where there is a small deviation. The explained variance varies between 0.60 and 0.71.

Year-Month	Charongo		Ngomberi		1DD1	
	Observed l/s	Simulated l/s	Observed l/s	Simulated l/s	Observed m^3/s	Simulated m^3/s
1998-01		45		230	48.8	42.2
1998-02		83		256	36.8	28.8
1998-03		86		281	27.3	27.6
1998-04		271		1305	89.9	95.2
1998-05		297		1658	93.9	107.8
1998-06		218		1054	35.3	45.1
1998-07		166		728	22.9	36.7
1998-08	137	126	312	385	18.0	26.2
1998-09	88	94	126	156	15.2	19.4
1998-10	65	69	33	39	14.1	16.2
1998-11	59	51	9	0	11.7	13.6
1998-12	49	38	6	0	11.4	12.1
1999-01	29	28	1	0	12.1	12.0
1999-02	15	21	0	0	11.4	11.9
1999-03	37	22	1	0	24.0	12.2
1999-04	99	155	275	550	43.3	68.2
1999-05	175	226	860	1127	55.7	72.2
1999-06	164	217	931	1092	38.1	45.1
1999-07	197	177	1077	813	28.0	37.0
1999-08	139	135	532	452	19.5	26.7
1999-09	94	103	143	215	15.4	20.0
1999-10	60	76	24	83	13.8	16.7
1999-11	54	57	18	4	15.2	14.1
1999-12	55	46	22	0	15.0	12.5
2000-01	44	34	15	0	12.0	12.1
2000-02	27	25	8	0	18.7	12.0
2000-03	35	21	5	0	17.7	11.9
2000-04	37	35	4	20	20.6	15.0
2000-05	52	74	18	315	26.2	24.9
2000-06	51	67	10	284	15.4	24.1
2000-07	81	58	55	170	14.1	20.1
2000-08	56	45	10	0	13.7	12.9
2000-09	38	34	5	0	13.1	11.5
2000-10	30	25	1	0	13.1	11.4
2000-11	42	19	0	0	14.3	11.3
2000-12	53	15	0	0	14.0	11.1
Average	71	72	155	197	25.3	27.7
R^2-value	0.65		0.71		0.60	

Table 8.6: Summary of post calibration simulation for the Charongo, Ngomberi and 1DD1 catchment showing monthly average discharge, average discharge and R^2-value.

8.6 Discussion of the modelling and the calibration results

The model tends to simulate the responses from the three catchments relatively well. The model simulates the increases in discharge during rainfall and subsequent recession periods quite well. The most apparent deviation between the simulated and observed discharge, is the smoothed simulated discharge versus the more flickering natural course found in the discharge observations. Also, "medium-extreme" rainfall events do not give any proper response in the simulation model.

The method of calculation applied by the model with the many linear tanks, tends to smooth out some of the responses compared to natural conditions. The simulation model somehow does not seem to be able to simulate fully the flexibility and dynamics of the natural system. This can also be seen in the recession period --- for example at the end of November 1999 --- where several rainfall events up to 26 mm influence the curve of the observed discharge, but the model does not simulate them properly.

Large spatial divergences in precipitation can give rise to local precipitation events and subsequent local runoff not reproduced by the model. A brief examination of the precipitation series from the three stations applied in the simulation shows that events with 40-50 mm of precipitation at the uppermost station may not have resulted in any precipitation at all at the lowermost station. The opposite is also the case; large precipitation events take place in the plains but do not reach the mountain slopes. Though precipitation is weighted with distance from the point of observation to the area element under consideration, all precipitation events observed at any station, will influence the calculation of precipitation in any area element. The description of the spatial distribution of precipitation in the model may deviate from the actual distribution in the field.

Direct errors in the observation of meteorological or stream gauge data can also result in unexpected results. For example, the discharge event on 15th March 1999 in Figure 8.14 can be due to such errors. No rainfall is observed at any of the three stations applied for the simulation for the three days preceding the peak event and the event cannot be traced on the discharge observations from any of the above gauging stations. It is difficult to see any reason for a tenfold increase in discharge over 2 days and then a sudden decrease to the pre-increase level.

On the other hand, the model does not simulate properly some events observed at all the three gauging stations simultaneously. This is the case for the event of 29th April 1999, which can be found as a peak on all the three curves with observed runoff. When inspecting the rainfall observations used in the simulations, there are no extreme rainfall events on this day compared to some days before or after. This can indicate that the error can be found in the precipitation observations and not in the simulation model.

However, the results here show that the model is capable of simulating the principal hydrological response from the catchment based on the meteorological data from the area. Figure 8.12, Figure 8.13, Figure 8.14 and Table 8.6 support this conclusion and summarise the results of the model development and calibration.

9. USE OF THE SIMULATION MODEL

9.1 Introduction to use of the simulation model

In this chapter, the simulation model developed for the 1DD1 catchment will be utilised for various studies in order to illustrate how the model can be used for planning purposes and as a tool in water management. The model will primarily be run for a long-term simulation of the catchment above the 1DD1 gauging station. Later, various land use and climatic change data will be introduced into the input data for the simulation model. The resulting hydrological response from the catchment above 1DD1 will thereafter be simulated. The land use and climatic change evaluated by the model are shown in Table 9.1. All scenarios are compared with the simulated present hydrological response of the 1DD1 catchment. One land use or climatic change is evaluated at a time. The change in temperature and precipitation is imposed on the input data series for the simulation. The land use changes are imposed on the distributed parameters of the model described in chapter 8. The present land cover situation in the basin based on Hunting Technical Services (1996) is shown in Figure 9.1. In addition, the changes in forest cover are illustrated with the black and red lines representing the border for the increased and the decreased area respectively.

Change	Increase	Decrease
Extend of forest cover around Mt Kilimanjaro	2 km downwards	2 km upwards
Water demand	10 %	10 %
Temperature	+2^{o}C	-2^{o}C
Precipitation	10 %	10 %

Table 9.1: Overview of feasible land use and climatic changes applied in simulation of the hydrologic response from the catchment above gauging station 1DD1 for the period 1958-2000.

The extent of the climatic changes concerning the increase in temperature and precipitation is based on the estimates in the IPCC reports by Watson (2001), Houghton et al. (2001) and McCarthy et al. (2001). However, their estimates vary depending on simulation model applied. The tendency is for increased temperature and precipitation. The simulation with decreased temperature and precipitation can contribute to identifying the sensitivity of these to the hydrological response from the catchment.

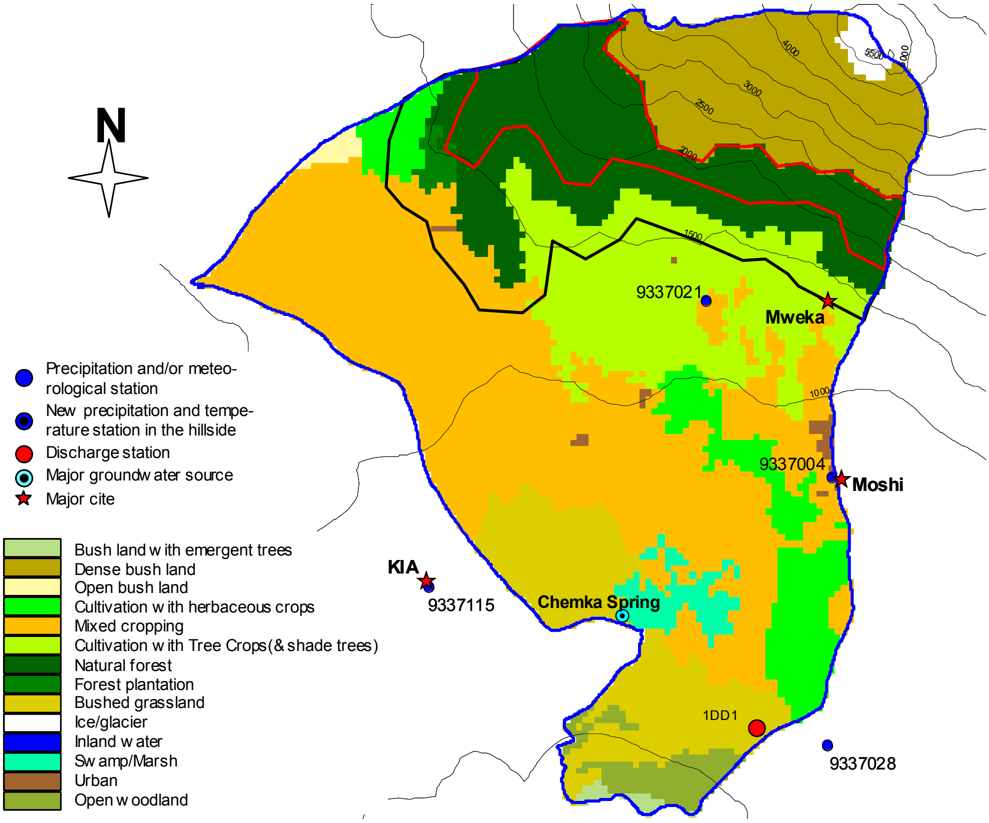

Figure 9.1: Present land use in the catchment above gauging station 1DD1. From Hunting Technical Services (1996). The two alternatives of change of forested area are shown with red and black line for 2 km decrease and 2 km increase of the forest area border respectively.

9.2 Simulation of the period 1958 to 2000

By collecting data from various sources, and filling in a smaller amount of temperature and runoff data and correcting some precipitation data with information from nearby stations, a continuous series of meteorological and discharge data from 1958 to 2000 was obtained. An summary of the source of data applied for the simulation can be seen in Table 9.2. For the temperature and precipitation data, observations from three different stations were used if available. If some data were missing from one station, then only the two others were utilised instead. For some periods, temperature or precipitation data from only one station was available.

The extent of the corrections in the meteorological data is shown in Table 9.3. The missing discharge data referred to the last day of February and whole March 1960. For simplicity's sake, the missing data was merely interpolated linearly for the missing period.

Station	Precipitation	Temperature	Discharge
9337021	X		
9337004	X	X	
9337028	X	X	
9337115		X	
1DD1			X

Table 9.2: Overview of source for meteorological data applied for simulation of the period 1958-2000.

Parameter	Missing data, days	Missing data, %
Discharge	32	0.20
Temperature	180	1.15
Precipitation	168	1.07

Table 9.3: Extent of missing or assumed wrong meteorological or discharge data which were filled inn or corrected.

The extent of missing temperature data was bigger. For some periods, there were no temperature data available for any of the three stations. For these cases, the average monthly temperature for the actual station based on the observations, was filled in. The missing temperature data generally appeared as an entire missing month, so that no observations were available for the actual month.

The precipitation records applied in the simulations were complete in that for no period was the record from all three stations missing at the same time. However, after the first run, the simulated discharge values from some precipitation events were rather extreme compared to the actually observed discharge. A thorough examination of the input data for these years, and a comparison of precipitation data from nearby stations revealed extremes, which were assumed incorrect. Precipitation observations can be found for nearby stations for two of the three precipitation stations and used for parts of the simulation period. One example is from station 9337028 for April 1978. The station is located on the lowland plain with an annual precipitation of about 500 mm/year. For April 1978, the observations indicate a total precipitation of about 1757 mm or about 3.5 times the annual precipitation in one month. Such extreme event can possibly take place, but would probably be reflected in the observations from nearby stations and in the discharge observations from gauging station 1DD1. When comparing the observations from April 1978 for station 9337028 with station 9337143 located some 11 km to the east, we see a total precipitation of 109 mm for April 1978. The two stations are located at the same elevation and within the same land use regime. Similar findings, although not so extreme were made for station 9337004 and station 9337091 located only 2 km apart at approximately the same elevation in the town of Moshi. In April 1984 where 554 mm of precipitation was observed at station 9337004, only 282 mm was observed at station 9337091.

On the basis of a plot from the first long-term simulation, years with extreme over- or underestimated simulated flow were investigated further and precipitation data was compared with nearby stations. In those cases where such extreme deviations were found, the entire month was replaced with the observations from the nearby stations. On some occasions it was not possible to compare, or to replace any data, so the original data was left unchanged. In total, precipitation data for three months each for station 9337004 and 9337028 was replaced in this way.

All the replaced precipitation data are for the month of April. That is also when the most intensive precipitation takes place. The number of precipitation events is bigger, the amount of precipitation is highest, and therefore the potential of making mistakes increase. During high precipitation events, the gauge reader may experience extreme precipitation events not common at other times of the year, and this may cause confusion and introduce errors in the recording. However, it is difficult today to investigate these events, which lie 20-40 years back in time.

The result from the simulation of the hydrological response from the catchment above gauging station 1DD1 for the period 1958 to 2000 is shown in Figure 9.4 where the parameters found during the calibration process described in chapter 8 were applied without any changes. Separate plots of the years referred to later in the text, are shown in the appendix. The plot of simulated and observed discharge on the figure, have an explained variance of R^2 = 0.26 for the whole simulation period. The average simulated discharge is 24.4 m^3/s and the average observed discharge for the same period is 24.5 m^3/s. The model simulates the annual flood peaks, but some deviations can be found. For example in the two years 1971 and 1981, the simulated peak is about twice the size of the observed peak. On the other hand, for example in

1965, 1966 and more recently in 1987, the simulated peak is only a fraction of the actual observed discharge. When considering the low flow discharge, the simulation shows good correspondence with the observed low flow, but the simulated low flow discharge is much smoother compared to the simulated flow. See later for comment. The good correspondence between the simulated and the observed discharge is illustrated by the plots for the years 1958, 1964, 1980 and 1998, all shown in the appendix. These plots show good correspondence between the observed and the simulated discharges at different periods in the simulation, that is in the beginning, in the middle and at the end.

More results from the long-term simulation can be seen in Figure 9.2, Figure 9.3 and Figure 9.5 to illustrate some of the output that can be evaluated and which can show some of the internal states of the model applicable for example in water resources planning or management. Figure 9.2 shows the spring yield simulated by the model. This is the water depleted from the groundwater reservoir in the model and can contribute to the identification of groundwater resources which can be utilised. It shows that the groundwater yield fluctuates over the year and from year to year. The curve on the figure represents the total groundwater yield from all the springs in the area. The actual discharge presented in the figure cannot therefore be observed at any physical location in the catchment.

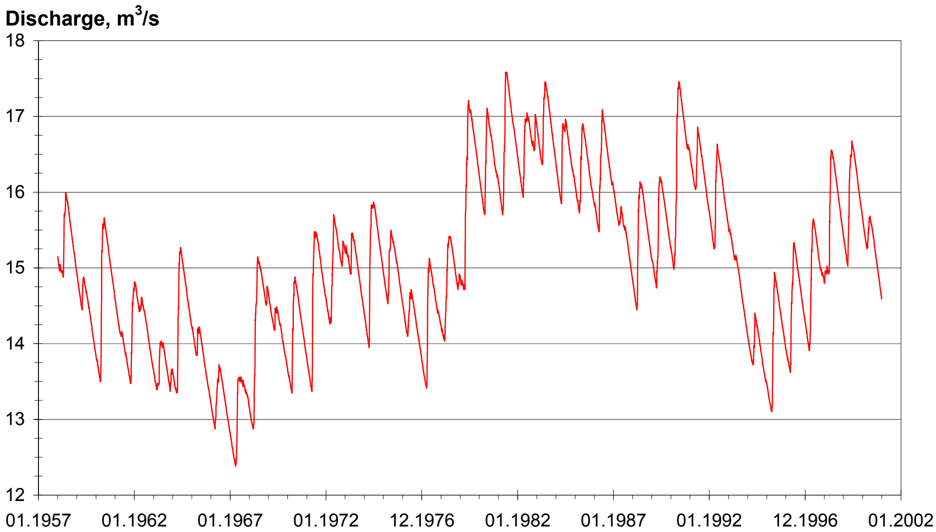

Figure 9.2: Simulated spring yield from the catchment above gaguging station 1DD1 for the period 1958-2000.

Figure 9.3 shows the duration curve for the observed and simulated discharge at gauging station 1DD1 for the period 1958 to 2000. The curves show some deviation, particularly for the high discharge period where there is a marked deviation. The deviation probably has some of the same causes as the deviation of the flood peaks. This is discussed below. On the duration curve in Figure 9.3, the observed and simulated discharge shows a relatively similar pattern for the low flow discharge. The pattern is relatively similar for the two. In an analysis of impact form land use change, this can be used for detecting changes in the low flow season.

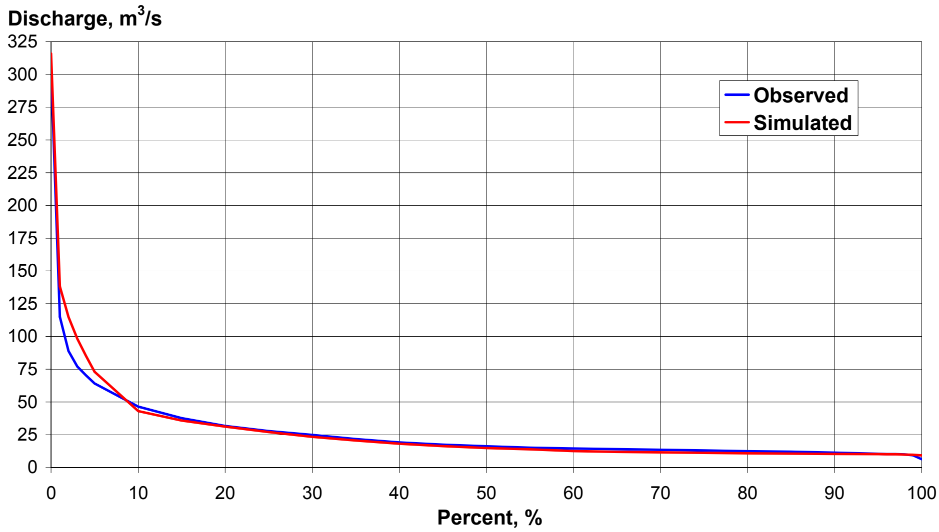

Figure 9.3: Duration curve for simulated and observed discharge from the catchment above gauging station 1DD1 for the period 1958-2000.

The deviation between the simulated and observed flood peaks for some of the years during the simulation can have several causes. The precipitation data can constitute a source of error. Checking selected years of precipitation data exposed a number of probable errors in the observations, which was corrected through replacement with observations from nearby stations. However, there are probably still errors within the precipitation data. An indication of this not shown here is the connection between the average annual precipitation and the observed and simulated annual discharge. A plot of the precipitation vs. observed annual discharge contains more outliers than a plot with the simulated discharge.

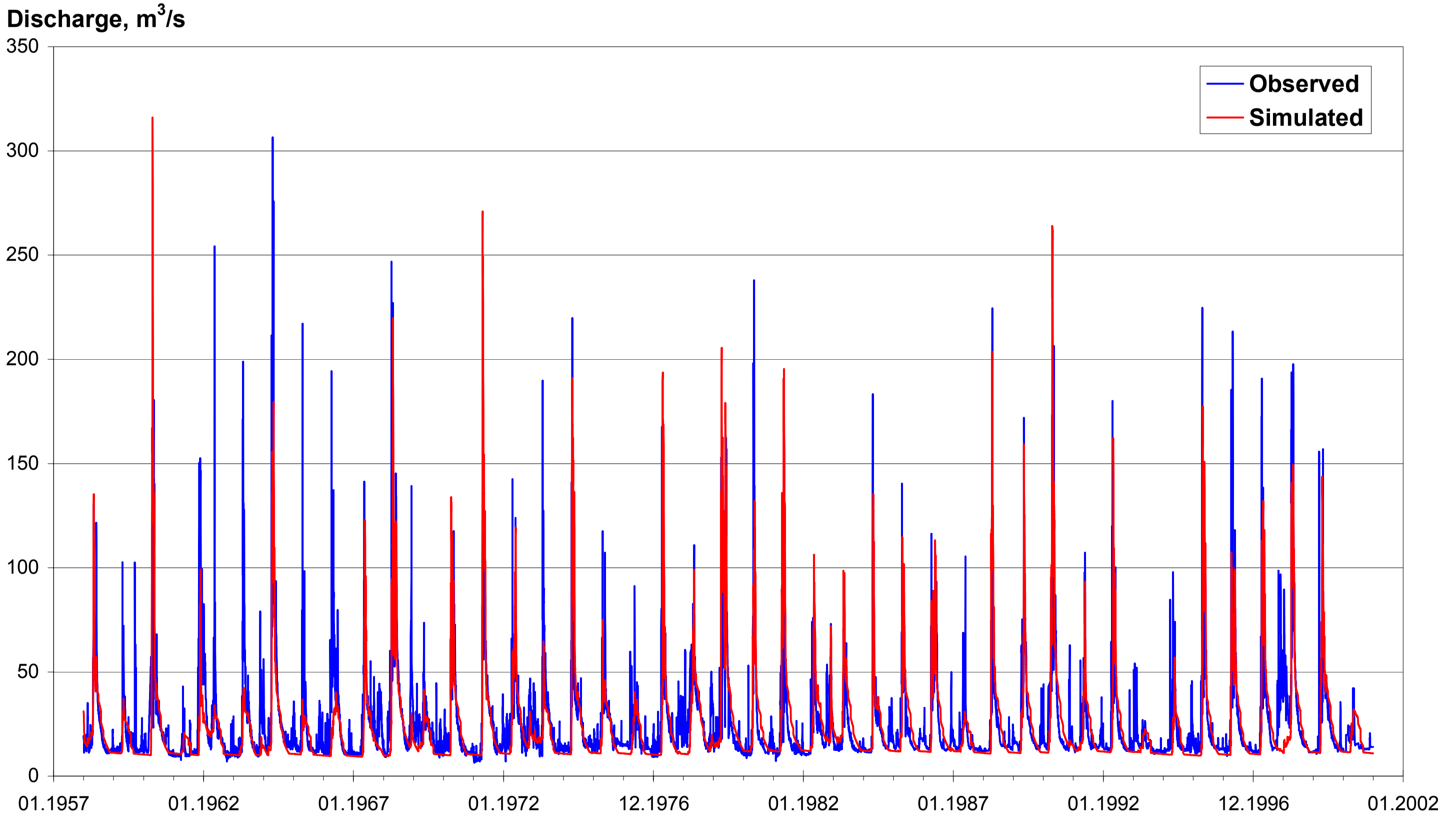

Figure 9.4: Simulated and observed discharge from the catchment above gauging staion 1DD1 for the period 1958-2000.

During some of the extreme precipitation events, the time of the reading can influence the records. If the precipitation record is done at 08.00 hours in the morning, the larger part of the precipitation could have fallen during the previous day or could be distributed evenly over the last 24-hour period. These processes are not represented in the model. This means that the large part of the precipitation may drain out from the basin a day earlier than in the simulation model if the precipitation fall as an intense event the previous day. This may explain some of the deviations between the simulated and observed discharge on the left side of the duration curve. With reference to Figure 9.4 and the explanation above, too many extreme discharge events are calculated and may therefore give the course of the duration curve as shown in Figure 9.3.

On Figure 9.4 the simulated discharge during the low flow period has a relatively smooth pattern compared to the jagged pattern of the observed discharge. The smoothing of the low flow is due to the treatment of the off take in the model and the high representation of spring yield in this period. The low flow period has a high percentage of spring yield, which is formed, by a slowly receding groundwater reservoir. In addition, the resulting discharge from the local catchment just upstream of the gauge due to smaller precipitation events, is smoothed out through merging with runoff response from the remaining catchment and subtraction of water demand for irrigation purposes.

Figure 9.5 shows the degree of fulfilment of the water demand for the catchment above 1DD1. With the present land use and water demand as incorporated in the simulation model the total water demand in the area is about 245-mill m^3/year. This is mainly water required for irrigation purposes as discussed previously, but though only a small fraction, the domestic water supply is also covered to some degree through the off takes and the furrow systems (Grove, 1993). Theoretically, Figure 9.5 shows that the water demand in the area is only met for one single year during the 43-year simulation period confirming that the numerous claims regarding water scarcity are realistic. Two particularly dry years are 1993 and 1994, which are known to have been difficult as regards the water situation in the area though written documentation for this has not been found. Also recently, the year 2000 seems to have experienced a considerable unmet water demand and this coincides with the dry conditions found in the area for this year. A brief survey of the report by the International Monetary Fund (2000) to disclose an agro-economic response to the water shortage for these 3 years in the 1990s did not show any clear relation, which might have been expected.

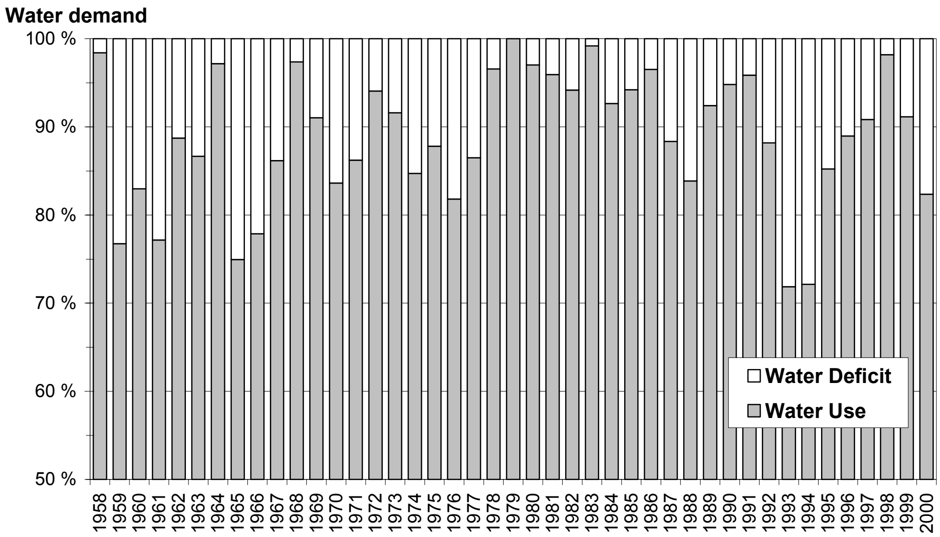

Figure 9.5: Simulated relative Water Use and Deficit for the catchment above gauging station 1DD1 for the period 1958-2000. See text for details.

9.3 Simulation with land use change

9.3.1 Change in forest cover

Today the forest around Mt Kilimanjaro is protected by a forest reserve designed to prevent human activities like settlements, logging and clearing for agriculture. The heavily populated areas below the forest reserve therefore exert constant pressure on this area for utilisation and serve as an alternative area for migration compared to the dry unproductive lowland plains. An alternative land use change could be to reduce the forest reserve for example 2 km upwards and allow clearing for annual cropping, thus securing food for a growing population. A more dramatic change would be to extend the forest reserve 2 km downwards to protect and extend the biodiversity within the forest from further encroachment by unauthorized activities. The author has no opinion about which of these management schemes to undertake, if any! However, the response from such management activities should probably be evaluated by a model simulation instead of full-scale field experiments.

The change in the forest limits is imposed in the model through changes in the parameters influenced by the forest. With reference to Table 8.2, the distributed parameters most relevant to change due to a move of the forest limits will be the coverage of high vegetation, the average tree height and the field capacity. These changes assume that the field capacity is related to the land use and vegetation cover, which may not be too unexpected in the long run. When the forest limits are moved upwards, the parameters for the area just below the present forest reserve are imposed on the ”deforested” areas. Conversely, the parameters for the forest are imposed on the “forested” areas when the forest limits are moved downwards.

9.3.2 Changes in water demand

As indicated in Table 9.1, the period 1958 to 2000 was simulated with changes in water demand for the catchment above 1DD1. The changes in water demand introduced, was a 10 percent increase and a 10 percent decrease. The change was done on the WD parameter seen in Table 8.1, which described distributed the water demand over the catchment.

9.3.3 Result from simulations with change in land use

The result from the simulation with changed land use shows a pattern, which could be expected in accordance with the findings from the literature. The result from the four simulations with alternative land use is shown in Table 9.4. The annual runoff increases with the reduction of forest cover and decreases for expansion of the forest cover. The evapotranspiration shows the opposite pattern.

Factor	Min discharge m^3/s	Change in annual runoff, %	Change in evapotranspi-ration, %	Change in water use %
10% increase in water demand	9.293	-1.6	0.0	5.7
10% decrease in water demand	9.296	1.9	0.0	-6.7
Calibration result	9.293	0.0	0.0	0.0
Forest border 2 km upwards	9.448	1.9	-1.2	0.8
Forest border 2 km downwards	9.158	-2.0	1.2	-0.7

Table 9.4: Some of the results from simulations with changed land use input to the model. The results are based on simulation of the period 1958-2000.

A result obtained from the model, is the change in water use arising from the change in forest cover. Figure 9.6 shows the change in water use for each year in the simulation period from 1958 to 2000. In addition, the original difference between the water demand and the water use is shown at the bottom of the figure. The figure shows that the influence of changed land use conditions is greater for marginal conditions. For example, in 1993 and 1994 when the deficit is already large, with no change in land use, the influence from changed land use conditions is greater. This result can for example be used for an analysis of the conditions for agriculture. The larger change of 1.5 percent in marginal years may have more influence than a smaller 0.7 percent average change.

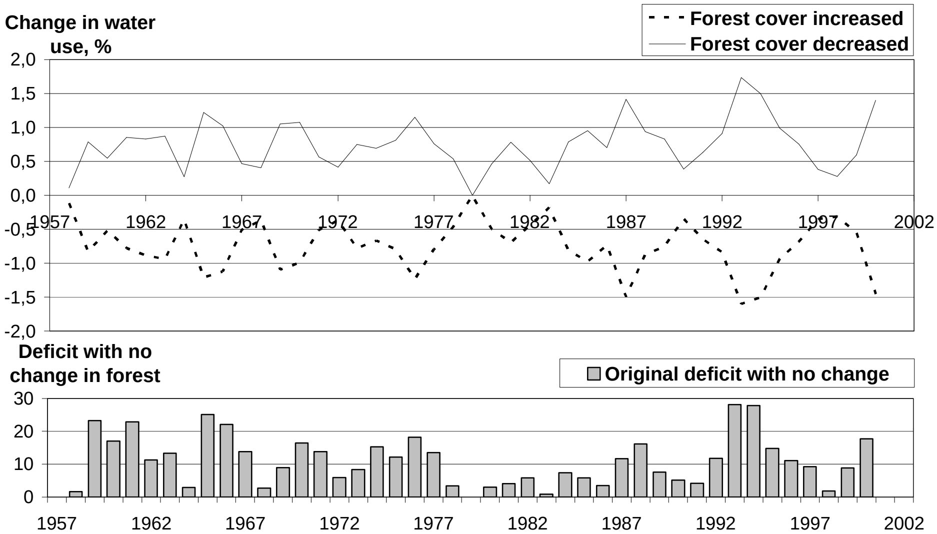

Figure 9.6: Influence on water use with change in forest cover. See text for details.

The result from the simulation of increase in water demand is that the system is not able to meet the increased demand for water. The system is also apparently not able to meet today's water demand (Figure 9.5). The 10 percent change in water demand is not reflected in a corresponding change in water use. The reduced water demand is used for meeting unmet water demand from other users and not for increased runoff. The increased water demand can on the other hand not be met completely by the existing water demand and the corresponding increase in water use will be less than the increase in demand.

A weakness in the simulation of minimum discharge when increasing the water demand is the restriction imposed on the utilisation of the groundwater resources between Chemka Spring and the 1DD1 gauging stations. The model does not allow much increase in the extraction of water between these two points. This will influence the calculation of minimum discharge. If other limits on the utilisation of this groundwater yield are imposed in the model, the change in minimum discharge will be more pronounced.

9.4 Simulation with climatic changes

9.4.1 Climatic changes imposed in the input data

A feasible scenario for climatic change would be changes in temperature. The hydrologic response to changes in temperature is investigated through simulations using changed temperature data. All the three temperature series were imposed with a 2-centigrade increase or decrease if measurements were available. The change in precipitation is another feasible climatic scenario for which the hydrological impacts are simulated. All precipitation data applied in the model were added or subtracted by 10 percent of their value. Zero-values were kept. The spatial distribution of the precipitation events was not evaluated nor changed. Both scenarios for climatic change were based on the IPPC reports as cited previously.

9.4.2 Results from simulation with climatic changes

The results from simulation with changed climatic conditions in the catchment are shown for all the 4 alternatives in Table 9.5. The results are compared to a simulation of the period 1958-2000 based on the input data and parameters found though the calibration process in chapter 8. In addition, Figure 9.7 shows a duration curve for the alternative with increased or decreased precipitation.

Factor	Min discharge m^3/s	Change in annual runoff, %	Change in evapotranspi-ration, %	Change in water use %
10% increase of precipitation	10.4	20.0	4.7	4.7
10% decrease of precipitaton	8.2	-18.7	-5.2	-6.4
Simulation with no change	9.3	0.0	0.0	0.0
2^oC increase in temperature	9.0	-3.9	2.6	-1.6
2^oC decrease in temperature	9.6	4.3	-3.0	1.6

Table 9.5: Some of the results from simulations with changed climatic input to the model. The results are based on simulation of the period 1958-2000.

Table 9.5 shows the minimum simulated discharge for the simulation period for the 4 alternatives. In addition, the change in annual runoff, in evapotranspiration and water use is shown relative to the no-change situation. The changes in water use are due to changes in the amount of water available during the season of abstraction.

The change in precipitation means that the amount of water in the model changes. The change in precipitation entering the model will result in a similar pattern of change for the output from the model. The relatively dramatic 20 percent change in annual runoff from the model compared to the 10 percent change in precipitation can probably be attributed to the spatial distribution of precipitation. A considerable amount of runoff is caused by a few concentrated and relatively intense rainfall events. The greater part, from 60 to 70 percent of the precipitation for the three stations, is to be found in the months March to April. The soil is then relatively saturated, and a small change in precipitation will then easily be reflected in the runoff. At other seasons, the retention capability of the soil is bigger and changes in precipitation are not so easily reflected in the runoff.

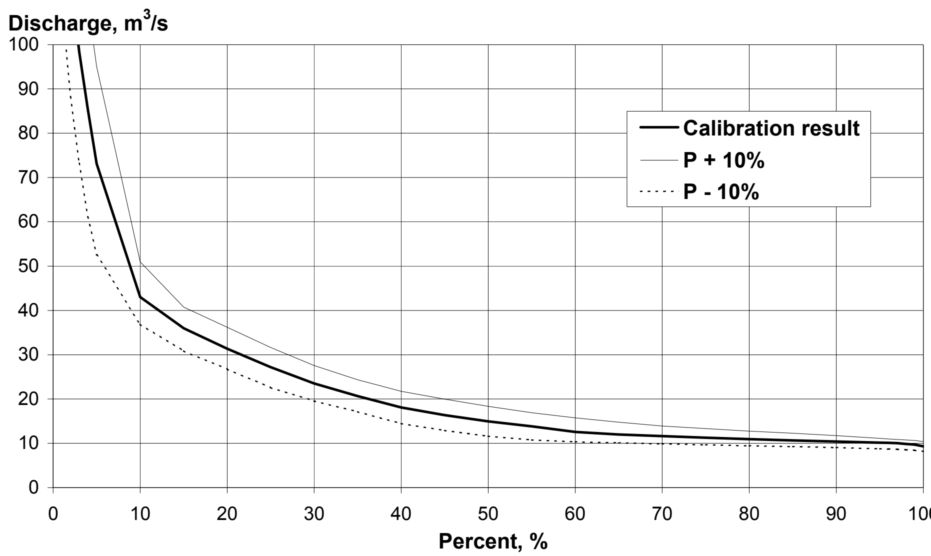

Figure 9.7: Duration curve from simulation of the period 1958-2000 with +/- 10 percent change in precipitation.

The influence on the low flow season due to climate change is illustrated by the duration curves in Figure 9.7. The figure shows that the low flow discharge can be influenced by as much as 20 percent during a considerable part of the low flow season. This will influence the off take of water as shown in Table 9.5. The influence from change in temperature is less than from change in precipitation and the resulting duration curve is not shown.

The change in temperature will primarily influence the evapotranspiration and so the annual runoff and water use. The increase in temperature causes an increase in the evapotranspiration. The resulting annual discharge decrease will mean less water for for irrigation purposes and vice versa in the case of a temperature decrease. Roughly every degree of increase in temperature gives a 0.5 m^3/s reduction of the average discharge at gauging station 1DD1.

9.5 Comment on simulations with land use and climatic changes

None of the simulations using changes in land use or climatic properties have any feedback mechanisms to other processes in the catchment. For example, the increased temperature causes some increase in evapotranspiration. The increased evapotranspiration may influence the precipitation through higher precipitable moisture content in the air as discussed in the study by de Groen & Savenije (1995). If climatic changes take place, they will most probably be a combination of changes of different elements influencing the hydrological cycle and not just a change of one element.

The scenario of precipitation change may also include spatial change of the precipitation events. Above, all precipitation data are changed linearly. Increased precipitation may result in more extreme events and not necessarily in a linear increase of all precipitation events. Also, the temperature change may not have undergone a linear increase for all seasons, but the spatial distribution of the alternative climatic change scenarios has not been investigated and is beyond the scope of this study.

The increase in temperature may also influence the peak of Mt Kilimanjaro visually due to a larger amount of precipitation falling as rain instead of as snow causing the white peak to decrease or disappear. However, as regards changes in the visual appearance, the hydrological consequences will most certainly not be as dramatic as those claimed by Amos (2001) who predicts dramatically worsened water supply, irrigation and power production.

The results from the simulation using the alternative land use show an expected pattern in the light of the findings from chapter 3. However, as discussed in chapter 11, there is scope for further development

URN:NBN:no-3437

.

10. CONCLUSIONS AND OVERALL DISCUSSIONS

10.1 Concluding the study

This study has revealed new information on three important areas of interest concerning the hydrology on the southern slopes of Mt Kilimanjaro:

Stream gauging:

- Runoff from different vegetation types on the southern slopes of Mt Kilimanjaro through gauging of three small catchments
- The area above about 2800 masl on the southern slopes of Mt Kilimanjaro contribute with little or no surface discharge

Precipitation distribution:

- Development of a homogeneous reference precipitation series for the area south of Mt Kilimanjaro through analysis of all available precipitation series. The reference series can be used for controlling other series
- Development of a function describing the change in precipitation by elevation for the southern slopes of Mt Kilimanjaro by use of the permanent regular and nine temporary precipitation stations
- Assessment of the elevation for maximum precipitation on the southern slopes of Mt Kilimanjaro which was found to about 2000-2200masl, which appears to be 400-500 m higher than assumed previously

Water Balance:

- Determination of the different elements of the hydrological cycle for different elevations on the southern slopes of Mt Kilimanjaro, including the areas where the major part of the groundwater most probably occurs

Hydrologic modelling:

- Development of a hydrological model describing the processes above, on and just under the soil surface

The elements above form a part of the complex picture of hydrological processes occurring on the slopes south of Mt Kilimanjaro. Assumptions have been made previously to explain the hydrological processes occurring on the slopes, but numerical proofs for these assumptions have seldom been produced before. The stepwise approach to the different processes has revealed new knowledge about the hydrology of the area. The knowledge has been used for development of a hydrological simulation model, which can be utilised for further study of the hydrological processes in the area and their interaction with the land use. If desired, the model can be applied for better water management in the light of land use change based on an assessment of the actual hydrological processes taking place in the area, instead of a lumped average assessment for the whole river basin.

The hydrologic simulation model developed on the basis of the processes examined has shown a noteworthy capability for reproducing the hydrological response from the catchment based on the meteorological input. The degree to which the results are based on an actually correct representation of the internal processes in the catchment or a on mutual concealment of errors smoothing each other out, is, of course, open to discussion. It should be noted that the development of the model is based on the consideration of separate sub-catchments, the processes within are investigated, modelled, and the results evaluated before a larger catchment is assessed using the same approach. The processes found in the smaller catchment are applied in the larger one as illustrated in Figure 2.2.

10.2 Overall discussion of findings

The results from the chapters, 5-8, have been discussed individually and critically at the end of each chapter as regards stream gauging, the rainfall distribution, the water balance and the hydrologic modelling.

It is clear that many factors influenced this study. There were many uncertainties and a number of choices had to be made, based on subjective considerations. The uncertainties are accounted for here and discussed. The assumptions in chapter 1 about the complex interrelations between the hydrological processes in the slopes south of Mt Kilimanjaro are essential for this study. It will be difficult to prove or disprove them conclusively. None of the findings directly exclude the assumptions set out in chapter 1, but the calculations and evaluations performed during this study have strengthened or maybe confirmed the assumptions.

The complex processes have been approached one by one as illustrated in Figure 2.1 and individually accounted for. The findings were utilised in the development of the hydrological simulation model described in chapter 8. The model simulated in an acceptable fashion, the response from the three catchments tested in this thesis. Later, the simulation model was applied to evaluate the hydrological response due to

URN:NBN:no-3437

potential changes in land use or climate. The responses correspond to findings from the literature.

A potential weakness in this study may be the lack of verification of the approach and of the simulation model. When dealing with model development, it is often common to test the model on another catchment for verification of the model system. The unique conditions found on the slopes south of Mt Kilimanjaro, make it difficult to find a similar area for verification of the model. However, the approach to the model development with three different catchments at different elevations and within different land use regimes and the long term simulation performed in chapter 9 should show that the model has some flexibility and is firmly rooted in the real conditions found in the catchment.

11. FURTHER WORK

Further work should focus more on specific land use related to agriculture and the representation of such land use in the model. The representation of the vegetation in the present model is approximate, considering high and low vegetation with the same approach and the same generalised processes. Implementation of routines taking the process of agricultural cropping into consideration could improve the model performance and representation of the processes in the catchment. The actual water demand could be modelled in more detail at field scale and give the hydrological response from the catchment for various cropping patterns in detail, which Bruijnzeel (1990) has claimed has not been done in many other studies. For example, this could be solved through use of the distributed parameter land use (Table 8.2), which could determine which processes could be calculated for the different types of land use. The results from an improved model could be coupled to an economic assessment concerning water use for agricultural or hydropower purposes.

The results from the further development of the hydrologic model can lead to the production of an overall tool for water management taking different water consuming activities into consideration. On the slopes south of Mt Kilimanjaro, irrigation for agricultural production is the biggest water consumer with a continuous demand for increased abstraction of water. An improved hydrologic simulation framework, can give the local water and the agricultural authorities a better tool for improved water management. The effect of changing cultivation or increased off take of water, can be evaluated in advance by way of a simulation rather than several years of full-scale experiments. Expensive investments, which later prove to be useless due to the lack of water, can be avoided and stopped before being implemented. Unnecessary conflicts over scarce water resources can then be avoided.

The groundwater situation in the area is another field, which should be paid more attention. Quantitative mapping of the yield outside the areas with extensive yield could also be another task. A combination of geological survey and the application of tracers can produce further understanding of groundwater movements. Such studies may reveal further information about the groundwater element in the hydrological cycle in the area.

Finally, the infrastructure established through this study should continue to be operated for the future without any unnecessary breaks. Particularly The discharge and precipitation measurements towards the upper slopes of Mt Kilimanjaro in particular give valuable information about the water resources in the area.

URN:NBN:no-3437

12. REFERENCES

Adokpo Migan, S. (2000). *The impact of forest conversion on hydrology - A synthesis of French work in West Africa and Madagascar* (Technical Documents in Hydrology 36). Paris: UNESCO, CEREG / UFR de Gbographie, ORSTOM.

Alexandersson, H. (1986). A homogeneity test applied to precipitation data. *Journal of Climatology, 6*, 661-675.

Ali, M. F., & Mawdsley, J. A. (1987). Comparison of 2 recent models for estimating actual evapotranspiration using only regularly recorded data. *Journal of Hydrology, 93*(3-4), 257-276.

Allen, R. G., Pereira, L. S., Raes, D., & Smith, M. (1998). *Crop evapotranspiration - Guidelines for computing crop water requirements - FAO Irrigation and drainage paper 56*. Rome.: FAO - Food and Agriculture Organization of the United Nations.

Amland, B. A. E. (1995, 27th July). Conflicts over Pangani dampen enthusiasm for hydro power in Tanzania. *Development Today. Nordic Outlook on Development Assistance, Business & the Environment, 5*, 1, 6-7,12.

Amos, J. (2001). Kilimanjaro's white peak to disappear . http://news.bbc.co.uk/2/hi/in_depth/sci_tech/2001/san_francisco/1177879.stm.

ASCE. (1996). *Hydrology handbook*. New York.: ASCE.

Bergstrøm, S., & Forsman, A. (1973). Development of a conceptual deterministic Rainfall-Runoff model. *Nordic Hydrology, 4*, 147-170.

Black, P. E. (1991). *Watershed Hydrology*: Prentice Hall International.

Bosch, J. M., & Hewlett, J. D. (1982). A review of catchment experiments to determine the effect of vegetation changes on water yield and evapotranspiration. *Journal of Hydrology, 55*, 3-23.

Bruijnzeel, L. A. (1990). *Hydrology of moist tropical forests and effects of conversion : A state of knowledge review*. Paris & Amsterdam: Unesco - International Hydrological Programme & Free university.

Bruijnzeel, L. A., & Critchley, W. R. S. (1994). *Environmental Impacts of Logging Moist Tropical Forests*. IHP Humid Tropics Programme Series: (Vol. 7): UNESCO.

Brutsaert, W. (1982). *Evaporation into the atmosphere : theory, history, and applications*. Dordrecht.: Reidel.

Brutsaert, W., & Stricker, H. (1979). An Advection-Aridity Approach to Estimate Actual Regional Evapotranspiration. *Water Resources Research, 15*(2), 443-450.

Buishand, T. A. (1982). Some methods for testing the homogenity of rainfall records. *Journal of Hydrology, 58*, 11-27.

Buishand, T. A. (1984). Tests for detecting a shift in the mean of hydrological time series. *Journal of Hydrology, 73*, 51-69.

Calder, I. R. (1993). Hydrologic effects of land-use change. In D. R. Maidment (Ed.), *Handbook of hydrology* (pp. 13.1-13.50). New York: McGraw-Hill.

Calder, I. R., Hall, R. L., Bastable, H. G., Gunston, H. M., Shela, O., Chirwa, A., & Kafundu, R. (1995). The impact of land-use change on water-resources in Sub-Saharan Africa - a modeling study of Lake Malawi. *Journal of Hydrology, 170*(1-4), 123-135.

Chiew, F. H. S., & Mcmahon, T. A. (1991). The applicability of Morton's and Penman's evapotranspiration estimates in Rainfall-Runoff Modeling. *Water Resources Bulletin, 27*(4), 611-620.

Critchley, W. R. S., & Bruijnzeel, L. A. (1996). *Environmental Impacts of Converting Moist Tropical Forest to Agriculture and Plantations*. IHP Humid Tropics Programme Series: (Vol. 10): UNESCO.

Daluti, R. L. (1999). *Irrigation Development and Water Management in Pangani River Basin* (Workshop contribution). Bahari Beach, Dar Es Salaam, Tanzania: Zonal Irrigation Office, Moshi, Tanzania.

de Groen, M. M., & Savenije, H. H. G. (1995). Do Land Use Induced Changes of Evaporation Affect Rainfall in Southeastern Africa? *Physics and Chemistry of The Earth, 20*(5-6), 515-519.

de Groen, M. M., & Savenije, H. H. G. (1998). A Rainfall Generator for Southeastern Central Africa. *Physics and Chemistry of The Earth, 23*(4), 399-403.

Dingman, S. L. (2002). *Physical hydrology, Second Edition*. (2nd ed.). Upper Saddle River, N.J.: Prentice Hall.

Doyle, P. (1990). Modeling catchment evaporation - an objective comparison of the Penman and morton approaches. *Journal of Hydrology, 121*(1-4), 257-276.

Foley, J. A., Levis, S., Prentice, I. C., Pollard, D., & Thompson, S. L. (1998). Coupling dynamic models of climate and vegetation. *Global Change Biology, 4*(5), 561-579.

Førland, E., Hanssen-Bauer, I., & Nordli, P. (1991). *Long term variation of precipitation. In Norwegian: "Langtidsvariasjon av nedbør"* (02/91 Klima). Oslo-Norway: Det Norske Meteorologiske Institutt.

Garbrecht, J., & Fernandez, G. P. (1994). Visualization of trends and fluctuations in climatic records. *Water Resources Bulletin, 30*(2), 297-306.

Gemini Data Loggers (UK) LTD. (1995). Tinytalk (R) II Data Loggers. In Orion Group of Companies (Ed.) (pp. 24). UK: Gemini Data Loggers (UK) Ltd, Scentific House, Terminus Road, Chichester, West Sussex, PO19 2UJ, UK.

Granger, R. J. (1989). A complementary relationship approach for evaporation from nonsaturated surfaces. *Journal of Hydrology, 111*(1-4), 31-38.

Griffiths, J. F. (1972). *Climates of Africa*. World Survey of Climatology: (Vol. 9). Amsterdam-London-New York: Elsevier Publishing Company.

Grove, A. (1993). Water-Use by the Chagga on Kilimanajro. *African Affairs, 92*(368), 431-448.

Hobbins, M. T., Ramirez, J. A., Brown, T. C., & Claessens, L. H. J. M. (2001). The complementary relationship in estimation of regional evapotranspiration: The Complementary Relationship Areal Evapotranspiration and Advection-Aridity models. *Water Resources Research, 37*(5), 1367-1387.

Houghton, J. T., Ding, Y., Griggs, D. J., Noguer, N., van der Linden, P. J., Dai, X., Maskell, K., & Johnson, C. A. (Eds.). (2001). *Climate Change 2001: The Scientific Basis*. Cambridge: Cambridge University Press.

Hughes, D., & Smakhtin, V. (1998, Novmber 1998). *Simulating the impacts of land-use change on streamflow time series for southern African rivers.* Paper presented at the Water Resources Variability in Africa during the XXth Century, Abidjan, Cõte d'lvoire.

Hunting Technical Services. (1996). Map: *Arusha, Sheet SA-37-13, Land Cover and Land Use.*1:250 000. Surveys and Mapping Division, Ministry of Lands, Ministry of Natural Resources and Tourism, The United Republic of Tanzania

International Monetary Fund. (2000). *Tanzania: Statistical Annex* (IMF Staff Country Report 00/122). Washington D.C.: International Monetary Fund.

IVO International Ltd, & Norplan AS. (1990). *Pangani Falls Redevelopment. Feasibility Study. Main Report.* (Consulting report for Tanzania Electric Supply Company Limited). Vantaa, Finland.

IVO International Ltd, & Norplan AS. (1995). *Pangani Falls Redevelopment. An analysis of the optimal Water Management in Pangani River Basin, Tanzania. The Summary Report* (Consulting report for Tanzania Electric Supply Company Limited). Ski, Norway.

Karongo, S. K., & Sharma, T. C. (1997). An evaluation of actual evapotranspiration in tropical East Africa. *Hydrological Processes, 11*(5), 501-510.

Klute, F. (1920). *Ergebnisse der forschungen am Kilimandscharo 1912*. Berlin: Dietrich Reimer (Ernst Vohsen) A-G.

Lefstad, L., & Bjørkenes, A. (1997). *Diploma Thesis in Water Resources Planning. Hydrological studies in The Upper Pangani River, Tanzania.*Diploma Thesis, The Norwegian University of Science and Technology, Trondheim, Norway.

Lein, H. (1998). Traditional versus modern water management systems in Pangani River Basin, Tanzania. In L. de Haan & P. Blaikie (Eds.), *Looking at maps in the dark. Directions for geographical research in land management and sustainable development in rural and urban environments of the Third World* (pp. 52-64). Utrecht/Amsterdam: Royal Dutch Geographical Society, Faculty of Environment Sciences, University of Amsterdam.

Lein, H. (2001, 14-15th June). *Immigration, irrigation and land use change in the lowlands of Mt Kilimanjaro, Tanzania.* Paper presented at the Pangani Conference, Moshi, Tanzania.

Lugomela, V., Mkhandi, S. H., & Mtalo, F. (2001, 14-15th June). *Assessment of the impact of irrigation on the water resources of Pangani River Basin.* Paper presented at the The Pangani Conference, Moshi, Tanzania.

Luhumbika, B. A. S. (1999). *Water Management in Pangani River Basin* (Workshop contribution). Bahari Beach, Dar Es Salaam, Tanzania: Idara Ya Maji, Moshi.

Lørup, J. K., Refsgaard, J. C., & Mazvimavi, D. (1998). Assessing the effect of land use change on catchment runoff by combined use of statistical tests and hydrological modelling: Case studies from Zimbabwe. *Journal of Hydrology, 205*(3-4), 147-163.

Maidment, D. R. (Ed.). (1993). *Handbook of hydrology*. New York: McGraw-Hill.

Manning, J. C. (1997). *Applied Principles of Hydrology*. (Third ed.): Prentice Hall Inc.

Martin, D. (Ed.). (2000). *Kilimanjaro, Tanzania. Land, people, history.* (ISBN 1-77901-145-8 ed.). Johannesbourg, South-Africa: African Publishing Group International and Tanzania National Parks.

Mbonile, M. J. (1999, 1st - 3rd July). *Population dynamics in Pangani Basin.* Paper presented at the Workshop on Water Management in Pangani Basin, Bahari Beach, Dar es Salaam, Tanzania.

McCarthy, J. J., Canziani, O. F., Leary, N. A., Dokken, D. J., & White, K. S. (Eds.). (2001). *Climate Change 2001: Impacts, Adaptation, and Vulnerability*. Cambridge: Cambridge University Press.

Morton, F. I. (1983a). Operational estimates of areal evapotranspiration and their significance to the science and practice of hydrology. *Journal of Hydrology, 66*, 1-76.

Morton, F. I. (1983b). Operational estimates of lake evaporation. *Journal of Hydrology, 66*, 77-100.

Morton, F. I. (1991). A discussion of four papers on evaporation in Volume 111. *Journal of Hydrology, 124*(3-4), 363-374.

Morton, F. I. (1994). Evaporation research - A critical-review and its lessons for the Environmental Sciences. *Critical Reviews in Environmental Science and Technology, 24*(3), 237-280.

Mujwahuzi, M. R. (1999, 20-22nd January). *Water Use Conflicts in the Pangani Basin.* Paper presented at the Workshop on Water Management in Pangani River Basin, Moshi, Tanzania.

NASA. (2002). http://www.jpl.nasa.gov/srtm/tanzania.htm : Visited 25th October 2002.

Nash, J. E. (1989). Potential evaporation and "The complementary relationship". *Journal of Hydrology, 111*(1-4), 1-7.

Ndege, M. M. (1996). Strain, Water Demand, and Supply. Directions in the most Stressed Water Systems of Eastern Africa. In E. Rached, E. Rathgeber, & D. B. Brooks (Eds.), *Water management in Africa and the Middle East : Challenges and Opportunities* . Ottawa: International Development Research Centre.

Nippon Koei CO. Ltd, & Pasco International Inc. (1998). *The Feasibility study on Lower Moshi Integrated Agriculture and Rural Development Project in The United Republic of Tanzania* : JICA, Japan International Cooperation Agency

The united Repuiblic og Tanzania, Ministry of Agriculture and Cooperatives.

Olaussen, E., & Roald, L. (1996). *Kvalitetskontroll av tilsigsserier* (82-594-0913-5). Trondheim.: Energiforsyningens forskningsinstitutt.

Perzyna, J. G. (1994a). *Pangani Basin Water Management: Assessment of inflow to Nyumba ya Mungu reservoir, Tanzania* : Ministry of Water, Tanzania, IVO International of Finland & Norplan A/S of Norway.

Perzyna, J. G. (1994b). *Pangani Basin Water Management: Assessment of inflow to Nyumba ya Mungu reservoir, Tanzania. Mission Report* : Ministry of Water, Tanzania, IVO International of Finland & Norplan A/S of Norway.

Post, D. A., Jakeman, A. J., Littlewood, I. G., Whitehead, P. G., & Jayasuriya, M. D. A. (1996). Modelling land-cover-induced variations in hydrologic response: Picaninny Creek, Victoria. *Ecological Modelling, 86*(2-3), 177-182.

Refsgaard, J. C. (1997). Parameterisation, calibration and validation of distributed hydrological models. *Journal of Hydrology, 198*(1-4), 69-97.

Rinde, T. (1998). *A flexible hydrological modelling system developed using an object-oriented methodology.*Doctoral Thesis, The Norwegian University of Science and Technology, Trondheim.

Rinde, T. (1999). *Landpine. En hydrologisk modell for simulering av arealbruksendringers innvirkning på avrenningsforhold. (In Norwegian: Landpine: A hydrologic model for describing the influence of landuse on changes in runoff)* (Notat). Trondheim: SINTEF Bygg og miljøteknikk.

Rusten, O. (1995). *Pangani Falls Redevelopment, An analysis of optimal water managment in Pangani River Basin, Tanzania. The Summary Report* . Ski, Norway: Made for Tanzania Electric Supply Company Limited by IVO International Ltd & Norplan AS j.v.

Sahin, V., & Hall, M. J. (1996). The effects of afforestation and deforestation on water yields. *Journal of Hydrology, 178*(1-4), 293-309.

Sandström, K. (1995). *Forests and water - friends or foes? Hydrological implications of deforestation and land degradation in semi-arid Tanzania*. Linköping.: Linköping University.

Sarmett, J. D. (1999, 1st - 2nd July). *Water Resources Management in Pangani River Basin with Particular Reference to Kilimanjaro Region.* Paper presented at the Workshop on Water Management in Pangani Basin, Bahari Beach, Dar Es Salaam, Tanzania.

Schulze, R. E. (2000). Modelling hydrological responses to land use and climate change: A southern African perspective. *AMBIO, 29*(1), 12-22.

Serneels, S., & Lambin, E. F. (2001). Proximate causes of land-use change in Narok District, Kenya: a spatial statistical model. *Agriculture Ecosystems & Environment, 85*(1-3), 65-81.

Shaw, E. M. (1994). *Hydrology in practice*. London: Chapman & Hall.

Sivertsgaard, T., & Skau, S. H. (1996). *Diploma Thesis in Water Resources Planning. Hydrological studies in The Pangani River, Tanzania.*Diploma Thesis, The Norwegian University of Science and Technology, Trondheim.

Staudenrausch, H., & Flugel, W. A. (2001). Development of an integrated water resources management system in southern african catchments. *Physics and Chemistry of the Earth, Part B: Hydrology, Oceans and Atmosphere, 26*(7-8), 561-564.

Stephenne, N., & Lambin, E. F. (2001). A dynamic simulation model of land-use changes in Sudano-sahelian countries of Africa (SALU). *Agriculture, Ecosystems & Environment, 85*(1-3), 145-161.

Stiles, G. (1996). Demand-side Management, Conservation, and Efficiency in the Use of Africa's Water Resources. In E. Rached, E. Rathgeber, & D. B. Brooks (Eds.), *Water management in Africa and the Middle East : Challenges and Opportunities* . Ottawa: International Development Research Centre.

Tanzanian Authorities. (1999). Tanzania, Enhanced Structural Adjustment Facility. Policy Framework paper for 1998/99-2000/01. In International Monetary Fund (Ed.) (pp. 15). http://www.imf.org/external/np/pfp/1999/tanzania/index.htm: International Monetary Fund.

Tauer, W., & Humborg, G. (1992). *Runoff irrigation in the Sahel Zone: Remote sensing and geographical information systems for determining potential sites* (Translation: Donald Baerg and John S. McNown, Trans.). Weikersheim.: Verlag J. Margraf (distr.).

Teale, E. O., & Gillman, C. (1935). *Report on the investigation of the proper control of water and the re-organization of water boards in the northern province of Tanganyika Territory : November-December, 1934* . Dar es Salaam : Government Printer.

The United Republic of Tanzania. (1977a). *Water Master Plan, Kilimanjaro Region, Hydrogeology* (Technical report Hydrogeology Volume III): Water Master Plan Team, Ministry of Water, Energy and Minerals, The United Republic of Tanzania.

The United Republic of Tanzania. (1977b). *Water Master Plan, Kilimanjaro Region, Hydrometeorology* (Technical report Hydrometeorology Volume II): Water Master

Plan Team, Ministry of Water, Energy and Minerals, The United Republic of Tanzania.

The United Republic of Tanzania. (1977c). *Water Master Plan, Kilimanjaro Region, Main Report* (Final report Volume I): Water Master Plan Team, Ministry of Water, Energy and Minerals, The United Republic of Tanzania.

The United Republic of Tanzania. (1994). *Report on agro/socio-Economic situation in Pangani River Basin* : Zonal Irrigation-Kilimanjaro-Moshi, Ministry of Agriculture & Ministry of Water, Energy and Minerals.

Tole, L. (1998). Sources of Deforestation in Tropical Developing Countries. *Environmental Management, 22*, 19-33.

Unknown. (1995, July). Making ends meet. *International Water Power & Dam Construction*, 2.

Valente, F., David, J. S., & Gash, J. H. C. (1997). Modelling interception loss for two sparse eucalypt and pine forests in central Portugal using reformulated Rutter and Gash analytical models. *Journal of Hydrology, 190*(1-2), 141-162.

Walker, W. R. (1989). *Guidelines for designing and evaluating surface irrigation systems: FAO Irrigation and drainage paper 45* . Rome: FAO - Food and Agricultural Organization of the United Nations.

Ward, R. C. (1990). *Principles of hydrology*. London: McGraw-Hill.

Watson, F., Vertessy, R., McMahon, T., Rhodes, B., & Watson, I. (2001). Improved methods to assess water yield changes from paired-catchment studies: application to the Maroondah catchments. *Forest Ecology and Management, 143*(1-3), 189-204.

Watson, R. T. (Ed.). (2001). *Climate Change 2001: Synthesis Report*. Cambridge: Cambridge University Press.

Wilk, J., & Hughes, D. A. (2002a). Calibrating a rainfall-runoff model for a catchment with limited data. *Hydrological-Sciences-Journal, 47*(1), 3-17.

Wilk, J., & Hughes, D. A. (2002b). Simulating the impacts of land-use and climate change on water resource availability for a large South Indian catchment. *Hydrological-Sciences-Journal, 47*(1), 19-30.

WMO. (1966). *Measurement and estimation of evaporation and evapotranspiration. Technical note no 83.* Geneva: Secretariat of the World Meteorological Organization.

WMO. (1994). *Guide to hydrological practices : data acquisition and processing, analysis, forecasting and other applications*. [Geneva]: World Meteorological Organization.

Worsley, K. J. (1979). On the likelihood ratio test for a shift in location of normal populations. *Journal of the American Statistical Association, 74*(366), 365-367.

Yanda, P. Z., & Shishira, E. K. (1999, 1st - 3rd July). *Forestry Conservation and Resource Utilisation on Southern Slopes of Mount Kilimanjaro: Trends, Conflicts and*

Resolutions. Paper presented at the Workshop on Pangani River Basin, Dar Es Salam.

Aanderaa-Instruments. (1997). *Water Level Sensors (WLS) 3190/3190A* (Data sheet for equipment). Bergen, Norway: Aanderaa Instruments.

Aanderaa-Instruments. (1998). *Specific Information for datalogger 3634* (Manual for equipment). Bergen, Norway: Aanderaa Instruments.

APPENDIX

This part contains appendix the thesis. The content is as follows:

Appendix 1: Discharge from the new river gauging stations

Appendix 2: Rainfall observations from reference stations

Appendix 3: Input data for the hydrological model

Appendix 4: Meteorological data for the water balance calculation

Appendix 5: Calculation of actual evapotranspiration

Appendix 6: Plot of long-term simulation results for selected years

Appendix 7: Discharge observations from 1DD1

Appendix 1: Discharge from the new river gauging stations

This appendix shows the discharge observations from the three gauging stations, Charongo, Ngomberi and Ghona River.

Observation: Discharge at gauging station Charongo, l/s
Year: 1998

Month Day	Jan	Feb	Mar	Apr	Mai	Jun	Jul	Aug	Sep	Oct	Nov	Dec
1								178	106	71	58	75
2								170	103	71	57	64
3								162	103	72	58	63
4								163	105	70	59	58
5								159	101	70	58	57
6								153	104	70	62	59
7								153	101	70	64	56
8								149	98	70	67	56
9							179	149	95	68	58	54
10							174	146	93	68	58	53
11							173	148	92	66	58	53
12							187	145	93	66	58	52
13							189	142	107	65	58	52
14							185	141	92	67	57	53
15							180	135	87	66	57	53
16							173	133	86	65	57	52
17							173	129	86	65	57	50
18							187	127	84	64	64	43
19							180	129	81	64	57	41
20							173	128	79	62	58	40
21							167	131	79	63	58	39
22							165	124	80	63	58	38
23							163	120	78	61	53	34
24							162	119	78	59	60	34
25							176	118	76	59	60	34
26							181	117	74	59	60	38
27							168	125	75	58	57	55
28							163	125	73	58	54	47
29							158	116	73	57	53	37
30							155	111	72	58	91	34
31							218	109		58		34

Observation: Discharge at gauging station Charongo, l/s
Year: 1999

Month Day	Jan	Feb	Mar	Apr	Mai	Jun	Jul	Aug	Sep	Oct	Nov	Dec
1	70	18	13	86	222	160	134	171	113	74	47	98
2	68	17	14	94	189	152	138	164	114	74	47	72
3	45	16	13	59	163	146	237	163	108	74	47	72
4	37	14	13	94	144	150	233	158	106	67	47	58
5	35	14	16	73	128	169	183	158	104	67	47	53
6	34	14	14	158	116	225	173	149	110	67	44	53
7	38	15	14	99	231	187	267	146	106	63	47	50
8	30	14	12	103	206	169	222	144	104	65	47	47
9	22	17	12	87	180	171	240	147	104	67	47	47
10	21	15	24	57	164	187	215	139	104	63	47	49
11	20	15	65	43	154	198	206	136	103	63	49	47
12	19	14	48	36	158	187	199	136	98	63	50	45
13	19	14	24	31	163	195	213	136	95	62	47	47
14	19	14	47	30	206	185	204	134	94	60	44	55
15	27	14	68	33	176	177	234	135	93	60	44	53
16	27	15	53	28	273	174	208	140	93	60	44	82
17	21	15	49	26	218	171	202	165	93	60	44	55
18	20	14	43	28	210	167	197	165	91	60	47	50
19	20	14	33	39	193	164	192	141	88	57	44	47
20	19	15	43	172	199	160	199	139	87	57	45	44
21	19	23	28	134	178	155	192	132	88	57	44	47
22	19	16	25	106	170	153	189	128	86	57	41	57
23	43	15	21	101	163	147	185	128	86	53	50	47
24	39	16	19	90	157	146	186	126	86	53	72	44
25	30	14	21	133	163	139	195	121	83	53	68	42
26	28	13	21	123	160	137	188	121	81	50	60	44
27	27	14	148	101	148	145	185	120	81	50	90	42
28	25	16	77	104	142	132	177	120	77	50	76	84
29	25		56	397	149	139	173	120	75	50	67	69
30	25		46	297	160	135	173	120	75	50	114	58
31	20		52		152		171	115		47		52

Observation: Discharge at gauging station Charongo, l/s
Year: 2000

Month Day	Jan	Feb	Mar	Apr	Mai	Jun	Jul	Aug	Sep	Oct	Nov	Dec
1	75	35	20	29	54	27	52	64	44	30	30	35
2	63	35	79	27	88	27	62	73	42	30	31	35
3	53	37	26	24	60	27	165	63	42	30	31	37
4	47	38	24	24	44	27	172	62	42	31	33	48
5	47	35	24	34	49	110	128	64	41	30	30	45
6	45	37	24	76	38	63	106	64	41	30	30	38
7	44	35	61	45	34	45	91	61	41	32	30	38
8	41	35	44	56	55	50	85	59	41	44	30	36
9	41	34	28	40	167	45	79	57	40	34	30	64
10	47	30	24	35	124	39	77	57	40	30	33	85
11	44	24	24	47	94	38	74	55	41	30	39	69
12	42	24	46	64	67	35	71	54	40	30	34	60
13	41	24	29	42	54	47	73	53	40	30	41	52
14	41	24	30	36	48	78	67	54	42	30	36	49
15	38	24	59	33	42	58	67	68	39	27	35	46
16	38	24	76	30	50	49	63	57	38	27	55	43
17	38	24	75	32	56	49	60	54	39	27	41	45
18	38	24	37	34	42	43	60	64	37	27	40	56
19	38	24	30	30	43	62	64	54	37	24	36	49
20	38	24	28	28	38	74	63	56	37	29	80	43
21	41	24	27	27	37	56	60	53	36	30	67	42
22	66	22	24	26	35	50	60	52	35	29	106	46
23	41	22	26	25	35	46	57	50	35	30	73	82
24	41	22	25	25	35	44	95	49	35	29	50	97
25	41	22	25	43	32	41	84	47	35	29	42	55
26	44	22	26	30	32	41	95	48	34	29	38	72
27	42	23	23	27	32	64	102	47	35	30	41	56
28	38	22	25	32	30	61	81	47	35	30	38	52
29	38	22	28	60	30	65	72	47	34	30	38	52
30	35		31	54	30	56	68	47	30	30	36	54
31	35		31		30		66	47		30		50

Observation: Discharge at gauging station Ngomberi, l/s
Year: 1998

Month Day	Jan	Feb	Mar	Apr	Mai	Jun	Jul	Aug	Sep	Oct	Nov	Dec
1								562	256	65	12	7
2								498	223	57	12	11
3								483	174	57	13	8
4								458	161	55	12	8
5								409	165	55	12	8
6								384	193	48	11	9
7								375	170	49	12	9
8								349	148	34	14	6
9								328	141	38	13	6
10								341	136	38	12	6
11								320	135	28	10	6
12								304	135	30	10	6
13								298	173	23	9	7
14								318	130	21	10	7
15							502	298	105	24	9	9
16							495	268	106	24	8	7
17							516	277	111	25	8	7
18							591	260	104	27	9	6
19							599	244	95	29	8	6
20							582	246	93	35	7	5
21							577	262	90	33	8	5
22							553	262	81	28	8	4
23							523	263	78	29	8	3
24							495	241	73	33	8	3
25							556	232	77	33	8	3
26							518	228	87	27	8	3
27							503	227	89	19	7	2
28							495	254	77	17	6	2
29							448	237	91	16	6	2
30							421	210	79	14	6	2
31							704	223		12		2

Observation: Discharge at gauging station Ngomberi, l/s
Year: 1999

Month Day	Jan	Feb	Mar	Apr	Mai	Jun	Jul	Aug	Sep	Oct	Nov	Dec
1	2	0	0	69	907	776	654	767	283	36	21	25
2	2	0	0	62	777	736	687	727	294	33	21	25
3	2	0	0	25	513	673	1105	747	273	29	21	27
4	2	0	0	19	472	647	1617	727	235	29	19	29
5	2	0	0	15	390	748	1000	727	217	29	17	27
6	2	0	0	157	331	1085	847	688	225	29	17	25
7	2	0	0	177	1128	951	1516	670	192	25	17	25
8	2	0	0	88	1362	874	1231	670	155	27	17	25
9	2	0	0	96	976	825	1338	689	162	25	17	25
10	2	0	0	33	858	917	1326	633	148	25	17	25
11	2	0	0	19	769	1126	1253	615	135	25	17	25
12	2	0	0	12	771	1059	1234	564	135	25	17	25
13	1	0	0	6	766	1333	1357	548	135	25	17	25
14	1	0	0	31	1048	1289	1089	516	135	25	17	25
15	1	0	0	7	957	1214	1245	471	135	23	19	21
16	1	0	0	5	1569	1132	1225	471	135	21	17	21
17	1	0	1	4	1187	1127	1116	651	155	25	14	21
18	1	0	0	3	1099	1143	1039	728	148	25	14	21
19	1	0	0	82	1006	1105	1014	581	135	25	14	21
20	1	0	0	557	1058	1029	1170	581	129	21	14	17
21	0	0	0	456	939	984	1039	516	122	21	14	17
22	0	0	0	360	953	910	990	428	111	21	16	14
23	1	0	0	297	837	852	990	414	95	21	16	14
24	1	0	0	189	745	850	1014	401	81	21	17	17
25	0	0	0	314	846	810	1090	388	69	17	25	21
26	0	0	0	263	816	772	1014	388	65	17	25	21
27	0	0	1	216	747	790	990	319	57	17	23	21
28	0	0	16	156	708	729	897	244	44	17	21	25
29	0		2	2932	670	744	830	217	41	17	25	21
30	0		1	1596	745	710	747	208	39	17	25	25
31	0		11		716		727	208		17		21

Observation: Discharge at gauging station Ngomberi, l/s
Year: 2000

Month Day	Jan	Feb	Mar	Apr	Mai	Jun	Jul	Aug	Sep	Oct	Nov	Dec
1	21	10	6	3	3	6	12	25	5	3	0	0
2	21	10	8	3	2	5	12	20	5	3	0	0
3	25	10	8	3	2	6	160	17	5	3	0	0
4	25	9	8	3	2	6	329	14	6	2	0	0
5	25	9	8	3	2	5	219	13	6	2	0	0
6	21	10	5	5	3	7	127	11	6	2	0	0
7	21	10	5	3	2	7	87	15	5	2	0	0
8	21	10	5	3	1	7	58	18	4	2	0	0
9	17	9	5	3	134	8	54	18	5	2	0	0
10	17	8	5	3	131	7	56	15	4	1	0	0
11	17	8	4	3	103	7	49	13	5	1	0	0
12	17	8	3	3	26	7	38	12	5	1	0	0
13	14	8	3	3	10	7	31	12	5	1	0	0
14	16	8	6	16	11	8	29	11	6	1	0	1
15	14	8	3	15	11	9	24	9	5	0	0	0
16	12	8	3	5	10	11	22	8	5	0	0	0
17	12	6	5	5	10	11	23	8	4	0	0	0
18	12	7	5	4	9	11	22	7	4	0	0	0
19	12	7	6	3	10	12	22	6	4	0	0	0
20	11	6	5	3	9	15	22	5	4	0	1	0
21	12	6	5	3	9	16	22	5	5	0	2	1
22	12	6	5	3	8	19	21	5	4	0	1	0
23	12	6	5	3	7	19	18	6	4	0	1	1
24	12	6	5	6	6	18	18	5	4	0	1	0
25	12	7	3	4	6	17	19	5	4	0	1	0
26	12	7	3	4	5	15	23	5	4	0	1	0
27	10	7	3	3	6	13	51	4	4	0	0	0
28	10	6	4	3	4	12	47	5	4	0	0	0
29	10	6	5	3	4	11	38	6	3	0	0	0
30	10		5	3	5	12	32	5	2	0	0	0
31	10		5		5		29	5		0		0

Observation: **Discharge at gauging station Ghona, l/s**
Year: **1998**

Month Day	Jan	Feb	Mar	Apr	Mai	Jun	Jul	Aug	Sep	Oct	Nov	Dec
1								2264	1206	962	377	337
2								2264	1168	962	369	327
3								2264	1168	962	346	320
4								2078	1168	824	353	315
5								1932	1168	686	354	314
6								1904	1206	596	360	319
7								1904	1168	596	362	304
8								1904	1095	596	1010	277
9								1822	1168	596	436	262
10								1795	1168	554	360	257
11								1743	1168	596	358	252
12								1691	1168	596	339	245
13								1691	1691	596	344	246
14								1743	1284	596	354	266
15								1691	1246	596	353	248
16								1717	1027	596	338	259
17								1691	1027	596	346	255
18								1691	1027	617	408	252
19								1691	1027	639	384	256
20								1691	1027	596	375	257
21								1691	1027	554	382	256
22								1592	1027	617	368	232
23							2535	1592	994	596	359	210
24							2535	1522	1027	639	353	210
25							2573	1498	1027	596	356	215
26							2500	1498	1027	596	364	217
27							2331	1498	1027	491	366	218
28							2234	1498	994	463	349	218
29							2141	1498	962	453	350	218
30							2138	1498	962	431	345	216
31							2912	1409		410		207

Observation: **Discharge at gauging station Ghona, l/s**
Year: **1999**

Month Day	Jan	Feb	Mar	Apr	Mai	Jun	Jul	Aug	Sep	Oct	Nov	Dec
1	206	178	145	1348	5584	1836	1328	1281	891	538	369	813
2	205	177	139	1438	5705	1783	1321	1225	940	553	356	802
3	194	174	140	972	4837	1730	1573	1203	980	553	361	623
4	193	176	142	1847	4745	1696	1643	1215	919	560	380	573
5	174	174	138	1219	4213	2003	1356	1244	881	543	356	554
6	173	172	141	1169	3903	3838	1308	1228	905	545	333	553
7	174	170	155	1192	4193	2420	1648	1213	886	569	327	556
8	176	169	160	1114	4142	2074	1485	1177	844	633	329	570
9	180	159	164	1141	3807	2101	1623	1165	837	563	327	516
10	182	149	299	860	3510	2161	1465	1162	840	548	330	516
11	194	167	315	788	3318	2131	1392	1140	805	572	386	501
12	182	161	423	712	3210	2004	1367	1122	801	575	360	487
13	185	162	307	665	2966	2216	1389	1092	754	517	436	481
14	420	163	310	1840	3808	2053	1371	1120	717	519	359	479
15	310	157	220	1717	3264	1995	1422	1132	722	500	407	469
16	231	147	244	1539	3464	1918	1346	1175	714	484	359	744
17	200	153	257	1207	3090	1845	1321	1328	775	479	352	493
18	208	152	258	1329	2794	1777	1284	1203	708	460	374	476
19	210	153	231	1547	2675	1799	1241	1168	680	445	359	481
20	213	154	238	2092	2578	1795	1459	1104	674	445	386	496
21	210	158	294	3158	2437	1777	1324	1151	676	438	368	494
22	208	146	240	9959	2303	1708	1321	1084	661	430	368	506
23	196	147	223	5549	2222	1666	1264	1044	621	419	385	491
24	203	147	211	4152	2113	1654	1264	989	618	421	366	466
25	199	147	214	3965	2119	1573	1381	994	608	415	351	450
26	186	145	335	3518	1999	1496	1399	960	599	411	417	473
27	179	145	1501	3063	1904	1503	1346	910	591	405	376	543
28	176	147	547	3089	1874	1409	1324	900	578	391	462	565
29	173		2129	6249	2101	1431	1321	898	592	385	1536	497
30	171		961	6699	2136	1381	1308	873	563	369	3193	479
31	175		1709		1827		1281	861		361		465

Observation: Discharge at gauging station Ghona, l/s
Year: 2000

Month Day	Jan	Feb	Mar	Apr	Mai	Jun	Jul	Aug	Sep	Oct	Nov	Dec
1	445	294	217	234	380	354	327	382	279	200	128	154
2	445	299	250	232	370	354	354	382	279	183	128	154
3	445	307	218	228	361	327	479	354	279	183	128	154
4	438	302	241	227	345	327	445	327	279	168	128	154
5	429	291	230	232	369	382	445	327	327	168	128	168
6	412	284	224	244	403	354	445	327	257	168	128	168
7	412	280	218	217	382	354	445	354	257	168	128	154
8	412	259	233	298	412	354	382	327	257	168	128	200
9	412	267	220	328	639	354	382	327	257	168	128	200
10	399	261	210	287	639	354	382	302	237	168	128	168
11	369	259	211	670	617	327	354	302	237	168	302	168
12	356	257	222	903	575	327	354	302	237	168	141	168
13	359	259	218	386	497	302	382	302	237	168	128	168
14	348	260	232	330	462	302	382	302	237	168	128	161
15	327	262	236	321	445	302	382	302	237	168	128	154
16	327	260	230	296	382	302	382	302	237	168	141	154
17	328	256	228	281	429	327	382	302	237	154	141	168
18	327	251	215	264	382	302	354	302	237	154	128	154
19	327	250	211	247	382	354	412	302	237	141	128	154
20	331	252	205	237	354	382	382	302	237	141	302	154
21	322	244	196	237	354	382	382	302	237	141	200	128
22	323	227	198	234	354	354	382	302	237	141	200	128
23	327	227	202	289	354	327	354	302	237	141	154	128
24	326	227	244	417	354	354	412	302	218	141	128	154
25	326	230	581	386	382	327	382	302	218	128	128	154
26	328	235	300	302	354	327	382	302	218	141	128	154
27	316	228	250	285	382	327	412	302	200	141	128	154
28	302	220	225	380	382	354	382	302	200	141	154	168
29	300	209	233	458	354	354	382	302	200	128	154	168
30	303		230	474	354	327	382	302	200	128	154	168
31	304		229		354		445	302		128		168

Appendix 2: Rainfall observations from reference stations

This appendix shows daily rainfall observations from the referense stations and the reference series itself.

Observation: **Rainfall at station 9337004 Moshi Airport**

Month Year	Jan	Feb	Mar	Apr	May	Jun	Jul	Aug	Sep	Oct	Nov	Dec	Annual
1938	5.1	100.0	336.2	243.8	334.9	13.2	4.0	7.1	5.1	151.1	53.6	23.2	1277.3
1939	10.9	5.1	97.0	431.0	344.2	10.2	4.1	13.4	11.2	7.9	10.9	26.9	972.8
1940	104.9	108.7	116.6	254.8	129.0	24.9	5.1	27.7	0.0	4.1	75.9	0.0	851.7
1941	26.2	18.0	68.8	183.4	27.9	34.8	0.0	1.5	10.9	0.0	46.2	216.2	634.1
1942	13.0	0.0	365.5	343.9	336.0	2.0	0.0	13.2	0.0	0.3	41.1	34.3	1149.3
1943	7.4	98.6	82.7	181.6	890.5	98.3	164.1	0.0	3.3	2.8	85.3	56.1	* 776.0
1944	49.0	27.2	123.2	392.7	138.2	5.3	4.6	7.9	47.2	73.9	99.6	108.5	1077.2
1945	18.3	14.7	102.6	106.9	226.1	7.9	24.6	16.0	1.8	0.3	44.5	20.6	584.2
1946	1.0	10.9	13.7	328.9	124.7	0.8	7.4	7.1	157.0	118.4	6.6	53.1	829.6
1947	65.5	33.5	110.5	440.4	205.2	110.0	2.5	12.4	18.3	22.9	36.1	24.6	1082.0
1948	0.0	2.0	112.0	196.3	153.7	20.3	8.4	9.4	0.5	24.9	4.1	126.7	658.4
1949	24.9	65.0	11.7	276.6	60.2	0.8	15.7	0.0	4.8	3.8	7.6	37.6	508.8
1950	8.6	34.8	218.7	203.5	255.8	17.0	18.0	26.4	8.4	2.3	11.4	62.0	866.9
1951	77.7	31.2	108.5	369.1	275.8	70.1	15.2	3.6	2.3	106.2	93.0	53.3	1206.0
1952	43.7	21.3	102.1	205.7	79.2	17.8	0.0	1.5	7.6	4.3	32.5	21.3	537.2
1953	16.8	0.0	68.6	177.8	176.0	0.8	16.5	33.3	20.1	49.0	78.0	19.8	656.6
1954	26.0	65.3	7.9	408.4	204.0	7.9	0.8	40.4	2.8	13.2	33.0	11.7	821.3
1955	14.0	103.4	152.9	323.1	102.6	68.1	8.9	12.7	0.0	0.0	17.8	113.8	917.2
1956	107.4	5.3	56.4	261.6	51.3	11.9	2.5	13.0	6.6	2.8	19.1	0.0	538.0
1957	165.9	16.3	30.2	271.0	187.5	10.4	8.9	0.0	5.1	114.0	74.2	66.3	949.7
1958	4.1	112.0	138.9	178.1	172.0	54.4	2.0	1.0	0.0	0.0	5.1	52.3	719.8
1959	39.4	45.5	38.1	205.7	25.9	15.7	26.9	16.8	0.0	5.6	21.3	21.1	462.0
1960	135.4	15.7	140.5	662.2	106.9	17.8	3.6	0.3	0.5	36.8	9.9	3.6	1133.1
1961	11.2	14.2	56.9	124.5	100.6	3.3	93.0	0.3	47.0	275.6	407.9	141.5	1275.8
1962	60.5	5.1	13.0	129.5	55.1	5.6	14.5	1.3	0.5	11.9	113.3	72.6	482.9
1963	13.8	136.8	277.4	240.8	57.0	68.8	5.9	0.0	0.0	0.0	178.2	88.0	1066.7
1964	2.5	85.0	69.5	326.3	100.4	5.2	2.8	5.5	16.0	43.0	23.2	33.1	712.5
1965	98.9	9.3	47.6	167.8	62.1	0.5	5.4	4.5	11.1	31.3	43.4	14.3	496.2
1966	21.6	32.1	171.9	148.1	125.7	26.5	8.1	0.0	0.5	2.5	6.2	45.5	588.7
1967	8.1	34.8	16.3	139.7	405.4	22.0	56.4	39.0	64.8	132.4	62.1	0.2	981.2
1968	0.6	134.2	138.0	331.2	206.5	91.4	19.6	21.7	51.0	29.1	103.7	170.2	1297.2
1969	7.9	62.2	28.0	58.0	192.6	45.1	11.0	55.7	2.1	78.2	70.9	1.0	612.7
1970	98.6	40.1	268.4	390.2	70.0	9.6	4.8	25.6	1.1	6.2	5.8	42.0	962.4
1971	43.3	1.9	51.9	540.3	149.4	52.9	15.4	2.0	0.4	0.0	15.2	146.1	1018.8
1972	11.3	57.2	201.9	281.0	197.9	4.6	22.6	12.8	57.1	57.3	145.4	22.3	1071.4
1973	92.6	34.4	5.3	205.3	51.8	26.1	1.9	5.2	0.1	7.8	44.3	37.1	511.9
1974	33.6	9.2	48.5	724.5	45.7	82.0	5.3	7.3	0.7	0.6	40.4	15.7	1013.5
1975	24.1	23.4	68.4	347.1	63.1	5.7	38.1	0.1	65.6	2.1	6.1	11.0	654.8
1976	7.5	42.5	119.3	236.8	83.6	32.2	3.5	2.2	20.5	0.1	16.2	51.5	615.9
1977	14.7	74.9	80.6	460.5	171.6	14.9	4.0	27.6	11.4	80.0	50.4	15.6	1006.2
1978	71.7	62.4	320.3	250.3	117.9	25.7	5.1	0.4	0.0	3.8	145.2	57.8	1060.6
1979	107.6	39.5	127.3	709.9	229.0	48.3	81.0	11.4	23.6	0.7	41.4	35.8	1455.5
1980	13.7	12.3	90.3	346.0	215.2	5.2	8.4	59.7	4.3	33.1	81.6	9.7	879.5
1981	15.6	11.3	119.5	441.1	244.9	9.7	2.9	13.8	4.7	76.2	32.8	38	1010.5
1982	13.5	19	113.9	90.7	216.6	83.7	44.7	14.2	23.3	51.5	263.6	111.8	1046.5
1983	11.6	31.9	54.1	217.4	217.3	34.6	26.9	0.0	3.3	8.8	35.2	67.7	708.8
1984	38.7	1.9	13.7	553.5	58.9	72.2	76.9	0.6	4.2	31.0	95.2	57.6	1004.4
1985	14.3	99.2	146.5	200.7	173.2	28.1	12.4	15.8	3.2	40.0	116.2	63.7	913.3
1986	87.6	5.4	164.5	387.6	208.1	29.5	2.2	7.0	1.4	43.8	58.7	89.2	1085.0
1987	39.8	8.8	25.0	116.0	97.1	0.3	58.4	60.8	3.4	0.6	13.4	19.6	443.2
1988	60.8	8.6	179.8	534.8	128.6	22.4	7.2	4.8	37.5	0.0	27.5	79.1	1091.1
1989	76.0	0.7	103.2	278.5	156.9	16.2	3.0	17.9	10.3	14.2	5.6	107.3	789.8
1990	52.0	45.7	244.9	630.9	48.5	6.4	3.6	6.2	4.0	39.8	173.7	43.0	1298.7
1991	126.3	18.0	78.4	168.5	283.7	5.5	5.6	29.7	26.8	16.7	38.1	105.6	902.9
1992	2.9	16.9	37.9	446.8	215.5	3.1	14.4	24.1	0.8	0.1	91.8	52.4	906.7
1993	111.1	54.7	73.5	46.6	103.6	5.8	8.2	12.5	0.0	35.0	45.2	32.2	528.4
1994	4.7	41.9	124.8	174.4	178.3	8.9	13.6	2.7	2.7	70.8	27.5	68.4	718.7
1995	11.1	38.8	71.9	508.0	210.9	4.1	6.4	17.7	1.8	34.4	9.5	47.5	962.1
1996	12.9	76.7	61.6	218.7	194.6	4.5	8.1	1.7	5	5.8	11.5	0	601.1
1997	0	12.6	127.5	375.2	179.1	26.2	14.7	0.6	1	127.5	105.8	65.7	1035.9
1998	287.2	151.2	44.4	402	135.3	12.9	25.4	1	4.8	15.2	19.2	16	1114.6
1999	20.8	0.6	229.8	362.9	96.7	74.5	15.1	24.9	13.8	1.7	68.4	23.1	932.3
Average	43.5	40.2	110.0	305.8	168.6	26.5	17.7	12.9	13.6	34.7	60.4	52.5	865.9

* Disagreement between sources. Annual value applied in calculation

Observation: Rainfall at station 9337021 Lyamungu ARI

Month Year	Jan	Feb	Mar	Apr	May	Jun	Jul	Aug	Sep	Oct	Nov	Dec	Annual
1938	14.1	74.7	360.8	321.6	540.0	77.0	47.4	16.4	5.5	66.3	81.3	27.8	1632.9
1939	8.4	10.6	129.8	682.3	685.3	212.6	23.5	14.4	42.1	2.1	15.8	12.9	1839.8
1940	81.7	130.7	100.7	568.7	276.3	67.6	59.9	74.4	9.2	33.1	21.5	32.3	1456.1
1941	29.6	51.8	62.6	451.4	290.4	136.5	24.2	67.9	79.7	1.7	121.8	254.1	1571.7
1942	38.7	11.9	370.5	1035	505.0	121.9	60.8	30.0	4.8	10.8	84.1	46.8	2319.8
1943	1.7	66.1	37.3	194.6	519.7	122.1	100.1	11.2	11.1	4.8	51.6	5.8	1126.1
1944	27.7	49.3	146.3	797.5	331.5	100.7	68.2	38.1	57.2	83.7	95.0	101.1	1896.3
1945	34.5	73.9	70.9	416.0	546.9	99.1	82.6	34.5	6.1	1.3	122.4	9.9	1498.1
1946	0.3	29.7	14.7	508.8	550.9	65.3	17.0	29.2	201.2	138.2	14.0	63.0	1632.2
1947	33.8	16.0	89.2	977.6	674.4	292.4	45.7	38.6	39.6	27.2	20.6	40.1	2295.1
1948	18.3	26.4	80.0	388.9	405.1	97.3	41.9	13.5	8.9	58.9	47.0	162.8	1349.0
1949	39.6	98.6	3.6	281.9	313.9	27.2	53.6	27.7	8.6	21.8	5.8	40.4	922.8
1950	49.8	79.5	187.2	452.9	651.5	141.0	59.4	46.0	52.1	15.2	22.1	20.1	1776.7
1951	117.6	72.1	103.6	541.5	512.8	203.7	65.5	45.2	7.9	83.3	221.2	188.5	2163.1
1952	45.5	39.9	87.1	349.0	359.4	95.8	46.2	18.3	80.3	11.7	67.6	10.7	1211.3
1953	35.3	15.2	27.2	370.6	357.1	42.4	54.6	66.8	45.5	56.9	124.7	32.8	1229.1
1954	42.4	62.7	3.8	628.9	422.7	37.3	11.7	44.7	10.7	11.2	33.0	31.2	1340.4
1955	18.5	182.4	111.3	450.6	447.3	166.9	58.4	18.0	2.0	3.0	71.1	72.4	1602.0
1956	214.4	24.6	111.8	418.3	227.8	80.5	44.5	33.8	74.9	5.3	44.2	*	1280.2
1957	89.7	19.1	50.3	677.9	666.5	108.2	74.9	6.1	21.3	41.1	242.6	127.0	2124.7
1958	12.2	185.9	126.7	350.0	379.5	176.0	65.3	4.1	3.6	0.3	10.2	65.5	1379.2
1959	4.6	27.7	60.5	446.0	115.3	47.0	134.6	53.6	0.3	10.4	40.4	59.4	999.7
1960	129.0	4.1	111.5	833.6	343.2	127.8	31.8	5.1	0.8	40.4	32.8	5.3	1665.2
1961	9.9	25.1	30.7	158.5	153.7	18.8	141.2	26.4	116.3	150.9	720.1	264.4	1816.1
1962	187.5	21.8	42.7	367.5	364.5	72.6	126.2	61.2	12.4	7.6	45.5	126.5	1436.1
1963	36.6	39.1	119.9	345.2	280.9	121.4	58.2	34.3	4.8	1.5	245.6	257.3	1544.8
1964	18.0	100.3	195.1	938.5	455.2	31.0	39.6	20.3	11.2	36.3	30.0	36.1	1911.6
1965	102.9	20.3	38.9	512.1	154.9	9.1	27.9	19.8	19.6	44.5	146.1	37.8	1133.9
1966	26.7	35.8	265.4	430.5	295.1	106.2	21.1	8.4	4.6	18.5	28.7	31.5	1272.5
1967	2.8	98.6	10.2	346.7	627.6	148.8	151.9	52.6	193.5	89.4	146.1	6.1	1874.3
1968	1.5	80.8	163.6	653.3	316.0	151.9	96.5	62.5	21.6	29.0	154.4	139.2	1870.2
1969	42.8	68.6	77.5	170.3	380.2	133.6	44.7	110.0	10.9	71.1	103.1	10.3	1223.1
1970	160.4	20.0	193.7	467.5	259.4	46.4	21.9	19.5	3.6	17.7	9.2	26.7	1246.0
1971	37.3	44.2	90.2	683.9	399.8	117.9	79.6	19.9	9.4	0.8	4.3	100.6	1587.9
1972	18.5	106.0	127.7	406.9	517.9	36.8	70.5	36.2	67.1	167.1	330.7	38.9	1924.3
1973	175.2	148.4	5.6	420.7	335.7	91.4	7.0	22.2	3.0	19.3	34.9	31.9	1295.3
1974	3.0	10.7	45.1	952.6	231.2	180.1	53.4	13.2	10.2	5.4	21.7	67.1	1593.7
1975	31.5	9.4	373.7	466.9	290.2	80.2	119.8	12.2	76.6	5.0	20.6	42.6	1528.7
1976	19.4	121.9	50.3	289.6	341.8	137.2	54.3	16.7	22.7	10.0	40.0	51.8	1155.7
1977	48.1	50.3	115.5	843.6	243.4	39.0	16.6	101.8	8.3	175.1	99.4	107.4	1848.5
1978	106.2	56.1	182.4	383.4	358.2	215.2	61.5	27.6	9.9	0.2	204.0	259.5	1864.2
1979	106.1	105.7	68.5	624.7	550.6	131.8	82.2	61.0	69.4	6.8	35.5	36.5	1878.8
1980	40.6	42.5	66.8	441.8	636.6	24.3	74.3	82.5	9.3	79.3	113.9	173.0	1784.9
1981	37.2	17.4	88.6	318.2	555.2	85.1	22.1	51.1	11.2	74.0	16.8	59.6	1336.5
1982	8.5	45.2	34.1	364.7	529.3	172.4	110.3	42.9	29.3	134.5	197.3	46.0	1714.5
1983	1.1	24.5	83.8	335.9	431.8	258.2	80.3	14.7	30.3	48.1	18.6	62.5	1389.8
1984	17.2	37.1	64.1	820.9	275.2	158.9	87.3	23.9	23.8	49.4	117.5	101.1	1776.4
1985	2.1	245.1	100.3	386.3	313.3	33.0	55.6	15.2	15.4	30.7	49.3	99.5	1345.8
1986	118.4	4.4	50.5	576.4	521.0	124.9	34.0	9.2	8.6	69.7	71.1	173.4	1761.6
1987	41.5	10.0	52.5	161.7	316.6	45.6	108.4	111.9	15.2	2.2	48.2	10.4	924.2
1988	60.3	6.5	110.6	703.1	203.0	145.5	17.3	8.3	23.0	2.5	57.7	85.3	1423.1
1989	94.5	12.4	19.0	303.1	810.6	137.4	63.6	65.1	21.7	25.0	33.3	85.8	1671.5
1990	27.4	54.3	329.2	698.5	509.0	87.3	33.5	30.5	5.9	56.1	174.6	118.4	2124.7
1991	72.8	0.0	140.0	199.6	522.9	51.5	7.0	68.6	8.8	6.5	89.4	108.9	1276.0
1992	0.0	66.7	25.6	536.7	404.6	47.4	73.4	35.4	4.8	1.1	59.3	50.1	1305.1
1993	177.9	59.4	28.9	150.7	297.5	77.5	50.6	18.6	2.3	28.5	18.0	78.5	988.4
1994	13.6	55.7	109.4	318.2	321.8	35.6	76.1	15.7	6.7	42.3	49.6	240.8	1285.5
1995	9.6	39.3	81.7	376.7	567.6	51.4	41.2	45.9	10.0	21.4	4.9	63.6	1313.3
1996	28.5	168.5	146.8	811.1	457.7	103.5	37.7	19.2	14	16.2	32.9	2.6	1838.7
1997	3.6	33.9	146.7	627.8	396.5	115.4	*	*	*	*	*	*	2117.0
1998	174.8	167	73.7	744	306.5	100.8	64.9	24.7	14.4	26.8	20.6	32	1750.2
1999	11.8	10.5	223.2	502.3	314.3	253.2	107.4	46.3	25.4	11.5	91.4	17.4	1614.7
Average	51.0	58.3	106.8	499.7	409.2	106.8	60.5	36.0	28.3	37.9	86.5	78.2	1565.5

* Montly value is missing. Annual value is found in separate files or summary.

Observation: Rainfall at station 9337031 Himo Sisal Estate

Month Year	Jan	Feb	Mar	Apr	May	Jun	Jul	Aug	Sep	Oct	Nov	Dec	Annual
1938	11.0	88.0	355.0	185.0	311.0	0.0	13.0	4.0	0.0	5.0	153.0	107.0	1232.0
1939	0.0	0.0	94.0	201.0	205.0	12.0	9.0	30.0	25.0	5.0	16.0	40.0	637.0
1940	135.0	150.0	141.0	275.0	113.0	15.0	0.0	29.0	10.0	0.0	44.0	24.5	936.5
1941	40.5	20.0	46.0	95.0	96.0	37.0	0.0	69.0	0.0	14.0	435.0	328.0	1180.5
1942	61.0	5.0	284.5	260	104.0	13.0	0.0	10.0	0.0	35.0	58.0	144.0	974.5
1943	19.1	179.8	65.3	103.9	71.6	27.2	16.8	0.0	0.0	0.0	57.7	4.1	545.3
1944	70.6	2.5	89.4	155.2	88.4	31.5	0.0	19.1	7.6	88.1	219.2	108.0	879.6
1945	52.1	13.2	24.6	83.6	174.5	13.5	24.4	9.7	0.0	0.0	111.3	15.5	522.2
1946	0.0	7.4	11.4	213.4	114.6	63.2	23.9	10.9	86.6	105.2	50.5	48.3	735.3
1947	37.6	18.3	120.1	287.0	150.6	120.9	9.4	5.1	9.7	6.1	107.7	28.4	900.9
1948	31.2	1.3	115.6	101.6	118.1	12.4	9.9	6.1	0.0	7.6	42.4	79.8	526.0
1949	42.2	82.8	0.0	106.2	83.3	0.0	0.0	10.2	0.0	13.2	3.3	152.4	493.5
1950	42.9	12.7	335.8	182.1	62.5	12.7	5.3	14.7	10.7	0.0	58.9	11.7	750.1
1951	37.6	41.9	59.4	365.3	189.0	48.8	19.1	0.0	2.3	58.4	115.8	96.3	1033.8
1952	50.8	142.7	184.2	245.4	45.2	0.0	11.7	2.8	9.4	50.3	27.4	6.6	776.5
1953	30.0	1.5	184.9	112.0	128.5	2.5	24.4	32.3	21.1	37.6	76.2	11.4	662.4
1954	47.5	2.5	45.2	353.1	109.7	6.6	0.0	6.9	17.0	171.4	34.5	42.9	837.4
1955	20.3	63.5	104.4	129.0	90.2	30.2	15.7	0.0	0.0	37.3	156.2	86.9	733.8
1956	124.0	124.5	95.3	142.7	49.8	0.0	4.1	26.4	6.9	1.0	88.9	15.0	678.4
1957	183.4	36.1	86.9	175.8	257.6	0.0	3.6	0.0	1.8	10.2	147.3	78.2	980.7
1958	17.3	173.2	195.3	79.5	103.4	70.1	3.0	0.0	0.0	1.0	34.0	54.6	731.5
1959	54.9	86.9	136.4	234.4	95.3	1.0	44.7	10.9	0.0	5.6	132.8	11.2	814.1
1960	48.5	22.9	126.7	263.4	65.5	4.3	4.1	0.0	0.0	30.2	17.5	0.0	583.2
1961	6.6	82.8	93.7	195.6	56.6	9.9	60.5	7.1	42.9	119.6	373.6	202.2	1251.2
1962	148.6	30.7	25.4	79.5	73.4	16.3	12.2	10.9	1.5	46.7	82.6	109.2	637.0
1963	116.1	55.9	178.8	87.1	99.1	46.5	2.0	3.6	3.8	1.8	190.5	61.2	846.3
1964	*	*	*	*	*	*	*	*	*	*	*	*	842.0
1965	*	*	*	*	*	*	*	*	*	*	*	*	569.0
1966	4.4	93.6	185.3	181.3	32.0	48.2	7.4	12.7	0.0	2.8	14.8	45.7	628.2
1967	0.0	66.8	31.5	272.0	135.6	13.4	34.0	76.2	75.7	8.4	271.8	66.3	1051.8
1968	0.0	0.0	239.0	289.5	88.1	4.9	0.0	58.2	0.0	4.1	85.2	17.8	786.8
1969	5.1	182.9	38.4	68.6	8.1	4.3	2.0	36.6	0.0	32.8	37.6	5.8	422.1
1970	60.5	35.8	243.3	378.6	63.2	0.0	8.0	10.1	15.2	2.1	37.2	109.2	963.2
1971	138.4	0.0	67.1	271.0	203.1	90.3	8.1	17.1	0.0	27.0	61.0	91.1	974.2
1972	96.6	104.5	210.5	123.8	208.6	58.2	21.6	24.4	44.5	34.5	211.8	83.4	1222.4
1973	89.3	40.4	0.0	61.0	72.5	27.5	0.0	0.0	0.0	0.0	38.2	7.0	335.9
1974	0.0	2.5	9.0	406.4	80.0	44.3	43.5	0.0	0.0	20.0	1.1	0.0	606.8
1975	10.4	7.6	21.8	38.4	7.1	25.0	18.0	1.6	36.6	17.3	60.1	43.0	286.9
1976	89.6	260.3	146.3	348.2	129.0	19.7	9.3	0.0	21.0	26.1	137.6	40.5	1227.6
1977	76.1	64.5	127.2	362.8	58.4	22.7	3.2	46.4	5.3	71.2	176.3	88.0	1102.1
1978	143.6	82.7					6.9		0.3	3.8	100.8	67.5	405.6
1979	46.2	130.1	110.3	203.5	107.4	17.4	13.0	47.4	13.9	3.3	12.1	21.5	726.1
1980	33.2	10.6	53.6	163.8	94.8	0.0	10.2	21.6	0.0	8.1	142.6	49.2	587.7
1981	21.5	34.5	140.9	148.1	142.8	0.0	0.0	16.3	33.4	33.6	41.1	64.9	677.1
1982	0.0	0	24.4	107.8	158.7	43.3	58.1	4.6	31.7	74.0	79.5	104.3	686.4
1983	0.0	51.7	3.2	53.8	48.2	13.9	4.5	0.0	10.2	4.3	16.9	98.8	305.5
1984	36.4	26.8	22.3	177.8	47.4	40.6	2.8	0.0	0.0	16.6	154.1	19.6	544.4
1985	3.9	89.8	76.0	159.0	64.0	9.7	18.5	0.4	0.0	69.7	93.7	82.0	666.7
1986	69	4.0	66.7	178.6	153.0	10.1	6.1	2.5	18.0	25.8	90.5	181.1	805.4
1987	20.6	3.2	44.5	76.1	64.4	4.9	10.4	35.7	9.5	2.6	22.7	7.9	302.5
1988	107.0	13.4	380.4	171.1	46.4	39.7	2.0	5.4	16.0	0.0	272.5	53.1	1107.0
1989	49.9	49.4	117.3	211.7	80.9	3.2	0.0	24.8	3.5	53.0	81.3	116.3	791.3
1990	24.1	36.4	110.1	120.9	57.1	0.6	14.5	5.5	0.0	16.9	93.5	76.1	555.7
1991	77.7	7.4	32.0	270.2	146.7	10.7	14.9	36.9	10.4	0.0	104.2	69.8	780.9
1992	0.0	20.3	50.3	148.8	53.7	3.2	0.0	3.4	0.0	0.0	112.1	71.3	463.1
1993	113.0	0.0	36.9	90.9	45.0	5.6	2.3	0.7	1.1	13.6	147.1	36.3	492.5
1994	13.7	149.6	54.4	68.5	115.2	19.6	7.3	4.2	3.3	10.9	38.8	151.2	636.7
1995	5.0	30.6	55.3	211.1	113.9	0.0	0.6	37.0	0.0	12.3	45.4	91.9	603.1
1996	29.9	129.3	11.6	264.1	157.7	0	1.2	6.3	1.8	0.3	77.3	0	679.5
1997	0	0	32.7	244.6	169.6	21.7	6.0	0.4	1.1	92.9	118.4	139.9	827.3
1998	252.3	122.1	72.4	313.5	216.9	0	25.4	0	28.3	5	53.9	6.6	1096.4
1999	23.6	0	174.1	106.8	169.6	66.5	5.6	6	0	0	133.3	36	721.5
Average	51.2	54.9	104.9	186.5	108.4	21.4	11.4	14.6	10.6	25.7	100.0	66.8	747.8

* Montly value is missing. Annual value is found in separate files or summary.

Weighted reference series based on station 9337004, 9337021 and 9337031

Month Year	Jan	Feb	Mar	Apr	May	Jun	Jul	Aug	Sep	Oct	Nov	Dec	Annual
1938	10.9	84.7	352.7	268.3	430.3	41.5	27.5	11.0	4.1	75.0	90.6	45.2	1441.7
1939	7.1	6.6	112.5	500.7	479.4	110.3	14.8	17.8	29.7	4.4	14.5	23.1	1320.7
1940	100.6	129.3	114.5	414.1	197.8	43.6	30.9	51.0	6.9	17.4	41.6	21.7	1169.3
1941	31.2	35.1	60.4	294.6	173.2	85.4	11.9	50.1	42.2	4.1	174.9	261.2	1224.3
1942	36.9	7.0	348.9	664.2	364.7	63.6	29.9	20.7	2.4	13.6	66.3	66.3	1684.6
1943	7.3	101.7	56.2	169.7	515.3	93.3	97.9	5.5	6.4	3.1	62.2	19.1	776.0
1944	43.6	32.3	126.6	536.2	221.7	58.4	34.8	25.4	42.8	82.1	125.5	104.7	1434.1
1945	34.2	43.5	68.6	253.7	371.9	54.1	53.1	23.6	3.5	0.7	98.6	14.1	1019.6
1946	0.4	19.3	13.7	390.3	332.2	47.2	16.0	18.9	162.2	125.0	20.6	56.8	1202.6
1947	43.3	21.3	102.3	668.9	423.4	202.4	25.4	23.6	26.8	21.0	45.3	33.2	1636.8
1948	16.4	13.9	97.1	268.9	269.1	56.4	25.3	10.6	4.5	37.6	34.2	133.5	967.3
1949	36.2	85.7	4.9	239.1	190.6	13.6	30.7	16.0	5.6	14.9	5.7	66.0	709.0
1950	37.0	51.6	230.7	321.3	405.2	77.0	35.4	33.3	30.4	8.1	27.9	29.5	1287.4
1951	87.9	53.9	94.6	453.1	372.1	130.9	40.9	23.2	5.0	83.7	161.5	130.0	1636.8
1952	46.2	59.0	114.0	285.6	209.2	52.0	25.5	10.1	43.8	18.8	48.6	12.6	925.4
1953	29.0	7.9	75.6	257.3	254.0	21.7	37.1	49.5	32.8	50.2	100.6	24.2	939.9
1954	39.1	49.3	14.7	504.0	289.5	22.1	6.0	34.6	10.0	49.4	33.4	28.7	1080.7
1955	17.7	132.9	121.0	340.2	269.4	107.8	34.9	12.3	1.0	10.3	76.6	87.1	1211.3
1956	164.0	42.9	92.8	310.8	137.9	42.9	23.5	26.4	40.3	3.6	47.9	*	936.5
1957	132.5	22.3	53.4	449.0	439.8	56.1	40.2	3.0	12.3	53.7	174.3	99.0	1535.6
1958	11.2	162.8	146.2	239.5	258.0	118.0	33.4	2.3	1.8	0.4	14.4	59.4	1047.3
1959	25.9	46.4	72.2	330.8	86.2	27.7	84.1	33.5	0.1	8.0	56.9	37.6	809.6
1960	111.8	11.7	123.0	652.8	213.5	68.8	17.6	2.6	0.5	37.0	23.0	3.6	1265.8
1961	9.5	35.7	52.7	157.9	116.4	12.5	109.1	14.7	80.2	177.5	553.6	216.3	1536.1
1962	143.7	19.4	30.5	235.0	211.8	41.1	69.0	33.1	6.6	18.0	72.7	107.8	988.5
1963	49.1	69.7	176.7	256.1	177.2	89.5	30.7	17.7	3.3	1.2	214.3	165.1	1250.3
1964	*	*	*	*	*	*	*	*	*	*	*	*	1333.4
1965	*	*	*	*	*	*	*	*	*	*	*	*	827.3
1966	20.1	48.4	221.1	295.0	187.1	70.8	14.3	7.1	2.4	10.5	19.3	38.7	934.7
1967	3.6	73.7	16.9	272.8	451.4	82.4	98.2	54.4	130.8	82.1	152.8	18.6	1437.6
1968	0.9	76.3	174.3	480.0	232.6	100.8	52.9	50.4	24.5	23.1	124.3	119.1	1459.3
1969	24.4	93.7	54.8	115.8	241.6	79.1	25.5	77.9	5.9	64.0	78.9	6.7	868.5
1970	120.1	29.2	225.7	425.5	161.7	25.5	14.0	19.0	5.6	10.9	14.9	50.3	1102.2
1971	62.7	22.3	74.3	547.7	285.3	93.7	45.3	14.4	4.7	6.7	20.6	110.8	1288.5
1972	34.9	92.4	167.4	306.0	358.0	33.1	46.0	27.1	59.1	106.0	252.3	44.8	1526.9
1973	132.5	91.9	4.2	277.4	196.5	58.6	4.0	12.3	1.5	11.6	38.2	27.5	856.3
1974	10.6	8.4	37.5	762.0	145.1	121.4	38.0	8.5	5.2	7.5	21.9	37.3	1203.5
1975	24.5	12.8	207.8	333.5	161.8	46.9	73.6	6.4	64.2	7.1	25.9	34.1	998.6
1976	32.7	132.8	91.7	289.0	221.4	81.0	29.9	8.8	21.7	11.1	56.5	49.1	1025.6
1977	45.6	60.3	108.7	626.2	180.3	28.6	10.0	68.6	8.4	124.8	104.1	77.8	1443.5
1978	105.6	64.1	177.1	257.0	208.5	113.0	33.3	13.7	4.9	2.0	163.7	159.4	1302.2
1979	92.4	93.4	94.3	548.8	358.8	82.1	65.6	44.3	43.9	4.3	31.6	32.8	1492.4
1980	31.5	26.8	70.1	350.3	394.4	13.4	41.3	62.0	5.8	50.0	111.9	99.4	1256.7
1981	27.6	19.8	109.3	311.7	373.7	44.5	11.7	32.8	14.7	65.1	26.9	55.0	1092.6
1982	7.9	27.4	53.6	229.6	357.0	117.9	80.2	26.1	28.2	97.7	187.7	77.6	1290.7
1983	3.7	32.9	56.8	237.3	283.1	139.8	47.9	7.2	18.2	27.1	22.7	72.5	949.3
1984	27.6	25.1	40.5	596.8	162.7	107.5	64.6	11.9	12.9	36.7	120.0	70.1	1276.3
1985	5.8	168.8	107.2	282.3	216.5	26.2	35.1	11.9	8.5	42.4	78.0	85.6	1068.3
1986	98.4	4.6	85.4	431.4	349.2	71.9	18.8	7.0	8.8	52.3	72.3	152.3	1352.4
1987	36.1	8.1	43.1	129.1	197.5	23.7	71.7	80.1	10.6	1.9	32.7	12.3	647.0
1988	71.4	8.7	192.9	532.1	145.9	87.1	11.0	6.7	25.3	1.2	100.0	76.0	1258.3
1989	79.0	17.9	65.1	274.9	460.9	72.8	32.1	42.8	14.3	28.6	37.0	98.8	1224.3
1990	33.3	47.7	254.7	544.2	277.3	44.9	20.9	18.0	4.0	42.4	155.3	87.9	1530.7
1991	88.5	6.6	97.8	207.7	369.3	29.4	8.5	50.5	14.1	7.7	78.9	98.8	1057.9
1992	0.8	42.2	34.8	421.0	270.6	24.9	40.1	24.8	2.6	0.6	80.6	55.7	998.5
1993	144.4	44.1	42.9	108.3	185.3	41.1	27.7	12.7	1.4	26.8	55.8	56.0	746.5
1994	11.2	74.0	100.7	220.3	234.1	24.6	42.9	9.5	4.8	42.7	41.0	172.8	978.5
1995	8.9	37.1	72.8	373.5	363.7	26.4	22.2	36.1	5.4	22.8	15.7	65.9	1050.6
1996	24.6	134.3	91.8	521.1	315.5	52.2	21.0	11.4	8.7	9.6	37.5	1.3	1228.9
1997	1.8	20.1	114.7	468.9	283.9	69.1	*	*	*	*	*	*	1519.2
1998	223.6	152.1	65.4	549.6	238.8	53.1	44.9	12.4	15.1	18.5	28.1	21.7	1423.3
1999	17.0	5.3	213.4	371.3	221.0	160.6	58.3	31.0	16.3	6.1	95.0	23.3	1218.7
Average	48.8	52.5	107.1	369.3	275.0	66.4	37.9	25.1	20.5	33.4	82.5	69.6	

* Montly values are missing. Annual values are calculated.

Appendix 3: Input data for the hydrological model

This appendix shows the meteorological observations applied as input to the hydrological model.

Observation: **Precipitation at station 9337021 Lyamungu ARI, mm**
Year: **1998**

Month / Day	Jan	Feb	Mar	Apr	Mai	Jun	Jul	Aug	Sep	Oct	Nov	Dec
1	1.2	2.3	0	0	52.1	14.3	0	0	0	0	0	24.1
2	1.1	1.8	0	0	25.8	4.5	0	0	0.4	0	0	0.7
3	2.8	0	0	0	17.4	7.9	0	0.5	0	0	0	0.4
4	9.8	0	0	1.3	51.6	1.6	0	0	0	0	0	0
5	2.5	0	0	0	19.2	1.5	0	0	0	0	0	0
6	0	0	0	52.9	7.6	0	0	0	1.9	0	0	4.7
7	1.7	0	0	0	11.8	0	0.9	2.2	0	0	0	0
8	4.3	2.7	0	0.7	1.3	0	0	0	0	0	0	0
9	0	11.1	0	0	14.5	0.5	0	0	0	0	0.4	0
10	0	20.5	1.5	107	1	0	0	0	0	0	0	0
11	1.5	31	0	37.2	0	0	0	0.3	0	0	0	0
12	55.7	0.5	0	97	25.4	0	1.9	0	0	0	0	0
13	3	0	0	76.6	35.7	0	0.6	0	7.7	0	0	0
14	10	0	0	0	0	0	1.1	0	0	0	0	0
15	15.2	14.8	0	0	0	0	5.7	0	0	4	0	1.3
16	2.1	2.4	0	4.6	13.1	0	0.6	0	0	0	0	0
17	39.8	6.4	0	1.4	11	19.7	2	0	0	0	2	0
18	6.3	0	0	65.1	0	2.2	12.2	0	0	0	14.2	0
19	0	26	2.8	34.1	0.3	7.4	0.9	0	0.9	0.8	0	0
20	1	12.6	0	12.8	0	3.8	0.6	12.2	0	4.5	0	0.8
21	0	10.4	0.5	27.2	0.1	0	0	4.8	0	17.5	0	0
22	0	24.5	7.8	7.6	0	0	0	0	0	0	0	0
23	3.2	0	6	6.3	0	3.7	0	0	0	0	0	0
24	0	0	15.4	34.7	0	14.2	0	0	1.5	0	0	0
25	0	0	7.8	56	0	19	8.4	0.5	0.5	0	0	0
26	0	0	15.8	28.4	1.7	0.4	6.4	0	0.8	0	3.4	0
27	0	0	13.5	5.6	13.3	0	0	0	0	0	0.6	0
28	0	0	2.6	7.7	3.6	0.1	0	1.1	0	0	0	0
29	13.6		0	42.7	0	0	0	0.9	0.7	0	0	0
30	0		0	37.3	0	0	1	2	0	0	0	0
31	0		0		0		22.6	0.2		0		0

Observation: **Precipitation at station 9337021 Lyamungu ARI, mm**
Year: **1999**

Month / Day	Jan	Feb	Mar	Apr	Mai	Jun	Jul	Aug	Sep	Oct	Nov	Dec
1	0	0	0	39.8	57	17.4	2.3	0.9	3	0	0	0
2	0	0	0	11.6	58.2	6	8.3	0.5	1.4	0	0	0
3	0	0	0	53	8.6	5.6	11.6	0	0	0	0	0.5
4	0	0	4.4	12.7	9.3	10.6	9.1	0	0	0	0	0
5	0	0	8.4	0	9.8	12.1	1.1	3.4	0	0.2	0	0
6	0	0	0	15.9	0	28.7	2.9	2.5	0	0	0	0
7	4	0	0	6.3	7.3	2.1	7.8	3	9	2.7	0	0
8	0	0	14	1.1	2.5	56.9	1.1	0.3	4.8	0	0	0
9	0	0	0	16	12	3.4	7.1	2	0	0	0	0
10	0	2	9.5	0.8	10	20	0.5	1	0	0	0	0
11	0	0	7.8	0	0.7	18.3	0	0	0	0	6	0
12	0	0	0	0.6	13	10.1	0	0	0	0	1.6	0
13	0	0	0	0	19.6	26.4	7.3	0	0	5.2	0	0
14	0	0	0	74.6	38.3	3.5	5.3	0.6	0	0.4	0	0
15	0	0	0	27.3	29.3	6.5	16.3	0	0	0	6.3	0
16	0	0	4	5	4.5	0	3.1	0	2.2	0	3.1	0
17	3.7	8.5	10.8	5.9	4.2	0	0.9	3.7	3.5	2	0	0
18	0	0	0	22.4	3	3.8	0	8.5	0	1	0.3	0
19	0	0	0	44.4	2.9	0	0	0	0	0	0	0
20	1.4	0	15.8	10.9	2.2	0	10.4	2.5	0	0	0	0
21	0	0	0	13	2.4	0	0.1	4	0	0	5.7	1.7
22	0	0	0	47.2	0	0	0	0.3	0	0	0	0
23	0	0	0	26.4	0	0.4	0.6	1.5	0	0	1.9	1.2
24	0	0	0	0.4	4.2	7.2	0.3	2.2	1.1	0	8.9	0
25	0	0	0	40.2	2	1.1	6	0	0	0	3.4	0
26	0	0	0.8	3.3	4.4	0	0	7.5	0	0	10.9	0.4
27	0	0	133	1	0.5	3.8	4.8	0	0	0	14.6	0.6
28	0	0	0	0	0	0	0	0	0	0	2.2	0
29	0		1.1	17.2	4.3	5.5	0	0	0	0	0.5	13
30	2.7		4	5.3	0.7	3.8	0.5	0.5	0.4	0	26	0
31	0		9.5		3.4		0	1.4		0		0

Observation: Precipitation at station 9337021 Lyamungu ARI, mm
Year: 2000

Month / Day	Jan	Feb	Mar	Apr	Mai	Jun	Jul	Aug	Sep	Oct	Nov	Dec
1	0	0	0	0	3.3	0	1.9	3.3	0	0	0	0.6
2	1	0	82	7	18.1	0	4	0	0	0	0	0
3	0	0	0	0.2	4.7	0	13	0	0	0	0	0
4	0	0	0	0	5.4	0	12.2	0	4	0	0	0
5	0	0	4.5	0.5	14.5	3.3	3.2	0	0	0	1	0
6	0	0	0	9.8	15.3	2.7	0	9.7	0.6	0	0	4.6
7	0	0	0	0	2.2	0	0	0.1	0.2	0	0	0
8	0	0	0	2	20.7	0.8	0	0	0	0	0	0
9	0	0	0	0	49.2	0	0	0.3	0	0	0	0
10	1.3	0	0	0	7.3	0	0.9	0	0	0	1.4	0
11	0	0	0	2.9	18.7	0	0	0	0	0	0	3.2
12	0	0	0	1.6	2.6	1.1	0	0	0	0	0	9.1
13	0	0	0.7	0	0	4.2	0	0	0	0	0	0
14	0	0	0	76.9	0	5.3	1.9	0	3	0	0.9	0
15	0	0	0.7	21.2	2	1.2	0	1.2	0	0.5	0	2.4
16	0	0	0	0.6	3.9	3.2	0	1.3	0	0	0	0
17	0	0	16.4	18.5	29.1	3.9	0	0	0	0	2.3	23
18	0	0	0	6.3	2.3	0.6	0	0	0	0	0.6	46.2
19	0	0	0	0	8.9	7.5	0	0	6.9	0	0	0
20	0	0	0	3.5	0.8	27.5	0.8	0	0.6	0	0	0
21	0	0	0	0	4	0	0	0	0	0	31.2	9.6
22	0	0	0.6	0.8	7.6	0	0	0	0	0	6.3	0.2
23	0	0	0	0	0.6	7.8	0	0	0	0	12.1	5.5
24	3.8	0	0	52	2	6.5	10.3	0	0	0	0.6	17.5
25	0	0	0	9	0.2	0	3	0	0	0	0.3	0
26	0	0	2.5	4.1	0.5	0	5	0	0	0	0	0
27	0	0	0	0.7	2.6	2.3	1.4	0	0	0	0	1.1
28	0	0	0	2.1	0	3.3	1.1	0	0	0	0	0
29	0	0	26.1	34.4	0	0.8	0	0	0	0	0.2	0
30	0		34.2	20.3	0	0	1	0	0	0	4.1	0
31	0		6.5		0		0	0		0		0

Observation: Precipitation at station 9337004 Moshi Airport, mm
Year: 1998

Month / Day	Jan	Feb	Mar	Apr	Mai	Jun	Jul	Aug	Sep	Oct	Nov	Dec
1	0	0	0	0	20	2.5	0	0	0	0	0	9.3
2	0	0	0	0	20.4	1.1	0	0	0	0	0	1.4
3	1	0	0	0	5.1	0	0	0	0	0	0	0
4	0	0	0	4	20.5	1.8	0	0	0	0	0	0
5	1	0	0	1	3.2	0	0	0	0	0	0	0
6	0	0	0	59.8	0	0	0	0	0	0	0	0
7	0	0	0	0	28.2	0	0	0	0	0	2	0
8	0.5	0	0	0	0	0	0	0	0	0	0	0
9	0.7	0	2.1	0	0	0.2	0	0	0	0	0	0
10	0	50	4.4	51	0	0	0	0	0	0	0	0
11	39.9	2	0	2	5.8	0	0	0	0	0	0	0
12	132	14.3	0	96	22.7	0	1	0	0	0	0	0
13	1	0	11.7	26.2	8.4	0	0	0	1.8	0	0	0
14	15	0	0	0	0	0	0	0	0	0	0	0
15	14.9	0	0	0	0	0	1.2	0	0	0	0	4.6
16	5	0	0	0	0	0	0	0	0	0	0	0
17	0	0	0	0	0	1.3	0	0	1.2	0	2	0
18	14	0	0	77.5	0	0.4	5.5	0	0	0	4.6	0
19	2.2	0	0	0	0	4.4	0	0	0	1.7	0	0
20	1.8	5.5	0	1	0	0	0	0	0	6.4	0	0.7
21	0.3	64	22.8	14.7	0	0	0	0	0	7.1	0	0
22	1	15.4	0	5.4	0	1.2	0	0	0	0	0	0
23	0	0	0	0	0	0	0	0	0	0	0	0
24	0	0	0.5	4.9	0	0	0	0	0	0	0	0
25	0	0	1.2	14	0	0	8.8	0	1.3	0	7.7	0
26	0	0	0	17.7	1	0	0	0	0.5	0	1.7	0
27	1.1	0	1.7	0	0	0	0	0	0	0	1.2	0
28	19.8	0	0	0	0	0	0	1	0	0	0	0
29	36.5		0	13.4	0	0	0	0	0	0	0	0
30	0		0	13.4	0	0	0.4	0	0	0	0	0
31	0		0		0		8.5	0		0		0

Observation: Precipitation at station 9337004 Moshi Airport, mm
Year: 1999

Month Day	Jan	Feb	Mar	Apr	Mai	Jun	Jul	Aug	Sep	Oct	Nov	Dec
1	0	0	0	0	4.7	6	0.3	0	2.2	0	0	0
2	0	0	0	20	11.5	1	1	0	0.2	0	0	1.2
3	0	0	0	14	0	0	0	0	0	0	0	1.4
4	0	0	0	5	4	10	2.7	0	0	0	0	0
5	0	0	2.7	0	0	9	0	0	0	0	0	0
6	0	0	0	0	0	35.9	0	0	3.8	1	0	0
7	0	0	0	12.2	0	1.2	0	0	2	0.7	0	0
8	0	0	0	0	0	0.8	0	0	1.8	0	0	0
9	0	0	0	1.3	10.8	0	0.1	0	0	0	0	0
10	0	0	19.1	1.9	6.8	1	0.2	0	0	0	1.4	0
11	0	0	34.6	0	0	3.2	0	0	0	0	14.2	0
12	0	0	0	0	6.7	0	0	0	0.2	0	0	0
13	0	0	0	50	6.7	2	0.7	0	0	0	0	0
14	0	0	0	10.3	24.2	0	2.2	0	0	0	1.8	0
15	0	0	1.8	0	9.8	0	4.3	0	0	0	11.6	0
16	0	0	0	0	0	0	0	1.5	0	0	0	0
17	0	0	41.6	7.6	0	0.6	0	0.3	0	0	0.8	0
18	0	0	0	2.7	0.6	1.4	0	12	0	0	0	0
19	0	0	0	32.4	1	0	0	2.5	0	0	0	0
20	11.4	0	0	57.5	0	0	0	6.9	0	0	1.6	0
21	0	0	0	51	0	0	0	0	0	0	0	14
22	7.6	0	0	62.8	0	0	0	0	0	0	1.8	0
23	1.8	0	2.8	1.2	0	0	1.5	0	0	0	5	0.4
24	0	0	0	15.5	2	1.4	0	0	0	0	0	0.2
25	0	0	0	9.5	0	0	0.4	1.5	0	0	10.8	2
26	0	0	0	0.8	0	0	0	0	0	0	5.4	0
27	0	0.6	49	0	0	0	1.1	0	0	0	0	0.3
28	0	0	1	1.4	0	0	0	0	0	0	0	3.6
29	0		1.6	0	2.9	1	0	0	3.6	0	0	0
30	0		0	5.8	0	0	0.6	0	0	0	14	0
31	0		75.6		5		0	0.2		0		0

Observation: Precipitation at station 9337004 Moshi Airport, mm
Year: 2000

Month Day	Jan	Feb	Mar	Apr	Mai	Jun	Jul	Aug	Sep	Oct	Nov	Dec
1	0	0	0	0	2.6	0	0	0	0	0	0	0
2	0	0	39	0	0	0	0.7	0	0	0	0	0
3	0	0	0	0	2.9	0	0.3	0	0	6	0	0
4	0	0	0	4.4	15.5	0	0	0	0.6	0	0	0
5	0	0	0	0	3.1	0	0	13.4	0	0	0	2.6
6	0	0	0	2	16.6	0	0	1.5	0.4	0	0	1.5
7	0	0	0	0.1	4.4	0	0	0	0	0	0	0
8	0	0	0	0	0.4	0	0	0	0	0	0	0
9	0	2	0	0	0	0.4	0	0	0	0	0	1.5
10	0	0	0	4.8	1.7	0	0	0	0	0	0	0
11	0	0	0	12.9	0	0	0	0	0	0	0	0
12	0	0	0	0	0	0	0	0	0	0	0	0
13	0	0	0	0	0	0	0	0	0	0	0	0
14	0	0	0	46.2	0.8	2.5	0	0.4	1	0	2.4	1.2
15	0	0	0	0	5.2	0	0	0.2	0	0	0	0
16	0	0	0	0	0	1.1	0	0	0	0	0.4	0.4
17	0	0	5.6	0	0	1.8	0	0	0	0	1.5	13.7
18	0	0	0	0	0	0	0	0	0	0	0	0
19	0	0	4.9	0	0	8	0	0	0	0	0	0
20	0	0	0	0	0.9	11.5	0	0	0	0	0	0
21	0	0	0	0	0	0	0	0	0	0	2	2.7
22	0	0	1.2	0	0	0	0	0	0	0	0.5	0
23	0	0	0	21	0	0	0	0	0	0	4.5	4.8
24	1.4	0	0	10.9	0	1.1	0	0	0	0	0	0
25	0	0	23.2	0.5	0	0	3.4	0	0	0	0	0
26	0	0	5	0	0	0	0	0	0	0	0	0
27	0	0	9.6	0	0	0	0	0	0	0	4.2	0
28	0	0	1.5	8.5	0	0.3	0	0	0	0	0	0
29	0	0	19.6	5.9	0	0	0	0	0	0	1.4	0
30	0		2	0	0	0.3	0	0	0	0	0	0
31	0		10		0		0	0		0		0

Observation: Precipitation at station 9337028 TPC, mm
Year: 1998

Month Day	Jan	Feb	Mar	Apr	Mai	Jun	Jul	Aug	Sep	Oct	Nov	Dec
1	3.2	0	0	0	17.2	0	0	0	0	0	0	0
2	0.8	0	0	0	0	0	0	0	0	0	0	0
3	0	0	0	1	0	0	0	0	0	0	0	0
4	0	0	0	0	0	0	0	0	0	0	0	0
5	0	0	0	32.3	0	0	0	0	15.4	0	0	0
6	0	0	0	0	0	0	0	0	0	0	0	0
7	0.6	0	0.2	0	0	0	0	0	0	0	1.5	0
8	0	0	0	0	0	0	0	0	0	0	0	0
9	0	25	0	140	6	0	0	0	0	0	0	0
10	0.6	0.5	3.3	0	26.3	0	0	0	0	0	0	0
11	36	1	0	18.3	0	0	0	0	0	0	0	0
12	0.5	0	0	0	0	0	0	0	5	0	0	0
13	16.2	0	0	0	0	0	0	0	0	0	0	0
14	25.5	12.5	0	0	0	0	0	0	0	0	0	0
15	0.8	0	0	0	0	0	0	0	0	0	0	0
16	0	0	0	33.5	0	0	0	0	0	0	0	0
17	0.6	0	0	5.1	0	0	0	0	0	0	0.4	0
18	0	0	0	0	0	0	0	0	0	0	0	0
19	0	0	0	0	0	0	0	0	0	0	0	0
20	0	0	0	2.3	0	0	0	0	0	0	0	0
21	0	0	0	0	0	0	0	0	0	0	0	0
22	0	0	0	0	0	0	0	0	0	0	0	0
23	0	0	0	10.6	0	0	0	0	0	0	0	0
24	0	0	20	10.4	0	0	0	0	0	0	1.2	0
25	0	0	27	7.5	2.1	0	0	0	0	0	2.5	0
26	0	0	5	0	0	0	0	0	0	0	0	0
27	29	0	0	36.6	0	0	0	0	0	0	0	0
28	23.5	0	0	2.6	0	0	0	0	0	0	0	0
29	0		0	0	0	0	0	0	0	0	0	0
30	0		0	0	0	0	0	0	0	0	0	0
31	1.7		0		0		0	0		0		0

Observation: Precipitation at station 9337028 TPC, mm
Year: 1999

Month Day	Jan	Feb	Mar	Apr	Mai	Jun	Jul	Aug	Sep	Oct	Nov	Dec
1	0	0	0	0	0	0	0	0	0	0	0	0
2	0	0	0	0	4.2	0	0	0	0	0	0	0
3	0	0	0	0	38	2	0	0	0	0	0	0
4	0	0	0.1	0	0	8	0	0	0	0	0	0
5	0	0	2.7	0	0	9	0	0	0	0	0	0
6	0	0	11.5	58	0	0	0	0	0	0	0	0
7	0	0	7.8	0.5	0	0	0	0	0	0	0	0
8	0	0	0	4.2	0	0	0	0	0	0	0	0
9	0	0	45.2	60	0.1	0	0	0	3.7	0	24.3	0
10	0	0	0	8.3	0	0	0	0	0	1.6	0	0
11	0	0	0	7.8	0.7	0	0	0	0	0	0	0
12	0	0	0	0	0	0	0	0	0	0	0	0
13	0	0	0	0	6	0	0	0	0	0	0	0
14	0	0	0	0	0	0	0	0	0	0	0	0
15	0	0	0	0	0	0	0	0	0	0	0	0
16	0	0	26	2.5	0	1.4	0	0	0	0	0	0
17	0	0	0	0	0	0	0	0	0	0	0	0
18	0	0	0	0	0	0	0	8.7	0	0	0	0
19	0	0	0	4.8	0	0	0	0	0	0	0	0
20	3	0	0	6.5	0	0	0	0	0	0	2	3.1
21	0	0	0	5	0	0	0	0	0	0	0	0
22	0	0	0	4.1	0	0	0	0	0	0	4.7	0
23	0	0	0	0	0	0	0	0	0	0	3.9	0
24	0	0	0	10.2	0	0	0	0	0	0	9.6	0
25	0	0	0	0	0	0	0	0.6	0	0	11	0
26	0	0	89.4	0	0	0	0	0	0	0	14.5	0
27	0	0	0	0	0	0	0	0	0	0	0	0
28	0	0	0	0	0	0	0.5	0	0	0	0	0
29	0		3	3.7	0	0	0	0	0	0	16	0
30	0		0	1.1	0	0	0	0	0	0	0	0
31	0		27.5		2.1		0	0		0		0

Observation: Precipitation at station 9337028 TPC, mm
Year: 2000

Month Day	Jan	Feb	Mar	Apr	Mai	Jun	Jul	Aug	Sep	Oct	Nov	Dec
1	0	0	41	0	2.2	0	0	0	0	0	0	0
2	0	0	0	0	0	0	0	0	0	0	0	0
3	0	0	0	0	0	0	0	0	0.3	0	0	0
4	0	0	0	0	4.9	0	0	0	0	0	0	0
5	0	0	0	0	5.4	0	0	10	0	0	0	0.2
6	0	0	0	0	4.3	0	0	0	0	0	0	0
7	0	0	0	53.3	1.5	0	0	0	0	0	0	0
8	0	0	0	0	0	0	0	0	0	0	0	0
9	0	0	0	2	0	0	0	0	0	0	0	0
10	0	0	0	0	0	0	0	0	0	0	0	2.6
11	0	0	0	1.9	0	0	0	0	0	0	0	0
12	0	0	0	1.5	0	0	0	0	0	0	2.3	0
13	0	0	0	0	0	0	0	0	7.5	0	0	1.1
14	0	0	0	0	0	0	0	0	0	0	0	0
15	0	0	0	4	0	0	0	0	0	0	0	0
16	0	0	12.8	0	0	0	0	0	0	0	0	0
17	0	0	0	0	0	8	0	0	0	0	12.8	0.6
18	0	0	0	0	0	4.1	0	0	0	0	0	0
19	0	0	0	0	0	0	0	0	0	0	0	0
20	0	0	4.2	0	0	0	0	0	0	0	0	0
21	0	0	0	0	0	0	0	0	0	0	3	0
22	0	0	0	0	0	0	0	0	0	0	0	0
23	0	0	0	0	0	0	0	0	0	0	0	2.6
24	0	0	6.5	0	0	0	0	0	0	0	0	0
25	0	0	3.3	0	0	0	0	0	0	0	0	0
26	0	0	0	0	0	0	0	0	0	0	0	0
27	0	0	0	0	0	0	0	0	0	0	2.2	0
28	0	0	0	0	0	0	0	0	0	0	4.2	0
29	0	0	9.3	0	0	0	0	0	0	0	0	0
30	0		0.5	2.2	0	0	0	0	0	0	0	0
31	0		0		0		0	0		0		0

Observation: Temperature at station 9337115 KIA, oC
Year: 1998

Month Day	Jan	Feb	Mar	Apr	Mai	Jun	Jul	Aug	Sep	Oct	Nov	Dec
1	23.8	25.5	23.9	26.7	22.2	21.4	17.5	20.9	23.5	20.3	25.3	24.8
2	25.3	24.8	25.1	27.4	23.2	22.4	18.2	19.1	23.6	21.0	22.1	25.1
3	25.0	25.2	23.9	26.1	22.7	22.3	17.2	20.8	23.9	21.9	21.8	25.0
4	24.4	24.3	24.4	27.4	22.9	22.8	18.3	22.3	23.0	22.1	25.0	25.7
5	25.7	23.6	24.7	27.0	24.0	22.5	18.7	21.1	22.8	23.3	25.5	25.1
6	25.2	23.2	26.3	26.2	23.8	22.0	17.5	22.4	23.6	21.0	25.5	26.7
7	25.4	24.9	24.9	24.3	24.3	22.3	20.6	19.7	23.1	21.7	26.8	25.0
8	25.1	25.4	25.2	26.1	24.9	23.5	19.4	21.3	22.3	21.0	26.6	24.6
9	26.5	26.9	25.2	26.8	24.9	21.6	20.2	21.9	21.9	21.0	25.6	25.8
10	25.8	25.8	26.5	24.6	24.8	20.0	18.4	20.6	21.0	21.5	22.2	26.4
11	25.4	24.0	26.2	24.4	24.2	21.1	19.5	21.2	22.2	24.4	21.6	26.1
12	24.2	24.1	25.6	23.6	24.0	20.7	20.9	20.7	23.2	23.3	25.7	25.3
13	25.2	25.7	25.2	25.5	23.0	20.1	21.1	21.8	22.9	22.3	23.0	24.5
14	21.5	24.4	25.5	24.9	24.8	18.3	19.5	19.2	23.2	24.3	23.5	26.4
15	24.0	25.6	26.3	26.1	22.7	17.9	19.0	19.4	20.9	24.2	22.6	25.7
16	24.5	24.5	26.0	26.2	22.1	18.1	19.5	20.5	23.3	23.8	24.7	26.9
17	24.4	25.1	26.7	25.0	21.6	21.3	18.2	20.7	23.0	24.9	23.6	26.6
18	23.5	24.8	26.8	25.3	20.7	21.8	19.3	20.7	23.5	23.6	23.4	26.3
19	24.5	23.1	25.9	24.7	22.2	20.1	19.7	21.0	21.9	24.4	24.3	26.1
20	25.0	24.7	26.7	24.0	22.6	20.4	19.0	21.7	21.1	23.1	25.2	27.1
21	25.3	25.1	26.9	20.3	22.4	22.5	19.7	22.1	20.4	25.7	25.4	26.3
22	23.9	25.0	26.0	22.9	22.5	19.9	17.9	22.0	20.3	25.3	27.0	27.0
23	25.6	24.8	26.3	24.9	21.5	22.3	18.6	21.4	21.9	26.0	27.3	26.7
24	24.8	24.9	26.0	23.3	21.9	21.5	21.1	22.6	24.3	23.9	26.7	26.1
25	24.7	25.2	26.4	22.7	21.2	22.7	21.0	20.7	22.3	22.6	26.3	26.0
26	25.0	23.3	26.1	24.2	21.8	22.3	20.9	21.1	22.9	21.9	26.5	26.1
27	25.1	23.1	27.3	25.0	23.0	20.1	18.6	20.2	23.4	22.6	26.3	26.3
28	22.5	26.2	26.9	26.0	22.5	20.4	20.8	20.2	21.9	22.9	26.4	26.7
29	23.8		26.0	24.5	20.5	20.5	21.9	19.6	22.8	24.2	26.5	26.7
30	24.1		26.0	22.7	21.7	19.4	21.4	22.7	23.2	23.5	26.6	26.9
31	25.2		27.0		19.6		20.6	23.3		24.1		26.7

Observation: **Temperature at station 9337115 KIA, oC**
Year: **1999**

Month Day	Jan	Feb	Mar	Apr	Mai	Jun	Jul	Aug	Sep	Oct	Nov	Dec
1	26.9	26.3	26.7	24.1	22.9	21.1	20.4	20.1	21.1	22.5	22.1	23.9
2	27.1	25.7	28.5	24.3	23.9	21.7	21.5	19.0	22.3	24.6	25.8	24.8
3	26.9	26.0	26.6	23.7	23.0	20.5	20.4	20.8	22.4	23.3	26.6	25.4
4	27.3	26.1	26.7	24.0	22.6	21.5	20.4	20.6	22.1	21.6	26.2	23.6
5	25.9	25.6	27.8	24.7	22.5	18.1	21.4	20.2	22.1	23.6	24.5	24.5
6	25.2	25.3	27.9	24.5	22.2	20.1	21.0	22.7	23.6	24.9	26.9	25.3
7	25.5	25.6	26.0	23.9	22.8	20.1	20.9	20.1	21.1	24.3	27.1	25.4
8	26.8	25.9	26.4	24.0	22.6	20.9	20.9	20.5	22.3	22.9	27.5	26.0
9	26.0	25.3	26.5	25.1	21.6	21.7	20.1	22.3	22.8	23.2	26.4	23.3
10	26.1	28.1	26.0	25.0	20.8	20.5	21.1	21.8	22.3	23.9	26.0	26.8
11	26.0	26.7	26.1	24.9	22.1	21.5	19.5	20.2	23.1	25.1	25.1	26.9
12	27.7	27.1	25.4	24.4	21.7	21.2	20.6	22.2	21.8	22.8	26.2	25.9
13	26.4	28.3	24.9	23.5	21.8	21.2	19.1	21.5	23.0	22.1	25.2	26.8
14	27.4	24.8	25.0	24.2	21.3	21.3	18.7	20.2	19.0	22.2	24.5	26.6
15	25.1	25.0	25.0	24.1	22.1	21.4	21.2	20.2	21.5	20.0	25.2	26.4
16	24.9	26.2	25.3	24.2	21.9	21.9	21.8	18.6	23.3	23.1	25.7	25.9
17	25.6	27.6	25.3	24.2	21.8	21.8	21.3	20.3	22.8	22.3	26.5	26.3
18	25.6	27.0	25.3	24.1	22.4	22.0	21.3	21.4	22.8	23.9	25.4	24.9
19	24.8	26.3	25.3	24.9	22.3	20.6	20.0	20.1	20.5	20.6	24.8	26.2
20	24.3	27.0	25.6	24.1	22.4	20.2	20.6	21.9	21.0	24.6	26.5	25.4
21	26.8	27.8	25.9	24.1	22.2	20.3	18.7	22.2	21.8	23.1	26.3	25.1
22	26.5	27.9	26.6	24.6	21.3	20.4	20.1	21.5	22.1	22.3	25.9	25.3
23	27.0	27.0	26.6	23.2	22.0	19.3	20.2	20.3	24.4	22.7	25.3	26.2
24	26.3	28.5	27.0	21.1	22.4	20.2	19.0	21.2	24.2	22.1	25.3	25.0
25	26.3	27.2	25.9	21.5	23.1	17.0	19.3	22.4	21.2	24.4	24.0	23.1
26	25.9	25.3	25.4	21.7	21.3	18.0	19.9	23.4	21.2	25.4	23.9	25.4
27	26.1	26.0	22.4	22.7	22.2	21.4	21.1	22.6	20.5	24.0	23.1	26.5
28	25.0	26.0	25.1	22.4	22.0	19.8	18.3	21.3	24.3	25.9	25.0	26.0
29	25.3		24.6	21.5	20.9	17.1	19.6	19.9	25.0	26.3	23.5	25.8
30	26.3		25.5	22.2	21.7	21.0	21.3	20.8	24.4	23.1	22.4	25.3
31	25.7		25.5		21.2		19.8	21.2		25.0		26.4

Observation: **Temperature at station 9337115 KIA, oC**
Year: **2000**

Month Day	Jan	Feb	Mar	Apr	Mai	Jun	Jul	Aug	Sep	Oct	Nov	Dec
1	28.0	29.4	29.9	26.7	21.1	24.8	20.8	23.4	24.5	25.9	26.7	26.8
2	27.9	28.8	25.6	26.3	23.1	24.0	21.3	23.7	22.4	26.3	26.7	26.6
3	28.8	28.5	28.9	27.6	24.0	25.6	22.2	23.4	25.3	25.5	26.7	27.2
4	28.3	29.5	24.5	27.8	24.6	24.8	19.9	22.8	23.7	25.4	26.7	27.6
5	28.3	29.1	26.3	25.7	21.9	23.8	21.7	20.8	24.3	25.8	26.7	27.8
6	28.5	28.1	28.7	26.1	22.9	21.8	22.1	20.1	24.1	27.1	26.7	26.5
7	29.1	28.3	29.2	27.1	23.3	22.8	23.0	22.6	22.2	26.7	26.7	26.4
8	29.0	28.4	27.5	25.0	21.7	23.3	22.2	20.9	23.2	24.7	26.7	26.8
9	29.2	29.0	28.7	25.9	19.9	23.0	21.5	22.5	24.8	27.0	26.7	27.6
10	28.4	28.5	28.4	25.0	22.1	23.0	21.5	23.2	22.8	27.0	26.7	26.3
11	29.8	28.5	28.8	24.3	23.7	23.5	22.6	23.0	23.9	26.5	26.7	25.9
12	29.7	27.6	28.5	24.5	23.0	22.2	22.6	22.7	23.4	25.1	26.7	26.8
13	29.5	29.5	28.8	24.0	22.9	21.3	23.2	22.8	24.4	26.5	26.7	27.6
14	30.0	29.0	29.1	26.0	24.0	21.4	22.9	23.2	22.8	26.1	26.7	27.7
15	29.5	30.4	28.2	25.3	24.1	22.9	21.2	21.3	23.6	25.9	26.7	27.7
16	28.9	30.2	28.5	25.8	22.7	23.3	21.2	20.5	25.5	25.7	26.7	25.3
17	30.2	28.8	27.0	26.6	22.6	23.1	22.5	20.6	24.8	27.0	26.7	23.4
18	28.5	29.6	27.1	27.2	23.2	23.7	22.1	23.3	22.6	27.5	26.7	25.0
19	28.4	29.8	27.8	26.3	23.0	20.6	21.3	24.4	23.1	26.3	26.7	26.8
20	28.2	29.1	27.6	26.5	23.2	21.3	22.1	22.1	22.8	24.2	26.7	25.3
21	29.3	30.2	27.0	26.0	23.3	21.6	22.9	24.2	24.4	26.2	26.7	23.5
22	28.2	31.3	27.6	26.5	23.7	23.4	22.8	22.2	23.1	26.1	26.7	24.7
23	29.4	30.6	27.3	26.4	24.3	23.7	22.1	24.7	24.2	25.7	26.7	27.3
24	27.4	29.6	27.0	25.3	23.2	22.3	21.1	23.9	23.5	26.4	26.7	26.5
25	27.9	29.3	26.0	25.5	24.8	23.1	20.5	22.3	23.5	27.2	26.7	27.7
26	29.0	29.3	25.8	25.6	24.5	21.6	20.6	21.6	23.8	27.4	26.7	28.9
27	29.9	29.9	26.8	26.6	23.5	23.1	21.0	19.5	25.0	27.7	26.7	28.9
28	29.0	29.4	27.3	22.6	22.8	21.0	22.4	23.2	23.3	27.8	26.7	25.1
29	29.4	30.3	26.3	23.9	22.0	21.3	22.4	24.1	23.2	27.7	26.7	27.9
30	31.8		26.4	24.4	24.1	22.2	24.3	23.2	22.8	27.3	26.7	28.1
31	28.9		25.4		23.1		21.8	22.6		26.6		27.8

Observation: Temperature at station Gauge 8, oC
Year: 2000

Month Day	Jan	Feb	Mar	Apr	Mai	Jun	Jul	Aug	Sep	Oct	Nov	Dec
1	18.5	19.9	20.4	17.2	15.5	15.7	13.1	15.4	16.1	18.5	16.9	19.1
2	19.0	19.3	18.4	17.9	16.2	14.7	13.4	15.5	15.4	16.6	17.2	19.1
3	19.3	19.8	21.4	18.6	16.2	15.4	13.7	15.9	15.5	17.0	17.6	19.2
4	19.8	20.7	19.0	19.4	16.2	15.9	12.9	15.9	15.9	17.6	17.2	18.6
5	19.3	21.1	19.2	18.7	16.0	14.3	13.2	14.1	15.2	17.3	19.5	18.8
6	19.6	20.3	20.0	17.1	16.1	14.2	13.6	14.4	16.6	16.5	18.6	18.8
7	21.3	19.2	19.3	18.4	16.4	14.7	14.0	15.1	15.1	16.1	17.7	17.7
8	20.1	19.5	19.0	18.2	15.2	15.1	13.6	13.8	16.4	15.2	17.4	18.7
9	20.0	20.8	19.4	19.0	14.6	14.8	14.2	14.3	17.4	18.8	17.5	16.8
10	18.7	19.9	20.5	17.5	15.4	14.4	13.9	15.2	15.2	17.6	18.1	18.7
11	20.3	20.0	20.8	16.8	16.1	14.5	15.1	16.3	14.4	17.7	20.3	19.0
12	20.4	19.9	18.2	17.3	15.7	14.5	14.9	15.7	15.2	17.0	17.6	19.4
13	21.0	19.2	18.9	16.1	16.6	14.0	14.4	15.2	14.6	18.4	17.6	19.4
14	21.3	21.1	17.9	16.5	15.8	14.1	14.2	14.3	15.2	17.6	17.8	18.8
15	20.2	21.9	18.5	16.7	16.2	14.5	13.3	13.1	16.4	17.4	19.0	18.6
16	21.0	21.1	19.4	17.1	15.5	15.2	14.5	13.2	18.5	16.9	17.4	18.8
17	21.2	20.2	19.2	16.9	15.3	14.7	14.6	14.1	16.9	17.9	19.7	18.4
18	19.5	21.2	18.5	18.1	15.4	16.1	14.6	14.7	15.2	18.6	18.8	18.0
19	19.7	21.7	18.9	16.6	15.8	14.9	13.3	15.1	14.8	17.8	19.9	19.1
20	17.3	21.2	17.7	18.0	15.2	13.9	13.5	14.6	15.7	16.6	16.2	19.6
21	17.8	22.0	17.3	17.9	16.2	13.4	14.8	16.0	16.5	18.5	18.3	19.2
22	17.9	22.9	18.7	17.6	15.7	15.0	14.0	15.2	15.2	18.3	16.0	18.7
23	19.3	22.9	18.2	17.8	15.6	16.1	13.9	15.6	16.7	18.0	18.7	19.0
24	18.8	21.7	18.2	17.2	16.3	15.8	12.3	15.6	15.0	19.1	19.0	18.2
25	19.5	20.5	17.9	16.9	16.6	14.8	13.2	14.7	14.9	19.3	19.9	20.5
26	21.3	20.1	17.4	17.0	15.2	14.7	12.7	14.4	16.8	19.1	19.3	19.6
27	21.6	22.6	17.4	17.2	15.3	12.7	13.2	14.0	15.8	17.1	18.3	19.8
28	21.2	20.4	16.4	15.9	15.4	12.8	14.6	14.4	15.3	18.4	17.7	19.4
29	21.3	22.3	15.9	16.4	14.6	12.9	15.2	16.4	15.3	18.7	17.7	20.2
30	22.3		16.9	16.0	15.8	13.9	15.3	14.9	15.6	18.6	18.8	20.3
31	21.1		17.4		15.7		15.1	14.4		17.9		19.3

Gauge 8 started recording in Januar 2000. No records for 1998-1999

Observation: Temperature at station 9337028 TPC, oC
Year: 1998

Month Day	Jan	Feb	Mar	Apr	Mai	Jun	Jul	Aug	Sep	Oct	Nov	Dec
1	25.5	26.5	25.3	27.5	25.0	22.9	19.0	22.0	24.5	24.5	24.5	26.5
2	25.8	24.9	26.9	28.5	24.0	23.5	20.8	22.4	24.5	23.8	22.3	26.7
3	25.4	27.0	28.5	27.0	23.6	23.5	18.5	22.3	25.0	25.0	24.0	26.5
4	25.0	25.8	26.2	27.0	22.5	24.8	20.5	23.0	23.5	24.9	25.8	27.5
5	26.2	25.8	26.3	27.5	25.0	24.0	24.0	23.8	25.0	25.0	24.8	27.8
6	26.0	25.5	26.4	26.5	25.5	23.0	20.5	22.5	23.5	22.0	26.3	27.8
7	26.0	26.5	26.3	27.3	25.5	24.0	21.5	22.6	23.5	24.0	26.8	27.3
8	25.4	26.3	26.3	27.4	25.4	22.3	19.5	22.5	23.5	22.6	25.8	26.3
9	25.9	27.3	26.1	27.8	24.5	22.0	21.0	23.9	23.5	24.0	24.5	28.0
10	26.2	22.5	26.3	26.0	25.0	21.8	20.6	23.0	22.0	22.3	25.3	26.5
11	26.2	25.5	27.0	24.8	24.3	22.0	20.5	21.5	24.8	25.5	24.5	26.0
12	23.8	26.3	26.5	24.5	24.3	22.1	22.5	21.5	24.5	25.5	24.3	26.2
13	27.0	26.8	26.5	26.0	25.0	20.8	20.5	22.8	23.5	24.5	25.5	26.9
14	22.0	27.0	27.0	26.0	25.0	23.0	19.5	22.3	21.5	23.0	25.0	27.8
15	26.2	26.5	28.0	26.5	24.3	20.5	21.3	22.5	23.5	25.0	26.3	27.8
16	25.8	26.8	27.0	26.4	25.2	24.8	21.0	23.8	24.0	27.3	26.9	28.0
17	25.0	26.0	27.5	26.0	25.0	23.0	20.5	21.8	23.5	24.5	27.0	28.1
18	24.9	26.3	28.1	26.0	23.1	22.3	21.3	23.0	25.0	24.8	25.5	27.4
19	25.5	28.1	28.6	26.0	23.5	22.9	19.5	23.5	23.5	24.8	26.8	27.5
20	25.5	25.0	27.9	26.0	22.9	22.5	20.0	23.0	24.5	23.8	27.5	27.4
21	26.9	26.3	27.9	24.0	24.8	24.0	21.0	23.0	22.0	26.5	27.2	27.7
22	25.6	27.0	27.4	24.5	23.5	21.5	19.8	23.5	22.5	26.0	25.0	28.3
23	25.4	26.5	27.5	25.0	22.0	22.5	20.5	23.5	22.0	26.5	28.0	27.8
24	24.6	26.3	26.0	24.0	22.5	23.5	21.0	22.4	24.6	24.8	28.0	26.8
25	25.3	25.8	26.3	25.0	21.8	23.8	22.8	23.5	24.0	25.0	26.0	27.8
26	26.7	26.3	26.3	25.0	22.5	22.5	22.0	23.8	23.0	23.0	26.0	27.8
27	23.7	25.0	26.7	25.0	24.5	24.3	19.8	23.0	24.7	24.3	26.6	26.4
28	24.5	26.0	27.5	25.1	23.3	24.0	21.5	23.0	25.3	24.3	27.4	27.9
29	24.7		26.3	24.8	21.3	21.0	23.0	21.5	25.5	25.3	27.7	28.0
30	24.5		26.3	23.5	22.5	21.2	22.0	23.0	24.0	25.0	28.3	28.8
31	26.4		27.8		23.6		22.3	23.0		26.0		28.0

Observation: **Temperature at station 9337028 TPC, oC**
Year: **1999**

Month Day	Jan	Feb	Mar	Apr	Mai	Jun	Jul	Aug	Sep	Oct	Nov	Dec
1	28.2	27.8	28.8	25.5	24.9	22.0	22.5	22.5	22.5	24.0	24.2	25.3
2	27.9	26.8	28.1	25.3	25.5	23.9	23.0	21.3	24.3	25.5	28.0	26.6
3	28.5	26.3	28.0	26.2	25.0	24.8	23.0	22.3	25.0	25.0	27.9	26.4
4	28.4	26.8	27.8	25.5	25.0	23.4	23.3	23.0	23.9	25.5	27.3	25.0
5	28.3	25.3	29.0	26.0	24.5	22.9	23.2	21.0	24.5	23.7	26.8	26.3
6	28.5	27.5	28.0	25.5	24.0	21.3	25.3	24.0	23.8	25.3	27.5	30.0
7	28.5	26.5	26.5	25.5	25.3	22.0	23.5	24.0	23.0	25.5	27.5	26.2
8	28.3	28.2	27.5	28.0	25.8	24.8	23.3	22.9	23.0	25.8	28.5	26.4
9	28.7	26.8	28.0	25.8	25.3	24.5	23.8	23.4	23.5	24.8	27.3	25.0
10	28.4	28.5	26.0	25.7	24.8	23.9	23.0	24.9	23.5	26.2	27.7	25.0
11	27.0	27.0	26.0	26.0	24.5	23.8	21.9	22.5	22.3	26.0	26.0	25.2
12	26.8	28.0	27.5	26.5	23.5	24.8	22.3	23.0	25.5	24.6	26.6	27.3
13	27.9	27.5	26.0	25.5	24.0	22.5	24.4	23.9	24.5	20.5	27.2	27.2
14	28.4	27.4	26.5	25.8	24.0	23.0	22.0	23.0	22.5	23.8	27.0	26.9
15	28.5	27.0	26.9	25.0	23.5	23.0	23.5	23.8	22.8	24.7	27.1	26.0
16	28.4	29.0	27.7	25.0	23.7	24.5	23.5	23.0	24.0	24.9	27.0	27.6
17	28.0	28.8	25.5	26.0	24.0	24.3	24.1	23.5	25.0	24.1	27.9	27.5
18	27.7	27.4	26.0	25.5	25.3	24.0	23.8	23.3	24.5	24.5	27.7	27.5
19	27.9	27.4	25.5	26.0	25.5	24.0	22.3	21.5	25.0	24.3	26.3	26.8
20	26.1	28.5	25.0	26.0	25.5	23.8	22.5	23.4	22.5	26.1	25.9	26.5
21	27.9	28.9	25.1	25.8	25.5	23.5	20.5	23.3	22.5	26.0	26.8	25.9
22	28.6	28.5	26.5	25.5	25.0	24.2	21.5	24.0	23.5	24.0	27.3	26.0
23	28.4	28.9	26.5	26.3	24.5	23.5	22.1	23.3	24.5	25.3	27.2	26.0
24	28.2	29.1	28.0	24.0	25.0	23.2	22.5	24.0	25.0	24.8	26.3	26.6
25	27.0	29.0	27.0	24.0	25.5	20.8	21.5	24.5	24.7	25.1	26.3	26.0
26	27.8	28.5	26.0	24.3	25.5	22.8	22.5	24.5	25.3	27.4	26.1	26.8
27	27.8	29.0	25.5	24.3	24.5	21.3	22.9	24.5	25.4	27.4	24.9	27.0
28	28.0	28.6	26.2	25.4	25.0	23.3	21.1	23.7	25.5	26.5	27.3	26.8
29	27.0		26.0	24.3	24.5	20.0	21.9	23.0	24.5	27.4	24.2	26.5
30	26.9		26.0	24.0	23.8	22.0	22.5	23.0	26.3	26.9	24.7	27.2
31	28.0		26.0		22.8		23.0	18.0		25.1		25.9

Observation: **Temperature at station 9337028 TPC, oC**
Year: **2000**

Month Day	Jan	Feb	Mar	Apr	Mai	Jun	Jul	Aug	Sep	Oct	Nov	Dec
1	26.0	NA	26.0	27.1	23.3	24.5	23.3	25.1	23.3	NA	NA	27.5
2	25.5	NA	25.8	27.5	24.7	21.5	22.3	23.5	23.8	NA	NA	27.0
3	26.0	NA	28.0	26.9	25.3	23.3	24.0	24.5	25.0	NA	NA	27.8
4	26.3	NA	29.0	28.2	26.0	24.0	24.3	23.7	24.3	NA	NA	28.5
5	26.9	NA	27.0	27.5	25.4	24.8	24.7	20.0	24.8	NA	NA	28.8
6	25.7	NA	27.9	26.8	24.8	24.0	22.3	22.3	24.0	NA	NA	28.5
7	26.5	NA	27.4	26.5	24.2	23.9	21.5	22.6	23.8	NA	27.5	28.8
8	26.8	NA	27.5	26.3	24.2	24.8	23.8	23.7	24.5	NA	28.0	28.3
9	25.6	NA	27.2	26.4	24.1	23.8	20.8	22.7	22.9	NA	27.5	29.3
10	26.8	NA	27.3	26.0	23.8	25.5	23.2	22.8	21.5	NA	27.5	28.4
11	26.9	NA	28.1	25.2	24.0	24.3	23.4	21.2	23.3	NA	28.3	27.8
12	27.3	NA	27.3	25.9	24.3	22.3	22.7	23.0	22.5	NA	27.3	29.0
13	26.3	NA	28.8	25.6	24.8	23.2	23.5	23.0	22.8	NA	29.0	28.0
14	26.0	NA	28.9	25.8	25.0	23.2	23.5	23.3	23.8	NA	28.3	27.3
15	27.2	NA	28.5	26.0	25.6	24.3	24.0	22.3	23.0	NA	25.3	27.8
16	26.1	NA	28.5	26.8	25.0	25.0	21.3	22.3	22.5	NA	28.3	28.3
17	26.7	NA	27.0	27.2	24.5	24.9	21.4	21.4	22.8	NA	25.8	27.5
18	26.6	NA	28.5	27.2	25.4	25.3	23.7	22.8	24.5	NA	26.3	26.8
19	26.0	NA	28.1	27.3	25.7	22.4	23.4	23.5	23.5	NA	27.0	27.3
20	26.8	NA	27.5	26.3	25.8	23.3	22.5	23.8	24.0	NA	23.5	27.8
21	27.2	NA	26.7	27.2	25.5	21.4	23.3	24.5	24.5	NA	29.0	26.5
22	27.5	NA	27.5	27.4	25.2	21.2	24.0	22.0	22.8	NA	26.0	27.0
23	27.8	NA	28.0	27.4	25.1	24.2	23.2	24.4	23.0	NA	27.3	27.0
24	27.9	NA	28.1	26.9	26.4	24.8	21.8	24.5	24.0	NA	27.5	27.3
25	27.5	NA	26.0	27.4	24.7	24.1	22.2	24.0	23.5	NA	27.0	28.3
26	26.5	NA	25.6	26.5	25.4	22.6	20.5	22.0	24.3	NA	27.8	28.5
27	25.0	NA	27.1	27.6	24.9	21.9	20.0	24.5	24.0	NA	28.3	26.0
28	25.4	NA	26.9	25.0	25.5	23.8	22.2	23.5	22.5	NA	27.8	27.0
29	26.5	NA	26.8	25.0	22.6	23.5	22.2	23.8	23.8	NA	27.0	28.3
30	27.3		27.3	25.3	24.0	23.5	24.1	23.5	24.8	NA	27.8	27.5
31	25.2		27.3		22.8		23.9	23.0		NA		27.8

NA No observation available

Appendix 4: Meteorological data for the water balance calculation

This appendix shows the meteorological observations applied in the water balance calculation.

9337004 Moshi Airport

Minimum temperature

Year	Jan	Feb	Mar	Apr	May	Jun	Jul	Aug	Sep	Oct	Nov	Dec
1970	21.2	21.9	18.4	19.8	18.1	19.4	16.0	15.2	16.2	16.3	17.1	17.8
1971	17.5	17.4	18.0	18.8	17.6	15.1	15.6	14.4	16.4	16.4	16.5	17.7
1972	16.3	17.7	17.6	19.4	18.5	17.0	16.7	15.9	15.8	17.8	18.0	18.5
1973	18.1	18.7	16.9	20.6	19.0	17.3	15.3	16.1	16.3	17.9	18.0	17.6
1974	17.1	17.6	18.8	19.2	18.2	17.8	16.2	15.3	15.6	15.1	17.3	17.1
1975	17.2	19.4	19.4	19.2	19.0	18.2	18.5	16.3	17.0	16.9	17.5	18.1
1976	17.2	18.4	18.9	19.3	19.0	17.1	15.5	15.7	16.7	17.3	17.9	17.4
1977	19.1	18.2	19.2	19.3	19.2	17.4	16.8	16.0	16.1	17.4	18.4	18.7
1978	17.7	17.8	18.3	19.5	17.8	17.4	16.0	16.1	16.1	17.8	18.0	18.3
1979	18.2	18.5	18.5	19.4	18.8	16.7	16.1	16.5	16.1	17.5	17.2	18.6
1980	18.2	18.4	19.0	19.9			17.0	16.2	16.5	17.0	18.6	
1981	17.7	18.4	19.3		18.2	16.3	15.6	16.2	16.4	17.3	17.5	18.3
1982	17.6	18.4	18.9	19.5	18.5	17.7	16.9	16.3	17.3	18.1	18.6	18.1
1983	17.7	18.6	20.4	20.6	19.4	18.8	17.6	16.7	16.8	17.2	17.9	18.1
1984	18.3	18.2	19.4	20.2	18.7	17.2	16.6	16.5	15.5	18.0	18.6	16.1
1985		19.4	18.5	19.3	18.4	16.5	16.2	16.5	16.6	17.1	21.7	18.5
1986	18.2	17.4	19.3	19.5	21.9		15.4	15.6		20.0		18.6
1987	17.7	18.0	19.2	19.8	18.9	17.4	16.1	16.1	17.3	18.1	19.3	18.6
1988	19.9	19.4	19.6	19.6	18.5	17.2	16.1	16.5	16.5	17.8	18.7	18.5
1989	18.4	17.4	18.9	18.6	18.3	16.7	16.5	15.9	17.0	17.7	18.6	18.9
1990	17.0	18.4	18.6	18.7	18.4	15.0	15.1	15.9	16.3	17.3	17.7	17.3
1991	17.4	16.9	18.2	18.9	18.2	16.2	16.1	15.2	15.2	17.1	17.7	18.2
1992	17.0	18.5	18.6	19.2	17.9	16.8	15.8	14.8	15.5	16.5	18.0	18.0
1993	17.9	16.9	17.8	19.2	18.7	17.3	15.9	15.8	15.4	17.4	18.7	18.9
1994	18.7	19.1		19.2	18.1	16.7	16.3	16.9	17.5	19.1	19.2	18.9
1995	18.6	19.2	19.8	19.9	18.9	17.1	16.6	16.5	16.4	18.0		
1996	18.7	19.6	20.5	19.4	18.7			15.9	17.1	17.8	18.4	18.4
Mean	18.0	18.4	18.8	19.5	18.7	17.1	16.3	16.0	16.4	17.5	18.2	18.1

9337004 Moshi Airport

Maximum temperature

Year	Jan	Feb	Mar	Apr	May	Jun	Jul	Aug	Sep	Oct	Nov	Dec
1970	30.9	32.6	31.1	27.2	26.0	25.0	26.6	26.6	28.6	30.7	32.6	31.3
1971	31.9	33.0	31.0	29.4	26.3	24.6	24.5	25.0	28.3	30.4	32.4	30.7
1972	30.3	30.9	30.9	29.4	25.9	25.1	25.1	26.3	27.9	28.8	29.2	31.1
1973	31.1	32.5	34.2	30.3	26.4	24.5	25.6	26.2	28.9	31.1	31.9	32.3
1974	32.8	34.0	32.1	28.0	28.3	25.1	27.7	26.7	27.5	30.5	31.5	32.5
1975	32.7	33.9	32.3	29.5	27.4	25.6	25.2	25.1	27.5	29.9	32.5	32.4
1976	33.8	32.5	32.9	29.5	26.5	25.7	25.7	26.6	28.4	31.2	31.0	32.2
1977	32.3	31.4	32.2	27.7	27.7	26.3	26.1	26.2	29.1	30.9	30.2	31.4
1978	31.5	31.7	29.9	26.6	26.1	25.0	24.0	26.4	29.3	31.3	30.5	29.4
1979	31.0	30.2	31.6	28.3	25.9	24.1	24.5	25.7	27.7	31.0	32.3	32.0
1980	33.6	33.0	32.8	30.0	27.5	25.8	25.5	25.7	28.9	31.4	30.6	
1981	33.2	34.3	32.1	28.0	25.2	25.6	24.6	26.4	27.3	30.3	31.7	30.8
1982	33.7	34.8	34.0	29.4	26.2	25.9	25.1	25.6	27.8	29.7	30.5	30.3
1983	32.4	33.7	33.7	31.1	27.7	26.3	26.5	27.0	28.9	30.9	32.7	31.1
1984	32.6	34.1	33.7	29.5	27.1	25.4	24.4	24.9	28.6	30.6	29.9	30.7
1985		30.9	32.6	28.9	26.0	25.2	25.7	26.2	29.1	29.9	30.1	30.0
1986	30.3	34.1	31.9	29.5	27.1		25.0	27.0		30.4		29.8
1987	31.8	33.8	34.0	31.0	27.0	26.1	26.7	25.8	29.2	32.4	31.5	34.4
1988	33.2	34.5	32.8	28.3	27.2	26.2	26.2	26.7	28.1	30.6	31.5	31.9
1989	29.5	33.1	32.3	28.2	26.3	25.4	25.2	25.2	28.0	30.6	31.6	31.7
1990	31.0	32.7	28.9	27.9	27.0	26.5	25.7	25.5	28.6	30.5	30.9	30.1
1991	33.0	33.6	33.6	29.8	26.8	25.7	25.6	26.3	28.3	31.6	32.0	30.8
1992	32.7	33.9	34.1	29.7	26.7	25.7	25.1	25.8	28.2	30.4	31.4	30.4
1993	29.8	30.8	31.9	31.6	29.4	26.4	25.9	26.6	29.1	30.6	33.0	32.1
1994	33.8	33.4		30.0	27.1	26.2	25.5	27.0	29.3	31.6	30.9	30.3
1995	33.5	33.3	31.9	29.5	26.9	25.6	25.4	27.5	29.0	30.9		
1996	33.3	32.5	32.8	28.4	26.7			26.4	29.0	30.3	31.8	34.5
Mean	32.1	32.9	32.4	29.1	26.8	25.6	25.5	26.2	28.5	30.7	31.4	31.4

9337021 Lyamungu ARI
Minimum temperature

Year	Jan	Feb	Mar	Apr	May	Jun	Jul	Aug	Sep	Oct	Nov	Dec
1970	14.6	14.6	15.5	16.2	15.3	13.8	13.2	12.6	12.7	12.8	13.7	14.0
1971	13.8	13.5	13.7	15.6	14.7	12.6	12.7	12.1	12.2	11.7	12.2	13.8
1972	12.9	14.4	13.8	14.9	15.2	13.6	13.1	12.5	12.4	14.2	14.8	14.4
1973	14.7	14.9	14.0	15.8	15.2	13.9	11.8	12.4	12.7	13.1	13.5	12.9
1974	11.8	12.2	13.3	15.3	13.9	13.4	12.5	11.7	11.8	11.6	12.7	12.5
1975	12.4	12.1	14.3	14.6	13.7	13.2	12.1	11.7	12.3	11.7	11.8	12.5
1976	11.6	12.4	12.8	14.0	14.2	12.9	11.2	11.4	11.7	11.4	12.7	12.7
1977	13.7	13.1	14.0	14.9	14.6	12.8	12.2	11.7	11.5	12.2	13.6	13.7
1978	12.8	12.5	14.4	15.1	13.6	13.0	11.9	11.6	11.1	11.5	13.4	14.0
1979	13.9	13.9	13.7	14.8	14.3	12.7	11.8	10.6	13.1	13.2	14.1	15.0
1980	14.5	14.2	14.7	16.0	16.2	13.4	13.7	13.2	12.9	12.3	14.6	14.4
1981	13.1	13.9	15.0	16.3	15.3	13.3	12.9	13.2	13.4	13.8	13.5	14.9
1982	13.4	14.0	14.6	15.8	15.6	14.6	14.1	13.4	14.0	14.1	15.0	14.7
1983	17.6	14.6	15.6	16.0	16.1	14.8	14.0	13.4	13.0	13.2	13.9	14.6
1984	14.3	14.1	14.2	16.3	15.2	13.9	13.6	13.2	11.7	13.8	15.1	14.2
1985	13.8	16.1	14.7	16.0	15.4	14.1	13.4	13.4	13.3	13.6	14.8	14.0
1986	14.8	13.0	15.4	14.9	16.0	13.6	12.4	11.9	11.9	13.3	15.3	15.3
1987	14.2	14.0	14.7	15.9	15.7	14.2	13.0	13.3	13.3	13.6	15.2	13.8
1988	15.6	14.4	16.0	16.5	15.6	14.1	13.0	13.4	12.8	12.9	14.0	14.4
1989	15.1	13.2	14.1	15.2	15.1	12.8	12.8	12.6	12.9	12.9	13.8	15.1
1990	13.7	15.3	16.1	16.6	16.0	14.1	12.8	13.9	13.4	13.9	14.8	14.7
1991	14.5	14.0	14.4	16.0	16.3	14.0	13.5	12.5	12.3	13.7	14.5	15.1
1992	13.4	15.1	14.8	16.5	15.6	14.5	13.2	12.6	13.1	13.1	14.7	15.0
1993	15.3	14.3	14.4	16.1	15.9	14.7	13.0	13.0	12.0	13.3	14.1	14.4
1994	14.5	15.5	15.2	15.8	15.5	14.0	13.3	13.7	13.6	14.3	15.0	15.9
1995	14.4	14.5	15.4	16.4	16.1	14.1	13.7	13.7	13.3	14.8	14.2	14.0
1996	13.9	15.5	15.6	16.4	15.9	14.6	13.2	12.6	13.5	13.1	14.3	14.0
Mean	14.0	14.0	14.6	15.7	15.3	13.7	12.9	12.6	12.7	13.1	14.0	14.2

9337021 Lyamungu ARI
Maximum temperature

Year	Jan	Feb	Mar	Apr	May	Jun	Jul	Aug	Sep	Oct	Nov	Dec
1970	26.1	27.4	26.7	23.1	21.8	21.4	20.9	21.9	23.9	25.9	27.8	26.8
1971	27.4	27.7	27.9	24.7	22.0	20.5	20.1	20.4	23.4	25.5	27.8	26.4
1972	27.1	26.3	26.7	24.8	22.4	20.9	20.4	21.7	23.4	25.0	24.6	26.6
1973	27.0	27.6	28.7	25.5	22.4	20.7	21.1	21.8	24.1	26.1	26.6	27.4
1974	28.3	29.0	27.1	23.9	22.7	20.4	20.0	21.7	22.6	25.6	26.1	27.4
1975	27.2	28.9	27.1	24.6	22.5	20.6	20.3	20.8	22.4	24.4	27.0	27.1
1976	28.2	27.2	27.1	25.0	22.0	21.2	21.0	21.3	23.6	25.9	26.1	27.1
1977	27.1	27.2	26.3	23.9	23.3	21.7	21.2	21.5	24.3	26.1	25.2	25.9
1978	26.8	26.8	25.5	23.7	21.6	20.3	19.9	21.4	24.3	26.0	25.5	24.8
1979	25.9	25.8	26.7	24.2	21.1	19.8	20.1	20.9	22.8	25.7	26.9	27.7
1980	28.9	27.6	27.7	25.6	22.6	21.3	20.8	21.1	23.7	26.1	25.6	26.6
1981	27.7	28.8	27.1	24.2	21.6	21.1	20.3	21.6	23.5	25.7	26.9	26.5
1982	29.1	29.9	29.6	25.1	21.5	21.8	20.7	21.2	22.8	24.4	25.8	26.4
1983	28.3	29.2	29.0	26.2	23.3	21.6	21.6	22.3	24.3	26.0	27.5	26.5
1984	28.0	31.9	28.0	25.2	22.6	21.2	19.9	20.2	24.0	25.5	25.2	26.1
1985	28.2	26.4	27.1	24.3	21.8	20.7	20.8	21.3	24.0	25.3	25.4	26.3
1986	26.0	29.2	27.9	24.1	21.9	20.5	20.3	22.0	23.9	26.8	25.6	26.1
1987	27.5	29.1	28.9	25.5	22.9	21.3	21.3	21.4	23.2	26.6	27.2	29.3
1988	28.5	29.9	28.0	24.2	22.7	21.6	21.6	22.0	23.5	27.0	26.3	27.3
1989	25.3	28.1	27.9	23.9	22.2	21.2	20.5	20.8	23.0	24.7	26.1	26.8
1990	26.8	28.0	24.8	24.1	22.6	21.9	21.2	20.6	24.0	25.5	26.2	25.9
1991	28.1	29.1	28.4	25.3	22.3	21.5	20.9	21.9	23.9	26.6	26.3	25.7
1992	28.2	28.9	29.2	25.1	22.6	21.3	20.2	20.9	23.3	26.0	26.0	26.3
1993	25.7	26.5	27.5	26.3	23.9	21.2	20.4	21.5	24.0	25.4	27.9	27.3
1994	29.0	28.7	27.1	25.1	22.4	21.5	21.0	22.1	24.3	26.6	26.1	25.6
1995	28.5	28.5	26.9	25.1	22.4	20.9	21.1	22.8	24.3	26.1	27.3	28.2
1996	28.6	27.5	27.3	23.9	22.2	21.1	21.0	21.5	23.9	25.5	26.4	29.6
Mean	27.5	28.2	27.5	24.7	22.3	21.1	20.7	21.4	23.6	25.8	26.3	26.8

9337004 Moshi Airport

Relative humidity at 09.

Year	Jan	Feb	Mar	Apr	May	Jun	Jul	Aug	Sep	Oct	Nov	Dec
1970												
1971	76	72	72	85	86	73	87	84	81	73	72	75
1972	76	75	76	88	92	82	83	82	83	77	83	77
1973	80	80	72	85	86	83	78	76	74	70	73	69
1974	69	67	74	89	86	87	82	81	75	73	71	67
1975	70	66	76	83	85	80	80	78	79	72	66	70
1976	67	71	74	82	86	78	77	76	76	67	68	70
1977	70	72	79	86	83	79	80	80	77	73	75	74
1978	71	75	84	87	85	85	85	81	78	70	79	82
1979	80	82	77	89		79	84	83	78	72	68	73
1980	68	74	74	82	86	80	81	83	77	67	76	73
1981	68	70	76	86	89	80	82	81	77	76	71	76
1982	71	67	70	81	85	81	83	84	77	76	75	75
1983	73	71	71	82	87	85	82	78	74	72	65	73
1984	69	66	70	83	83	80	83	82	75	70	79	74
1985	71	79	74		86	81	80	77	72	71	76	77
1986	79	66	76	86	90	82	81	79	74	71	75	82
1987	75	68	71	80	85	78	85	82	78	70	70	69
1988	76	74	76	88	84	85	83	82	78	71	71	76
1989	81	71	76	87	86	83	81	83	80	74	73	77
1990	75	74	84	88	85	80	81	82	79		79	79
1991												
1992												
1993												
1994												
1995												
1996												
Mean	73.3	72.1	75.1	85.1	86.0	81.0	81.9	80.8	77.1	71.8	73.3	74.4

9337004 Moshi Airport

Relative humidity at 15.

Year	Jan	Feb	Mar	Apr	May	Jun	Jul	Aug	Sep	Oct	Nov	Dec
1970												
1971	43	36	34	54	64	56	58	60	48	40	30	47
1972	47	45	48	57	69	59	55	45	48	46	58	50
1973	50	45	36	54	64	58	48	45	44	37	39	39
1974	38	33	40	63	57	62	57	48	43	36	32	39
1975	36	36	41	56	59	60	52	40	47	38	30	36
1976	32	41	42	51	63	55	47	43	40	35	39	43
1977	41	38	48	59	58	53	50	51	42	39	47	47
1978	45	48	55	65	63	62	55	49	40	36	51	59
1979	49	55	50	66	69	63	58	54	48	39	39	46
1980	35	41	41	57	63	54	53	52	45	35	46	46
1981	37	34	46	61	66	55	53	50	43	42	41	47
1982	35	35	36	54	66	58	57	53	47	48	48	54
1983	44	40	40	49	61	59	52	48	39	36	36	47
1984	39	31	33	52	57	54	58	53	39	37	51	50
1985	39	48	41	56	62	59	52	46	38	38	48	46
1986	49	35	44	57	65	58	54	42	39	37	43	57
1987	46	36	40	51	55	55	53	56	44	37	38	39
1988	46	41	49	62	61	60	53	53	48	36	39	48
1989	57	42	45	62	65	61	54	53	48	42	44	46
1990	49	47	61	67	61	53	52	55	46	47	47	52
1991	40	40	43	55	65	60	53	53	45	37	38	51
1992	42	39	37	59	63	59	55	48	43	40	43	49
1993	54	50	49	47	52	53	48	47	38	40	35	43
1994	38	40		52	63	54	52	46	40	37	44	54
1995	41	44	5	59	65	60	55	47	41	41		
1996	39	47	55	61	64			48	41	39	34	33
Mean	42.7	41.0	42.3	57.2	62.3	57.6	53.4	49.4	43.2	39.0	41.6	46.7

9337021 Lyamungu ARI
Relative humidity at 09.

Year	Jan	Feb	Mar	Apr	May	Jun	Jul	Aug	Sep	Oct	Nov	Dec
1970	82	80	86	93	90	88	88	87	79	78	75	77
1971	79	72	75	88	92	85	90	88	83	76	72	75
1972	73	78	78	90	93	89	90	88	85	81	84	79
1973	80	79	79	91	91	88	85	84	83	77	80	72
1974	68	68	79	91	90	91	89	89	81	78	78	74
1975	72	69	79	89	90	90	86	88	86	79	73	74
1976	71	77	79	88	92	86	84	84	84	76	75	75
1977	77	75	85	92	91	87	87	86	86	79	86	83
1978	77	79	86	92	90	91	92	90	83	78	83	87
1979	85	82	80	92	94	89	89	90	82	81	80	80
1980	71	80	77	85	91	85	89	89	87	78	81	83
1981	77	76	83	90	93	85	79	90	87	81	80	82
1982	76	72	74	90	78	87	87	90	90	88	80	82
1983	77	73	79	88	93	90	90	87	88	82	77	79
1984	76	72	79	91	90	90	90	78	83	82	85	80
1985	79	81	83	90	93	90	90	89	83	82	85	83
1986	83	63	83	93	95	90	86	85	83	79	85	83
1987	79	76	77	85	93	90	93	90	90	80	83	72
1988	79	74	80	93	91	90	90	90	80	79	81	80
1989	81	73	77	90	91	90	90	90	87	87	83	82
1990	79	77	87	90	91	87	90	90	85	81	82	82
1991	77	73	73	88	93	85	89	90	83	77	80	84
1992	77	76	74	90	91	90	86	86	85	81	81	81
1993	82	79	77	87	90	90	86	90	78	82	76	76
1994	72	67	90	86	77	85	87	87	81	80	82	85
1995	74	74	83	90	93	87	85	81	83	81	79	74
1996	73	73	83	95	93	93	89	90	87	84	83	71
Mean	76.9	74.7	80.2	89.9	90.7	88.4	88.0	87.6	84.1	80.3	80.3	79.1

9337021 Lyamungu ARI
Relative humidity at 15.

Year	Jan	Feb	Mar	Apr	May	Jun	Jul	Aug	Sep	Oct	Nov	Dec
1970	63	62	64	77	74	64	63	57	52	45	47	56
1971	53	50	46	68	73	68	67	63	54	48	46	57
1972	52	61	59	67	77	71	68	60	59	59	72	63
1973	61	62	51	69	75	70	59	59	54	49	56	49
1974	44	44	53	73	69	73	71	58	57	49	56	53
1975	51	45	59	69	71	69	67	60	62	52	48	56
1976	50	57	56	67	74	69	65	62	59	52	60	58
1977	58	62	68	74	72	67	65	65	54	53	67	66
1978	60	64	73	79	75	76	70	65	55	52	67	69
1979	65	68	60	79	80	74	68	67	59	68	58	57
1980	46	56	56	69	73	66	66	62	58	52	67	51
1981	57	54	63	77	77	70	70	55	60	73	60	66
1982	59	58	62	72	80	72	85	66	65	66	66	68
1983	58	55	59	62	78	76	70	69	60	58	59	68
1984	62	63	63	69	75	75	76	73	56	61	62	65
1985	57	68	59	73	76	69	63	58	54	54	65	66
1986	71	54	59	74	80	90	64	59	60	56	63	66
1987	61	50	47	51	75	74	70	68	58	52	65	60
1988	58	53	63	77	72	73	65	64	61	49	61	57
1989	67	52	61	73	75	71	64	67	64	69	68	64
1990	60	58	75	79	73	65	63	66	55	56	61	67
1991	56	48	53	67	78	72	66	65	58	52	54	67
1992	54	57	52	69	77	72	68	62	55	56	57	66
1993	67	63	56	64	70	68	64	64	53	51	51	61
1994	49	49	65	65	73	66	66	61	55	52	58	67
1995	54	52	58	73	78	69	62	58	56	55	53	54
1996	54	59	62	75	78	75	66	68	59	49	58	46
Mean	57.3	56.4	59.3	70.8	75.1	71.3	67.1	63.0	57.5	55.1	59.4	60.9

9337004 Moshi Airport
Sunshine Hours

Year	Jan	Feb	Mar	Apr	May	Jun	Jul	Aug	Sep	Oct	Nov	Dec
1970												
1971												
1972	9.3	6.8	6.2	8.1	5.7	4.9	3.8	6.2	6.9	8.4	7.5	9.4
1973	8.3	8.2	9.2	6.3	4.5	2.8	6.0	5.8	6.5	8.3	6.7	9.1
1974	9.9	9.1	8.0	5.3	6.7	4.1	6.7	7.2	6.2	8.0	9.5	10.0
1975												
1976		8.5		7.5	5.5	5.0	6.2	6.5	7.6	8.9		
1977	8.7	7.2		5.0	5.7	5.8	4.8	5.2	7.4	8.8	8.1	8.3
1978	8.2	8.9	5.4	5.5	4.7	3.2	4.2	5.1	8.1	8.4	6.7	8.3
1979								4.9	6.6	7.8	8.4	8.3
1980	8.7	8.0	7.8	6.4	4.2	4.8	4.3	4.5	7.0	8.9	8.1	7.9
1981	9.8	9.5	6.3	5.7	3.0	5.4	3.7	5.1	6.8	8.1	8.5	7.7
1982	10.1	9.8	9.2	6.5	3.7	5.3	3.9	5.3	5.5	7.1	7.9	8.8
1983	9.7	9.8	7.9	6.4	6.4	4.8	4.4	5.5	7.1	7.2	9.1	6.8
1984	8.7	9.6	7.9	6.2	5.7	5.3	3.1	3.3	7.8	7.6	8.3	8.1
1985	9.2	5.7	7.9	6.5	2.3	3.6	5.1	4.9	7.6	4.7	7.1	8.2
1986	8.5	10.5	7.8	6.7	3.2	4.5	5.2	7.0	8.0	8.3	7.5	7.5
1987	9.3	9.7	9.2	6.5	7.4	3.9	4.9	5.1	10.6	8.9	7.9	10.2
1988	8.4	4.5	6.8	5.9	4.6	4.9	5.5	4.4	7.0	8.9	7.7	8.3
1989	6.3	8.9	7.6	5.9	3.7	4.1	3.6	3.3	5.9	7.8	7.9	7.9
1990	9.1	6.1	6.1	5.1	4.5	5.8	5.2	3.4	6.5	7.8	8.8	8.3
1991	9.7	10.5	8.3	6.9	4.3	5.2	4.5	5.6	7.4	8.5	9.1	7.0
1992	10.4	8.7	8.4	5.7	4.7	3.7	3.8	5.5	6.5	8.2	7.6	7.8
1993	6.2	9.1	8.2	7.2				5.0	8.1	7.6	9.2	9.5
1994	9.7	8.2		5.9	4.7	4.7	4.5	5.5	6.6	7.6	6.9	7.1
1995	9.6	7.9	6.3	5.6	3.9	4.7	4.8	7.2	7.3	7.2		
1996	9.3	8.9	7.1	5.9	4.3			5.9	6.4	7.6	7.1	10.6
Mean	9.0	8.4	7.6	6.2	4.7	4.6	4.7	5.3	7.1	7.9	8.0	8.4

9337021 Lyamungu ARI
Sunshine Hours

Year	Jan	Feb	Mar	Apr	May	Jun	Jul	Aug	Sep	Oct	Nov	Dec
1970	5.4	8.2	5.9	3.2	2.5	3.8	3.8	5.2	6.5	7.5	7.5	6.5
1971	7.4	8.0	7.3	5.3	3.5	4.2	3.4	4.0	6.5	8.1	8.4	7.3
1972	8.7	6.8	8.2	6.1	3.6	4.5	2.8	5.1	6.4	6.5	5.8	8.1
1973	7.8	8.0	8.8	5.1	3.2	2.5	5.5	4.9	5.8	7.4	6.6	8.5
1974	9.2	9.0	6.5	3.5	4.8	2.7	3.0	5.0	5.7	8.6	7.0	8.1
1975	7.7	8.8	6.9	4.9	4.0	2.8	3.4	4.2	4.8	6.4	8.2	7.7
1976	9.0	7.4	7.4	5.6	2.9	3.8	5.1	5.0	5.6	7.9	7.1	7.4
1977	7.1	7.0	6.1	3.8	4.4	4.5	4.1	5.3	6.3	8.6	6.4	6.6
1978	7.7	8.6	4.2	3.3	3.4	2.1	3.2	4.2	7.0	6.7	4.9	5.2
1979	6.3	6.9	7.6	3.8	1.5	2.0	3.8	3.9	5.6	6.6	6.8	7.2
1980	8.4	7.6	7.3	5.1	2.8	4.1	3.1	3.8	6.3	7.6	5.8	7.2
1981	8.9	9.0	5.6	4.2	2.1	4.2	3.2	4.1	2.0	7.0	5.7	6.1
1982	8.7	9.1	8.2	5.2	2.3	3.7	3.2	4.2	3.2	5.6	6.5	7.5
1983	8.8	8.3	6.7	5.1	4.1	3.6	3.7	5.3	6.6	6.2	8.2	5.9
1984	8.1	9.3	7.4	5.0	4.4	4.4	2.2	2.4	6.7	5.9	5.7	7.1
1985	8.0	4.8	6.7	4.0	2.2	3.0	4.1	4.4	6.2	6.5	5.3	5.5
1986	6.8	9.8	6.4	3.6	1.8	3.3	3.9	6.0	6.5	7.0	5.3	5.9
1987	8.2	9.0	8.0	5.0	3.8	3.3	4.3	4.6	5.6	7.3	6.4	8.9
1988	7.4	8.1	6.0	4.2	3.3	3.9	4.8	3.7	6.4	8.4	6.0	6.6
1989	5.4	8.3	6.6	3.6	2.5	3.4	3.0	3.4	3.0	5.8	6.2	5.4
1990	7.4	6.4	4.1	3.5	3.0	4.8	4.3	2.5	5.3	5.9	6.0	6.5
1991	8.4	9.6	7.4	5.3	2.1	4.1	3.3	1.8	6.5	7.3	3.3	5.3
1992	8.8	7.4	7.5	4.5	3.1	2.7	2.8	4.1	4.8	7.1	4.9	5.3
1993	4.5	7.7	7.4	5.5	4.2	2.5	3.9	3.5	7.1	5.9	7.1	6.9
1994	8.4	7.1	6.5	5.2	3.0	4.1	3.5	4.3	5.3	6.3	5.3	4.3
1995	9.0	7.5	5.4	4.8	2.0	3.6	3.5	5.9	5.6	5.2	7.1	7.6
1996	8.4	7.1	6.3	3.4	2.9	2.5	3.8	4.2	5.2	6.0	4.7	9.2
Mean	7.8	8.0	6.8	4.5	3.1	3.5	3.7	4.3	5.6	6.9	6.2	6.8

Annual rainfall at some stations

Station	9337028	9337115	9337143/4	9337147
Year	TPC	KIA	Kahe Nafco	Shia
1970	588.8			
1971	701.3			
1972	804.8	591.0		
1973	399.3	530.9		
1974	547.6	306.8		
1975	242.6	261.3		
1976	361.1	426.8		
1977	497.2	446.9	578.6	
1978	870.0	1016.4	676.5	
1979	683.6	752.5	454.9	
1980	414.9	391.9		1425.0
1981	832.3	633.4		1204.0
1982	839.7	985.9		1234.8
1983	354.2	341.5	373.2	887.0
1984	374.6	332.1	392.2	1112.0
1985	674.1	552.0	351.1	1693.0
1986	545.5	728.9	535.0	2351.0
1987	521.1	452.8	357.7	1098.0
1988	579.7	561.8	461.2	2548.8
1989	594.4	548.3	505.6	1336.8
1990	1142.2		745.4	1795.2
1991	336.3		354.8	1425.0
1992	351.6	444.1	335.7	1129.2
1993	267.9	319.7	337.2	937.2
1994	384.5	367.0	477.1	1038.0
1995	673.1	530.9	545.1	1108.0
1996	569.1	288.2	296.1	1092.8
Average	561.2	513.5	457.5	1377.4

Appendix 5: Calculation of actual evapotranspiration

The example shows the calculation of the actual evapotranspiration for station 9337021 located at 1250 masl for the year 1976. See text for description of calculation procedure. Equal calculation is performed for each month for the period 1970 to 1996 and the average is used in the water balance calculation. The value 1214 found in table 7.9 is the average of all the monthly calculations at 1250 masl.

Date	T_{max}	T_{min}	RH 09	RH 15	n	T_p	E_{TP}	E_{TW}	E_T	E_T
	°C	°C	%	%	hrs	°C	mm/d	mm/d	mm/d	mm/month
1976-01	28.2	11.6	71	50	9	18.6	5.7	4.7	3.6	110.9
1976-02	27.2	12.4	77	57	7.4	19.1	5.1	4.5	3.8	110.7
1976-03	27.1	12.8	79	56	7.4	19.2	5.1	4.5	3.8	118.7
1976-04	25.0	14.0	88	67	5.6	19.4	4.0	3.8	3.7	111.3
1976-05	22.0	14.2	92	74	2.9	18.1	2.9	2.9	2.9	91.1
1976-06	21.2	12.9	86	69	3.8	16.6	3.3	2.9	2.6	77.0
1976-07	21.0	11.2	84	65	5.1	15.6	3.6	3.1	2.7	83.3
1976-08	21.3	11.4	84	62	5	15.9	3.9	3.4	2.9	88.6
1976-09	23.6	11.7	84	59	5.6	17.2	4.3	3.8	3.3	99.4
1976-10	25.9	11.4	76	52	7.9	17.7	5.3	4.4	3.6	110.2
1976-11	26.1	12.7	75	60	7.1	18.6	5.0	4.3	3.6	106.6
1976-12	27.1	12.7	75	58	7.4	18.9	5.1	4.3	3.5	109.8
									Sum	**1217.6**

Appendix 6: Plot of long-term simulation results for selected years

This appendix shows the plot of simulated and observed discharge for gauging station 1DD1 for a selected number of years referred in the text.

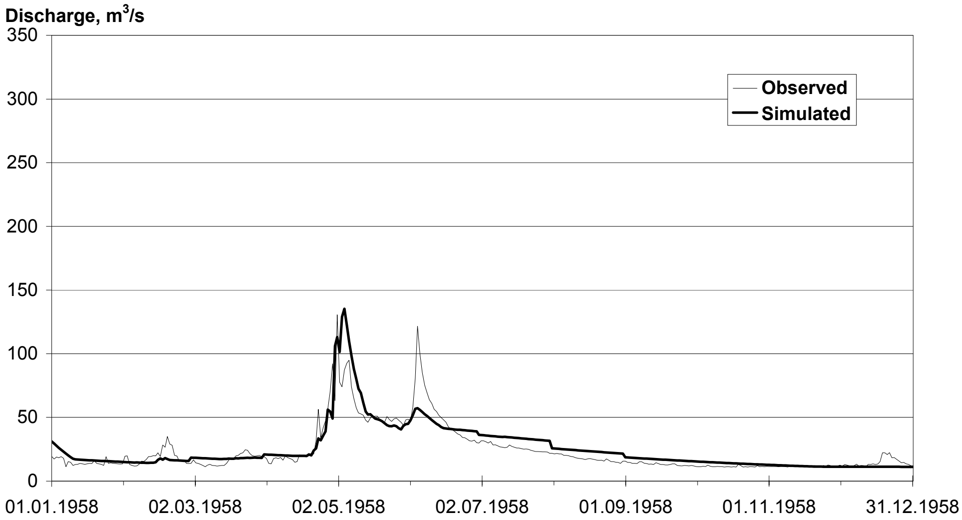

Figure A6.1: Plot of simulated and observed discharge at 1DD1 for 1958.

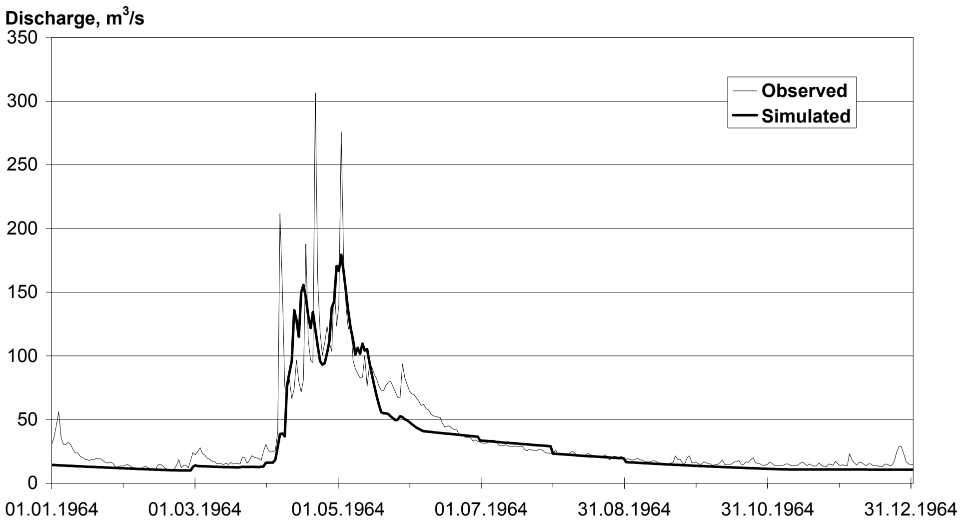

Figure A6.2: Plot of simulated and observed discharge at 1DD1 for 1964.

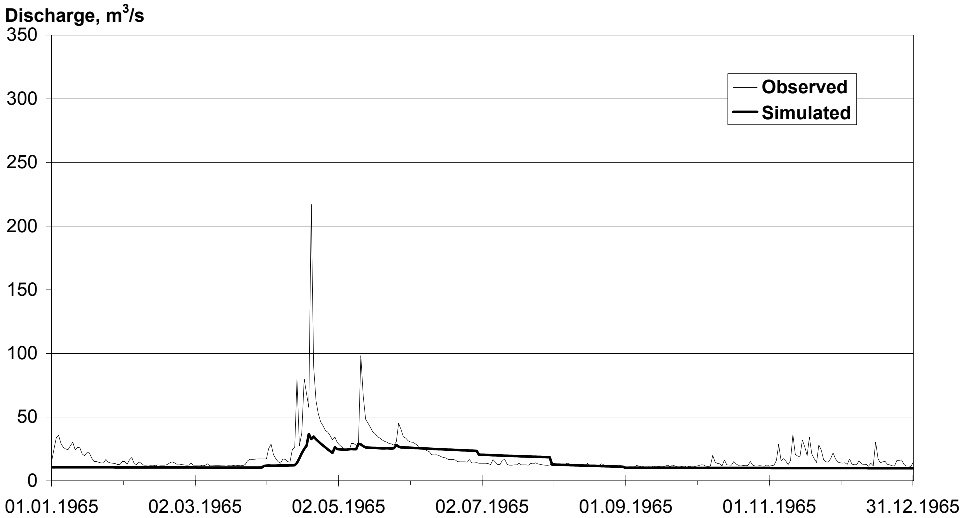

Figure A6.3: Plot of simulated and observed discharge at 1DD1 for 1965.

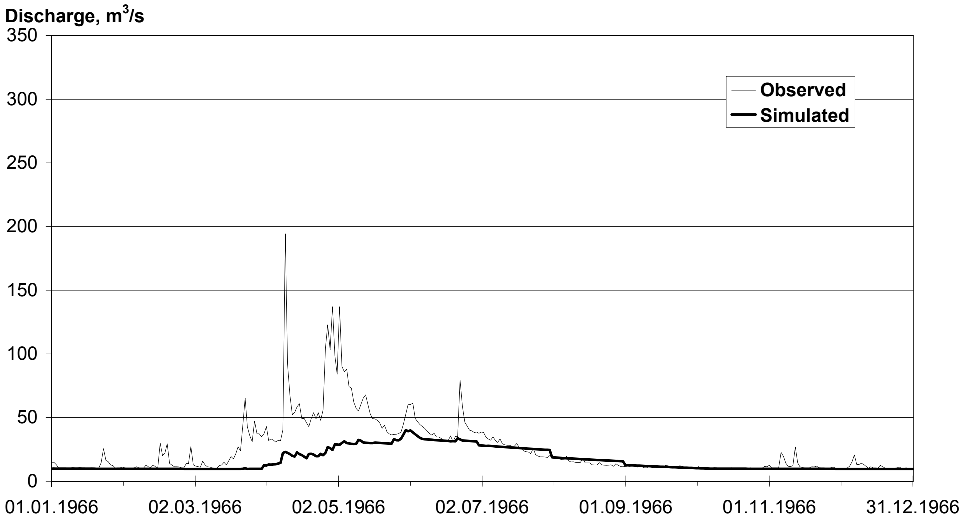

Figure A6.4: Plot of simulated and observed discharge at 1DD1 for 1966.

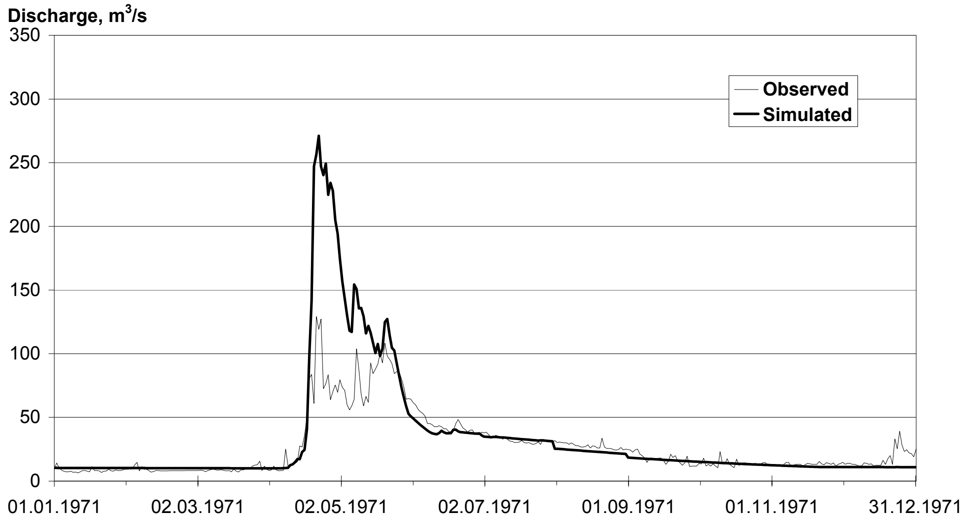

Figure A6.5: Plot of simulated and observed discharge at 1DD1 for 1971.

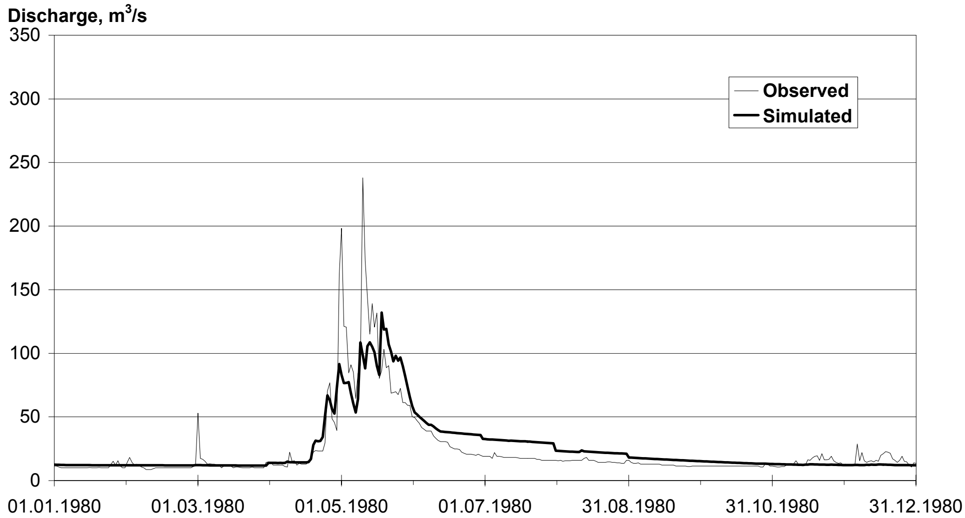

Figure A6.6: Plot of simulated and observed discharge at 1DD1 for 1980.

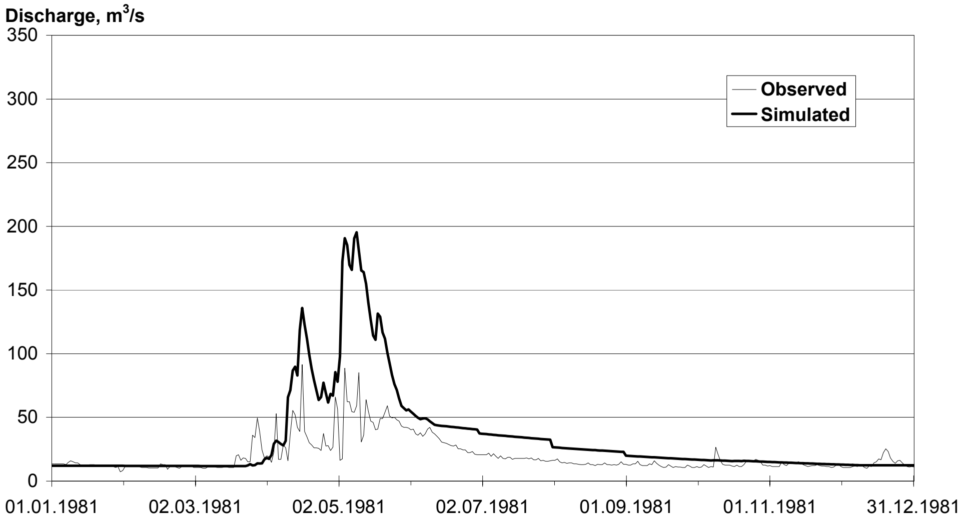

Figure A6.7: Plot of simulated and observed discharge at 1DD1 for 1981.

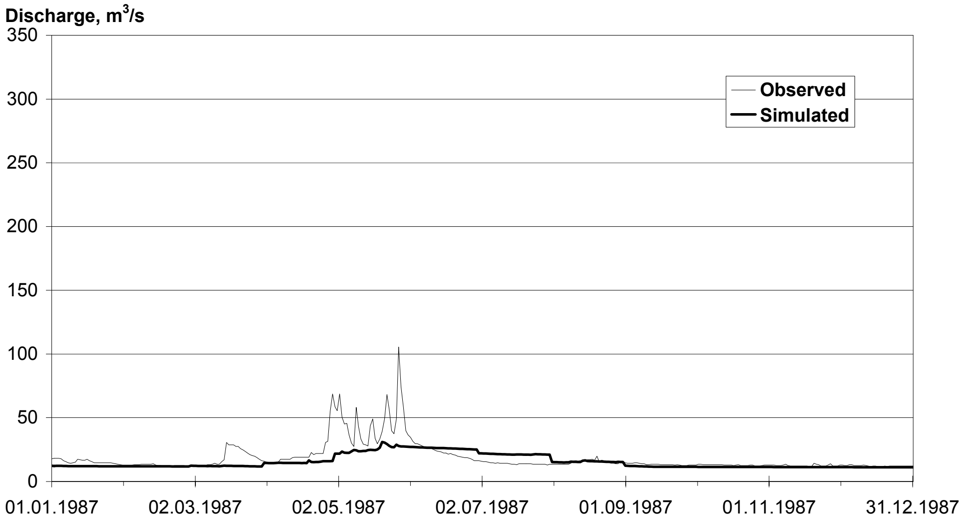

Figure A6.8: Plot of simulated and observed discharge at 1DD1 for 1987

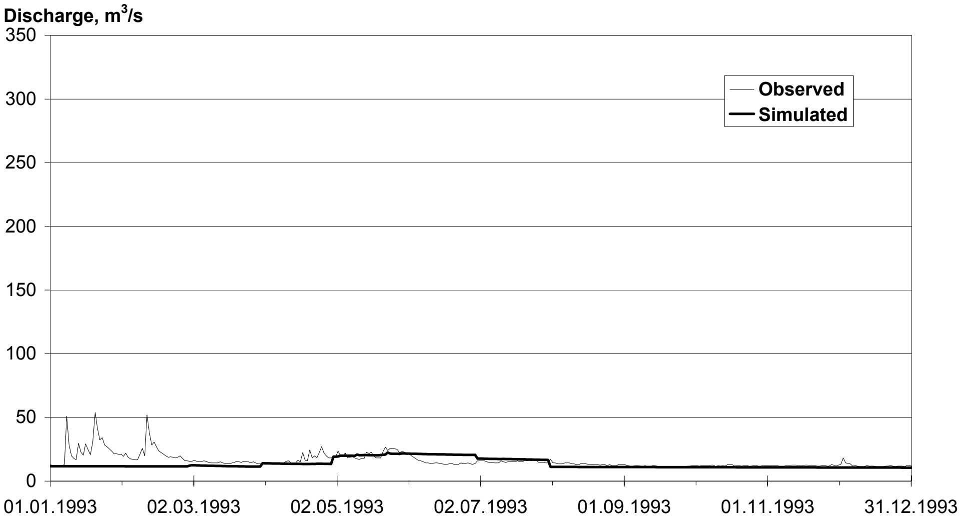

Figure A6.9: Plot of simulated and observed discharge at 1DD1 for 1993

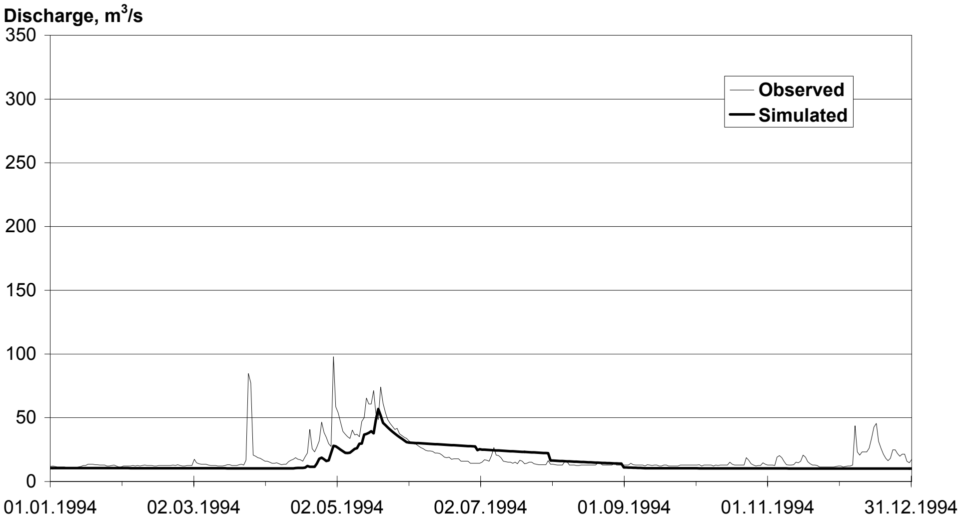

Figure A6.10: Plot of simulated and observed discharge at 1DD1 for 1994

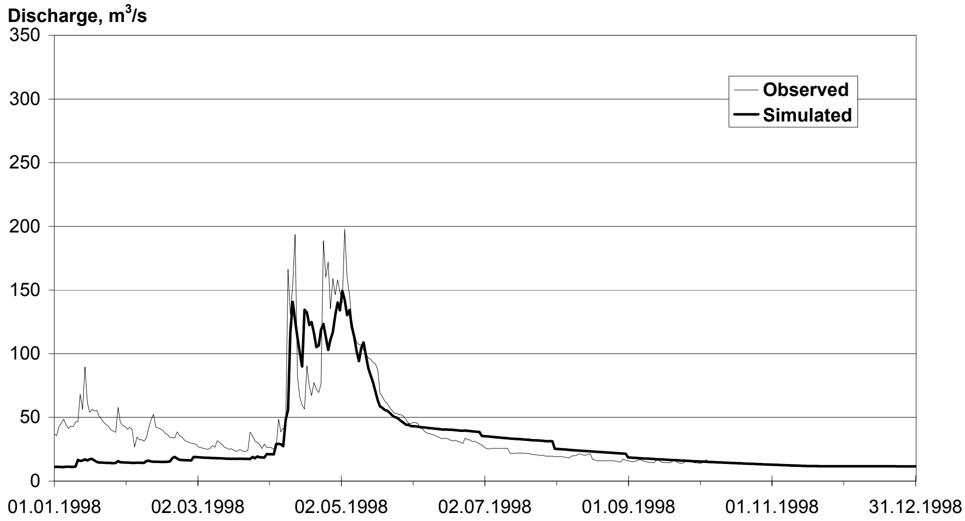

Figure A6.11: Plot of simulated and observed discharge at 1DD1 for 1998

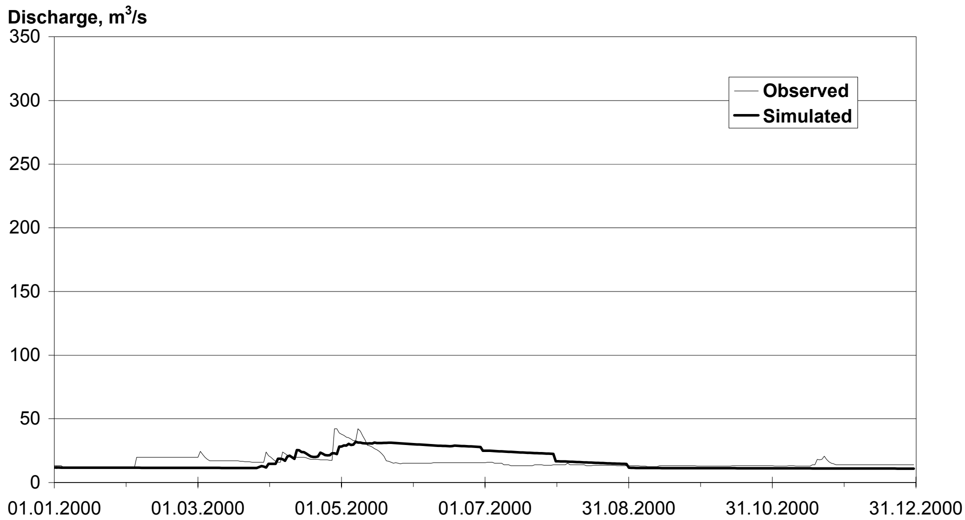

Figure A6.12: Plot of simulated and observed discharge at 1DD1 for 2000

Appendix 7: Discharge observations from 1DD1

This appendix shows discharge observations from river gauging station 1DD1.

Discharge observations from river gauging station 1DD1. Values in m^3/s

Year	Jan	Feb	Mar	Apr	May	Jun	Jul	Aug	Sep	Oct	Nov	Dec
1958	14.8	19.0	16.6	27.7	59.4	52.7	26.4	17.8	13.4	11.4	11.7	14.6
1959	12.2	11.8	12.4	29.1	36.4	16.9	18.7	16.5	29.2	12.0	12.3	15.1
1960	14.9	12.1	NA	47.9	77.7	36.6	25.3	19.6	16.3	20.8	11.0	10.6
1961	9.9	10.0	9.9	14.2	13.7	10.1	13.9	11.6	11.1	18.3	95.9	60.9
1962	51.0	23.9	16.1	25.2	61.7	24.0	20.3	16.3	12.7	9.6	10.0	14.1
1963	12.9	10.8	13.2	49.6	69.9	32.5	27.2	16.3	12.9	10.8	23.6	28.0
1964	23.5	12.7	18.9	100.6	98.8	49.1	28.6	22.0	17.5	15.8	14.6	16.6
1965	20.6	13.3	13.2	42.6	35.9	20.2	13.4	12.4	11.2	12.8	19.6	14.2
1966	12.0	13.4	22.9	61.9	59.7	42.6	27.5	14.7	11.2	10.4	12.4	11.5
1967	10.4	10.6	10.7	21.8	64.7	40.1	30.2	25.1	24.7	19.9	29.6	22.4
1968	10.7	14.0	31.6	79.3	80.6	73.9	38.5	28.1	18.2	13.8	26.5	50.6
1969	20.1	25.6	24.0	20.4	38.4	28.9	21.4	19.8	14.1	15.1	15.2	12.8
1970	16.7	14.8	19.0	59.7	66.3	28.9	19.1	13.7	12.7	11.0	11.1	12.0
1971	8.4	8.8	9.2	44.9	79.5	45.2	32.4	27.6	17.7	13.8	13.2	17.4
1972	16.6	19.6	20.6	36.0	55.9	41.7	26.7	19.3	18.9	19.5	32.1	25.8
1973	28.1	19.9	13.9	43.9	66.9	35.7	28.1	20.4	14.7	12.5	14.2	13.1
1974	13.2	12.9	12.9	66.2	42.0	31.9	33.6	24.6	15.2	14.7	15.4	14.6
1975	15.6	17.2	15.1	38.3	45.2	32.2	29.7	20.4	15.5	16.4	15.7	15.7
1976	14.7	14.8	16.0	22.5	34.2	29.6	20.3	13.3	14.2	13.5	13.0	10.8
1977	12.4	12.4	15.1	61.6	54.5	33.1	23.2	21.8	15.0	15.3	27.0	25.3
1978	25.0	20.7	33.8	51.5	55.5	36.7	34.8	26.8	18.3	13.8	18.8	36.1
1979	15.9	22.1	23.7	61.1	90.5	85.9	35.0	22.7	15.9	13.3	14.5	11.7
1980	10.7	10.7	13.0	22.9	103.3	30.8	17.8	15.3	12.4	11.5	14.4	16.2
1981	12.5	11.2	16.5	31.6	50.6	31.5	18.2	13.8	12.3	13.7	12.5	13.9
1982	10.8	10.4	11.2	28.3	48.0	27.5	24.2	18.7	14.6	27.3	26.5	32.1
1983	15.0	13.4	13.2	19.1	47.3	35.6	21.3	15.8	13.1	12.3	12.7	14.1
1984	12.9	12.0	11.9	34.6	45.2	27.9	26.3	19.3	14.9	13.5	22.1	20.9
1985	14.0	17.1	15.8	48.9	46.7	26.6	19.6	15.1	13.1	13.8	16.7	17.8
1986	19.0	13.7	14.1	40.2	59.7	52.0	21.9	14.6	13.8	12.8	13.8	22.8
1987	15.6	12.8	18.8	22.0	46.6	23.7	14.2	15.3	13.5	12.9	12.5	12.3
1988	12.3	12.2	16.4	55.9	41.8	28.1	20.0	14.7	15.0	14.1	15.5	15.3
1989	16.5	15.6	13.8	44.6	75.0	41.8	25.3	18.4	16.0	13.6	16.0	20.1
1990	18.6	14.2	35.2	68.0	90.2	41.5	21.2	16.3	14.1	13.7	20.9	17.0
1991	13.5	13.2	15.8	21.5	55.2	28.7	16.4	14.4	14.8	14.0	15.2	19.9
1992	13.5	13.5	12.3	41.9	51.9	34.4	20.4	16.6	14.0	12.7	13.8	14.0
1993	24.2	22.1	14.8	16.9	21.1	15.0	15.3	13.4	11.6	12.1	12.2	12.2
1994	12.1	12.4	18.4	21.6	49.2	21.8	15.9	13.2	12.7	13.3	14.0	22.1
1995	13.5	12.6	14.5	46.5	58.4	40.2	20.6	16.3	14.0	13.7	13.4	13.4
1996	12.6	13.3	14.6	66.8	69.9	38.9	23.4	16.6	14.5	12.5	13.6	12.4
1997	11.4	11.9	14.1	53.2	51.5	34.7	24.0	14.5	13.6	20.9	37.9	52.5
1998	48.8	36.8	27.3	89.9	93.9	35.3	22.9	18.0	15.2	14.1	11.7	11.4
1999	12.1	11.4	24.0	43.3	55.7	38.1	28.0	19.5	15.4	13.8	15.2	15.0
2000	12.0	18.7	17.7	20.6	26.2	15.4	14.1	13.7	13.1	13.1	14.3	14.0
Average	16.5	15.1	17.2	42.9	57.6	34.8	23.4	17.8	14.9	14.3	18.7	19.6
Max	51.0	36.8	35.2	100.6	103.3	85.9	38.5	28.1	29.2	27.3	95.9	60.9
Min	8.4	8.8	9.2	14.2	13.7	10.1	13.4	11.6	11.1	9.6	10.0	10.6

URN:NBN:no-3437

Daily discharge at river gauging station 1DD1 Kikuletwa TPC for the year 1998

Day	Jan	Feb	Mar	Apr	May	Jun	Jul	Aug	Sep	Oct	Nov	Dec
1	36.9	40.6	29.4	26.3	158.1	45.1	28.3	19.2	15.9	14	12.9	11.4
2	35.6	42.2	28.8	26.6	148.4	46.1	26.8	19.2	15.5	14	12.9	11.4
3	42.9	40	26.7	26.2	140.2	46.1	25.5	19.2	15.1	14.9	12.9	11.4
4	45.3	26.7	26.4	24.9	197.8	44.9	25.2	19.2	15.6	16.7	12.4	11.4
5	48.7	34.5	25.7	26.6	160	41.7	25.6	18.8	16	15.5	12.1	11.4
6	44	32.4	25.2	48.7	146.4	40.6	25.7	18.4	17.1	14.5	12.1	11.4
7	41.2	32.5	25	38.7	126.3	38.7	25.7	18.1	16	14.4	12	11.4
8	43	31.2	25.7	41.5	116.3	37.6	25.6	19.6	15.6	14.4	11.8	11.4
9	42.8	33.9	27.8	40.9	109.1	37.1	25.6	19.9	15	14.4	11.4	11.4
10	46.3	42	26.6	166.4	107.1	36.5	25.7	19.9	14.8	14.4	11.4	11.4
11	46.7	48	31.8	131	106.9	36	25.7	21.5	14.5	15.1	11.4	11.4
12	68.2	52.6	30.1	153.4	102.7	35	25.7	21.2	14.4	14.1	11.4	11.4
13	56.5	42.2	28.9	193.7	100	34.2	21.8	20.4	16.3	13.9	11.4	11.4
14	89.6	41.6	26.6	81.9	96.6	33.3	21.8	20.3	16.3	13.8	11.4	11.4
15	61.7	40.8	25.9	66.4	95.7	33.7	21.8	21.1	15.1	14	11.4	11.4
16	54.1	39.8	25	59.4	93.1	33.35	21.9	21.5	14.6	14	11.4	11.4
17	56.3	37.4	25.3	56.6	92.1	33	21.9	17.1	14.5	14	11.4	11.4
18	55.1	36.4	24.2	90.3	87.2	31.9	21.9	16.4	14.4	15.1	11.4	11.4
19	55.6	34.2	23.2	74.7	69.1	31.5	21.9	15.9	14.4	14.1	11.4	11.4
20	50.9	34	24.3	67.3	66.1	32.1	21.7	15.9	16.7	13.6	11.4	11.4
21	48.7	33.9	24.4	77.3	62.9	30.9	21.7	15.9	16	13.6	11.4	11.4
22	46.1	38.7	23.2	72.2	61.1	30.6	21.1	15.9	14.5	13.6	11.4	11.4
23	44.1	35.6	23.3	69.5	57.8	29.5	20.8	15.9	14	13.6	11.4	11.4
24	43	34.7	24.2	76.2	55.6	33.7	20.6	15.9	14	13.6	11.4	11.4
25	40.1	32.4	38.4	188.7	53.4	32.4	20.4	15.9	15	13.6	11.4	11.4
26	39.3	31.2	35.6	160	53.1	32.4	19.9	15.9	15.3	13.6	11.4	11.4
27	38.3	30.3	31.6	172.1	52.2	31	20.4	15.5	16.2	13.6	11.4	11.4
28	58	29.7	30.1	135.4	52.1	31.2	19.6	15.1	15	13.4	11.4	11.4
29	46.1		28.7	159.2	50.7	30.4	19.6	15.1	14.4	12.9	11.4	11.4
30	43.5		25.5	146.1	48.2	29.2	19.6	17.5	14.3	13.4	11.4	11.4
31	42.8		29.1		45.3		19.6	16.3		12.9		11.4
Average	48.8	36.8	27.3	89.9	93.9	35.3	22.9	18.0	15.2	14.1	11.7	11.4
Max	89.6	52.6	38.4	193.7	197.8	46.1	28.3	21.5	17.1	16.7	12.9	11.4
Min	35.6	26.7	23.2	24.9	45.3	29.2	19.6	15.1	14.0	12.9	11.4	11.4

Daily discharge at river gauging station 1DD1 Kikuletwa TPC for the year 1999

Day	Jan	Feb	Mar	Apr	May	Jun	Jul	Aug	Sep	Oct	Nov	Dec
1	11.9	12.1	19.1	16.5	72.0	40.3	28.8	23.2	17.1	13.6	13.2	31.9
2	12.1	12.1	17.1	43.8	88.7	38.4	27.9	23.6	17.1	13.6	13.2	27.0
3	12.1	12.9	16.5	42.5	78.6	37.4	27.0	23.2	17.1	13.6	13.2	24.9
4	12.1	12.9	16.3	40.1	70.9	38.4	34.2	22.7	17.4	13.6	13.2	19.0
5	12.1	12.9	15.8	39.3	59.7	37.9	31.5	21.9	17.8	13.6	13.2	16.7
6	12.1	12.9	14.1	39.3	58.7	48.0	30.6	21.5	18.2	13.6	13.2	15.9
7	12.1	10.7	13.8	38.9	56.1	46.1	35.6	21.1	18.2	14.7	13.2	14.4
8	12.1	10.7	14.6	38.4	57.2	44.6	31.5	21.5	16.3	14.4	13.2	14.4
9	12.1	10.7	14.5	37.9	58.2	40.7	31.0	20.7	16.3	14.4	13.2	13.6
10	12.1	10.7	14.9	38.4	58.2	40.7	30.1	20.3	15.5	15.9	13.2	13.2
11	12.1	10.7	14.6	38.4	56.6	41.2	29.2	19.9	15.9	15.5	13.2	13.2
12	12.1	10.7	14.6	39.3	57.2	42.7	28.3	19.9	15.5	15.5	13.2	13.2
13	12.1	10.7	16.1	38.5	66.1	43.6	27.9	19.0	15.5	14.7	13.2	13.2
14	12.1	10.7	62.2	38.7	62.4	43.1	28.3	18.2	15.5	14.4	13.2	13.2
15	12.1	10.7	155.8	38.4	60.3	41.7	29.2	18.6	15.1	14.4	13.2	13.2
16	12.1	10.7	140.5	25.6	58.2	39.8	28.8	18.6	15.1	14.0	13.6	13.2
17	12.1	11.4	17.1	47.9	67.1	38.8	27.9	18.2	15.1	14.0	14.0	12.9
18	12.1	11.4	11.4	26.3	64.5	38.4	27.9	18.6	15.1	14.0	12.5	12.9
19	12.1	11.4	11.4	27.2	59.2	37.0	27.5	19.0	15.1	13.6	13.2	12.9
20	12.1	11.4	11.4	26.6	54.6	36.5	25.7	18.6	14.7	13.6	12.9	12.9
21	12.1	11.4	11.4	34.7	50.5	35.6	26.1	18.2	14.4	13.2	16.3	12.9
22	12.1	11.4	11.4	34.7	49.5	35.6	27.0	19.4	14.4	13.2	13.6	13.2
23	12.1	11.4	11.4	37.9	43.1	35.1	27.0	19.9	14.0	13.2	12.5	13.2
24	12.1	11.4	11.4	37.4	41.7	35.1	26.6	18.2	13.6	12.9	14.0	12.9
25	12.1	11.4	11	35.6	42.7	32.8	27.9	17.8	13.6	12.9	13.6	12.9
26	12.1	11.4	11.4	38.9	40.7	31.9	26.1	17.1	13.6	14.4	14.0	12.9
27	12.1	11.4	11.4	38.9	41.7	31.9	25.3	17.1	13.6	11.8	25.3	13.2
28	12.1	11.4	11.4	35.6	37.9	30.6	23.6	17.1	13.6	13.2	29.2	13.2
29	12.1		11.4	157	37.4	30.1	23.6	17.1	13.6	13.2	16.3	13.2
30	12.1		14.3	125.4	38.8	29.2	22.7	17.1	13.6	13.2	35.6	13.2
31	12.1		15.1		37.9		22.7	17.1		13.2		13.2
Average	12.1	11.4	24.0	43.3	55.7	38.1	28.0	19.5	15.4	13.8	15.2	15.0
Max	12.1	12.9	155.8	157.0	88.7	48.0	35.6	23.6	18.2	15.9	35.6	31.9
Min	11.9	10.7	11.0	16.5	37.4	29.2	22.7	17.1	13.6	11.8	12.5	12.9

Daily discharge at river gauging station 1DD1 Kikuletwa TPC for the year 2000

Day	Jan	Feb	Mar	Apr	May	Jun	Jul	Aug	Sep	Oct	Nov	Dec
1	13.2	11.8	19.9	21.1	38.8	15.1	15.5	14.0	13.2	12.9	13.2	14.0
2	13.2	11.8	19.9	19.9	37.9	15.1	15.5	14.0	13.2	12.9	12.9	14.0
3	13.2	11.8	24.4	18.2	37.0	15.1	15.9	14.0	13.2	12.9	12.9	14.0
4	13.2	11.8	21.9	16.7	35.6	15.1	15.9	14.0	13.2	12.9	12.9	14.0
5	11.8	19.9	19.9	15.9	35.1	15.1	15.9	14.0	13.2	12.9	12.9	14.0
6	11.8	19.9	18.2	15.9	34.2	15.1	15.1	15.1	12.9	12.9	12.9	14.0
7	11.8	19.9	17.1	24.0	32.8	15.1	15.1	14.0	12.9	12.9	12.9	14.0
8	11.8	19.9	17.1	22.7	32.8	15.1	15.1	14.0	12.9	12.9	13.2	14.0
9	11.8	19.9	17.1	21.5	42.2	15.1	15.1	14.0	12.5	12.9	13.2	14.0
10	11.8	19.9	17.1	20.3	40.3	15.5	14.0	14.0	12.5	12.9	13.2	14.0
11	11.8	19.9	17.1	19.9	36.5	15.5	14.0	14.0	12.5	12.9	12.9	14.0
12	11.8	19.9	17.1	19.9	33.3	15.5	14.0	14.0	12.5	12.9	12.9	14.0
13	11.8	19.9	17.1	19.9	29.2	15.5	13.2	14.0	12.5	12.9	12.9	14.0
14	11.8	19.9	17.1	19.9	28.8	15.5	13.2	13.2	13.2	12.9	12.9	14.0
15	11.8	19.9	17.1	19.9	27.9	15.5	13.2	13.2	13.2	13.2	12.9	14.0
16	11.8	19.9	17.1	19.9	26.6	15.5	13.2	13.2	13.2	13.2	12.9	14.0
17	11.8	19.9	17.1	19.4	25.7	15.5	13.2	13.6	13.2	13.2	12.9	14.0
18	11.8	19.9	17.1	18.6	24.4	15.5	13.2	13.6	13.2	13.2	14.0	14.0
19	11.8	19.9	17.1	18.2	22.7	15.5	13.2	13.6	13.2	13.2	14.0	14.0
20	11.8	19.9	16.7	18.2	20.7	15.5	13.2	13.6	13.2	13.2	18.2	14.0
21	11.8	19.9	16.7	18.2	17.1	15.5	13.2	13.6	13.2	13.2	17.8	14.0
22	11.8	19.9	16.3	18.2	16.7	15.5	13.2	13.6	13.2	13.2	18.2	14.0
23	11.8	19.9	16.3	17.8	15.9	15.5	14.0	13.6	13.2	13.2	20.7	14.0
24	11.8	19.9	16.3	17.8	15.1	15.5	14.0	13.6	13.2	13.2	18.2	14.0
25	11.8	19.9	15.9	17.8	15.5	15.5	14.0	13.6	13.2	13.2	16.3	14.0
26	11.8	19.9	15.9	17.8	15.1	15.5	14.0	13.6	13.2	13.2	15.1	14.0
27	11.8	19.9	15.9	17.4	14.7	15.5	13.6	13.2	13.2	13.2	14.7	14.0
28	11.8	19.9	15.9	17.4	15.1	15.5	13.6	13.2	13.2	13.2	14.0	14.0
29	11.8	19.85	15.9	42.2	15.1	15.5	13.6	13.2	13.2	13.2	14.0	14.0
30	11.8		15.9	42.2	15.1	15.5	13.6	13.2	12.9	13.2	14.0	14.0
31	11.8		24.0		15.1		14.0	13.2		13.2		14.0
Average	12.0	18.7	17.7	20.6	26.2	15.4	14.1	13.7	13.1	13.1	14.3	14.0
Max	13.2	19.9	24.4	42.2	42.2	15.5	15.9	15.1	13.2	13.2	20.7	14.0
Min	11.8	11.8	15.9	15.9	14.7	15.1	13.2	13.2	12.5	12.9	12.9	14.0